Understanding the molecular mechanisms of the T6SS in *Photorhabdus luminescens* and their potential for biotechnology

Dissertation

zur Erlangung des Grades

Doktorin der Naturwissenschaften

(Dr. rer. nat.)

Am Fachbereich Biologie

der Johannes Gutenberg-Universität Mainz

Friederike Pisarz

Frankfurt, Januar 2025

Dekan: Prof. Dr. Eckhard Thines

1. Berichterstatter:

2. Berichterstatterin:

Tag der mündlichen Prüfung:

Eidesstattliche Erklärung

Ich versichere hiermit an Eides statt, dass die vorgelegte Dissertation von mir selbstständig und ohne unerlaubte Hilfe angefertigt wurde. Des weiteren erkläre ich, dass ich nicht anderweitig ohne Erfolg versucht habe, eine Dissertation einzureichen oder mich der Doktorprüfung zu unterziehen. Die folgende Dissertation liegt weder ganz noch in wesentlichen Teilen einer anderen Prüfungskommission vor.

Mainz, den _____ _____

Friederike Pisarz

Statutory Declaration

I declare that I have authored this thesis independently, that I have not used other than the declared sources/references. As well I declare that I have not submitted a dissertation without success and neither passed the oral exam. The present dissertation has not been presented to another examination board, neither as entire dissertation nor parts.

Mainz, _____ _____

Friederike Pisarz

Table of content

Nomenclature

The two distinct cell forms of *Photorhabdus luminescens* subsp. *luminescens* strain DJC are called primary (1°) and secondary (2°) cells and referred to 1° and 2° cells.

The symbol "Δ" is used to indicate gene deletions in *P. luminescens* DJC. While gene integration is marked with "::" followed by the respective gene or vector used.

Core components of the Type VI Secretion System are named as TssA-M. The effector and immunity proteins are named e.g. Tme and Tmi for Type VI membrane disrupting effector and Type VI membrane immunity protein.

Figures and tables are numbered according to the chapters (i.e. Figure 1 of Chapter 2 = Fig. 2.1).

Abbreviations

AA	Amino acid
AF2	AlphaFold2
ALA	5-amino levulinic acid
BACTH	Bacterial Adenylate Cyclase-based two hybrid
bp	Base pairs
Carb	Carbenicillin
CASO	Casein soy peptone medium
CFU	Colony forming unit
Cm	Chloramphenicol
ddH_2O	Double-distilled water
DNA	Deoxyribonucleic acid
DNase	Deoxyribonuclease
dNTPs	Deoxyribonucleotides
EPNs	Entomopathogenic nematodes
EtOH	Ethanol
E-I pair	Effector-immunity pair
fwd	Forward
gDNA	Genomic DNA
Gent	Gentamycin
HGT	Horizontal gene transfer
HPLC	High Performance Liquid Chromatography
IJs	Infective juveniles
IN	Inner membrane
IPM	Integrated pest management
IPTG	Isopropyl-ß-D-thiogalactopyranoside
Kan	Kanamycin

kDa	Kilo-Dalton
LB	Lysogeny broth
MSA	Multiple sequence alignment
OD	Optical density
OM	Outer membrane
PAE	Predicted aligned error
PCR	Polymerase chain reaction
PRE	Plant root exudates
rev	Reverse
Rif	Rifampicin
rpm	Rounds per minute
RT	Room temperature
Strep	Streptomycin
Suc	Sucrose
Tme	Type VI membrane-disrupting effector
TMH	Transmembrane helix
Tmi	Type VI membrane disrupting immunity
Tss	Type VI core component
T3SS	Type III Secretion System
T6SS	Type VI Secretion System
WT	Wildtype
X-Gal	5-Brom-4-chlor-3indoxyl-ß-galactopyranoside

Publications and manuscripts presented in this thesis

Chapter 2:

Friederike Pisarz, Timo Glatter, Dhana-Theresa M. Süss, Ralf Heermann, Alice Regaiolo.

The Type VI Secretion Systems of the insect pathogen *Photorhabdus luminescens* are involved in interbacterial competition, motility and secondary metabolism. *The Microbe* (2024) doi:10.1016/j.microb.2024.100067

Chapter 3:

Friederike Pisarz, Kira Götz, Dhana-Theresa M. Süss, Ralf Heermann, Alice Regaiolo

Functional insights into the T6SS-3 of *Photorhabdus luminescens*: Effector dynamics and environmental stress response.

Chapter 4:

Friederike Pisarz, Luca Rabbachin, Melanie Hoos, Ralf Heermann. Alice Regaiolo

Mechanisms of T6SS effectors in *Photorhabdus luminescens*: insights into Tme1 interactions and Tmi1 neutralization.

Chapter 5:

Friederike Pisarz, Luca Rabbachin, Fabio Platz, Alice Regaiolo, Ralf Heermann.

Lights off – Role of bioluminescence for the biology of the biocontrol agent *Photorhabdus luminescens. iScience* (accepted, 2024) doi: 10.1016/j.isci.2024.110977

Chapter 6:

Judith Mehler, Kim Ina Behringer, Robert Ethan Rollins, Friederike Pisarz, Andreas Klingl, Thomas Henle, Ralf Heermann, Noémie S. Becker, Michael Hellwig, Jürgen Lassak.

Identification of *Pseudomonas asiatica* subsp. *bavariensis* str. JM1 as the first Nε-carboxy(m) ethyllysine-degrading soil bacterium. *Environmental Microbiology* (accepted, 2022) doi: 10.111/1462-2920.16079

Contributions to publications and manuscripts presented in this thesis

Chapter 2:

F.P. performed the bioinformatics study, performed the microbiological and molecular biological experiments. T.G. performed the mass spectrometry analysis and F.P. performed the analyses of the data. A.R. and F. P. designed the study and A.R. supervised the experiments. D.S. performed the motility assay and mutants' phenotypic characterisation. R.H. and A.R. critically overviewed the experimental results. F.P. and A.R. wrote the manuscript.

Chapter 3:

F.P., A.R. and R.H. designed the experiments. R.H. and A.R. coordinated the project. F.P., K.G. and D.S. performed the experiments. F.P. and A.R. wrote the manuscript.

Chapter 4:

A.R. conceptualized the study. F.P. performed the formal analysis. F.P., L.R., M.H., and A.R. conducted the investigation. R.H. provided the resources. A.R. and R.H. supervised the work. F.P. and A.R. wrote the original draft, while R.H. and A.R. reviewed and edited the manuscript.

Chapter 5:

Fr.P and L.R. performed the molecular biological and microbiological experiments and analysed the data. Fa.P. performed the nematode bioassays. Fr.P. and R.H. designed, and R.H. and A.R. supervised the experiments. Fr.P., A.R. and R.H. wrote the manuscript.

Chapter 6:

J.M. isolated and characterized the CML degrading isolate unless indicated otherwise. She also initially classified the bacterium as *pseudomonad* of the *P. putida* group. All other bioinformatic analyses were done by R.E.R. and N.S.B. A.K. performed electron microscopy experiments. F.P. and R.H. performed entomopathogenicity assays and analysed plant root colonization. K.I.B. and M.H. synthesized CML/CEL and analysed their degradation and metabolic derivatives. J.L. and M.H. wrote the manuscript with contributions from all other authors. The study was designed by J.L. and M.H. with contributions from all other authors.

Summary

Biotechnology focuses on harnessing biological processes and organisms for practical applications, studying microbial systems to better understand their mechanisms and improving human health, agriculture, and industry. Bacterial secretion systems hold immense potential for the field, symbolising molecular weapons found in bacteria, like the type VI secretion system (T6SS). The T6SS facilitates competition by secreting toxic effectors to eliminate competitors thus being essential for bacterial fitness. Despite its significance, much remains unknown about how T6SSs act in different bacterial species and their contribution to microbial interactions. Investigating the T6SS in bacteria like *Photorhabdus luminescens*, which inhabits polymicrobial niches, is crucial to uncover bacterial strategies utilized to dominate and thrive in competitive environments. *P. luminescens* is an insect-pathogenic bacterium that colonizes various polymicrobial environments, such as nematode guts, plant roots and insect larvae. *P. luminescens*' ability to inhabit these diverse niches suggests the employing of complex competitive mechanisms, possibly involving T6SSs. Nevertheless, the roles of T6SSs in *P. luminescens* remain poorly understood. Therefore, this study aims to investigate the T6SSs in *P. luminescens* to elucidate its role in bacterial competition and fitness, which could increase knowledge into microbial ecology and host-pathogen interactions.

Initially, bioinformatic analyses identified four T6SS gene clusters in the *P. luminescens* DJC genome, alongside several auxiliary clusters encoding effector-immunity pairs, indicating T6SSs as a crucial mechanism to outcompete other organisms. Comparative proteome analysis between wild-type and T6SS-deficient strains revealed significant differences in protein abundance, demonstrating crucial role of T6SSs in enhancing the bacterial fitness. In particular, the T6SS-2 was found essential for interbacterial competition, underlining its role in microbial interactions. Further, the T6SSs were found linked to regulate other bacterial fitness factors, such as motility and secondary metabolism. Thus, strains lacking T6SS-2 showed increased movement and higher anthraquinone levels, suggesting that T6SSs not only impact bacterial competition but also influences other virulent key aspects found in *P. luminescens*.

Additionally, T6SS protein abundance varied in strains lacking T6SS function, indicating a compensatory mechanism. The T6SS-3 was particularly intriguing due to its novel structure and function, lacking diverse core components. However, the T6SS-3 was found involved in interbacterial competition, encoding four lipase effectors: including Tle4A, an antibacterial effector. The unique genetic structure of T6SS-3, encoding multiple VgrG tip-proteins with different C-terminal domains, likely facilitates the assembly of a multi-effector complex. This allows the system to inject a cocktail of toxic effectors into competitor cells, enhancing *P. luminescens*' ability to compete in diverse environments. Fluorophore reporter microscopy showed a high expression rate of the T6SS-3 under various rhizosphere-similar environmental conditions, such as acidic, alkaline, and high salt concentrations. Moreover, expression was observed at 37°C, indicating a role in insect pathogenesis. This adaptability suggests a critical role of the T6SS-3 in enabling the bacterium to thrive in different environments.

Furthermore, two membrane-disrupting effectors (Tme1) with antibacterial activity and related to the T6SS were identified. These effectors disrupt bacterial membranes putatively through pore formation and reduce bacterial cell growth. Time-lapse microscopy confirmed that Tme1A induces cell rounding, a hallmark of pore formation. Moreover, the Tmi immunity proteins (Tmi1A-F) neutralize these toxic effectors throughout binding on its C-terminal loop. Further, to assess the activity of the Tme1 effectors, luminescence-based reporter assays were established in *P. luminescens* through deletion of the *lux* operon. Thus, a new approach to study *P. luminescens* was implemented and further, reporter plasmids were used to monitor the role of Tme1 against bacterial competitors *in vivo*. Indeed, Tme1A was found active against bacterial cells and deletion of *tme1A* altered the killing capacity of *P. luminescens*. Thus, a role of those effectors in interbacterial competition could be assigned.

In summary, this research advances our understanding of the complex role of T6SSs in *P. luminescens*, revealing their critical functions in bacterial competition and adaptation across diverse environments. These insights not only deepen our knowledge of interspecies interactions but also open avenues for future biotechnological applications, such as engineering bacterial systems for targeted antimicrobial strategies or sustainable agricultural.

Zusammenfassung

Die Biotechnologie befasst sich mit der Nutzung biologischer Prozesse und Organismen für praktische Anwendungen, insbesondere zur Erforschung mikrobieller Systeme. Ziel ist es, deren Mechanismen detaillierter zu verstehen, um Fortschritte in der Medizin, Landwirtschaft und Industrie zu ermöglichen. Bakterielle Sekretionssysteme bergen ein beträchtliches Potenzial für die Biotechnologie, da sie als molekulare Waffen in Bakterien dienen, so beispielsweise das Typ VI-Sekretionssystem (T6SS). Das T6SS ermöglicht es Bakterien, toxische Effektoren zu sekretieren und somit Konkurrenzorganismen zu eliminieren, was essenziell für die Fitness und den Erfolg in komplexen Umgebungen ist. Trotz seiner zentralen Bedeutung sind viele Aspekte des T6SS, insbesondere in spezifischen Bakterienarten und dessen Beitrag zu mikrobiellen Interaktionen, noch weitgehend unbekannt.

Die Untersuchung des T6SS in *Photorhabdus luminescens*, einem Insektenpathogen, das polymikrobielle Lebensräume wie Nematodendärme, Pflanzenwurzeln und Insektenlarven besiedelt, ist von besonderer Relevanz. Die Fähigkeit von *P. luminescens*, in derart unterschiedlichen Lebensräumen zu existieren, deutet auf komplexe Konkurrenzmechanismen hin, bei denen das T6SS vermutlich eine zentrale Rolle spielt. Ziel dieser Arbeit war es, die Funktion des T6SS in *P. luminescens* zu analysieren, um dessen Bedeutung für bakterielle Konkurrenz, Fitness und Interaktionen innerhalb mikrobieller Gemeinschaften sowie mit Wirtsorganismen besser zu verstehen, sowie das Potenzial des T6SS für die biotechnologische Anwendung zu ermitteln.

Mittels bioinformatischer Analysen konnten vier T6SS-Gencluster im Genom von *P. luminescens* DJC identifiziert werden, zusätzlich zu mehreren zusätzlichen Clustern, die für Effektor-Immunitäts-Paare kodieren. Diese Ergebnisse weisen auf das T6SS als entscheidenden Mechanismus hin, mit dem *P. luminescens* mit Konkurrenzorganismen interagiert. Proteomanalysen von Wildtyp- und T6SS-defizienten Stämmen zeigten signifikante Unterschiede in der Proteinexpression und verdeutlichten die Rolle des T6SS für die bakterielle Fitness. Insbesondere das T6SS-2 erwies sich als essenziell für die interbakterielle Konkurrenz und beeinflusste zugleich weitere Fitnessfaktoren wie die Motilität und den

Sekundärstoffwechsel. T6SS-2-defiziente Stämme zeigten beispielsweise eine erhöhte Motilität und eine verstärkte Produktion von Anthrachinon, was darauf hindeutet, dass das T6SS nicht nur die bakterielle Konkurrenzfähigkeit, sondern auch andere essenzielle physiologische Prozesse beeinflusst.

Darüber hinaus variierte die T6SS- Proteinkonzentration in Stämmen ohne T6SS-Funktion, was auf einen Kompensationsmechanismus hindeutet, da T6SS-1- und T6SS-2-defiziente Stämme höhere Proteinkonzentrationen von T6SS-3 und T6SS-4 aufwiesen. Insbesondere das T6SS-3 war aufgrund seiner neuartigen Struktur und Funktion, bei der verschiedene Kernkomponenten fehlen, besonders interessant. Es wurde festgestellt, dass das T6SS-3 an der interbakteriellen Konkurrenz beteiligt ist und für vier Lipase-Effektoren kodiert, darunter Tle4A, ein antibakterieller Effektor. Die einzigartige genetische Struktur des T6SS-3, die für mehrere VgrG-Tip-Proteine mit unterschiedlichen C-terminalen Domänen kodiert, ermöglicht vermutlich den Aufbau eines Multi-Effektorkomplexes. Dadurch kann das System einen Cocktail aus toxischen Effektoren in konkurrierende Zellen injizieren und so die Konkurrenzfähigkeit von *P. luminescens* in verschiedenen Lebensräumen verbessern. Fluorophore Reportermikroskopie zeigte eine hohe Expressionsrate von T6SS-3 unter verschiedenen Rhizosphären ähnlichen Umweltbedingungen, wie z. B. sauren, alkalischen und hohen Salzkonzentrationen. Darüber hinaus wurde die Expression bei 37°C beobachtet, was auf eine Rolle des T6SS-3 bei der Pathogenese von Insekten hinweist. Diese Anpassungsfähigkeit deutet darauf hin, dass das T6SS-3 eine entscheidende Rolle dabei spielt, dass das Bakterium in verschiedenen Umgebungen überleben kann.

Darüber hinaus wurden zwei membranstörende Effektoren (Tme1) mit antibakterieller Aktivität identifiziert, die mit dem T6SS in Zusammenhang stehen. Diese Effektoren zerstören bakterielle Membranen, vermutlich durch Porenbildung und hemmen das bakterielle Zellwachstum. Mittels Zeitraffermikroskopie wurde gezeigt, dass Tme1A die Zellrundung, ein Kennzeichen der Porenbildung, induziert. Gleichzeitig neutralisieren die Tmi-Immunproteine (Tmi1A-F) diese toxischen Effektoren durch Bindung an die C-terminale Schleife der Tme-Effektorproteine. Um die Aktivität der Tme1-Effektoren zu ermitteln, wurden in *P. luminescens*

durch Deletion des *lux*-Operons Lumineszenz-Reporter-Assays durchgeführt. So wurde ein neuer Ansatz zur Untersuchung von *P. luminescens* implementiert und außerdem konnte durch Reporterplasmide die Rolle von Tme1 gegen bakterielle Konkurrenten *in vivo* untersucht werden. Tatsächlich erwies sich Tme1A als aktiv gegen bakterielle Zellen und die Deletion von *tme1A* veränderte die Tötungsfähigkeit von *P. luminescens*. Folglich konnte die Rolle dieser Effektoren im interbakteriellen Wettbewerb eingeordnet werden.

Zusammenfassend lässt sich sagen, dass diese Forschungsarbeit das Verständnis der komplexen Rolle der T6SSs in *P. luminescens* vertieft und wichtige Funktion für die bakterielle Konkurrenz und Anpassung in verschiedenen Umgebungen aufzeigt. Diese Einblicke vertiefen nicht nur das Wissen über die interbakteriellen Interaktionen, sondern eröffnen auch Möglichkeiten für zukünftige biotechnologische Anwendungen, wie die Entwicklung bakterieller Systeme für gezielte antimikrobielle Strategien.

1. Introduction

1.1 Biotechnology: Sustainable solutions and microbial applications

In light of global challenges such as food insecurity, antibiotic resistance, climate change, and environmental degradation, biotechnology offers cutting-edge solutions across various fields when compared to traditional methods (Tyczewska et al. 2023). Conventional approaches in agriculture, medicine and environmental management — including chemical treatments, synthetic drugs, and fossil-fuel-based processes — have often resulted in adverse effects such as resource depletion, increased carbon dioxide emissions and the emergence of resistances in pests and pathogens (Rathore und Singh 2022; Jurick II. 2022). Thus, biotechnology provides a more efficient, targeted, and sustainable alternative that minimizes these risks and helps overcome limitations (Villadsen 2007; Ghosh et al. 2019). For example, microorganisms can be genetically manipulated to be employed in different industrial processes (Tripathi et al. 2017). However, ethical concerns arise regarding the use of genetically modified organisms (GMO). Nevertheless, contemporary biotechnological techniques can be employed to identify novel microorganisms with diverse capabilities (van Dorst et al. 2016). These newly identified bacteria have the potential to be used in diverse industrial processes, nowadays as a polymicrobial solution (Tripathi et al. 2015). Yet, inter- and intraspecies competition can alter microbial ratios, leading to inefficient substrate transport thus having negative impact on the biotechnological process in which they are employed (Hays et al. 2015). While competition among microbial species can reduce process efficiency, it also opens valuable avenues for studying underlying mechanisms that could enhance biotechnological applications (Pourhassan et al. 2021). Bacterial secretion systems hold immense potential for the field, especially in the production and secretion of recombinant proteins. By facilitating the export of proteins into the extracellular environment, these systems offer distinct advantages over traditional intracellular expression (Burdette et al. 2018; Kanonenberg et al. 2018). One key benefit of bacterial secretion systems is that they simplify downstream processing and

purification, as the target proteins are secreted directly into the surrounding medium (Filloux 2011). This not only reduces the toxicity to host cells but also allows for proper protein folding outside the cell, enhancing protein stability and functionality (Choi und Lee 2004). Additionally, secretion systems enable continuous protein production, which can increase yield and streamline industrial processes.

In exploring bacterial secretion systems, biotechnology can benefit from these natural mechanisms to develop novel, sustainable solutions for environmental and medical challenges. As a case in point, microorganisms from the *Photorhabdus* genus serve as valuable models, providing insights into competitive microbial interactions that can inform more efficient and targeted biotechnological applications.

1.2 The genus *Photorhabdus*: diversity, pathogenicity and symbiosis

The *Photorhabdus* species belong to the Gram-negative bacteria and are generally known for their insect pathogenicity as well as being the only terrestrial bacterium able to produce light (Akhurst 1980; Peat et al. 2010; Daborn et al. 2001). Back in 1977, Khan and Brooks identified the first *Photorhabdus* species which led to subsequent analyses and currently 19 different *Photorhabdus* species have been identified (Khan und Brooks 1977; Machado et al. 2018). All 19 *Photorhabdus* species are pathogenic towards insect larvae like *Galleria mellonella* or *Manducta sexta* and exist in a symbiotic relationship with EPNs of the genus *Heterorhabditis* (Akhurst 1980; Akhurst und Boemare 1988; Khan und Brooks 1977). In this symbiosis the bacteria provide the nematodes with a hospitable environment inside the insect host, facilitated by the bacterial production of toxins and enzymes that kill the insect and degrade the cadaver (Waterfield et al. 2009).

However, certain *Photorhabdus* species have been shown to also interact with different eukaryotic hosts. For example, the species *Photorhabdus asymbiotica* was found to be associated with human infections, highlighting its pathogenic potential beyond insect hosts (Gerrard et al. 2003). In contrary, *Photorhabdus luminescens* DJC, was shown to colonize

plant roots, thereby suggesting a broader role in the rhizosphere besides insect pathogenicity (Regaiolo et al. 2020). However, the best characterized species of the *Photorhabdus* genus, is the strain *Photorhabdus luminescens* subsp. *laumondii* TTO1 (Machado et al. 2018). Yet, recent findings on the *P. luminescens* strain DJC regarding its ability to colonize plant roots and further protect plants against phytopathogens has made it a research candidate with the prospect of potential application as a biocontrol agent or unravel new biotechnological targeted approaches (Dominelli et al. 2022b; Regaiolo et al. 2020).

1.2.1 The life cycle of *P. luminescens*: a model organism for bacteria-host interactions

The life cycle of *P. luminescens,* also designated as *P. laumondii* subsp. l*aumondii*, includes multiple interactions with various eukaryotic hosts and therefore, *P. luminescens* is considered a model-organism to study bacteria-host interactions (Clarke 2008; Machado et al. 2018). Throughout the life cycle, the bacteria colonize the gut of soil-living infective juveniles of the *Heterorhabditidiae* family (**Fig 1.1**) (Forst et al. 1997). The infective juvenile (IJ) is the non-feeding stage of the nematodes, crucial for infection of new insect hosts (Bedding und Molyneux 1982; Stock und Kaya 1996). Through the mouth, anus or spiracles, the IJs can enter the insect body and move towards the insect haemocoel, where the *P. luminescens* cells are regurgitated from the nematode gut into the insect's haemolymph (Kaya und Gaugler 1993; Bedding und Molyneux 1982; Ciche und Ensign 2003). Inside the larvae, the bacterial cells enter the pathogenic lifestyle and start the production of various virulence factors, including the Tc toxins (insecticidal toxin complexes) and Mcf toxin (makes caterpillars floppy) as well as various proteases and lipases (Bowen et al. 1998; Blackburn et al. 1998; Daborn et al. 2002; Rajagopal und Bhatnagar 2002; Zamora-Lagos et al. 2018). Meanwhile, *P. luminescens* cells protect themself against the insect immune system through the production of bioactive inhibitor molecules like isopropylstilbene or rhabduscin (Crawford et al. 2012; Eleftherianos et al. 2007). Following, through the secretion of exoenzymes, *Photorhabdus* degrades the dead insect cadaver to provide nutrition for its own growth as well as for the growth of a new cycle of nematodes (Waterfield et al. 2009). The *P. luminescens* cells re-enter their symbiotic lifestyle

and provide the nematodes with essential nutrients and secondary metabolites, which support the nematodes development (Han und Ehlers 2001). Once the nutrients are depleted, *P. luminescens* reassociates with the new generation of infective juveniles, which now leave the insect cadaver in search of a new prey, thereby restarting the symbiosis- and pathogenic-lifestyle (ffrench-Constant et al. 2003). Thus, *P. luminescens* shares a similar pathogenic life cycle as *P. temperata* and *P. asymbiotica*: nevertheless, the *P. luminescens* strain DJC has recently been found to have an alternative lifestyle in the soil. Hence, *P. luminescens* colonizes plant roots in the rhizosphere and promotes the development of plant growth while protecting the plants through chitinolytic and fungicidal activity against fungal phytopathogens such as *Fusarium graminearum* (Regaiolo et al. 2020; Dominelli et al. 2022b).

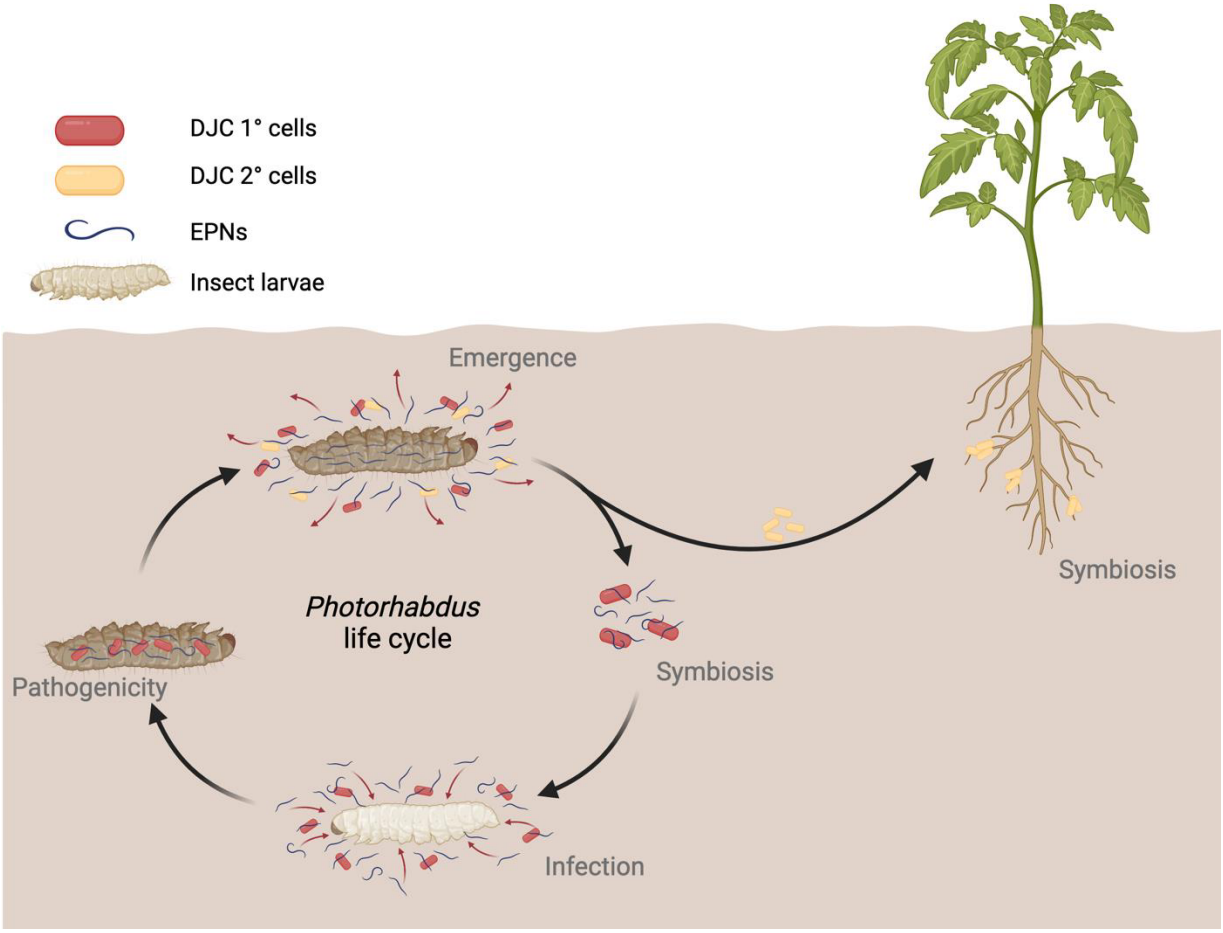

Figure 1.1 Life cycle and phenotypic heterogeneity of the insect pathogenic *Photorhabdus luminescens*. The life cycle of *P. luminescens* is characterized by two symbiotic lifestyles as well as a pathogenic lifestyle. The *P. luminescens* cells establish a symbiosis within the gut of nematodes of the *Heterorhabditidiae* family. Upon invading insect larvae of e.g. *Galleria mellonella*, the bacteria are released into the haemolymph and start to produce different toxins. Within 24 h, the larvae die and are

degraded into a nutrient source for the new generation of nematodes. Within this phase, part of the 1° cells switch to 2° cells. While the 1° cells reassociate with the nematodes, the 2° cells remain in the rhizosphere, entering the second symbiotic lifestyle by colonizing plant roots.

1.2.2 Phenotypic heterogeneity in *Photorhabdus luminescens*

One of the reasons behind the complex life cycle of *Photorhabdus luminescens* is the phenotypic heterogeneity represented in the *Photorhabdus* species (Forst et al. 1997; Waterfield et al. 2009). Phenotypic heterogeneity is the result of evolutionary pressure to adapt to different conditions in order to preserve the bacterial fitness and bacteria can face those environmental stresses through genomic rearrangements or through the methylation of DNA (Smits et al. 2006). However, in terms of phenotypic heterogeneity the cells are genetically identical, yet, the gene expression is altered to enhance the bacterial fitness and therefore results in different cell forms with various phenotypic traits (Elowitz et al. 2002; Dominelli et al. 2022a).

Recent studies confirmed that the different cell forms found in *P. luminescens* are based on phenotypic heterogeneity. The primary (1°) and secondary (2°) cells are genetically identical, although their phenotypic characteristics differ greatly from each other (Dominelli et al. 2022a). There are multiple prominent features found in 1° cells which are absent or reduced in the 2° cell form like i) mutualistic symbiosis with nematodes, ii) bioluminescence and red pigmentation, iii) production of antibiotics like carbapenem and diverse secondary metabolites like IPS and anthraquinone, and iv) production of crystalline inclusion bodies (CipA and CipB) as well as cell clumping through the *Photorhabdus* cell clumping factors (PCF) (Akhurst und Boemare 1988; Akhurst 1980; Langer et al. 2017; Richardson et al. 1988; You et al. 2006). Although both cell variants are pathogenic towards insect larvae, their lifecycles are very distinct and so far, it has only been reported that the 1° cells are found in the symbiotic stage with nematodes and the pathogenic stage. Therefore it is assumed, that part of the 1° cells switch to the 2° cells after depletion of the larvae nutrients (Han und Ehlers 2001).

While it was known that the 1° cells re-associate with nematodes and re-enter their symbiotic life cycle, it was long unclear whether the 2° cell forms enter a yet unidentified alternative life cycle. Initial studies have shown that the 2° cells are better adapted to an alternative lifestyle in the soil, with increased motility and temperature tolerance, as well as an alternative metabolism to adapt to nutrient limitation (Eckstein et al. 2019). The open question of what happens to the 2° cells in the soil has been resolved, as their colonization of plant roots has been observed for the first time, together with plant protection against phytopathogens by inhibiting fungal growth through chitin hydrolyzation (Regaiolo et al. 2020; Dominelli et al. 2022b). However, many aspects of the lifestyle and life cycle of *P. luminescens* remain unclear, such as the ability of 2° cells to revert to 1° cells and the role of bioluminescence and anthraquinones. Nevertheless, the distinct phenotypic traits exhibited by the two cell forms of *P. luminescens* provide a promising foundation to uncover novel biotechnological tools, ranging from advanced bioinsecticides to sustainable methods for plant protection.

1.3 Virulence factors in *Photorhabdus luminescens*

Besides the phenotypic heterogeneity and symbiotic features which contribute to the symbiotic relationship between *Photorhabdus* and its hosts, various virulence factors are also important for maintaining the symbiosis and protecting the insect carcass against other microbes (Zamora-Lagos et al. 2018). Generally, four different groups of toxins that exhibit insecticidal activity are well-studied in *P. luminescens*: i) the makes caterpillars floppy (MCF) toxins, ii) the toxin complexes (Tcs), iii) the *Photorhabdus* insect related proteins (Pir) and iv) the *Photorhabdus* virulence cassettes (PVCs) (Yang et al. 2006; Ffrench-Constant et al. 2007). The Tcs are located on pathogenicity islands distributed throughout the *Photorhabdus* genome and are high-molecular-weight insecticidal toxins composed of multiple subunits (Waterfield et al. 2001; Ffrench-Constant et al. 2007). PirAB proteins are cytotoxic to insect cells, inducing apoptosis through DNA fragmentation or cell shrinkage, while the MCF toxins cause a "floppy" phenotype by destroying haemocytes and the midgut epithelium (Dowling et al. 2004; Li et al. 2014). The fourth group, the PVCs, are extracellular injection systems (eCIS) consisting of

multiple proteins encoded by a single operon, and they are hypothesized to target eukaryotic cells, such as insect cells. Unlike the previously mentioned toxins, the PVCs share structural similarities with bacterial secretion systems like the type VI secretion system (T6SS) and R-type pyocins (Vlisidou et al. 2019).

1.4 Bacterial secretion systems in *Photorhabdus luminescens*

Bacterial secretion systems, which are commonly found in Gram-negative bacteria, are used for the translocation of small molecules, DNA, or proteins into the surrounding environment or another cellular space (Costa et al. 2015; Tseng et al. 2009). The proteins produced in the cytoplasm must be transported out, the inner membrane (IM), the outer membrane (OM), and the periplasmic space, which requires a complex system. There are two known mechanisms: one-step secretion, where a channel spans the IM and OM and two-step secretion, where a protein is first transported into the periplasm through an embedded complex and then transferred through the OM (Kostakioti et al. 2005; El-Sharoud 2008).

Secretion systems in *P. luminescens* are critical for its pathogenicity and symbiosis with nematodes (Rodou et al. 2010). This Gram-negative bacterium employs a variety of secretion systems, including type I, type II, type III, and type VI secretion systems, each with specific roles in its lifecycle and interaction with hosts. For instance, the Type III secretion system (T3SS) is essential for injecting effector proteins directly into the host cells, facilitating infection and immune evasion (Brugirard-Ricaud et al. 2005). The type I secretion system (T1SS) of *P. luminescens* is involved in the secretion of enzymes and toxins that degrade host tissues and promote nutrient acquisition (Bowen et al. 2003). The type II secretion systems (T2SS) can secrete a variety of extracellular enzymes, however only bioinformatic analysis confirmed the presence of T2SS core components and it was suggested, that the Pdl1 lipase can be transported via a T2SS (Yang et al. 2012; Rodou et al. 2010). These secretion systems collectively support *P. luminescens* to successfully infect insect hosts, evade their immune responses, and to convert the cadaver into a nutrient rich mass. One of those secretion systems, the type VI secretion system (T6SS), has gained a lot of interest throughout the last

years but the understanding of its role in the insect pathogen *P. luminescens* is limited. However, the diverse secretion systems employed by *P. luminescens* are not only vital for its pathogenicity and symbiosis but also present significant opportunities for biotechnological innovation, such as developing targeted pest control strategies and novel antimicrobial agents inspired by these molecular mechanisms.

1.5 The Type VI Secretion System

Since the first discovery of the T6SS (2006), the secretion system gained more and more attention as a nano-molecular weapon used by Gram-negative bacteria to fight against prokaryotic or eukaryotic cells (Pukatzki et al. 2006). While it was initially discovered in *P. aeruginosa* and *V. cholerae*, it is now estimated to be found in around 25% of pathogenic and non-pathogenic Gram-negative bacteria (Mougous et al. 2006; Pukatzki et al. 2006; Russell et al. 2014). After the first identification of the T6SS, numerous further studies followed to find out more about its role, composition and underlying mechanism of the system, as it may play a role in both interbacterial and interkingdom competition.

Generally, the T6SS apparatus shares structural and functional homology with the contractile sheath of bacteriophages and can transfer toxins, so-called effectors into a neighboring target cells (Basler und Mekalanos 2012). It is composed of a complex assembly of proteins forming a dynamic structure, which is span across the cell envelope, capable of puncturing the cell membranes of target organisms (Durand et al. 2015). This system is not only crucial for bacterial survival and competitiveness but also for niche adaptation and virulence. Moreover, the versatility of the T6SS allows it to deliver a wide range of effector proteins, enabling bacteria to perform diverse functions such as intoxicating bacterial cells, host cell manipulation and also biofilm formation (Wood et al. 2019; Chen et al. 2020; Fridman et al. 2020).

1.5.1 Structure of the Type VI Secretion System

Generally, T6SSs consist of 13 core components, which are commonly encoded within one gene cluster, yet bacteria can harbor more than one operon encoding for T6SSs (Russell et al. 2014). Further, so called pathogenicity islands or auxiliary clusters are often found spread on

the bacterial genome, encoding for additional structural components, adaptor proteins or effector and immunity proteins and can be a result of a prior horizontal gene transfer (Russell et al. 2014; Thomas et al. 2017).

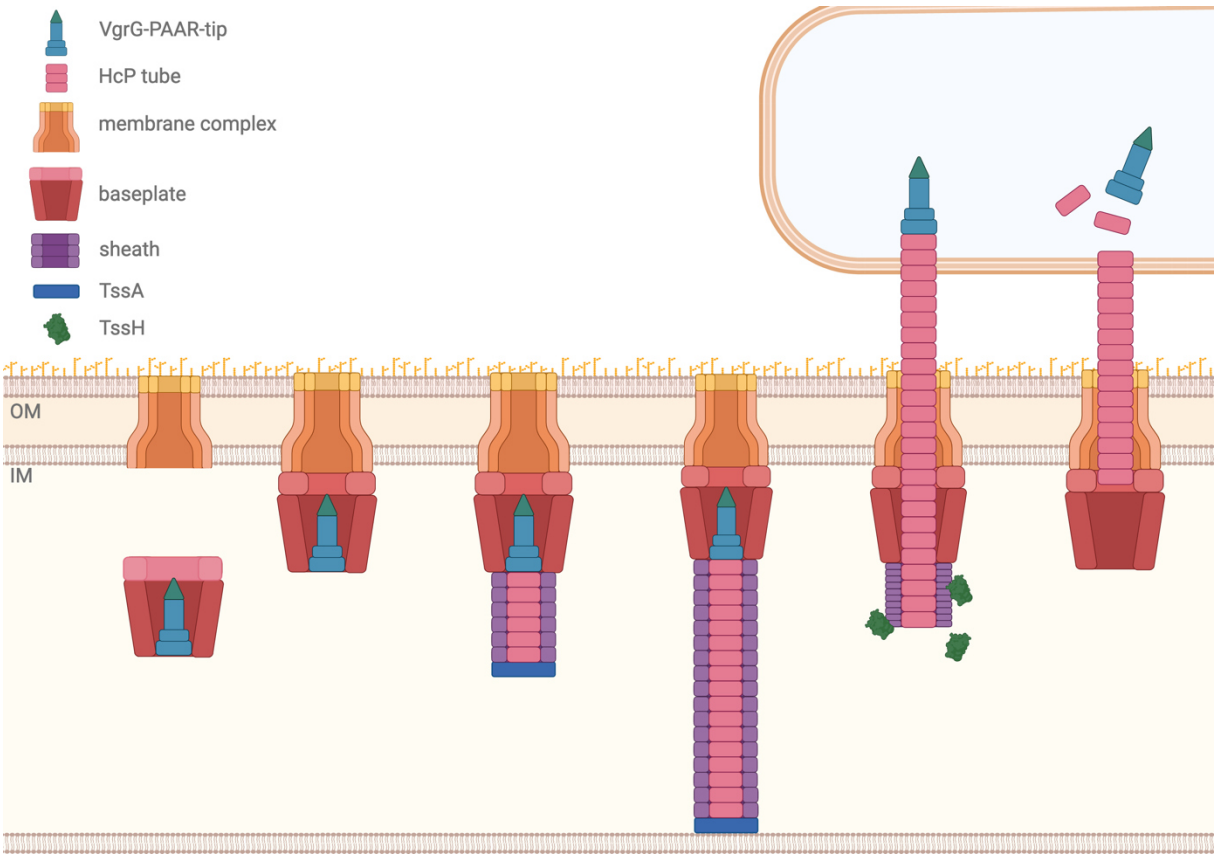

Figure 1.2 Assembly and activation of the T6SS. Assembly of the T6SS starts with the membrane complex, followed by the baseplate, docking to the membrane complex. Next, the tip is assembled, followed by the sheath-tube complex. The core component, TssA, locks the whole structure to the opposite inner membrane, maintaining it in a high-energy state, ready to fire. Upon activation, the sheath contracts and the tube is propelled out of the cell into a target cell, delivering toxic effectors. The sheath gets dissembled by the ATPase TssH, while the baseplate and membrane remain intact, ready for another round of assembly and firing.

The structure is divided into six parts: i) the membrane complex consisting of TssJ, TssL and TssM, ii) the baseplate consisting of TssE, TssF, TssG and TssK, iii) the tube assembled of hemolysin-coregulated proteins (HcPs), iv) the spike consisting of trimeric valine-glycine repeat proteins G (VgrG) and proline-alanine-alanine-arginine repeat proteins (PAAR), v) the sheath consisting of TssB and TssC and vi) TssA, a protein required for sheath stabilization (**Fig. 1.2**) (Durand et al. 2015; Brunet et al. 2015; Shneider et al. 2013; Wang et al. 2017;

Bernal et al. 2021). The assembly of the T6SS starts with the recruitment of the membrane complex to the inner membrane, defining the position for the secretion system (Durand et al. 2015). Thereby, TssJ reaches in the outer membrane and TssM in the inner membrane, while TssL is required for the interaction of the membrane complex with the baseplate (Durand et al. 2012; Durand et al. 2015; Aschtgen et al. 2008). Following, the baseplate, which is similar to the baseplate of contractile phages, forms a wedge-like structure that docks onto the membrane complex and initiates the assembly of the VgrG tip, which in turn provides a platform for the polymerization of the hexameric HcP tube (Cherrak et al. 2018; Nazarov et al. 2018; Park et al. 2018). The sheath is composed of TssB and TssC subunits, polymerizing around the HcP tube and locks the whole complex in a high-energy status (Clemens et al. 2015; Kudryashev et al. 2015). The core component TssA is located at the cytosolic end of the T6SS, initiating the sheath polymerization and thereby migrating to the opposite site of the cell, anchoring the sheath-tube complex. Accessory proteins like TagA can anchor TssA to the membrane, leading to a longer duration time of the T6SS in a ready-to-fire state, while accessory proteins as TagB or TagJ only stabilize the sheath until the assembly is completed, followed by direct firing (Bernal et al. 2021; Dix et al. 2018; Schneider et al. 2019; Zoued et al. 2017).

Upon activation of the T6SS, a conformation change of the sheath leads to the re-location of the tip-tube complex outside of the cell into another target cell within a few milliseconds (Kudryashev et al. 2015; Wang et al. 2017; Vettiger et al. 2017). Thereby, the tip punctures the target cell and the effectors, bound to the tip are relocated inside the target (Brunet et al. 2013). Following, the sheath is recycled by the ATPase TssH/ ClpV, while the membrane complex remains intact, allowing another round of T6SS assembly and firing (Durand et al. 2015; Kapitein et al. 2013).

1.5.2 The diversity of T6SS effectors and immunity proteins

Besides the complexity of the T6SS apparatus which is shared among different bacteria, the variety regarding its effectors seems even broader, as those effectors can be anti-bacterial or anti-eukaryotic (Fridman et al. 2020; Hachani et al. 2016; Trunk et al. 2018). Those effectors

can be delivered inside a target cell through either direct or indirect binding to the tip, which requires so called adaptor proteins (Durand et al. 2014; Unterweger et al. 2017). Upon direct binding, the effector either interacts directly with the VgrG tip through covalent binding or a C-terminal extension of the VgrG, or similarly with a PAAR protein or its C-terminal extension (Hernandez et al. 2020). In contrary, for indirect binding an adaptor protein is required, which interacts with the tip proteins and harbors a C-terminal extension, where the effectors can bind to (Cherrak et al. 2019). Further, T6SS effectors can also be secreted through the HcP tube and bind upon assembly to HcP and are following located inside of the HcP lumen. Yet, the tube diameter of 40 Å restricts this option to smaller effectors (Mougous et al. 2006). While the mechanism of effector delivery through the T6SS involves complex interactions with adaptor proteins, VgrG tips, PAAR proteins, or the HcP tube, the purpose of these effectors is to neutralize competitors or manipulate host cells (Allsopp und Bernal 2023).

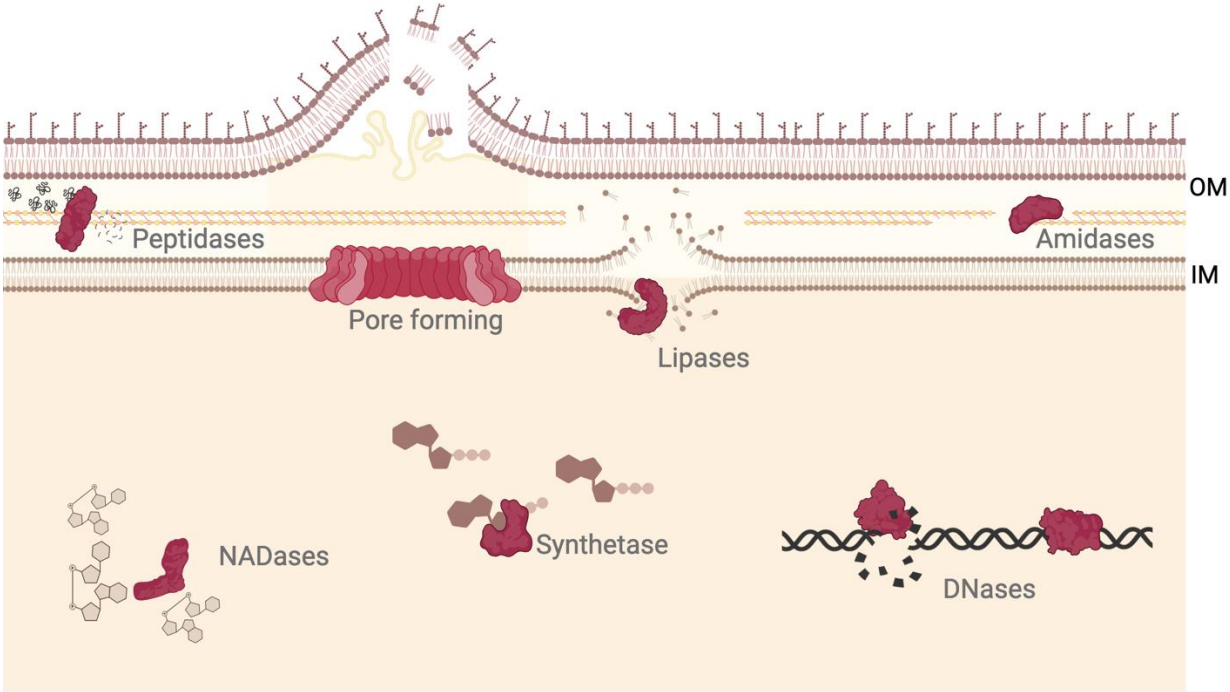

Figure 1.3 Diversity of antibacterial T6SS effectors. The model shows different enzymatic activities of T6SS effectors. Different toxins are shown in red. Tde effectors deploy DNase activity, targeting the DNA, while Tne effectors deploy NADase activity, degrading NAD(P) to nicotinamide and ADP-ribose. Effectors with synthetase activities like Tas can phosphorylate ATP and ADP, leading to accumulation of (p)ppApp. Other effectors can target the periplasm, like pore-forming effectors (Tme) or effectors with peptidase (Tpe), lipase (Tle) or amidase (Tae) activity (Adapted from Jurénas *et al*., 2021)

Studies throughout the last years identified multiple T6SS effectors, targeting different cell compartments (**Fig. 1.3**): i) the Type VI lipase effectors (Tle) target the cell membrane and hydrolyse phospholipids, considered as trans-kingdom effectors, ii) the Type VI DNase effectors (Tde) target chromosomal DNA leading to complete DNA degradation, iii) the T6SS membrane disrupting effectors (Tme) targeting the inner membrane can cause membrane depolarization or iv) the T6SS antifungal effectors (Tfe), leading to fungal cell death by disrupting the plasma membrane potential (Jiang et al. 2016; Jiang et al. 2014; Jana et al. 2019; Pissaridou et al. 2018; Fridman et al. 2020; Trunk et al. 2018). Further, to avoid killing of sister cells or self-intoxication, cognate immunity proteins are co-produced in combination with the effector and often named as effector-immunity (E-I) pairs. The respective genes encoding for immunity proteins are found on auxiliary clusters together with the upstream or downstream of the effector gene and mostly also with an additional gene encoding for an adaptor protein or for HcP, VgrG or a PAAR protein (Yang et al. 2018). Thus, T6SS-deploying bacteria often encode for multiple effector proteins of different effector classes, which enables T6SSs to attack a broad spectrum of organisms (Allsopp und Bernal 2023). However, while a considerable number of T6SS effectors have been identified throughout recent years; new effectors continue to emerge and thus, analysis of these effectors is still a valuable endeavor.

1.5.3 Role of T6SSs in the lifestyle of bacteria

With the T6SS, bacteria have a versatile and sophisticated molecular weapon used to deliver toxins into neighboring cells. While the structure and assembly of the T6SS is quite conserved, the underlying regulation and activity is often related to the bacteria's lifestyle and ecological niche. As bacteria can have more than one T6SS and various effectors found in auxiliary clusters, different roles can be assigned regarding their function in the bacteria's fitness (MacIntyre et al. 2010). For instance, *Burkholderia thailandensis* T6SS-1 is primarily involved in antibacterial activity, targeting competing bacteria, whereas the T6SS-5 is utilized for anti-host activity, playing a role in pathogenicity against eukaryotic cells. This specialization highlights the ability of bacteria to diversify the functions of different T6SSs to enhance their fitness and adaptability (Si et al. 2017).

In contrast, *Vibrio cholerae* employs a single T6SS for both antibacterial and anti-eukaryotic competition, showcasing a multifunctional use of its T6SS machinery within different contexts. This dual role emphasizes the efficiency and adaptability of the T6SS in mediating interactions with various types of cells (MacIntyre et al. 2010; Schwarz et al. 2010). Moreover, post-translational regulation of a T6SS in *P. aeruginosa* was observed, as the activity was based on a “tit-for-tat” strategy, where the T6SS was activated after an initial T6SS attack by other bacteria (Basler et al. 2013). On the contrary, T6SSs of *V. parahaemolyticus* strains can be constitutive expressed under marine warm conditions or low salt concentrations, independently of cell-cell contact (Salomon et al. 2013). While the role and activity in certain bacteria is well-studied and investigated, other bacteria like *P. luminescens* with great potential for biotechnological application still need to be analysed. First studies confirmed the presence of the T6SS effector Tre23 in the *P. luminescens* strain TTO1, which is an antibacterial effector, inhibiting translation in targeted bacteria (Jurėnas et al. 2021a; Jurėnas et al. 2021b). Further, recent transcriptomic analysis of the *P. luminescens* 2° cells discovered a modulation of T6SSs genes upon sensing plant root signals, indicating a role of the T6SS during plant root colonization (Regaiolo et al. 2020). Given the importance of the T6SS in other bacterial species, it is crucial to investigate its role in *P. luminescens* to fully understand the bacterium's and the T6SS’s potential. Further, the diverse functionalities underscore the adaptability and critical roles of T6SSs in ecological interactions, highlighting their immense biotechnological potential for applications such as precision biocontrol, plant-microbe symbiosis enhancement, and the development of novel antibacterial therapies.

1.6 Bacterial bioluminescence: occurrence and role

To study complex bacterial systems like the T6SS at gene expression level, tools that provide precise and real-time insights are essential. Fluorescence and bioluminescence-based reporter assays offer powerful methods to track gene activity, enabling studies to monitor effector expression, regulation, and bacterial interactions (Guckes et al. 2020; Manera et al. 2021). Bioluminescence, widely used in these assays, not only allows non-invasive tracking

but also plays a significant role in biotechnology, where it aids in unravelling bacterial infection process in animal-model in real-time or their colonization mechanism and distribution in polymicrobial environment (Jiang et al. 2024; Girotti et al. 2008). The emission of light by an organism, which is referred to as bioluminescence, is a phenomenon observed in nature, found in a broad variety of organisms like fungi, insects, marine animals as well as bacteria (Brodl et al. 2018). Among those bioluminescent organisms, bacteria evolved a highly efficient mechanism for light production, but the role of bioluminescence for their fitness is still mostly unknown (Peat et al. 2010; Daborn et al. 2001). Briefly, bioluminescence is a biochemical enzyme-catalyzed reaction, that results in a light emission in a spectra from 400 to 700 nm (Widder 2010). The proteins required for bioluminescence are encoded in the *lux* operon, containing the core genes *luxCDABE*, found in a conserved gene architecture (Dunlap 2009). While this cluster can be found in various bacterial families like *Vibrionaceae*, *Shewanellaceae* and *Enterobacteriaceae*, it is still unclear whether bioluminescence evolved independently or as a result of gene transfer or gene duplications (Widder 2010; Haddock et al. 2010; Dunlap 2009; Dunlap 2014; Urbanczyk et al. 2011).

The luciferase enzyme consists of the α and β-subunits LuxA and LuxB, while LuxC, LuxD and LuxE are the components of a fatty acid reductase complex, required to synthesize and recycle fatty acids to aldehydes (**Fig. 1.4**) (Dunlap 2009; Meighen und Dunlap 1993). During the light emitting reaction, the luciferase catalyses a long-chain aldehyde and a reduced flavin mononucleotide (FMNH2) under the consumption of oxygen, thereby emitting light as a byproduct (Ulitzur und Hastings 1979). Generally, the reaction of light emission is well studied but the biological function is still mostly unknown, although it can consume up to 10% of the energy from the metabolism and count up to 20% of the total oxygen consumption (Nealson und Hastings 1979).

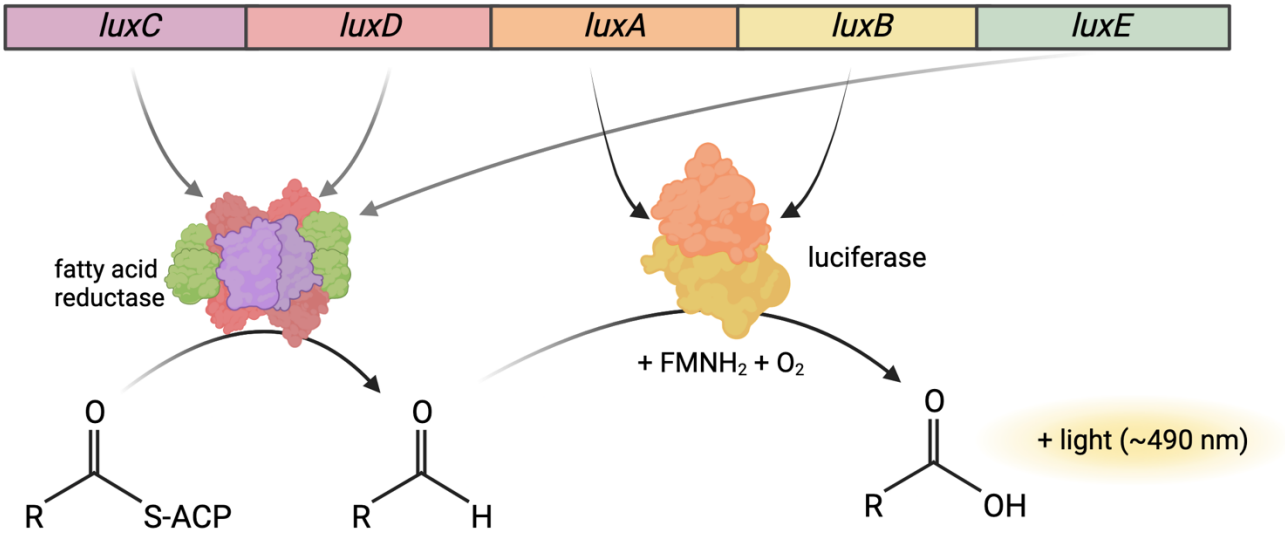

Figure 1.4 Overview of the mechanism underlying bioluminescence in bacteria. The lux operon consists of the five genes *luxCDABE*, encoding the enzymes required for the bioluminescent reaction. The fatty acid reductase consists of LuxC, LuxD and LuxE which synthesises the long chain aldehyde substrate. Luciferase consists of the subunits LuxA and LuxB which produces light through the monooxygenation of long chain aldehydes consuming $FMNH_2$ and reactive oxygen, resulting in the emission of light.

Among bioluminescent bacteria, all are Gram-negative, motile and facultative anaerobic and mainly found in marine environments, such as *Vibrio fischeri* (Dunlap 2009; Meighen 1991; Visick et al. 2000). In *V. fischeri*, the bioluminescence is important to establish a bacteria-host interaction with the squid *Eupymna scolopes* and benefits the squid with an escape mechanism against predators (Visick et al. 2000; Jones und Nishiguchi 2004). Unlikely, the exact ecological role of bioluminescence in freshwater *V. cholera* is still unclear and it is hypothesized, that bioluminescence aids in nutrient acquisition and survival in symbiosis with specific zooplankton (Zo et al. 2009). Similarly, *P. luminescens* is bioluminescent and to date the only know terrestrial bacterium, capable of light emission but a biological function could not be assigned yet (Peat et al. 2010; Daborn et al. 2001). Different hypotheses suggest a similar supporting role of bioluminescence during symbiosis with nematodes as reported for *V. fischeri* with squids or rather the acquisition of bioluminescence through an event of horizontal gene transfer (Patterson 2015; Peat et al. 2010). However, none of these hypotheses could be confirmed yet and thus, the role of bioluminescence in *P. luminescens* is still an open question.

Additionally, no luminescence-based reporter assays have been established in *P. luminescens*, but developing such a system through targeted deletion of the *lux* operon should provide a valuable tool for studying gene expression dynamics in this bacterium. This approach could not only shed light on the role of bioluminescence in *P. luminescens* but also unlock biotechnological applications, such as tracking bacterial interactions in complex environments or optimizing symbiotic relationships for agricultural benefits.

1.7 Scope of this thesis

Understanding the role of the type VI secretion system (T6SS) in *P. luminescens* is crucial not only for unravelling the bacterium's function in polymicrobial environments but also for utilising its mechanisms in biotechnological applications. The T6SS, known for its role in microbial competition and host interactions, has great potential for the development of antimicrobial agents, synthetic biology, and environmental biotechnology. Thus, this study aimed to identify and characterize T6SS gene clusters and effectors, broadening the knowledge of their genomic organization, diversity, and involvement in key stages of the *P. luminescens* life cycle, with a focus on their potential interbacterial and interkingdom interactions.

The core objective of this thesis was to investigate the T6SS in *P. luminescens* 1° and 2° cells and determine its relevance in microbial competition and adaptation. Bioinformatic analyses should reveal the T6SS core components and related genes, laying the groundwork for understanding their function. By comparing these components and effectors to those in other organisms, hypotheses can be drawn about their role in shaping microbial communities.

To directly address whether the T6SS contributes to interbacterial competition, deletion mutants of T6SS core components should be developed and analysed. Whole-cell proteome analyses of these mutants uncovered significant changes, revealing how T6SSs impact bacterial fitness by influencing not only competition but also processes like motility, secondary metabolism, and pathogenicity. These insights are particularly relevant for designing engineered microbial strains for biocontrol or industrial processes where microbial interactions are key.

Although previous research on *P. luminescens* TTO1 identified an antibacterial effector, no similar studies had been conducted in strain DJC, leaving a gap in knowledge about T6SS effectors. To address this, key effector candidates should be overexpressed and tested for their ability to inhibit or kill competitor bacteria, with accompanying immunity proteins analysed to confirm effector-immunity (E-I) pairs. These studies should provide crucial insights into the toxin-antitoxin mechanisms that govern T6SS-mediated interactions. In addition, BACTH assays should be performed to investigate the protein-protein interactions involved in effector delivery, contributing to a deeper understanding of the T6SS's machinery. This knowledge may be exploited in synthetic biology to develop bacteria capable of precise molecular delivery in various biotechnological contexts, such as targeted antimicrobial delivery systems that attack pathogenic bacteria while sparing beneficial microbiota.

Lastly, to study the regulation of T6SS genes, luminescence-based reporter assays should be established. By generating luminescence-deficient reporter strains, the environmental conditions and signals that modulate T6SS activity were explored. These assays should provide not only a tool for monitoring gene expression in real time but also insights into how T6SS activity can be controlled and harnessed for biotechnological applications, such as biosensors or microbial community management.

1.8 References of introduction

Akhurst, R. J. (1980): Morphological and Functional Dimorphism in *Xenorhabdus* spp., Bacteria Symbiotically Associated with the Insect Pathogenic Nematodes *Neoaplectana* and *Heterorhabditis*. In: *Microbiology* 121 (2), S. 303–309. DOI: 10.1099/00221287-121-2-303.

Akhurst, R. J.; Boemare, N. E. (1988): A numerical taxonomic study of the genus *Xenorhabdus* (*Enterobacteriaceae*) and proposed elevation of the subspecies of *X. nematophilus* to species. In: *Journal of general microbiology* 134 (7), S. 1835–1845. DOI: 10.1099/00221287-134-7-1835.

Allsopp, Luke P.; Bernal, Patricia (2023): Killing in the name of: T6SS structure and effector diversity. In: *Microbiology (Reading, England)* 169 (7). DOI: 10.1099/mic.0.001367.

Aschtgen, Marie-Stéphanie; Bernard, Christophe S.; Bentzmann, Sophie de; Lloubès, Roland; Cascales, Eric (2008): SciN is an outer membrane lipoprotein required for type VI secretion in enteroaggregative *Escherichia coli*. In: *Journal of bacteriology* 190 (22), S. 7523–7531. DOI: 10.1128/JB.00945-08.

Basler, M.; Mekalanos, J. J. (2012): Type 6 secretion dynamics within and between bacterial cells. In: *Science (New York, N.Y.)* 337 (6096), S. 815. DOI: 10.1126/science.1222901.

Basler, Marek; Ho, Brian T.; Mekalanos, John J. (2013): Tit-for-tat: type VI secretion system counterattack during bacterial cell-cell interactions. In: *Cell* 152 (4), S. 884–894. DOI: 10.1016/j.cell.2013.01.042.

Bedding, R. A.; Molyneux, A. S. (1982): Penetration of Insect Cuticle By Infective Juveniles of *Heterorhabditis* Spp. (*Heterorhabditidae*: Nematoda). In: *Nematol* 28 (3), S. 354–359. DOI: 10.1163/187529282X00402.

Bernal, Patricia; Furniss, R. Christopher D.; Fecht, Selina; Leung, Rhoda C. Y.; Spiga, Livia; Mavridou, Despoina A. I.; Filloux, Alain (2021): A novel stabilization mechanism for the type VI secretion system sheath. In: *Proceedings of the National Academy of Sciences of the United States of America* 118 (7). DOI: 10.1073/pnas.2008500118.

Blackburn, M.; Golubeva, E.; Bowen, D.; ffrench-Constant, R. H. (1998): A Novel Insecticidal Toxin from *Photorhabdus luminescens*, Toxin Complex a (Tca), and Its Histopathological Effects on the Midgut of *Manduca sexta*. In: *Applied and environmental microbiology* 64 (8), S. 3036–3041. DOI: 10.1128/AEM.64.8.3036-3041.1998.

Bowen, D.; Rocheleau, T. A.; Blackburn, M.; Andreev, O.; Golubeva, E.; Bhartia, R.; ffrench-Constant, R. H. (1998): Insecticidal toxins from the bacterium *Photorhabdus luminescens*. In: *Science (New York, N.Y.)* 280 (5372), S. 2129–2132. DOI: 10.1126/science.280.5372.2129.

Bowen, David J.; Rocheleau, Thomas A.; Grutzmacher, Cathy K.; Meslet, Laurence; Valens, Michelle; Marble, Daniel et al. (2003): Genetic and biochemical characterization of PrtA, an RTX-like metalloprotease from *Photorhabdus*. In: *Microbiology (Reading, England)* 149 (Pt 6), S. 1581–1591. DOI: 10.1099/mic.0.26171-0.

Brodl, Eveline; Winkler, Andreas; Macheroux, Peter (2018): Molecular Mechanisms of Bacterial Bioluminescence. In: *Computational and structural biotechnology journal* 16, S. 551–564. DOI: 10.1016/j.csbj.2018.11.003.

Brugirard-Ricaud, Karine; Duchaud, Eric; Givaudan, Alain; Girard, Pierre Alain; Kunst, Frank; Boemare, Noel et al. (2005): Site-specific antiphagocytic function of the *Photorhabdus luminescens* type III secretion system during insect colonization. In: *Cellular microbiology* 7 (3), S. 363–371. DOI: 10.1111/j.1462-5822.2004.00466.x.

Brunet, Yannick R.; Espinosa, Leon; Harchouni, Seddik; Mignot, Tâm; Cascales, Eric (2013): Imaging type VI secretion-mediated bacterial killing. In: *Cell reports* 3 (1), S. 36–41. DOI: 10.1016/j.celrep.2012.11.027.

Brunet, Yannick R.; Zoued, Abdelrahim; Boyer, Frédéric; Douzi, Badreddine; Cascales, Eric (2015): The Type VI Secretion TssEFGK-VgrG Phage-Like Baseplate Is Recruited to the TssJLM Membrane Complex via Multiple Contacts and Serves As Assembly Platform for Tail Tube/Sheath Polymerization. In: *PLoS genetics* 11 (10), e1005545. DOI: 10.1371/journal.pgen.1005545.

Burdette, Lisa Ann; Leach, Samuel Alexander; Wong, Han Teng; Tullman-Ercek, Danielle (2018): Developing Gram-negative bacteria for the secretion of heterologous proteins. In: *Microbial cell factories* 17 (1), S. 196. DOI: 10.1186/s12934-018-1041-5.

Chen, Lihua; Zou, Yaru; Kronfl, Asmaa Abbas; Wu, Yong (2020): Type VI secretion system of *Pseudomonas aeruginos*a is associated with biofilm formation but not environmental adaptation. In: *MicrobiologyOpen* 9 (3), e991. DOI: 10.1002/mbo3.991.

Cherrak, Yassine; Flaugnatti, Nicolas; Durand, Eric; Journet, Laure; Cascales, Eric (2019): Structure and Activity of the Type VI Secretion System. In: *Microbiology spectrum* 7 (4). DOI: 10.1128/microbiolspec.PSIB-0031-2019.

Cherrak, Yassine; Rapisarda, Chiara; Pellarin, Riccardo; Bouvier, Guillaume; Bardiaux, Benjamin; Allain, Fabrice et al. (2018): Biogenesis and structure of a type VI secretion baseplate. In: *Nature microbiology* 3 (12), S. 1404–1416. DOI: 10.1038/s41564-018-0260-1.

Choi, J. H.; Lee, S. Y. (2004): Secretory and extracellular production of recombinant proteins using *Escherichia coli*. In: *Applied microbiology and biotechnology* 64 (5), S. 625–635. DOI: 10.1007/s00253-004-1559-9.

Ciche, Todd A.; Ensign, Jerald C. (2003): For the insect pathogen *Photorhabdus luminescens*, which end of a nematode is out? In: *Applied and environmental microbiology* 69 (4), S. 1890–1897. DOI: 10.1128/AEM.69.4.1890-1897.2003.

Clarke, David J. (2008): *Photorhabdus*: a model for the analysis of pathogenicity and mutualism. In: *Cellular microbiology* 10 (11), S. 2159–2167. DOI: 10.1111/j.1462-5822.2008.01209.x.

Clemens, Daniel L.; Ge, Peng; Lee, Bai-Yu; Horwitz, Marcus A.; Zhou, Z. Hong (2015): Atomic structure of T6SS reveals interlaced array essential to function. In: *Cell* 160 (5), S. 940–951. DOI: 10.1016/j.cell.2015.02.005.

Costa, Tiago R. D.; Felisberto-Rodrigues, Catarina; Meir, Amit; Prevost, Marie S.; Redzej, Adam; Trokter, Martina; Waksman, Gabriel (2015): Secretion systems in Gram-negative bacteria: structural and mechanistic insights. In: *Nature reviews. Microbiology* 13 (6), S. 343–359. DOI: 10.1038/nrmicro3456.

Crawford, Jason M.; Portmann, Cyril; Zhang, Xu; Roeffaers, Maarten B. J.; Clardy, Jon (2012): Small molecule perimeter defense in entomopathogenic bacteria. In: *Proceedings of the National Academy of Sciences of the United States of America* 109 (27), S. 10821–10826. DOI: 10.1073/pnas.1201160109.

Daborn, P. J.; Waterfield, N.; Blight, M. A.; ffrench-Constant, R. H. (2001): Measuring virulence factor expression by the pathogenic bacterium *Photorhabdus luminescens* in culture and during insect infection. In: *Journal of bacteriology* 183 (20), S. 5834–5839. DOI: 10.1128/JB.183.20.5834-5839.2001.

Daborn, P. J.; Waterfield, N.; Silva, C. P.; Au, C. P. Y.; Sharma, S.; ffrench-Constant, R. H. (2002): A single *Photorhabdus* gene, makes caterpillars floppy (*mcf*), allows *Escherichia coli* to persist within and kill insects. In: *Proceedings of the National Academy of Sciences of the United States of America* 99 (16), S. 10742–10747. DOI: 10.1073/pnas.102068099.

Dix, Samuel R.; Owen, Hayley J.; Sun, Ruyue; Ahmad, Asma; Shastri, Sravanthi; Spiewak, Helena L. et al. (2018): Structural insights into the function of type VI secretion system TssA subunits. In: *Nature communications* 9 (1), S. 4765. DOI: 10.1038/s41467-018-07247-1.

Dominelli, Nazzareno; Jäger, Heidi Yoko; Langer, Angela; Brachmann, Andreas; Heermann, Ralf (2022a): High-throughput sequencing analysis reveals genomic similarity in phenotypic heterogeneous *Photorhabdus luminescens* cell populations. In: *Ann Microbiol* 72 (1). DOI: 10.1186/s13213-022-01677-5.

Dominelli, Nazzareno; Platz, Fabio; Heermann, Ralf (2022b): The Insect Pathogen *Photorhabdus luminescens* Protects Plants from Phytopathogenic *Fusarium graminearum* via Chitin Degradation. In: *Applied and environmental microbiology* 88 (11), e0064522. DOI: 10.1128/aem.00645-22.

Dowling, A. J.; Daborn, P. J.; Waterfield, N. R.; Wang, P.; Streuli, C. H.; ffrench-Constant, R. H. (2004): The insecticidal toxin Makes caterpillars floppy (Mcf) promotes apoptosis in mammalian cells. In: *Cellular microbiology* 6 (4), S. 345–353. DOI: 10.1046/j.1462-5822.2003.00357.x.

Dunlap, P. V. (2009): Bioluminescence, microbial. In: Encyclopedia of Microbiology: Elsevier, S. 45–61.DOI: 10.1016/B978-012373944-5.00066-3

Dunlap, Paul (2014): Biochemistry and genetics of bacterial bioluminescence. In: *Advances in biochemical engineering/biotechnology* 144, S. 37–64. DOI: 10.1007/978-3-662-43385-0_2.

Durand, Eric; Cambillau, Christian; Cascales, Eric; Journet, Laure (2014): VgrG, Tae, Tle, and beyond: the versatile arsenal of Type VI secretion effectors. In: *Trends in microbiology* 22 (9), S. 498–507. DOI: 10.1016/j.tim.2014.06.004.

Durand, Eric; van Nguyen, Son; Zoued, Abdelrahim; Logger, Laureen; Péhau-Arnaudet, Gérard; Aschtgen, Marie-Stéphanie et al. (2015): Biogenesis and structure of a type VI secretion membrane core complex. In: *Nature* 523 (7562), S. 555–560. DOI: 10.1038/nature14667.

Durand, Eric; Zoued, Abdelrahim; Spinelli, Silvia; Watson, Paul J. H.; Aschtgen, Marie-Stéphanie; Journet, Laure et al. (2012): Structural characterization and oligomerization of the TssL protein, a component shared by bacterial type VI and type IVb secretion systems. In: *The Journal of biological chemistry* 287 (17), S. 14157–14168. DOI: 10.1074/jbc.M111.338731.

Eckstein, Simone; Dominelli, Nazzareno; Brachmann, Andreas; Heermann, Ralf (2019): Phenotypic Heterogeneity of the Insect Pathogen *Photorhabdus luminescens*: Insights into the Fate of Secondary Cells. In: *Applied and environmental microbiology* 85 (22). DOI: 10.1128/AEM.01910-19.

Eleftherianos, Ioannis; Boundy, Sam; Joyce, Susan A.; Aslam, Shazia; Marshall, James W.; Cox, Russell J. et al. (2007): An antibiotic produced by an insect-pathogenic bacterium suppresses host defenses through phenoloxidase inhibition. In: *Proceedings of the National Academy of Sciences of the United States of America* 104 (7), S. 2419–2424. DOI: 10.1073/pnas.0610525104.

Elowitz, Michael B.; Levine, Arnold J.; Siggia, Eric D.; Swain, Peter S. (2002): Stochastic gene expression in a single cell. In: *Science (New York, N.Y.)* 297 (5584), S. 1183–1186. DOI: 10.1126/science.1070919.

El-Sharoud, Walid (2008): Bacterial Physiology. Berlin, Heidelberg: Springer Berlin Heidelberg. doi.org/10.1007/978-3-540-74921-9

ffrench-Constant, Richard; Waterfield, Nicholas; Daborn, Phillip; Joyce, Susan; Bennett, Helen; Au, Candy et al. (2003): *Photorhabdus*: towards a functional genomic analysis of a symbiont and pathogen. In: *FEMS microbiology reviews* 26 (5), S. 433–456. DOI: 10.1111/j.1574-6976.2003.tb00625.x.

Ffrench-Constant, Richard H.; Dowling, Andrea; Waterfield, Nicholas R. (2007): Insecticidal toxins from *Photorhabdus* bacteria and their potential use in agriculture. In: *Toxicon* 49 (4), S. 436–451. DOI: 10.1016/j.toxicon.2006.11.019.

Filloux, Alain (2011): Protein Secretion Systems in *Pseudomonas aeruginosa*: An Essay on Diversity, Evolution, and Function. In: *Frontiers in microbiology* 2, S. 155. DOI: 10.3389/fmicb.2011.00155.

Forst, S.; Dowds, B.; Boemare, N.; Stackebrandt, E. (1997): *Xenorhabdus* and *Photorhabdus* spp.: bugs that kill bugs. In: *Annual review of microbiology* 51 (Volume 51, 1997), S. 47–72. DOI: 10.1146/annurev.micro.51.1.47.

Fridman, Chaya M.; Keppel, Kinga; Gerlic, Motti; Bosis, Eran; Salomon, Dor (2020): A comparative genomics methodology reveals a widespread family of membrane-disrupting T6SS effectors. In: *Nature communications* 11 (1), S. 1085. DOI: 10.1038/s41467-020-14951-4.

Gerrard, John G.; McNevin, Samantha; Alfredson, David; Forgan-Smith, Ross; Fraser, Neil (2003): *Photorhabdus* species: bioluminescent bacteria as emerging human pathogens? In: *Emerging Infectious Diseases* 9 (2), S. 251–254. DOI: 10.3201/eid0902.020222.

Ghosh, Chandradhish; Sarkar, Paramita; Issa, Rahaf; Haldar, Jayanta (2019): Alternatives to Conventional Antibiotics in the Era of Antimicrobial Resistance. In: *Trends in microbiology* 27 (4), S. 323–338. DOI: 10.1016/j.tim.2018.12.010.

Girotti, Stefano; Ferri, Elida Nora; Fumo, Maria Grazia; Maiolini, Elisabetta (2008): Monitoring of environmental pollutants by bioluminescent bacteria. In: *Analytica chimica acta* 608 (1), S. 2–29. DOI: 10.1016/j.aca.2007.12.008.

Guckes, Kirsten R.; Cecere, Andrew G.; Williams, Amanda L.; McNeil, Anjali E.; Miyashiro, Tim (2020): The Bacterial Enhancer Binding Protein VasH Promotes Expression of a Type VI Secretion System in *Vibrio fischeri* during Symbiosis. In: *Journal of bacteriology* 202 (7). DOI: 10.1128/JB.00777-19.

Hachani, Abderrahman; Wood, Thomas E.; Filloux, Alain (2016): Type VI secretion and anti-host effectors. In: *Current opinion in microbiology* 29, S. 81–93. DOI: 10.1016/j.mib.2015.11.006.

Haddock, Steven H. D.; Moline, Mark A.; Case, James F. (2010): Bioluminescence in the sea. In: *Annual review of marine science* 2, S. 443–493. DOI: 10.1146/annurev-marine-120308-081028.

Han, R.; Ehlers, R-U. (2001): Effect of *Photorhabdus luminescens* phase variants on the in vivo and in vitro development and reproduction of the entomopathogenic nematodes *Heterorhabditis bacteriophora* and *Steinernema carpocapsae*. In: *FEMS microbiology ecology* 35 (3), S. 239–247. DOI: 10.1111/j.1574-6941.2001.tb00809.x.

Hays, Stephanie G.; Patrick, William G.; Ziesack, Marika; Oxman, Neri; Silver, Pamela A. (2015): Better together: engineering and application of microbial symbioses. In: *Current opinion in biotechnology* 36, S. 40–49. DOI: 10.1016/j.copbio.2015.08.008.

Hernandez, Ruth E.; Gallegos-Monterrosa, Ramses; Coulthurst, Sarah J. (2020): Type VI secretion system effector proteins: Effective weapons for bacterial competitiveness. In: *Cellular microbiology* 22 (9), e13241. DOI: 10.1111/cmi.13241.

Jana, Biswanath; Fridman, Chaya M.; Bosis, Eran; Salomon, Dor (2019): A modular effector with a DNase domain and a marker for T6SS substrates. In: *Nature communications* 10 (1), S. 3595. DOI: 10.1038/s41467-019-11546-6.

Jiang, Feng; Wang, Xia; Wang, Bei; Chen, Lihong; Zhao, Zhendong; Waterfield, Nicholas R. et al. (2016): The *Pseudomonas aeruginosa* Type VI Secretion PGAP1-like Effector Induces Host Autophagy by Activating Endoplasmic Reticulum Stress. In: *Cell reports* 16 (6), S. 1502–1509. DOI: 10.1016/j.celrep.2016.07.012.

Jiang, Feng; Waterfield, Nicholas R.; Yang, Jian; Yang, Guowei; Jin, Qi (2014): A *Pseudomonas aeruginosa* type VI secretion phospholipase D effector targets both prokaryotic and eukaryotic cells. In: *Cell host & microbe* 15 (5), S. 600–610. DOI: 10.1016/j.chom.2014.04.010.

Jiang, Tianyu; Bai, Xiaoyu; Li, Minyong (2024): Advances in the Development of Bacterial Bioluminescence Imaging. In: *Annual review of analytical chemistry (Palo Alto, Calif.)* 17 (1), S. 265–288. DOI: 10.1146/annurev-anchem-061622-034229.

Jones, B. W.; Nishiguchi, M. K. (2004): Counterillumination in the Hawaiian bobtail squid, *Euprymna scolopes* Berry (Mollusca: Cephalopoda). In: *Marine Biology* 144 (6), S. 1151–1155. DOI: 10.1007/s00227-003-1285-3.

Jurėnas, Dukas; Payelleville, Amaury; Roghanian, Mohammad; Turnbull, Kathryn J.; Givaudan, Alain; Brillard, Julien et al. (2021a): *Photorhabdus* antibacterial Rhs polymorphic toxin inhibits translation through ADP-ribosylation of 23S ribosomal RNA. In: *Nucleic acids research* 49 (14), S. 8384–8395. DOI: 10.1093/nar/gkab608.

Jurėnas, Dukas; Rosa, Leonardo Talachia; Rey, Martial; Chamot-Rooke, Julia; Fronzes, Rémi; Cascales, Eric (2021b): Mounting, structure and autocleavage of a type VI secretion-associated Rhs polymorphic toxin. In: *Nature communications* 12 (1), S. 6998. DOI: 10.1038/s41467-021-27388-0.

Jurick II., Wayne M. (2022): Biotechnology approaches to reduce antimicrobial resistant postharvest pathogens, mycotoxin contamination, and resulting product losses. In: *Current opinion in biotechnology* 78, S. 102791. DOI: 10.1016/j.copbio.2022.102791.

Kanonenberg, Kerstin; Spitz, Olivia; Erenburg, Isabelle N.; Beer, Tobias; Schmitt, Lutz (2018): Type I secretion system-it takes three and a substrate. In: *FEMS microbiology letters* 365 (11). DOI: 10.1093/femsle/fny094.

Kapitein, Nicole; Bönemann, Gabriele; Pietrosiuk, Aleksandra; Seyffer, Fabian; Hausser, Ingrid; Locker, Jacomine Krijnse; Mogk, Axel (2013): ClpV recycles VipA/VipB tubules and prevents non-productive tubule formation to ensure efficient type VI protein secretion. In: *Molecular microbiology* 87 (5), S. 1013–1028. DOI: 10.1111/mmi.12147.

Kaya, H. K.; Gaugler, R. (1993): Entomopathogenic Nematodes. In: *Annu. Rev. Entomol.* 38 (1), S. 181–206. DOI: 10.1146/annurev.en.38.010193.001145.

Khan, A.; Brooks, W. M. (1977): A Chromogenic Bioluminescent Bacterium Associated with the Entomophilic Nematode *Chromonema heliothidis*[1]. In: *Journal of invertebrate pathology* 29 (3), S. 253–261. DOI: 10.1016/S0022-2011(77)80030-X.

Kostakioti, Maria; Newman, Cheryl L.; Thanassi, David G.; Stathopoulos, Christos (2005): Mechanisms of protein export across the bacterial outer membrane. In: *Journal of bacteriology* 187 (13), S. 4306–4314. DOI: 10.1128/JB.187.13.4306-4314.2005.

Kudryashev, Mikhail; Wang, Ray Yu-Ruei; Brackmann, Maximilian; Scherer, Sebastian; Maier, Timm; Baker, David et al. (2015): Structure of the type VI secretion system contractile sheath. In: *Cell* 160 (5), S. 952–962. DOI: 10.1016/j.cell.2015.01.037.

Langer, Angela; Moldovan, Adriana; Harmath, Christian; Joyce, Susan A.; Clarke, David J.; Heermann, Ralf (2017): HexA is a versatile regulator involved in the control of phenotypic heterogeneity of *Photorhabdus luminescens*. In: *PLOS ONE* 12 (4), e0176535. DOI: 10.1371/journal.pone.0176535.

Li, Yusheng; Hu, Xiaofeng; Zhang, Xu; Liu, Zhengqiang; Ding, Xuezhi; Xia, Liqiu; Hu, Shengbiao (2014): *Photorhabdus luminescens* PirAB-fusion protein exhibits both cytotoxicity and insecticidal activity. In: *FEMS microbiology letters* 356 (1), S. 23–31. DOI: 10.1111/1574-6968.12474.

Machado, Ricardo A. R.; Wüthrich, Daniel; Kuhnert, Peter; Arce, Carla C. M.; Thönen, Lisa; Ruiz, Celia et al. (2018): Whole-genome-based revisit of *Photorhabdus* phylogeny: proposal for the elevation of most *Photorhabdus* subspecies to the species level and description of one novel species *Photorhabdus bodei* sp. nov., and one novel subspecies *Photorhabdus laumondii* subsp. *clarkei* subsp. nov. In: *International journal of systematic and evolutionary microbiology* 68 (8), S. 2664–2681. DOI: 10.1099/ijsem.0.002820.

MacIntyre, Dana L.; Miyata, Sarah T.; Kitaoka, Maya; Pukatzki, Stefan (2010): The *Vibrio cholerae* type VI secretion system displays antimicrobial properties. In: *Proceedings of the National Academy of Sciences of the United States of America* 107 (45), S. 19520–19524. DOI: 10.1073/pnas.1012931107.

Manera, Kevin; Caro, Florence; Li, Hao; Pei, Tong-Tong; Hersch, Steven J.; Mekalanos, John J.; Dong, Tao G. (2021): Sensing of intracellular Hcp levels controls T6SS expression in *Vibrio cholerae*. In: *Proceedings of the National Academy of Sciences of the United States of America* 118 (25). DOI: 10.1073/pnas.2104813118.

Meighen, E. A. (1991): Molecular biology of bacterial bioluminescence. In: *Microbiological reviews* 55 (1), S. 123–142. DOI: 10.1128/mr.55.1.123-142.1991.

Meighen, E. A.; Dunlap, P. V. (1993): Physiological, biochemical and genetic control of bacterial bioluminescence. In: *Advances in microbial physiology* 34, S. 1–67. DOI: 10.1016/S0065-2911(08)60027-2.

Mougous, Joseph D.; Cuff, Marianne E.; Raunser, Stefan; Shen, Aimee; Zhou, Min; Gifford, Casey A. et al. (2006): A virulence locus of *Pseudomonas aeruginosa* encodes a protein secretion apparatus. In: *Science (New York, N.Y.)* 312 (5779), S. 1526–1530. DOI: 10.1126/science.1128393.

Nazarov, Sergey; Schneider, Johannes P.; Brackmann, Maximilian; Goldie, Kenneth N.; Stahlberg, Henning; Basler, Marek (2018): Cryo-EM reconstruction of Type VI secretion system baseplate and sheath distal end. In: *The EMBO journal* 37 (4). DOI: 10.15252/embj.201797103.

Nealson, K. H.; Hastings, J. W. (1979): Bacterial bioluminescence: its control and ecological significance. In: *Microbiological reviews* 43 (4), S. 496–518. DOI: 10.1128/mr.43.4.496-518.1979.

Park, Young-Jun; Lacourse, Kaitlyn D.; Cambillau, Christian; DiMaio, Frank; Mougous, Joseph D.; Veesler, David (2018): Structure of the type VI secretion system TssK-TssF-TssG baseplate subcomplex revealed by cryo-electron microscopy. In: *Nature communications* 9 (1), S. 5385. DOI: 10.1038/s41467-018-07796-5.

Patterson, Walter (2015): Attractant Role of Bacterial Bioluminescence of *Photorhabdus luminescens* on a *Galleria mellonella* Model. In: *AJLS* 3 (4), S. 290. DOI: 10.11648/j.ajls.20150304.16.

Peat, Scott M.; Ffrench-Constant, Richard H.; Waterfield, Nick R.; Marokházi, Judit; Fodor, Andras; Adams, Byron J. (2010): A robust phylogenetic framework for the bacterial genus *Photorhabdus* and its use in studying the evolution and maintenance of bioluminescence: a case for 16S, *gyrB*, and *glnA*. In: *Molecular phylogenetics and evolution* 57 (2), S. 728–740. DOI: 10.1016/j.ympev.2010.08.012.

Pissaridou, Panayiota; Allsopp, Luke P.; Wettstadt, Sarah; Howard, Sophie A.; Mavridou, Despoina A. I.; Filloux, Alain (2018): The *Pseudomonas aeruginosa* T6SS-VgrG1b spike is topped by a PAAR protein eliciting DNA damage to bacterial competitors. In: *Proceedings of the National Academy of Sciences of the United States of America* 115 (49), S. 12519–12524. DOI: 10.1073/pnas.1814181115.

Pourhassan, Zohreh N.; Smits, Sander H. J.; Ahn, Jung Hoon; Schmitt, Lutz (2021): Biotechnological applications of type 1 secretion systems. In: *Biotechnology advances* 53, S. 107864. DOI: 10.1016/j.biotechadv.2021.107864.

Pukatzki, Stefan; Ma, Amy T.; Sturtevant, Derek; Krastins, Bryan; Sarracino, David; Nelson, William C. et al. (2006): Identification of a conserved bacterial protein secretion system in *Vibrio cholerae* using the *Dictyostelium* host model system. In: *Proceedings of the National Academy of Sciences of the United States of America* 103 (5), S. 1528–1533. DOI: 10.1073/pnas.0510322103.

Rajagopal, RAMAN; Bhatnagar, R. K.A.J. (2002): Insecticidal Toxic Proteins Produced by *Photorhabdus akhurstii*, a Symbiont of *Heterorhabditis indica*. In: *Journal of Nematology* 34 (1), S. 23–27. PMID: 19265903

Rathore, Anurag S.; Singh, Anurag (2022): Biomass to fuels and chemicals: A review of enabling processes and technologies. In: *J of Chemical Tech & Biotech* 97 (3), S. 597–607. DOI: 10.1002/jctb.6960.

Regaiolo, Alice; Dominelli, Nazzareno; Andresen, Karsten; Heermann, Ralf (2020): The Biocontrol Agent and Insect Pathogen *Photorhabdus luminescens* Interacts with Plant Roots. In: *Applied and environmental microbiology* 86 (17). DOI: 10.1128/AEM.00891-20.

Richardson, W. H.; Schmidt, T. M.; Nealson, K. H. (1988): Identification of an anthraquinone pigment and a hydroxystilbene antibiotic from *Xenorhabdus luminescens*. In: *Applied and environmental microbiology* 54 (6), S. 1602–1605. DOI: 10.1128/aem.54.6.1602-1605.1988.

Rodou, Athina; Ankrah, Dennis O.; Stathopoulos, Christos (2010): Toxins and secretion systems of *Photorhabdus luminescens*. In: *Toxins* 2 (6), S. 1250–1264. DOI: 10.3390/toxins2061250.

Russell, Alistair B.; Peterson, S. Brook; Mougous, Joseph D. (2014): Type VI secretion system effectors: poisons with a purpose. In: *Nature reviews. Microbiology* 12 (2), S. 137–148. DOI: 10.1038/nrmicro3185.

Salomon, Dor; Gonzalez, Herman; Updegraff, Barrett L.; Orth, Kim (2013): *Vibrio parahaemolyticus* type VI secretion system 1 is activated in marine conditions to target bacteria, and is differentially regulated from system 2. In: *PloS one* 8 (4), e61086. DOI: 10.1371/journal.pone.0061086.

Schneider, Johannes Paul; Nazarov, Sergey; Adaixo, Ricardo; Liuzzo, Martina; Ringel, Peter David; Stahlberg, Henning; Basler, Marek (2019): Diverse roles of TssA-like proteins in the assembly of bacterial type VI secretion systems. In: *The EMBO journal* 38 (18), e100825. DOI: 10.15252/embj.2018100825.

Schwarz S, West TE, Boyer F, Chiang WC, Carl MA, Hood RD, Rohmer L, Tolker-Nielsen T, Skerrett SJ, Mougous JD. (2010): *Burkholderia* type VI secretion systems have distinct roles in eukaryotic and bacterial cell interactions. *PLoS Pathog*. DOI: 10.1371/journal.ppat.1001068.

Shneider, Mikhail M.; Buth, Sergey A.; Ho, Brian T.; Basler, Marek; Mekalanos, John J.; Leiman, Petr G. (2013): PAAR-repeat proteins sharpen and diversify the type VI secretion system spike. In: *Nature* 500 (7462), S. 350–353. DOI: 10.1038/nature12453.

Si, Meiru; Zhao, Chao; Burkinshaw, Brianne; Zhang, Bing; Wei, Dawei; Wang, Yao et al. (2017): Manganese scavenging and oxidative stress response mediated by type VI secretion system in *Burkholderia thailandensis*. In: *Proceedings of the National Academy of Sciences of the United States of America* 114 (11), E2233-E2242. DOI: 10.1073/pnas.1614902114.

Smits, Wiep Klaas; Kuipers, Oscar P.; Veening, Jan-Willem (2006): Phenotypic variation in bacteria: the role of feedback regulation. In: *Nature reviews. Microbiology* 4 (4), S. 259–271. DOI: 10.1038/nrmicro1381.

Stock, S. P.; Kaya, H. K. (1996): A multivariate analysis of morphometric characters of *Heterorhabditis* species (Nemata: *Heterorhabditidae*) and the role of morphometrics in the taxonomy of species of the genus. In: *The Journal of parasitology* 82 (5), S. 806–813. DOI: 10.2307/3283895

Thomas, Jacob; Watve, Samit S.; Ratcliff, William C.; Hammer, Brian K. (2017): Horizontal Gene Transfer of Functional Type VI Killing Genes by Natural Transformation. In: *mBio* 8 (4). DOI: 10.1128/mbio.00654-17.

Tripathi, Vishal; Edrisi, Sheikh Adil; Chen, Bin; Gupta, Vijai K.; Vilu, Raivo; Gathergood, Nicholas; Abhilash, P. C. (2017): Biotechnological Advances for Restoring Degraded Land for Sustainable Development. In: *Trends in biotechnology* 35 (9), S. 847–859. DOI: 10.1016/j.tibtech.2017.05.001.

Tripathi, Vishal; Fraceto, Leonardo F.; Abhilash, P. C. (2015): Sustainable clean-up technologies for soils contaminated with multiple pollutants: Plant-microbe-pollutant and climate nexus. In: *Ecological Engineering* 82, S. 330–335. DOI: 10.1016/j.ecoleng.2015.05.027.

Trunk, Katharina; Peltier, Julien; Liu, Yi-Chia; Dill, Brian D.; Walker, Louise; Gow, Neil A. R. et al. (2018): The type VI secretion system deploys antifungal effectors against microbial competitors. In: *Nature microbiology* 3 (8), S. 920–931. DOI: 10.1038/s41564-018-0191-x.

Tseng, Tsai-Tien; Tyler, Brett M.; Setubal, João C. (2009): Protein secretion systems in bacterial-host associations, and their description in the Gene Ontology. In: *BMC microbiology* 9 Suppl 1 (Suppl 1), S2. DOI: 10.1186/1471-2180-9-S1-S2.

Tyczewska, Agata; Twardowski, Tomasz; Woźniak-Gientka, Ewa (2023): Agricultural biotechnology for sustainable food security. In: *Trends in biotechnology* 41 (3), S. 331–341. DOI: 10.1016/j.tibtech.2022.12.013.

Ulitzur, S.; Hastings, J. W. (1979): Evidence for tetradecanal as the natural aldehyde in bacterial bioluminescence. In: *Proceedings of the National Academy of Sciences of the United States of America* 76 (1), S. 265–267. DOI: 10.1073/pnas.76.1.265.

Unterweger, Daniel; Kostiuk, Benjamin; Pukatzki, Stefan (2017): Adaptor Proteins of Type VI Secretion System Effectors. In: *Trends in microbiology* 25 (1), S. 8–10. DOI: 10.1016/j.tim.2016.10.003.

Urbanczyk, Henryk; Ast, Jennifer C.; Dunlap, Paul V. (2011): Phylogeny, genomics, and symbiosis of *Photobacterium*. In: *FEMS microbiology reviews* 35 (2), S. 324–342. DOI: 10.1111/j.1574-6976.2010.00250.x.

van Dorst, J. M.; Hince, G.; Snape, I.; Ferrari, B. C. (2016): Novel Culturing Techniques Select for Heterotrophs and Hydrocarbon Degraders in a Subantarctic Soil. In: *Scientific reports* 6, S. 36724. DOI: 10.1038/srep36724.

Vettiger, Andrea; Winter, Julius; Lin, Lin; Basler, Marek (2017): The type VI secretion system sheath assembles at the end distal from the membrane anchor. In: *Nature communications* 8, S. 16088. DOI: 10.1038/ncomms16088.

Villadsen, John (2007): Innovative technology to meet the demands of the white biotechnology revolution of chemical production. In: *Chemical Engineering Science* 62 (24), S. 6957–6968. DOI: 10.1016/j.ces.2007.08.017.

Visick, K. L.; Foster, J.; Doino, J.; McFall-Ngai, M.; Ruby, E. G. (2000): *Vibrio fischeri* lux genes play an important role in colonization and development of the host light organ. In: *Journal of bacteriology* 182 (16), S. 4578–4586. DOI: 10.1128/JB.182.16.4578-4586.2000.

Vlisidou, Isabella; Hapeshi, Alexia; Healey, Joseph Rj; Smart, Katie; Yang, Guowei; Waterfield, Nicholas R. (2019): The *Photorhabdus asymbiotica* virulence cassettes deliver protein effectors directly into target eukaryotic cells. In: *eLife* 8. DOI: 10.7554/eLife.46259.

Wang, Jing; Brackmann, Maximilian; Castaño-Díez, Daniel; Kudryashev, Mikhail; Goldie, Kenneth N.; Maier, Timm et al. (2017): Cryo-EM structure of the extended type VI secretion system sheath-tube complex. In: *Nature microbiology* 2 (11), S. 1507–1512. DOI: 10.1038/s41564-017-0020-7.

Waterfield, Nicholas R.; Bowen, David J.; Fetherston, Jacqueline D.; Perry, Robert D.; Ffrench-Constant, Richard H. (2001): The tc genes of *Photorhabdus*: a growing family. In: *Trends in Microbiology* 9 (4), S. 185–191. DOI: 10.1016/s0966-842x(01)01978-3.

Waterfield, Nick R.; Ciche, Todd; Clarke, David (2009): *Photorhabdus* and a host of hosts. In: *Annual review of microbiology* 63, S. 557–574. DOI: 10.1146/annurev.micro.091208.073507.

Widder, E. A. (2010): Bioluminescence in the ocean: origins of biological, chemical, and ecological diversity. In: *Science (New York, N.Y.)* 328 (5979), S. 704–708. DOI: 10.1126/science.1174269.

Wood, Thomas E.; Howard, Sophie A.; Förster, Andreas; Nolan, Laura M.; Manoli, Eleni; Bullen, Nathan P. et al. (2019): The *Pseudomonas aeruginosa* T6SS Delivers a Periplasmic Toxin that Disrupts Bacterial Cell Morphology. In: *Cell reports* 29 (1), 187-201.e7. DOI: 10.1016/j.celrep.2019.08.094.

Yang, G.; Dowling, A. J.; Gerike, U.; ffrench-Constant, R. H.; Waterfield, N. R. (2006): *Photorhabdus* virulence cassettes confer injectable insecticidal activity against the wax moth. In: *Journal of bacteriology* 188 (6), S. 2254–2261. DOI: 10.1128/JB.188.6.2254–2261.2006.

Yang, Guowei; Hernández-Rodríguez, Carmen Sara; Beeton, Michael L.; Wilkinson, Paul; Ffrench-Constant, Richard H.; Waterfield, Nicholas R. (2012): PdI1 is a putative lipase that enhances *Photorhabdus* toxin complex secretion. In: *PLoS pathogens* 8 (5), e1002692. DOI: 10.1371/journal.ppat.1002692.

Yang, Xiaobing; Long, Mingxiu; Shen, Xihui (2018): Effector⁻Immunity Pairs Provide the T6SS Nanomachine its Offensive and Defensive Capabilities. In: *Molecules (Basel, Switzerland)* 23 (5). DOI: 10.3390/molecules23051009.

You, Juan; Liang, Shizhong; Cao, Li; Liu, Xiuling; Han, Richou (2006): Nutritive significance of crystalline inclusion proteins of *Photorhabdus luminescens* in *Steinernema* nematodes. In: *FEMS microbiology ecology* 55 (2), S. 178–185. DOI: 10.1111/j.1574-6941.2005.00015.x.

Zamora-Lagos, Maria-Antonia; Eckstein, Simone; Langer, Angela; Gazanis, Athanasios; Pfeiffer, Friedhelm; Habermann, Bianca; Heermann, Ralf (2018): Phenotypic and genomic comparison of *Photorhabdus luminescens* subsp. *laumondii* TT01 and a widely used rifampicin-resistant *Photorhabdus luminescens* laboratory strain. In: *BMC genomics* 19 (1), S. 854. DOI: 10.1186/s12864-018-5121-z.

Zo, Young-Gun; Chokesajjawatee, Nipa; Grim, Christopher; Arakawa, Eiji; Watanabe, Haruo; Colwell, Rita R. (2009): Diversity and seasonality of bioluminescent *Vibrio cholerae* populations in Chesapeake Bay. In: *Applied and environmental microbiology* 75 (1), S. 135–146. DOI: 10.1128/AEM.02894-07.

Zoued, Abdelrahim; Durand, Eric; Santin, Yoann G.; Journet, Laure; Roussel, Alain; Cambillau, Christian; Cascales, Eric (2017): TssA: The cap protein of the Type VI secretion system tail. In: *BioEssays : news and reviews in molecular, cellular and developmental biology* 39 (10). DOI: 10.1002/bies.201600262.

2. The Type VI secretion systems of the insect pathogen *Photorhabdus luminescens* are involved in interbacterial competition, motility and secondary metabolism

Friederike Pisarz, Timo Glatter, Dhana-Theresa M. Süss, Ralf Heermann, Alice Regaiolo (2024). The Type VI secretion systems of the insect pathogen *Photorhabdus luminescens* are involved in interbacterial competition, motility and secondary metabolism.

The Microbe 3. doi:10.1016/j.microb.2024.100067

Full-text article:

https://www.sciencedirect.com/science/article/pii/S2950194624000347?via%3Dihub

Supplementary material:

https://www.sciencedirect.com/science/article/pii/S2950194624000347?via%3Dihub#sec0160

The Microbe 3 (2024) 100067

Contents lists available at ScienceDirect

The Microbe

journal homepage: www.sciencedirect.com/journal/the-microbe

The Type VI secretion systems of the insect pathogen *Photorhabdus luminescens* are involved in interbacterial competition, motility and secondary metabolism

Friederike Pisarz [a], Timo Glatter [b], Dhana-Theresa M. Süss [a], Ralf Heermann [a], Alice Regaiolo [a,*]

[a] Johannes Gutenberg University Mainz, Institute of Molecular Physiology, Microbiology and Biotechnology, Mainz, Germany
[b] Facility for Bacterial Proteomics and Mass Spectrometry, Max-Planck Institute for Terrestrial Microbiology, Marburg, Germany

ARTICLE INFO

Keywords:
Secretion systems
Type VI secretion system
Interbacterial competition
Secondary metabolism
Insect pathogenicity
Entomopathogenic bacteria

ABSTRACT

The Type VI Secretion System (T6SS) is used as weapon by a variety of Gram-negative bacteria in polymicrobial niche competition. Its characterization and study gained more interest in recent years. The system functions as a molecular nano-weapon: it is used in inter-kingdom competition by various bacteria to deliver toxic effectors in target cells. In this context, *Photorhabdus luminescens* subsp. *luminescens* strain DJC is a microorganism able to colonize different polymicrobial environments, like nematode guts, plant roots and larvae hemolymph. However, the mechanisms used by this microorganism to compete against other bacteria in the same environment have not been clearly described yet. We hypothesis that the T6SS of *Photorhabdus luminescens* subsp. *luminescens* strain DJC can play a role in same-niche environments. In this study we focused our attention on the characterization of the T6SS clusters in *P. luminescens* and its role in this bacteria lifestyle thought bioinformatic, proteomics analyses and inter-bacterial killing assays. Using bioinformatics analysis, we identified four T6SS gene clusters (T6SS-1, T6SS-2, T6SS-3 and T6SS-4) and multiple orphan T6SS related genes in the genome of *P. luminescens*. Furthermore, we highlighted 11 T6SS effector-immunity pairs, including three undescribed membrane disrupting effectors, each with putatively different antibacterial activities. By comparing the proteomes of *P. luminescens* wild type cells and the respective isogenic T6SS-deficient strains, we could point out a putative link between T6SS and other *P. luminescens* related defense mechanisms such as PVCs, T3SS and pyocins. Furthermore, T6SS-deficiency led to a change in phenotypic traits such as motility and secondary metabolism. Our findings shed light on the T6SS of *P. luminescens* DJC, suggesting a role of the system in the complex life cycle with a putative cross-link with various defense mechanisms and secondary metabolism. This study could help to gain more knowledge on bacterial T6SSs and better understand the *P. luminescens* ability to live in polymicrobial environments.

1. Introduction

Bacterial secretion systems play an essential role in interbacterial competition and inter-kingdom pathogenicity. The assembly of the secretion systems and the nature of the secreted proteins are highly diverse among different bacteria (Green and Mecsas, 2016). Bacteria inhabit different ecological niches, living in proximity with other microorganisms, thus requiring interbacterial interactions (Russell et al., 2014). Among the systems mediating this interaction, one remarkable mechanism is the type VI secretion system (T6SS). The T6SS is a contact-dependent, nano-molecular weapon, utilised by Gram-negative bacteria to puncture bacterial and eukaryotic membranes to deliver toxins, so called effectors, into the adjacent target cells (Boyer et al., 2009; Brackmann et al., 2017; Russell et al., 2014). In general, many bacterial species such as *Vibrio cholera*, *Pseudomonas aeruginosa* or the plant pathogen *Xanthomonas campestris* are characterized by a single or multiple gene loci encoding T6SSs (Abendroth et al., 2017; Mougous et al., 2006; Pukatzki et al., 2006). The T6SSs share structural and functional similarities with the contractile tail of bacteriophages and R-type pyocins and consist of 13 core components, commonly encoded in one genomic region, which can also comprise coding regions for accessory proteins (Russell et al., 2014). The membrane complex built by TssJ, TssL and TssM assembles crossing the inner membrane and defines the position for the T6SS assembly (Durand et al., 2015). The

* Correspondence to: Johannes Gutenberg University, Institute for Molecular Physiology, Microbiology and Biotechnology, Hanns-Dieter-Hüsch-Weg 17, Bio-Zentrum II, Mainz 55128 , Germany
E-mail address: aregaiol@uni-mainz.de (A. Regaiolo).

https://doi.org/10.1016/j.microb.2024.100067
Received 7 November 2023; Received in revised form 5 April 2024; Accepted 5 April 2024
Available online 7 April 2024

baseplate, formed by the multi-protein complex composed of TssE, TssF, TssG and TssK subunits, docks on the membrane complex and promotes assembly of the sheath-tube complex (Brunet et al., 2015). The tube is assembled by HcPs, forming hexametric rings with a triplet VgrG spike, sharpened by a PAAR protein and enveloped by the sheath complex TssB, TssC (Shneider et al., 2013; Wang et al., 2017). TssA, an essential core component for the sheath polymerisation, is located at the distal end of the T6SS. After full assembly of the T6SS, TssA locks the sheath-tube complex in an extended, high-energy state, ready to fire (Bernal et al., 2021; Dix et al., 2018; Schneider et al., 2019; Zoued et al., 2016). The T6SS effectors are located at the tip of the T6SS and can bind directly, or with the support of adaptor proteins, to the tail components (Bernal et al., 2017). Furthermore, some VgrG proteins exist as so-called 'evolved VgrGs', harbouring an additional C-terminal toxic domain and therefore have dual functions as core components as well as effectors (Blondel et al., 2009). Upon T6SS activity, the sheath contracts and the tube-spike complex translocates into the target cell, delivering the toxic effectors (Brunet et al., 2013). After contraction, the sheath is disassembled by the AAA+ ClpV ATPase TssH, allowing the assembly of a new extended sheath to increase the delivery of toxic effectors into target cells by repeated T6SS firing events (Durand et al., 2015; Kapitein et al., 2013).

Over the years, different experimental approaches, such as comparative proteomics, helped to identify the diversity of bacterial T6SSs and further, to identify a broad spectrum of antibacterial and anti-eukaryotic effectors (Jurėnas and Journet, 2021; Ray et al., 2017; Salomon et al., 2014).

A transcriptional analysis of the soil-living bacterium *Photorhabdus luminescens* subsp. *luminescens* strain DJC (Zamora-Lagos et al., 2018), also designated as *Photorhabdus laumondii* subsp. *laumondii* (Machado et al., 2018) - a Gram-negative, rifampicin-resistant entomopathogenic bacterium belonging to the family of *Enterobacteriaceae* - revealed the regulation of T6SS related genes upon cultivation with the addition of plant root exudates (Regaiolo et al., 2020). *P. luminescens* is highly pathogenic towards insect larvae, lives in symbiosis with entomopathogenic nematodes (EPNs) and can colonise plant roots (Joyce et al., 2006; Regaiolo et al., 2020). Throughout its complex life cycle, *P. luminescens* is likely to interact with other microbes and therefore needs a variety of ways to compete. To date, its best known and characterized virulence factors include: i) toxin complexes (Tcs), ii) *Photorhabdus* insect related proteins (Pir) and iii) *Photorhabdus* virulence cassettes (PVCs) (Brillard et al., 2002; Rodou et al., 2010). However, little is known about the T6SSs in *P. luminescens* and main studies were focused on the effector proteins Tre23 and its interaction with Rhs1 (Jurėnas et al., 2021b, 2021a). Here we report a phenotypic characterization, e.g., interbacterial killing assays, motility assays and pathogenicity assays, of the T6SSs in *Photorhabdus luminescens* subsp. *luminescens* strain DJC. In more detail, we classified the *P. luminescens* T6SSs and generated T6SS-deficient strains of the two main T6SS clusters and further analysed their role in interbacterial competition. To determine the role of a putative new T6SS effector protein, we performed *in silico* and *in vivo* assays. Finally, we performed a proteomic analysis to characterize the role of the two main T6SSs and their impact on the *Photorhabdus* fitness and lifestyle on proteome level.

2. Material and Methods

2.1. Bacterial strains

Photorhabdus luminescens subsp. *luminescens* strain DJC (primary cells) were used (Zamora-Lagos et al., 2018). In-frame deletion mutants Δ*tssA*1b (*PluDJC_01760*) and Δ*tssA*2 (*PluDJC_12150*) were obtained through conjugation and double homologous recombination as previously described (Lassak et al., 2010). Briefly, 300 bp upstream and downstream of the gene to be deleted were amplified from the *P. luminescens* DJC genome (ref. NZ_CP024900.1) and inserted into the pNTPS138-R6KT suicide vector (respective primers listed in Supplementary Material S1). To ensure a clean deletion of the *tssA*1b and *tssA*2 locus, the respective genomic regions were amplified by PCR and checked by sequencing. Given that, the genes of *tssA*1a (*PluDJC_01750*) and *tssA*4 (*PluDJC_20770*) are homologous to *tssA*1b and *tssA*2, these sequences were also checked to rule out aberrant mutations.

The bacteria were cultivated aerobically in CASO medium (1.5% [w/v] peptone, 0.5% [w/v] peptone from soy, 0.5% [w/v] NaCl). *P. luminescens* DJC was aerobically incubated at 30°C. For interbacterial competition assays, *Escherichia coli* Top10 tnGFP were aerobically cultivated at 37°C supplemented with respective antibiotics.

2.2. Bioinformatics analysis

P. luminescens subsp. *luminescens* strain DJC gene and protein sequences were obtained from the public sequence database National Center for Biotechnology Information NCBI (https://www.ncbi.nlm.nih.gov/genome/, ref. NZ_CP024900.1). *P. luminescens* DJC T6SS-gene clusters were identified by comparison with the T6SS clusters in *P. luminescens* strain TT01 and by using the SecReT6 database (Zhang et al., 2023). Through BLASTP analysis using *P. aeruginosa* PAO1 (ref. NC_002516.2) T6SS proteins as query, additional previous undescribed T6SS proteins were identified (Boratyn, 2013). Protein functional motif analysis using Hidden Markov models (HMM) were retrieved from the HMMER website (https://www.ebi.ac.uk/Tools/hmmer/) (Potter et al., 2018) and the NCBI conserved domain database (https://www.ncbi.nlm.nih.gov/cdd); then analysed with Pfam (El-Gebali et al., 2019). Proteins with unknown function where analysed using the MPI Bioinformatics Toolkit HHpred and MUSCLE (Gabler et al., 2020; Zimmermann et al., 2018).

2.3. Bacterial cultivation

Bacterial growth was monitored to check whether T6SSs-impaired mutants had different growth rates compared to the wild type. 50 ml CASO medium were inoculated at $OD_{600} = 0.01$. Cultures were grown under aerobic conditions at 30°C for 24 h. OD_{600} was measured every hour until 6 h and after 24 h. Three biological replicates were performed.

2.4. Proteomic analysis using data independent acquisition-mass spectrometry (DIA-MS)

For comparative proteome analyses, *P. luminescens* DJC wild type and the respective T6SSs-impaired mutants Δ*tssA*1b and Δ*tssA*2 were cultivated for 5 h in 50 ml CASO medium under aerobic conditions at 30°C, starting $OD_{600} = 0.1$. Cells were centrifuged at 11'000 rpm, the cell pellets were washed twice with sterile 1x PBS-buffer (137 mM NaCl, 2.7 mM KCl, 10 mM Na_2HPO_4, 1.8 mM KH_2PO_4) and stored at −80°C until use. Cell pellets were then resuspended in buffer containing 2% sodium lauroyl sarcosinate (SLS) in 100 mM ammonium bicarbonate and heated for 15 min at 90°C. Extracted proteins were reduced by adding 5 mM Tris (2-caboxyethyl) phosphine for 15 minutes at 90°C, followed by alkylation (10 mM iodoacetamide, 30 min at 25°C). The concentration of extracted proteins was measured using BCA protein assay (Thermo Fisher Scientific). 50 µg total protein was then digested with 1 µg trypsin (Promega) overnight at 30°C in presence of 0.5% SLS. Following digestion, SLS was precipitated with trifluoroacetic acid (TFA, 1.5% final concentration) and peptides were purified using Chromabond C18 microspin columns (Macherey-Nagel). Acidified peptides were loaded on spin column that were equilibrated with 400 µl acetonitrile and then 400 µl 0.15% TFA. After peptide load, a washing step with 0.15% TFA was performed, followed by elution using 400 µl 50% acetonitrile. Eluted peptides were then dried and reconstituted in 0.15% TFA. Peptide mixtures were then analysed using liquid chromatography-mass spectrometry carried out on an Exploris 480 instrument connected

to an Ultimate 3000 RSLC nano with a Prowflow upgrade and a nanospray flex ion source (all Thermo Scientific). Peptide separation was performed on a reverse phase HPLC column (75 µm x 42 cm) packed in-house with C18 resin (2.4 µm, Dr. Maisch). The following separating gradient was used: 94% solvent A (0.15% formic acid) and 6% solvent B (99.85% acetonitrile, 0.15% formic acid) to 25% solvent B over 95 minutes and to 35% B for additional 25 minutes at a flow rate of 300 nl/min. DIA-MS acquisition method was adapted from Bekker-Jensen (Bekker-Jensen et al., 2020). In short, spray voltage was set to 2.0 kV, funnel RF level at 55, and heated capillary temperature at 275°C. For DIA experiments full MS resolutions were set to 120.000 at *m/z* 200 and full MS AGC target was 300% with an IT of 50 ms. Mass range was set to 350–1400. AGC target value for fragment spectra was set at 3000%. 45 windows of 15 Da were used with an overlap of 1 Da. Resolution was set to 15,000 and IT to 22 ms. Stepped HCD collision energy of 25, 27.5, 30% was used. MS1 data was acquired in profile, MS2 DIA data in centroid mode. Analysis of DIA data was performed using Spectronaut 15 (Rubin) DIA-NN version 1.8 (Biognosys) using the Uniprot protein database of *P. luminescens* sp. *luminescens* strain DJC (UP000253755). Full tryptic digest was allowed with two missed cleavage sites, and oxidized methionines, acetylated N-termini and carbamidomethylated cysteines. Spectronaut was executed in otherwise default settings. Spectronaut exports were further statistically evaluated using a modified SafeQuant (Glatter et al., 2012) script made compatible to process Spectronaut data.

2.5. Interbacterial competition assays

Streptomycin resistant *E. coli* Top10 tnGFP strain were used as prey for the interbacterial competition assays. The assays were performed according to the previous described protocol (Borgeaud et al., 2015). Briefly, daily cultures of *P. luminescens* DJC wild type and the respective T6SSs-impaired mutants Δ*tssA*1b and Δ*tssA*2 (hunter) were prepared of overnight cultures and grown for 2 h in culture medium. Strains were washed three times with sterile 1x PBS buffer and mixed with *E. coli* Top10 tnGFP strain (prey) in a OD_{600} 10:1 ratio (hunter vs prey). 100 µl of the mixture was spotted onto a small sterile nitrocellulose membrane placed on a pre-heated CASO plate to ensure bacterial contact and incubated for 5 h at 30°C. Then, bacteria were washed of the membrane with sterile 1x PBS buffer and serial dilutions were spotted onto LB agar plates supplemented with streptomycin for prey-survival *E. coli* Top10 selection and colony count. Three biological replicates were performed. *E. coli* alone was used as negative control.

2.6. Insect pathogenicity assays

Insect pathogenicity assays were performed as previously described (Mehler et al., 2022). Briefly, larvae of *Galleria mellonella* (reared in JGU Mainz, Heermann group) were surface sterilized with 80% [v/v] ethanol and numbed on ice. $2*10^4$ cells of *P. luminescens* DJC wild type, and the respective T6SSs-impaired mutants Δ*tssA*1b and Δ*tssA*2 were injected into the hemocoel of the larvae with a sterilized microlight syringe (1702 RN, 25 µl, Hamilton). Injected larvae were incubated at 30°C for 48 h and dead larvae were counted after 24 h and 48 h. Three independent biological replicates were performed with 7 larvae for each trial. Sterile medium was injected into the larvae as negative control.

2.7. Effector protein functionality assays

To determine the toxic effect of $Tme_{PL}1$ and $Tme_{PL}2$, the respective encoding genes were cloned into pBAD24 (pBAD24::effector). *E. coli* BL21 star cells were transformed with the respective plasmids and cultivated overnight in LB supplemented with carbenicillin and 0.1% (w/v) glucose to repress the leaky expression of the P_{BAD} promoter. Cell cultures were adjusted to $OD_{600} = 0.02$ and 200 µl were transferred into a 96-well plate in triplicates. Samples were incubated for 7 h at 37°C with shaking (135 rpm) and the OD_{600} was measured every 10 minutes with a microplate reader (Tecan). After 2 h, heterologous protein expression was induced with either 0.1% (w/v) L-arabinose or repressed with 0.1% (w/v) glucose. Three biological replicates were performed with similar results. *E. coli* BL21 star cells containing the empty pBAD24 vector served as control.

2.8. Motility assays

Motility assays were performed using semi-solid agar plates (1.5% [w/v] peptone, 0.5% [w/v] peptone from soy, 0.5% [w/v] NaCl) containing 0.4% [w/v] agar. Briefly, overnight cultures of *P. luminescens* DJC wild type and the respective T6SSs-impaired mutants Δ*tssA1b* and Δ*tssA2* were washed three times with sterile 1x PBS buffer and adjusted to $OD_{600} = 0.1$. Then, 20 µl were spotted onto the centre of a semi-solid agar plate and the plates were incubated for 48 h at 30°C. The resulting motility halo was monitored and quantified using ImageJ (https://imagej.nih.gov/ij/). Three independent biological replicates were performed.

2.9. HPLC-DAD analyses

To analyse whether a difference in the secondary metabolism of *P. luminescens* DJC wild type and T6SS-deficient mutants occurred, a HPLC-DAD analysis was performed. Therefore, *P. luminescens* DJC wild type and the respective T6SSs-impaired mutants Δ*tssA*1b and Δ*tssA*2 were inoculated at $OD_{600} = 0.05$ in 50 ml CASO medium, under shaking conditions at 140 rpm for 5 h at 30°C. The cultures were centrifuged for 30 min at 4500 rpm and the supernatant was mixed 1:1 with ethyl acetate. The hydrophilic phase was discarded, and the organic phase filtrated with Na_2SO_4. Separation of the solvent from the extract was performed with a vacuum rotary evaporator at 45°C, 200 mbar. Extracts were resuspended in acetonitrile and used in a final concentration of 5 mg/ml. High-performance liquid chromatography with diode array detector (HPLC-DAD) of the respective *P. luminescens* culture supernatants were performed on a Shimadzu LC 20 A Prominence system (Shimadzu, Griesheim, Germany). Separations were performed with a reversed-phase C18 column (Waters Sunfire C18, particle size 5 µm, 4.6 ×250 nm) at 20°C. With a flow rate of 1 ml/min, a linear gradient starting from 99% 0.1% [v/v] trifluoroacetic acid (TCA) and 1% [v/v] to 100% acetonitrile in 20 min, then 3 min maintaining with 100% acetonitrile and final equilibration time of 7 min was used with an injection volume of 20 µl. A Shimadzu SPD-M20A diode was used, with measurements from 200 – 800 nm to record and detect spectra at 300 nm and 350 nm. Data and spectra were analysed using the software LabSolution 5.54 (Shimadzu, Griesheim, Germany).

3. Results

3.1. The P. luminescens genome encodes four putative T6SS gene clusters

To identify T6SS genes in *P. luminescens* strain DJC, we performed a bioinformatics analysis (BLASTP, HMMER; HHpred and MUSCLE) screening for putative T6SS-related genes using *P. luminescens* TT01 as well as the SecReT6 database and the well-studied *Pseudomonas aeruginosa* PAO1 genome as reference. We identified four genomic regions encoding for T6SS clusters in the *P. luminescens* genome that we named T6SS-1, T6SS-2, T6SS-3 and T6SS-4 (Fig. 1 **A and B,** list in Supplementary Table S1). We classified the identified T6SSs in T6SS family groups following the nomenclature of Boyer et al. 2009 and Bernal et al. 2018 (Bernal et al., 2018; Boyer et al., 2009); thus categorising T6SS-1 in group 1.2b, T6SS-2 in group 4b and T6SS-3 and T6SS-4 in group 2.

The T6SS-1 region contains 16 genes, including 12 of 13 core components and 3 accessory genes (Fig. 1**B**). The lacking core component VgrG forms the syringe part of the T6SS and might be crucial for T6SS effector delivery (Pukatzki et al., 2007). Additionally, the T6SS-1 cluster

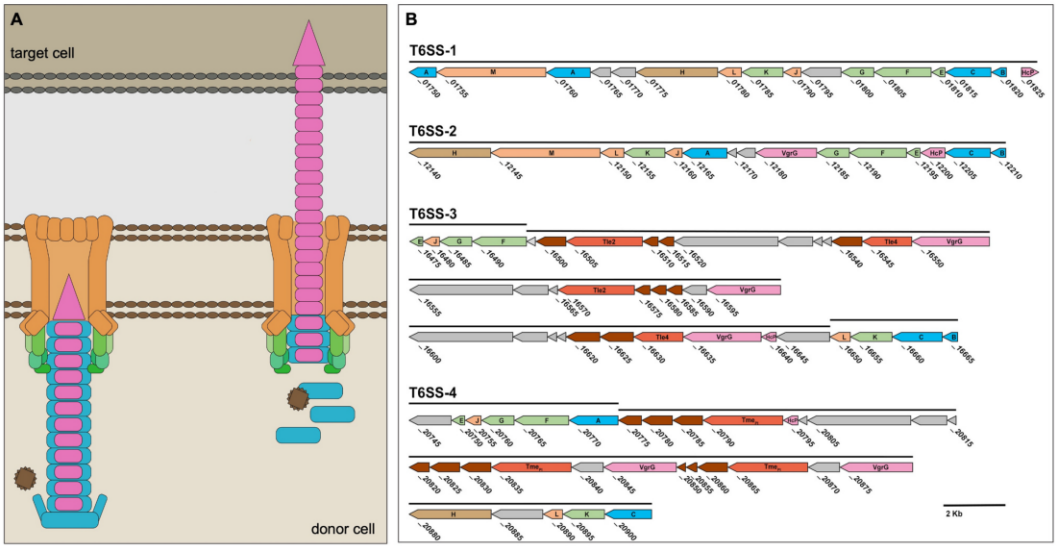

Fig. 1. (**A**) Schematic overview of the T6SS complex. Colour code in **A** corresponds with the colours in **B**. (**B**) Genomic organisation of the T6SS-1, T6SS-2, T6SS-3 and T6SS-4 clusters in *Photorhabdus luminescens* subsp. *luminescens* DJC genome. T6SS-Proteins of the membrane complex are shown in orange, sheath in blue, tube and spike in pink, baseplate proteins in green, accessory proteins and hypothetical proteins in grey. A more detailed picture is provided in Supplementary Material (Fig. S1).

encodes two *tssA* genes, in the following named *tssA1a* and *tssA1b*, encoding the short and long TssA cap component (Dix et al., 2018; Schneider et al., 2019). TssA is a core component, promoting sheath recruitment and is found in all T6SSs (Zoued et al., 2016). Bernal et al. 2021 showed different sheath stabilisation mechanisms for the two TssA conformations, leading to distinct firing mechanisms depending on the presence of two accessory proteins (TagA or TagB/J), which are absent in T6SS-1 [15]. The accessory gene *tagO* has a yet unknown function, while the *tagH* gene product is proposed to act as a regulator for T6SS activity in *P. aeruginosa* and *fis* encodes a transcriptional regulator responding to nutrient-limitation, proposed to regulate the T6SS gene expression in *Klebsiella pneumoniae* (Barbosa and Lery, 2019; Mallik et al., 2004). This suggests a putative regulation of the T6SS-1 activity upon nutrient availability but considering the missing VgrG and effector proteins, however, the role of the T6SS-1 in *P. luminescens* remains unclear. The T6SS-2 gene cluster consists of 15 genes (Fig. 1**B**), encoding all 13 T6SS core components, a hypothetical protein with unknown function and a PAAR-domain containing protein. No effector or regulatory genes were found in the T6SS-2 gene cluster. Therefore, the function of T6SS-2 in *P. luminescens* remains unclear. The T6SS-3 cluster (Fig. 1**B**) consists of 37 genes divided into two structural operons and one effector operon with a total of 10 core components. The effector operon contains 3 copies encoding VgrG, 4 genes encoding for effector proteins with 9 respective immunity proteins, one HcP, 7 accessory proteins and 7 hypothetical proteins with unknown function. Two structural operons flank the effector operon, containing the core components *tssE, tssJ, tssG, tssF* and *tssL, tssK, tssB, tssC,* while *tssA, tssM* and *tssH* are missing.

The structure of the T6SS-4 gene cluster (Fig. 1**B**) is similar to the T6SS-3 structure, which consists of 30 genes, including 11 core components, missing *tssM* and *tssB*. Furthermore, this cluster harbours 3 genes encoding effector proteins with 9 respective immunity proteins, 6 accessory proteins and 2 hypothetical proteins.

3.2. *P. luminescens harbours multiple T6SS E-I pairs*

In silico analysis of the T6SS-3 and T6SS-4 revealed multiple putative T6SS effectors and their cognate immunity proteins in the genome of *P. luminescens* strain DJC. We identified a total of four E-I pairs, which are located within the T6SS-3 effector operon (Fig. 1**B**). HMMER analysis identified them as the previously reported type VI lipase effectors Tle2 and Tle4 with the cognate immunity proteins Tli2 and Tli4 (Russell et al., 2013). Analysis of the putative effectors in the T6SS-4 cluster (*PluDJC_20790*, *PluDJC_20835* and *PluDJC_20865*) with the NCBI CDD revealed a Mix_III motif in the N-terminal region and a transmembrane helix (TMH) at C-terminal. Effectors containing Mix motifs and TMCs are predicted to have pore-forming activity (Salomon et al., 2014). Prediction of the C-terminal region using HHpred identified a putative Colicin N structure (1col: 688–822, probability: 77.3%), suggesting the putative effectors are Tme-like effectors (Fridman et al., 2020) and therefore named Tme_{Pl} and their cognate immunity protein, Tmi_{Pl} (Fig. S2 Supplementary Material S1). To determine the antibacterial activity of $Tme_{Pl}1$ and $Tme_{Pl}2$, the respective coding sequences were cloned into the pBAD24 vector. However, no significant toxic effect of $Tme_{Pl}1$ and $Tme_{Pl}2$ could be observed after induction with 0.1% arabinose within 5 h incubation time (Fig. S3 Supplementary Material S1).

3.3. *Conservation of the T6SSs in P. luminescens strain DJC and strain TT01*

Upon analysing the diverse spectrum of the T6SS related genes in *P. luminescens* strain DJC, conservation among the T6SS clusters of the strain DJC and TT01 was determined. While the T6SS-2 is highly conserved in the two strains, the T6SS-1 of strain TT01 harbours the well-studied toxin Rhs1 along with the respective immunity proteins. However, no effector could be identified in the T6SS-1 of the strain DJC. But unlike in TT01, an additional gene encoding for TssA1a is found in *P. luminescens* DJC. Interestingly, the T6SS-1, T6SS-3 and T6SS-4 of TT01 all harbour one or multiple transposases, whereas no transposases are located in the T6SS clusters of the strain DJC. Furthermore, a third homologous of the putative effector protein Tme_{Pl} is missing in TT01. However, conservation among the T6SSs of DJC and TT01 is high, despite the different lifestyles of the two strains.

3.4. T6SS-1 and T6SS-2 are not essential for P. luminescens growth

TssA, the cap component of the T6SS, is crucial for the assembly and sheath stability and therefore necessary for the T6SS activity (Dix et al., 2018). Previous studies showed, that TssA proteins can be distinguished in different classes, such as short TssA and long TssA. However, the sheath stabilization with short TssAs relies on the accessory proteins TagB or TagJ (Bernal et al., 2021), therefore the short TssA is not crucial as the long TssA in the T6SS assembly mechanism.

In order to study the role of T6SS-1 and T6SS-2, the two complete T6SSs, in *Photorhabdus*, we generated T6SSs deficient mutants lacking this cap protein – TssA –, thus impairing the T6SS assembly and functionality. Therefore, *tssA*1b (corresponding to the previously mentioned long TssA, which is crucial for the T6SS assembly) in T6SS1 and *tssA*2 in T6SS2 were deleted in the *P. luminescens* genome, and the mutant strains were following named Δ*tssA*1b and Δ*tssA*2. Once again, the deletion of *tssA1a*, the second short putative cap protein of the T6SS-1 was not considered for this study, as the accessory proteins TagB or TagJ are missing thus suggesting that this protein is not as crucial in impairing the T6SS stability as *tssA*1b. To exclude differential phenotype behaviour due to different bacterial growths, the growth rate was monitored. Wild type and the mutant strains showed no significant differences in their growth rate (Fig. 2**A**).

3.5. P. luminescens T6SS-1 and T6SS-2 are involved in interbacterial killing activity

Multiple T6SS loci in bacteria are likely to be differently expressed, depending on the presence of competitors, to enhance bacterial fitness in multi-microbial environments (Ma et al., 2014). To determine whether the T6SS-1 or T6SS-2 of *P. luminescens* are involved in antibacterial activity of *P. luminescens* we performed an interbacterial competition assay. For that purpose, *E. coli* Top10 tnGFP was picked as Gram-negative prey strain and co-cultivated (on CASO agar-plates to ensure bacterial contact) with *P. luminescens* wild type and T6SS-1 and T6SS-2 deficient strains for 5 h. Co-cultivation of the wild type *P. luminescens* with *E. coli* resulted in a 10'000-fold decrease of colony forming units (CFUs) of *E. coli* (Fig. 2**B**). Deletion of *tssA*1b increased the killing capacity of *P. luminescens* compared to the wild type by 10-fold, with even less survival. However, deletion of *tssA*2 decreased the killing capacity of *P. luminescens* by a 10-fold decrease. These results suggested a role of the T6SS-1 and T6SS-2 of *P. luminescens* as an antibacterial strategy to compete against other bacteria.

3.6. Proteome comparison of P. luminescens wild type and its T6SS-1 and T6SS-2 impaired mutants

To gain more insights into the T6SS activity in *P. luminescens*, we performed a proteome analysis and compared the proteome of *P. luminescens* wild type and its two T6SS impaired mutants (T6SS-1 and T6SS-2). Therefore, we analysed the proteomes of the wild type, Δ*tssA*1b

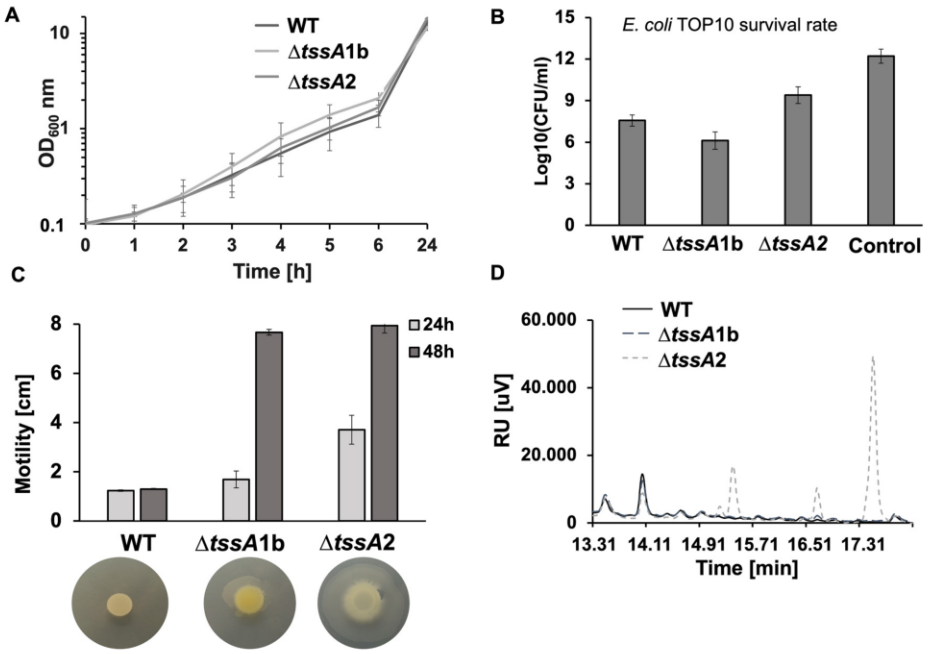

Fig. 2. Impairing the T6SS-1 and T6SS-2 of *P. luminescens* influences the interbacterial competition, motility and the secondary metabolism. (**A**) Growth of *P. luminescens* DJC wild type and the respective T6SS-deficient strains. Growth was monitored over 24 h starting at OD_{600} = 0.1. Values are means of three independent biological replicates; error bars represent standard deviation. (**B**) Survival of *E. coli* Top10 prey cells after co-cultivation for 5 h with *P. luminescens* DJC wild type and the respective T6SS-deficient mutants. Quantification is indicated upon colony forming units per ml (CFU/ml) of five independent replicates, error bars indicate standard deviation. (**C**) Motility assays of *P. luminescens* DJC wild type and the respective T6SS-deficient strains. The figure shows CASO semi-solid agar plates inoculated with the respective *P. luminescens* strains; the pictures are representative of three independently performed experiments with similar outcomes. The plot shows the average of the quantification of three independent replicates. Error bars indicate standard deviation. WT= wild type. (**D**) HPLC-DAD analysis of *P. luminescens* subsp. *luminescens* DJC wild type and Δ*tssA* mutants supernatant. Peaks at 15.4 min and 17.6 min indicate anthraquinone in Δ*tssA*2. The response unit RU [uv] is plotted against the retention time [min] at a wavelength of 350 nm.

and Δ*tssA*2 cells by label-free mass spectrometry. The different sets of proteins analysed were then compared between the respective mutant and the wild type to identify differences in protein production. The different bacterial strains were cultured for 5 h in CASO medium, setting the time point of collection and medium in agreement with our inter-bacterial competition assay previously conducted. Respective protein identifiers were obtained from Uniprot and protein identification was achieved by BLASTP and HMMER analysis. Out of 2682 quantified proteins, a total of 724 proteins in *P. luminescens* Δ*tssA*1b and 1108 in *P. luminescens* Δ*tssA*2 were over- or underrepresented ($q < 0.01$, $n \geq 3$ detected peptides) compared to the wild type (Fig. 3, Supplementary Table S2). Proteins with a $> \pm$ 1.5-fold abundance were considered as significantly abundant.

3.6.1. Abundance of T6SS related proteins in P. luminescens DJC wild type and its T6SS-1 and T6SS-2 impaired mutants

T6SS activity requires the assembly of all core components as well as synthesis and delivery of toxic effectors. To determine whether the observed killing behaviour is T6SS-dependent, we focused the proteome analysis on the presence of putative T6SS related proteins. A total of 80 proteins related to the T6SS were detected in the *P. luminescens* wild type. Among the 80 identified proteins, 42 proteins were less and 3 more represented in the *P. luminescens* Δ*tssA*1b mutant, while 43 proteins were less and 19 more represented in the Δ*tssA*2 mutant (Table 1). Unexpectedly, multiple proteins belonging to the T6SS-1 were significantly more abundant in the Δ*tssA*2 strain, only lacking TssL1, TssE1 and TssJ1, proteins belonging to the membrane complex and the baseplate of the T6SS. Additionally, 4 proteins of the T6SS-2 were more abundant, including HcP7 and TssH2. In contrast, 3 proteins of the T6SS-1 were more abundant in the Δ*tssA*1b strain, including HcP2 and TssH1. Thus, in both deletion mutants, both the corresponding HcP and TssH proteins were shown to still be produced, although T6SS assembly is impaired due to the deletion of the TssA encoding gene. Furthermore, the analyses revealed that the deletion from the TssA subunit results in a lower abundance of proteins of the T6SS-3 and T6SS-4, as multiple proteins were found significantly less abundant in the mutant strains. Overall, a general decrease in T6SS proteins could be observed in the T6SS-1 and T6SS-2 impaired *P. luminescens* strains.

3.7. Abundance of fitness factors in the P. luminescens T6SS-deficient strains

The complex life cycle of *P. luminescens* requires a diverse spectrum of defence and attack mechanisms to colonise eukaryotic hosts, such as insect larvae as e.g., *Galleria mellonella.* In addition, the bacteria must defend the larvae carcass against other microbes. Therefore, by screening for T6SS related proteins and putative effectors, we further investigated whether a change in different fitness factors could be observed. Indeed, multiple proteins involved in pyocin synthesis, *Photorhabdus* virulence cassettes (PVCs), T3SS and flagellar systems were detected with significant changes in the *P. luminescens* T6SS-deficient strains Δ*tssA*1b and Δ*tssA*2 (Table 2).

3.7.1. Abundance of PVC and pyocin proteins

The *Photorhabdus* virulence cassettes share structure similarity with R-type pyocins but so far, an antibacterial effect has not been shown yet (Yang et al., 2006). *P. luminescens* harbours three gene loci encoding for S-type pyocins and one gene loci encoding for R-type pyocins (Wilkinson et al., 2009). A total of 23 proteins related to pyocins were detected in the wild type, while in each T6SS-deficient strain only 16 proteins were found differently represented. Five proteins of the R-type pyocins where significantly more represented in Δ*tssA*2, while proteins related to S-type pyocins were significantly less abundant in both T6SS-deficient strains. 9 out of the 16 detected PVC predicted proteins in the wild type showed a significant higher abundance in Δ*tssA*1b, with a similar representation pattern in Δ*tssA*2, thus pointing out a role in

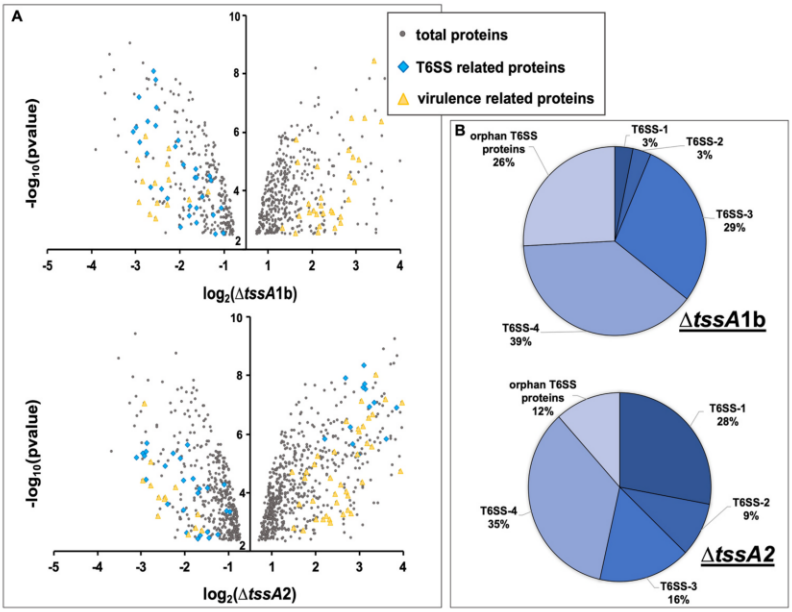

Fig. 3. Proteome comparison of Δ*tssA*1*b*, Δ*tssA*2 and P. luminescens WT cells. (**A**) Volcano plots summarizing proteome comparison between *P. luminescens* wild type and Δ*tssA*1b or Δ*tssA*2 strains. The -$\log_{10}$ (p value) is plotted against the $\log_2$ ratio of peptide intensities. Proteins detected with $n \geq 3$ and $q < 0.01$ were considered. Blue squares indicate T6SS related proteins, yellow triangles show virulence related proteins, grey circles represent the total proteins. (**B**) Distribution of T6SS related proteins detected in the proteome analysis of Δ*tssA*1b and Δ*tssA*2 strains into the different T6SS clusters.

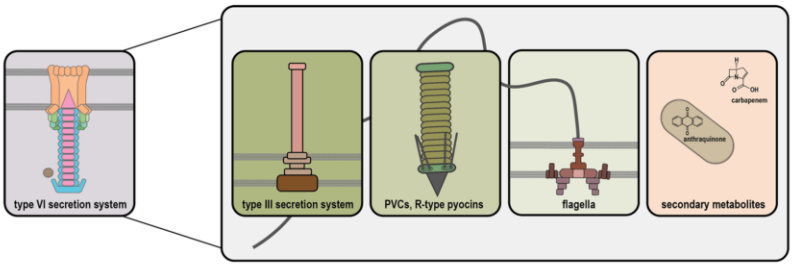

Fig. 4. : Putative link of different defence mechanism in *P. luminescens*. Schematic presentation of the correlation between T6SS activity and different virulence mechanisms such as type III secretion system, PVCs, R-type pyocins, flagella and secondary metabolites. As T6SS-deficiency can increase motility and killing capacity, eventually a master regulator for virulence factors exists in *P. luminescens* DJC.

interbacterial competition in *P. luminescens,* once T6SSs are impaired.

3.7.2. Role of P. luminescens T6SSs in insect pathogenicity

The T3SS is essential for the interaction of Gram-negative bacteria with eukaryotic cells and is involved in the infection process of insect larvae by *P. luminescens* (Brugirard-Ricaud et al., 2005). *P. luminescens* strain DJC harbours one gene loci consisting of 39 genes encoding for a T3SS. 10 proteins of the T3SS were detected in the *P. luminescens* wild type proteome, of which 5 proteins were detected in higher abundance in *P. luminescens* Δ*tssA*1b and no proteins in Δ*tssA2*. The T3SS is involved in the infection process of insect larvae by *P. luminescens* and therefore it was determined, whether one of the *P. luminescens* mutants is more pathogenic (Brugirard-Ricaud et al., 2005). However, the insect pathogenicity of the *P. luminescens* wild type, Δ*tssA*1b and Δ*tssA*2 showed no significant changes in mortality among the investigated strains (Fig. S4 Supplementary Material S1).

3.7.3. Increased motility in T6SS impaired P. luminescens strains

Motility is a key factor in interbacterial competition, giving bacteria the ability to move towards their hosts or competitors and is described in diverse *Xanthomonas* and *Pseudomonas* strains to be correlated with T6SS activity (Bouteiller et al., 2020; Montenegro Benavides et al., 2021). Among 20 detected flagellar proteins in the wild type, 12 were significantly more abundant in Δ*tssA*1b and 11 in Δ*tssA*2. FliA, a transcriptional regulator of flagellar filament synthesis, was detected slightly more abundant in *P. luminescens* Δ*tssA*2. *In vivo* analysis of the motility of the wild type, Δ*tssA*1b and Δ*tssA*2 showed a significant higher motility in the T6SS-deficient strains, i.e., the motility of Δ*tssA*2 was already increased after 24 h and no motility was observed for the wild type (Fig. 2**C**).

3.7.4. The P. luminescens T6SS-2 impaired mutant showed a more active secondary metabolism compared to the wild type

P. luminescens produces a broad spectrum of secondary metabolites among which are compounds with antibiotic activity like carbapenem, stilbene and anthraquinone (Derzelle et al., 2002; Heinrich et al., 2016; Williams et al., 2005). The analysis showed that 8 out of 9 proteins involved in anthraquinone biosynthesis were detected in the *P. luminescens* wild type proteome and were significantly more abundant in *P. luminescens* Δ*tssA*2, whereas none of these proteins were detected in Δ*tssA*1b. To examine whether the anthraquinone biosynthesis was altered in *P. luminescens* Δ*tssA*2, supernatants were extracted after 5 h of cultivation and analysed through HPLC-DAD analysis. No anthraquinone synthesis could be detected in the *P. luminescens* wild type and Δ*tssA*1b supernatant, but *P. luminescens* Δ*tssA*2 showed anthraquinone production already at this early time-point (Fig. 2**D**). Furthermore, 6 non-ribosomal peptide synthases (NRPS) were detected in the wild type-proteome as well as in *P. luminescens* Δ*tssA*2, but four of them were significantly more abundant in Δ*tssA*2. Three NRPS were detected in *P. luminescens* Δ*tssA*1b with similar levels as the wild type. Five proteins involved in carbapenem synthesis were found significantly higher abundant in the *P. luminescens* Δ*tssA*2 than in the wild type and therefore suggesting that the carbapenem synthesis could be increased in the *P. luminescens* Δ*tssA*2 strain.

4. Discussion

Since the first report on the T6SS in 2006, many Gram-negative bacteria have been described harbouring one or more active T6SSs. However, many questions remain elusive such as the impact of T6SS-deficiency on protein abundance at cell level and the understanding of the T6SSs in context with bacteria used as biocontrol agent. In this study, we confirmed four clusters encoding T6SSs in the genome of *P. luminescens* DJC, suggesting a role of the T6SSs in bacterial competition of this versatile bacterium. Previous studies performed in the *P. luminescens* strain TT01 revealed a highly toxic effector, which is not present in the genome of the strain DJC (Jurėnas et al., 2021b, 2021a). To study the role of the T6SSs in the strain DJC, further bioinformatic analysis were carried out. Our findings showed, that the T6SSs belong to different phylogenetic groups, one from group 1.2b (T6SS-1), two from group 2 (T6SS-3 and T6SS-4) and one belonging to group 4b (T6SS-2). Recent studies have attempted to assign functions to the T6SSs in the different phylogenetic groups, but no pattern could be discerned and thus the function of the *P. luminescens* T6SSs remains unclear (Bernal et al., 2018). While the T6SS-2 is considered functional as it harbours all core components, the function is yet unknown. Interestingly, no T6SS-2 activity was observed in the wild type and T6SS-deficient strains and therefore no role for T6SS-2 could be identified yet. However, T6SS-1 lacks a gene encoding for VgrG, the tip of the T6SS but further investigations showed a broad variety of VgrGs spread on the genome of *P. luminescens* DJC (Supplementary Table S1). Researchers suggested in different bacteria, that VgrGs can be shared across different T6SSs, therefore we consider the T6SS-1 as functional (Bernal et al., 2017). Furthermore, orphan VgrGs are located in so-called pathogenicity islands together with effectors and their cognate immunity proteins. The pathogenicity islands can be encoded separately of the T6SSs clusters, suggesting a different assembly mechanism of the tube and tip including the orphan VgrGs or HcPs (Zhang et al., 2021). Therefore, the T6SS-1 activity could be dependent on co-regulation of *vgrG* orphan islands; but this hypothesis needs to be further investigated.

Upon impairing the T6SS-1 and T6SS-2, we highlighted different representations of T6SS proteins. While deletion of *tssA*2 led to the activation of the T6SS-1, deletion of *tssA*1b resulted in lower abundance of T6SS-1 proteins. TssA promotes the sheath assembly and can lock the assembled T6SS in a high-energy state (Bernal et al., 2021; Dix et al., 2018; Schneider et al., 2019; Zoued et al., 2016). As *tssA*1b is missing in the first T6SS cluster, sheath instability could lead to abridged firing, not allowing the T6SS-1 to build up the sheath length for optimised T6SS

Table 1
T6SS related proteins detected in *P. luminescens* DJC Δ*tssA*1b and Δ*tssA*2 by label-free mass spectrometry (h.p. = hypothetical protein).

	Uniprot ID	T6SS name	Gene	Δ*tssA1b* log2ratio	Δ*tssA2* log2ratio	Δ*tssA1b* -log10 pvalue	Δ*tssA2* -log10 pvalue
T6SS-1	Q7N9H7	TssM1	*PluDJC_01755*	-1.1515	2.6389	4.7241	7.5263
	Q7N9H6	TssA1b	*PluDJC_07160*	-0.8696	2.6045	2.3943	8.3294
	Q7N9H5	TagO	*PluDJC_01765*	-	2.1788	-	7.8963
	Q7N9H4	Fis	*PluDJC_01770*	-	3.9678	-	5.8911
	Q7N9H3	TssH1	*PluDJC_01775*	0.6704	2.6131	2.0776	7.7122
	Q7N9H1	TssK1	*PluDJC_01785*	0.8576	2.7339	2.2886	6.9165
	Q7N9G9	TagH	*PluDJC_01795*	-	2.5912	-	7.5794
	Q7N9G8	TssG1	*PluDJC_01800*	-	3.3491	-	6.8867
	Q7N9G7	TssF1	*PluDJC_01805*	-	2.4802	-	5.2756
	Q7N9G5	TssC1	*PluDJC_01815*	-	2.3482	-	5.6424
	Q7N9G4	TssB1	*PluDJC_01820*	-	2.2996	-	6.2250
	Q7N9G3	HcP2	*PluDJC_01825*	1.0587	3.5346	1.6308	5.8152
T6SS-2							
	Q7N4N8	TssH2	*PluDJC_12140*	-	2.8398	-	7.0758
	Q7N4N7	TssM2	*PluDJC_12145*	-	1.7093	-	5.8209
	Q7N4N4	TssJ2	*PluDJC_12160*	-	3.7085	-	8.5060
	Q7N4M6	HcP7	*PluDJC_12200*	-0.7044	2.5192	-0.5395	3.3633
T6SS-3	Q7N265	Tle2A	*PluDJC_16505*	-0.5645	-0.6051	3.4062	4.2762
	Q7MB15	Tli2A	*PluDJC_16510*	-1.5373	-1,1704	5.7036	4.2235
	Q7MB14	Tli2B	*PluDJC_16515*	-	-0.9517	-	2.4639
	Q7N249	h.p.	*PluDJC_16525*	-2.1661	-1.8976	4.1078	3.6067
	Q7N259	Tli4B	*PluDJC_16540*	-1.1559	-0.9173	4.4397	2.6636
	Q7N258	Tle4A	*PluDJC_16545*	-0.4170	-0.2624	1.8717	1.4991
	Q7N256	VasK2	*PluDJC_16555*	-0.7611	-0.7851	2.1160	2.3135
	Q7N263	VasK3	*PluDJC_16600*	-0.9536	-0.4107	1.6146	0.4767
	Q7N247	Tli4C	*PluDJC_16620*	-0.7405	-0.3249	3.1753	1.0021
	Q7MB10	Tli4D	*PluDJC_16625*	-	-0.3606	-	0.7515
	Q7N245	VgrG8	*PluDJC_16635*	-0.5780	-0.4419	2.1385	1.6272
	Q7N244	HcP11	*PluDJC_16640*	-1.2749	-1.1921	3.4656	3.9951
	Q7N243	OmpA1	*PluDJC_16645*	-0.5244	-0.3727	1.6555	1.0822
	Q7N242	TssK3	*PluDJC_16655*	-0.5245	-0.2981	2.5618	1.2987
	Q7N241	TssC3	*PluDJC_16660*	-1.1340	-0.8805	2.9079	2.0147
	Q7N240	TssB3	*PluDJC_16665*	-1.7934	-1.2022	3–7183	2.4117
T6SS-4	Q7MZS5	TssE4	*PluDJC_20750*	-1.8012	-1.5245	2.2368	4.4064
	Q7MSZ4	TssJ4	*PluDJC_20755*	-1.2927	-1.3092	3.1277	4.4741
	Q7MSZ2	TssF4	*PluDJC_20765*	-1.4211	-1.4365	4.8935	5.6128
	Q7MZR8	h.p.	*PluDJC_20780*	-	-0.7374	-	2.5618
	Q7MZR7	$Tme_{PI}1$	*PluDJC_20790*	-1.6110	-1.7623	5.5046	5.3340
	Q7MRZ6	HcP12	*PluDJC_20795*	-0.9462	-0.9772	2.2009	4.1438
	Q7MZR1	PaaR8	*PluDJC_20815*	-1.9207	-1.5693	4.0609	5.1701
	Q7MZQ8	h.p.	*PluDJC_20830*	-2.0553	-2.6077	7.7907	5.1824
	Q7MZQ7	$Tme_{PI}2$	*PluDJC_20835*	-2.1018	-2.3665	8.0810	5.6790
	Q7MZQ6	Tap1C	*PluDJC_20840*	-2.4157	-2.3933	5.6423	4.4341
	Q7MZQ5	VgrG10/11	*PluDJC_20845*	-2.5070	-2.4702	6.1496	5.3355
	Q7MZQ4	TssH3	*PluDJC_20880*	-2.4386	-2.4174	7.1849	5.2584
	Q7MZQ3	OmpA2	*PluDJC_20885*	-2.5643	-2.3855	5.9970	5.3861
	Q7MZQ1	TssK4	*PluDJC_20895*	-2.0367	-1.9430	6.8243	4.9154
	Q7MZQ0	TssC4	*PluDJC_20900*	-1.4841	-1.4609	2.7622	2.6242
Orphan T6SS related proteins	Q7NAC9	HcP1	*PluDJC_00025*	-0.8033	-0.4620	4.3600	3.3570
	Q7N980	TseV1a	*PluDJC_02265*	-0.2843	0.2499	1.5713	0.9583
	Q7N5M2	VgrG4	*PluDJC_10005*	-	-0.4667	-	1.1878
	Q7N3Y9	HcP8	*PluDJC_13450*	-2.0180	-0.6898	2.5192	0.7435
	Q7N2U6	HcP9	*PluDJC_15210*	-	3.1223	-	5.8248
	Q7N2D1	HcP10	*PluDJC_16115*	-1.1365	0.1349	3.4075	0.2123
	Q7MZK5	Tke2	*PluDJC_21170*	-	0.6648	-	2.7373
	Q7MYS3	TssF5	*PluDJC_22815*	-2.2375	-1.5252	6.3617	3.4141
	Q7MYS2	VgrG12	*PluDJC_22820*	-2.0486	-1.1501	6.2240	2.5453
	Q7MYR9	TseT1a	*PluDJC_22835*	-2.2464	-1.2538	5.2687	2.0936
	Q7MYR8	TsiT1a	*PluDJC_22840*	-1.1220	-0.4525	5.2687	2.0936
	Q7MYR7	PaaR11	*PluDJC_22845*	-0.8248	-0.5180	4.4971	1.1049
	Q7MYR6	TseT1b	*PluDJC_22850*	-	-0.5187	-	0.9424
	Q7MYR5	TsiT1b	*PluDJC_22855*	-0.5442	0.1150	2.3270	0.2192
	Q7MYR	TsiT1c	*PluDJC_22870*	-0.9986	-0.4290	3.7970	1.1932

activity. Taking the differently representation in context with the interbacterial killing assay, it could be concluded, that the higher abundance of T6SS-1 proteins would lead to increased killing of the prey cells which was not the case. Since no T6SS related effector has been found more abundant, the single upregulation of the T6SS-1 alone could not be sufficient to restore the killing capacity and cognate antibacterial effectors are required.

The T6SS-3 and T6SS-4 were classified as non-functional because both clusters lack several core components such as TssM, TssH and TssA in T6SS-3 and TssM, TssB in T6SS-4. Further, the structural operons are separated by an effector operon with several E-I pairs and accessory proteins. Interestingly, multiple proteins of T6SS-3 and −4 clusters were detected less abundant in the proteomics and recent studies of the T6SS in *Yersinia pestis* showed, that an incomplete T6SS can be active

Table 2
Proteins related to virulence and secondary metabolism detected in P. luminescens DJC ΔtssA1b and ΔtssA2 by label-free mass spectrometry.

	Uniprot ID	protein	Gene	ΔtssA1b log2ratio	ΔtssA2 log2ratio	ΔtssA1b -log10 pvalue	ΔtssA2 -log10 pvalue
R-type pyocin	Q7NAC1	Phage tail assembly protein	*PluDJC_00075*	-	2.1312	-	3.2749
	Q7NAB9	Phage tail sheath protein	*PluDJC_00085*	-	1.8140	-	3.1032
	Q7NAB5	Tail fiber assembly protein	*PluDJC_00110*	0.8137	1.5350	2.7370	5.2406
	Q7NAB3	Phage tail protein	*PluDJC_00120*	1.8040	3.4444	2.0137	4.7268
	Q7NAB1	Baseplate J/gp47 family protein	*PluDJC_00130*	-	1.2949	-	4.7149
S-type Pyocin	Q7N861	Pyosin/cloacin T domain-containing protein	*PluDJC_04515*	-2.1847	-2.2854	3.2105	4.2424
	Q7N860	Hypothetical protein	*PluDJC_04520*	-2.0466	-2.0909	3.0401	3–8306
	Q7N859	Hypothetical protein	*PluDJC_04525*	-2.4656	-2.4278	5.0715	7.0405
	Q7N858	Bacteriocin immunity protein	*PluDJC_04535*	2.4320	-2.4167	3.6235	4.4084
	Q7N857	Hypothetical protein	*PluDJC_04545*	-2–3512	-2.2829	4.3316	5.0613
	Q7N5Q3	Hypothetical protein	*PluDJC_09840*	-0.8676	-	3.9821	-
	Q7N5Q2	Bacteriocin immunity protein	*PluDJC_09850*	-0.7687	-	1.8956	-
	Q7N5Q1	S-type pyocin domain-containing protein	*PluDJC_09855*	-1.7955	-	4.9182	-
	Q7MZV3	Hypothetical protein	*PluDJC_20605*	-1.3012	-1.1139	3.7021	2.7200
	Q7MZV2	Hypothetical protein	*PluDJC_20610*	-1.7862	-1.2608	3.5255	2.7865
	Q7MZV1	Hypothetical protein	*PluDJC_20615*	-1.7530	-1.1962	5.4534	3.2606
	Q7MZV0	Hypothetical protein	*PluDJC_20620*	-1.7640	-1.7072	4.3812	4.1898
	Q7MZU9	Hypothetical protein	*PluDJC_20625*	-2.2905	-2.1227	5.8680	3.2095
	Q7MZU8	Hypothetical protein	*PluDJC_20630*	-2.0280	-1.9559	3.5743	3.8249
	Q7MZU7	S-type pyocin domain-containing protein	*PluDJC_20635*	-2.0623	-1.9727	4.2599	3.7846
PVC	Q7N661	Phage tail sheath family protein	*PluDJC_08805*	-	-1.4222	-	2.5719
	Q7MB50	Hypothetical protein	*PluDJC_08835*	2.3919	1.8279	6.4759	4.4912
	Q7N651	Tail fiber protein	*PluDJC_08860*	3.0720	2.8127	6.3757	6.6789
	Q7N650	Hypothetical protein	*PluDJC_08865*	2.8961	2.6727	8.4346	5.6778
	Q7N649	Hypothetical protein	*PluDJC_08870*	2.4182	2.0786	5.1464	4.2640
	Q7N648	Hypothetical protein	*PluDJC_08875*	2.3403	2.2064	4.4915	4.0431
	Q7N647	Hypothetical protein	*PluDJC_08890*	2.6948	2.4614	6.4779	5.3181
	Q7N642	Phage tail sheath family protein	*PluDJC_08915*	2.4496	1.6620	4.2930	3.0883
	Q7N641	Phage tail sheath family protein	*PluDJC_08920*	2.4077	1.1220	3.5584	3.5938
	Q7N640	Phage tail protein	*PluDJC_08925*	1.6091	0.9952	4.8376	2.7884
T3SS	Q7N0×4	YopD family T3SS translocon subunit	*PluDJC_18550*	1.5987	-	3.2050	-
	Q7N0×1	Virulence-associated V antigen	*PluDJC_18565*	2.5490	-	5.0487	-
	Q7N0W0	T6SS needle length determinant	*PluDJC_18625*	3.7514	-	5.7037	-
	Q7N0V3	T3SS regulon anti-activator ExsD protein	*PluDJC_18660*	1.1225	-	2.5416	-
	Q7N0V1	T3SS outer membrane ring protein	*PluDJC_18670*	1.4315	-	3.2700	-
Flagellen	Q7N5N2	FlgC	*PluDJC_09955*	1.5268	1.5120	3.3079	3.0770
	Q7N5N1	FlgD	*PluDJC_09960*	1.9677	2.2405	3.2717	3.8965
	Q7N5N0	FlgE	*PluDJC_09965*	2.0100	1.8441	2.7232	2.9651
	Q7N5M8	FlgG	*PluDJC_09975*	1.750	1.7372	3.2286	3.2178
	Q7N5M6	FlgH	*PluDJC_09980*	1.6974	1.9530	3.5009	3.9605
	Q7N5M4	FlgK	*PluDJC_09995*	1.1291	-	2.3769	-
	Q7N5M3	FlgL	*PluDJC_10000*	1.6627	-	2.7804	-
	Q7N5K7	FliM	*PluDJC_10080*	2.1372	2.3086	2.9020	3.3036
	Q7N5K5	FliK	*PluDJC_10090*	2.3294	2.7859	5.4022	5.5565
	Q7N5K3	FliI	*PluDJC_10100*	1.9348	1.9881	3.3122	3.6696
	Q7N5K1	FliG	*PluDJC_10110*	2.1459	2.2461	3.1172	3.3935
	Q7N5K0	FliF	*PluDJC_10115*	2.3203	2.5725	3.6928	4.3451
	Q7N5J5	FliD	*PluDJC_10150*	1.6293	1.2150	2.5857	2.7233
	Q7N5J4	FliC	*PluDJC_10155*	1.7664	-	2.2959	-
	Q7N5J3	FliA	*PluDJC_10160*	0.5143	0.5471	1.3160	2.7465
NRPS	Q7N850	Non-ribosomal peptide synthase	*PluDJC_04580*	-	2.5914	-	6.2492
	Q7N849	Non-ribosomal peptide synthase	*PluDJC_04585*	-	3.0998	-	7.1779
	Q7N848	Non-ribosomal peptide synthase	*PluDJC_04590*	-	2.2065	-	6.4279
	Q7N3P5	Non-ribosomal peptide synthase	*PluDJC_14010*	1.2025	1.4289	3.1497	3.7204
	Q7N239	Non-ribosomal peptide synthase	*PluDJC_16670*	1.1470	1.4726	4.9841	4.9610
	Q7N1E3	Non-ribosomal peptide synthase	*PluDJC_17430*	1.1432	1.8803	5.7303	7.7307
Anthraquinone	Q7MZT8	AntI	*PluDJC_20685*	-	3.4806	-	7.0595
	Q7MZT7	AntH	*PluDJC_20690*	-	4.5915	-	4.5154
	Q7MZT6	AntG	*PluDJC_20695*	-	3.9893	-	6.1349
	Q7MZT5	AntF	*PluDJC_20700*	-	3.9554	-	3.5917
	Q7MZT4	AntE	*PluDJC_20705*	-	4.5816	-	7.4605
	Q7MZT3	AntD	*PluDJC_20710*	-	3.7427	-	6.8419
	Q7MZT2	AntC	*PluDJC_20715*	-	2.4882	-	6.0944
	Q7MZT0	AntA	*PluDJC_20725*	-	3.7585	-	3.5567
CPM	F5HGM6	CpmA	*PluDJC_00990*	1.1426	2.7195	1.6721	6.5611
	F5HGP5	CpmB	*PluDJC_00995*	1.0663	2.4747	1.9354	6.1699
	F5HC75	CpmC	*PluDJC_01000*	1.1557	2.5568	2.1864	7.1243
	F5HIJ2	CpmD	*PluDJC_01005*	0.8272	1.9330	2.1302	5.3909
	F5HC69	CpmE	*PluDJC_01010*	1.6926	2.8749	3.7577	8.0247

(Andersson et al., 2017). Thus, suggesting that T6SS-3 and T6SS-4 could have a functional role in *P. luminescens*.

Studies reported that for *P. aeruginosa*, different master regulators are involved in the regulation of multiple virulence pathways such as quorum sensing (QS), type III secretion system (T3SS) and T6SS (Huang et al., 2019). As *P. luminescens* is a highly pathogenic bacterium and also deploys antifungal activity, it was also investigated whether different mechanisms involved in the pathogenicity of *Photorhabdus* are affected by T6SS-impairing (Dominelli et al., 2022). Indeed, mutation of *tssA*1b and *tssA*2 had an impact on different mechanisms at proteomics level, i. e. PVCs, T3SS, pyocins and motility. The PVCs of *P. asymbiotica* and the T3SS of *P. luminescens* strain TT01 are essential for infection and interaction with eukaryotic hosts, such as the common wax moth *Galleria mellonella* (Brugirard-Ricaud et al., 2005; Yang et al., 2006). To determine whether the higher abundance of PVC and T3SS proteins increase the insect pathogenicity of *P. luminescens* DJC, we performed larvae infection assays. The results indicate no change in pathogenicity since all strains showed the same capability to kill the insect larvae. As mentioned before, *P. luminescens* harbours multiple mechanisms to kill insect larvae rapidly and therefore a role of the T6SSs in larvae pathogenicity cannot be excluded but is unlikely.

Besides the PVCs, a T3SS and 4 T6SSs, *P. luminescens* also harbours 3 gene loci encoding for S-type pyocins and one loci encoding for R-type pyocins (Wilkinson et al., 2009). Pyocins are described as bacteriocins, exhibiting antibacterial activity towards related strains as it has been reported in *P. luminescens* strain TT01 (Gaudriault et al., 2004). Proteomics showed a differential representation of various pyocin related proteins in the mutant strains and bioinformatic analysis of the S-type pyocins identified a N-terminal PAAR domain in *PluDJC_04515*, *PluDJC_09855* and *PluDJC_20635*. PAAR proteins are described to take part in T6SS assembly and may have a role in translocating the effector-VgrG spike into the target cell (Shneider et al., 2013). Fusion of C-terminal toxic domains to VgrG, HcP or PAAR has been described before and interestingly, a *Salmonella* species harbours two evolved VgrGs with a C-terminal extension of a S-type pyocin family domain (Blondel et al., 2009; Salomon et al., 2014). Therefore, we considered the S-type pyocins as putative T6SS effectors, but further experiments must be carried out to confirm this hypothesis. Then, through bioinformatics analyses, we could further identify 3 novel T6SS effectors, namely $Tme_{Pl}1$–3 and the cognate immunity proteins $Tmi_{Pl}1$–3 in the genome of *P. luminescens* with a putative pore-forming activity, as it has been described for Tme, a pore-forming toxin in *Vibrio parahaemolyticus* (Fridman et al., 2020). However, no antibacterial activity of $Tme_{Pl}1$ could be determined *in vivo* upon heterologous expression in the cytoplasm. Potentially, the site of action could be in the periplasm, as it has been shown for Tle1 in *E. coli*, where periplasmic expression was toxic but cytoplasmic expression had no effect (Flaugnatti et al., 2016).

Zhang *et al.* reported in T6SS-deficient strains of the plant pathogen *Ralstonia solanacearum*, that the deletion of *tssB* reduced the strain motility and the expression of the genes *fliA, flgM, flhC* and *flhD* was significantly decreased compared to the wild type (Zhang et al., 2021). *Xanthomonas phaseoli* pv. *manihotis*, a plant pathogen of the *Xanthomonas* genus was investigated regarding T6SSs and motility and a decrease in motility upon *tssH, vgrG* and *hcP* deficiency could be observed as well (Montenegro Benavides et al., 2021). On the contrary, we observed that the motility in both *P. luminescens* Δ*tssA*1b and *P. luminescens* Δ*tssA*2, respectively, was increased and absent in the wild type; moreover, proteins related to motility were significantly more abundant in the *P. luminescens* ΔtssA1b and Δ*tssA*2 strains. These data support a direct or indirect role of T6SS-1 and T6SS-2 in the *P. luminescens* motility.

Finally, analysis of the *P. luminescens* Δ*tssA*1b and Δ*tssA*2 culture supernatants showed a change in anthraquinone production and carbapenem synthesis, both secondary metabolites are involved in interaction with bacteria (Derzelle et al., 2002; Heinrich et al., 2016). A shift in the production of secondary metabolites with antimicrobial activity upon T6SS-deficiency has not been reported before. Since the proteome data indicate a shift in different pathways related to competition, such as the T3SS, PVCs and pyocins, the regulation of *P. luminescens* secondary metabolism regarding metabolites with antimicrobial activity could be shifted as well. These data suggest *P. luminescens* harbours a complex regulatory pathway, controlling its pathogenicity. Global regulators controlling T3SSs, T6SSs and flagella synthesis have been reported before in *P. aeruginosa* (Huang et al., 2019). Whether *P. luminescens* harbours a similar regulatory pattern needs to be further investigated, as only the *fis* and *tagH* transcriptional regulators have been identified so far.

Additionally, the identification of 4 T6SS clusters and 11 effector proteins indicates an important role of the T6SSs in *P. luminescens* lifestyle. The external factors leading to the activity of the different T6SSs, however, need to be further investigated. As *Photorhabdus luminescens* is proposed as a biocontrol agent, it is crucial to understand the different mechanisms leading to the bacteria's fitness in a polymicrobial environment. With this study we can conclude a role of the T6SS-1 and T6SS-2 of *P. luminescens* in interbacterial competition. Furthermore, we propose that the T6SSs are not independent of other *Photorhabdus* fitness factors and that there is a correlation between the different fitness features such as T3SS, PVCs, R-type pyocins, secondary metabolites and flagella.

5. Conclusions

In this study, our findings on the *P. luminescens* T6SSs suggested a link between various competition mechanisms of the bacteria, thus shedding light on the complex interaction of *P. luminescens* with its hosts and competition with other bacteria in the same ecological niche. Moreover, these outcomes could help to gain more knowledge on bacterial T6SSs, in general. Finally, the application of *P. luminescens* as a biocontrol agent could be optimised by understanding how the overall *P. luminescens* virulence is activated and regulated.

Ethics approval and consent to participate

Not applicable

Funding

Inneruniversitäre Forschungsförderung („Stufe I"), University of Mainz, Germany.

CRediT authorship contribution statement

Friederike Pisarz: Conceptualization, Data curation, Investigation, Methodology, Writing – original draft. **Timo Glatter:** Formal analysis, Investigation, Methodology, Writing – original draft. **Dhana-Theresa M. Süss:** Formal analysis, Investigation. **Ralf Heermann:** Conceptualization, Investigation, Validation, Writing – review & editing. **Alice Regaiolo:** Conceptualization, Formal analysis, Funding acquisition, Investigation, Methodology, Project administration, Supervision, Validation, Writing – review & editing.

Declaration of Competing Interest

The authors declare that they have no known competing financial interests or personal relationships that could have appeared to influence the work reported in this paper

Data availability

Data are accessible via http://www.ebi.ac.uk/pride/archive/projects/PXD035720. ProteomeXchange accession: PXD035720.

Acknowledgements

We thank Kirsten Schaubruch for excellent technical assistance. We are also grateful to Christiane Grünwald (JGU Mainz) for support with the HPLC analyses.

Consent for publication

Not applicable

Appendix A. Supporting information

Supplementary data associated with this article can be found in the online version at doi:10.1016/j.microb.2024.100067.

References

Abendroth, U., Adlung, N., Otto, A., Grüneisen, B., Becher, D., Bonas, U., 2017. Identification of new protein-coding genes with a potential role in the virulence of the plant pathogen *Xanthomonas euvesicatoria*. BMC Genom. 18, 625. https://doi.org/10.1186/s12864-017-4041-7.

Andersson, J.A., Sha, J., Erova, T.E., Fitts, E.C., Ponnusamy, D., Kozlova, E.V., Kirtley, M. L., Chopra, A.K., 2017. Identification of new virulence factors and vaccine candidates for *Yersinia pestis*. Front. Cell. Infect. Microbiol. 7, 448. https://doi.org/10.3389/fcimb.2017.00448.

Barbosa, V.A.A., Lery, L.M.S., 2019. Insights into *Klebsiella pneumoniae* type VI secretion system transcriptional regulation. BMC Genom. 20, 506. https://doi.org/10.1186/s12864-019-5885-9.

Bekker-Jensen, D.B., Martínez-Val, A., Steigerwald, S., Rüther, P., Fort, K.L., Arrey, T.N., Harder, A., Makarov, A., Olsen, J.V., 2020. A compact quadrupole-orbitrap mass spectrometer with FAIMS interface improves proteome coverage in short LC gradients. Mol. Cell. Proteom. 19, 716–729. https://doi.org/10.1074/mcp.TIR119.001906.

Bernal, P., Allsopp, L.P., Filloux, A., Llamas, M.A., 2017. The *Pseudomonas putida* T6SS is a plant warden against phytopathogens. ISME J. 11, 972–987. https://doi.org/10.1038/ismej.2016.169.

Bernal, P., Furniss, R.C.D., Fecht, S., Leung, R.C.Y., Spiga, L., Mavridou, D.A.I., Filloux, A., 2021. A novel stabilization mechanism for the type VI secretion system sheath. Proc. Natl. Acad. Sci. USA 118, e2008500118. https://doi.org/10.1073/pnas.2008500118.

Bernal, P., Llamas, M.A., Filloux, A., 2018. Type VI secretion systems in plant-associated bacteria: T6SS in phytobacteria. Environ. Microbiol. 20, 1–15. https://doi.org/10.1111/1462-2920.13956.

Blondel, C.J., Jiménez, J.C., Contreras, I., Santiviago, C.A., 2009. Comparative genomic analysis uncovers 3 novel loci encoding type six secretion systems differentially distributed in *Salmonella* serotypes. BMC Genom. 10, 354. https://doi.org/10.1186/1471-2164-10-354.

Borgeaud, S., Metzger, L.C., Scrignari, T., Blokesch, M., 2015. The type VI secretion system of *Vibrio cholerae* fosters horizontal gene transfer. Science 347, 63–67. https://doi.org/10.1126/science.1260064.

Bouteiller, M., Gallique, M., Bourigault, Y., Kosta, A., Hardouin, J., Massier, S., Konto-Ghiorghi, Y., Barbey, C., Latour, X., Chane, A., Feuilloley, M., Merieau, A., 2020. Crosstalk between the type VI secretion system and the expression of class IV flagellar genes in the *Pseudomonas fluorescens* MFE01 Strain. Microorganisms 8, 622. https://doi.org/10.3390/microorganisms8050622.

Boyer, F., Fichant, G., Berthod, J., Vandenbrouck, Y., Attree, I., 2009. Dissecting the bacterial type VI secretion system by a genome wide in silico analysis: what can be learned from available microbial genomic resources? BMC Genom. 10, 104. https://doi.org/10.1186/1471-2164-10-104.

Brackmann, M., Nazarov, S., Wang, J., Basler, M., 2017. Using force to punch holes: mechanics of contractile nanomachines. Trends Cell Biol. 27, 623–632. https://doi.org/10.1016/j.tcb.2017.05.003.

Brillard, J., Duchaud, E., Boemare, N., Kunst, F., Givaudan, A., 2002. The PhlA hemolysin from the entomopathogenic bacterium *Photorhabdus luminescens* belongs to the two-partner secretion family of hemolysins. J. Bacteriol. 184, 3871–3878. https://doi.org/10.1128/JB.184.14.3871-3878.2002.

Brugirard-Ricaud, K., Duchaud, E., Givaudan, A., Girard, P.A., Kunst, F., Boemare, N., Brehelin, M., Zumbihl, R., 2005. Site-specific antiphagocytic function of the *Photorhabdus luminescens* type III secretion system during insect colonization. Cell. Microbiol. 7, 363–371. https://doi.org/10.1111/j.1462-5822.2004.00466.x.

Brunet, Y.R., Espinosa, L., Harchouni, S., Mignot, T., Cascales, E., 2013. Imaging type VI secretion-mediated bacterial killing. Cell Rep. 3, 36–41. https://doi.org/10.1016/j.celrep.2012.11.027.

Brunet, Y.R., Zoued, A., Boyer, F., Douzi, B., Cascales, E., 2015. The type VI secretion TssEFGK-VgrG phage-like baseplate is recruited to the TssJLM membrane complex via multiple contacts and serves as assembly platform for tail tube/sheath polymerization. PLoS Genet. 11, e1005545 https://doi.org/10.1371/journal.pgen.1005545.

Derzelle, S., Duchaud, E., Kunst, F., Danchin, A., Bertin, P., 2002. Identification, characterization, and regulation of a cluster of genes involved in carbapenem biosynthesis in *Photorhabdus luminescens*. Appl. Environ. Microbiol. 68, 3780–3789. https://doi.org/10.1128/AEM.68.8.3780-3789.2002.

Dix, S.R., Owen, H.J., Sun, R., Ahmad, A., Shastri, S., Spiewak, H.L., Mosby, D.J., Harris, M.J., Batters, S.L., Brooker, T.A., Tzokov, S.B., Sedelnikova, S.E., Baker, P.J., Bullough, P.A., Rice, D.W., Thomas, M.S., 2018. Structural insights into the function of type VI secretion system TssA subunits. Nat. Commun. 9, 4765. https://doi.org/10.1038/s41467-018-07247-1.

Dominelli, N., Platz, F., Heermann, R., 2022. The insect pathogen *Photorhabdus luminescens* protects plants from phytopathogenic *Fusarium graminearum* via chitin degradation. Appl. Environ. Microbiol. 88, e00645-22 https://doi.org/10.1128/aem.00645-22.

Durand, E., Nguyen, V.S., Zoued, A., Logger, L., Péhau-Arnaudet, G., Aschtgen, M.-S., Spinelli, S., Desmyter, A., Bardiaux, B., Dujeancourt, A., Roussel, A., Cambillau, C., Cascales, E., Fronzes, R., 2015. Biogenesis and structure of a type VI secretion membrane core complex. Nature 523, 555–560. https://doi.org/10.1038/nature14667.

El-Gebali, S., Mistry, J., Bateman, A., Eddy, S.R., Luciani, A., Potter, S.C., Qureshi, M., Richardson, L.J., Salazar, G.A., Smart, A., Sonnhammer, E.L.L., Hirsh, L., Paladin, L., Piovesan, D., Tosatto, S.C.E., Finn, R.D., 2019. The Pfam protein families database in 2019. Nucleic Acids Res. 47, D427–D432. https://doi.org/10.1093/nar/gky995.

Flaugnatti, N., Le, T.T.H., Canaan, S., Aschtgen, M., Nguyen, V.S., Blangy, S., Kellenberger, C., Roussel, A., Cambillau, C., Cascales, E., Journet, L., 2016. A phospholipase A $_1$ antibacterial Type VI secretion effector interacts directly with the C-terminal domain of the VgrG spike protein for delivery. Mol. Microbiol. 99, 1099–1118. https://doi.org/10.1111/mmi.13292.

Fridman, C.M., Keppel, K., Gerlic, M., Bosis, E., Salomon, D., 2020. A comparative genomics methodology reveals a widespread family of membrane-disrupting T6SS effectors. Nat. Commun. 11, 1085. https://doi.org/10.1038/s41467-020-14951-4.

Gabler, F., Nam, S., Till, S., Mirdita, M., Steinegger, M., Söding, J., Lupas, A.N., Alva, V., 2020. Protein sequence analysis using the MPI bioinformatics toolkit. Curr. Protoc. Bioinform. 72 https://doi.org/10.1002/cpbi.108.

Gaudriault, S., Thaler, J.-O., Duchaud, E., Kunst, F., Boemare, N., Givaudan, A., 2004. Identification of a P2-related prophage remnant locus of *Photorhabdus luminescens* encoding an R-type phage tail-like particle. FEMS Microbiol. Lett. 233, 223–231. https://doi.org/10.1111/j.1574-6968.2004.tb09486.x.

Glatter, T., Ludwig, C., Ahrné, E., Aebersold, R., Heck, A.J.R., Schmidt, A., 2012. Large-scale quantitative assessment of different in-solution protein digestion protocols reveals superior cleavage efficiency of tandem Lys-C/trypsin proteolysis over trypsin digestion. J. Proteome Res. 11, 5145–5156. https://doi.org/10.1021/pr300273g.

Green, E.R., Mecsas, J., 2016. Bacterial secretion systems: an overview, 4.1.13 Microbiol. Spectr. 4. https://doi.org/10.1128/microbiolspec.VMBF-0012-2015.

Heinrich, A.K., Glaeser, A., Tobias, N.J., Heermann, R., Bode, H.B., 2016. Heterogeneous regulation of bacterial natural product biosynthesis via a novel transcription factor. Heliyon 2, e00197. https://doi.org/10.1016/j.heliyon.2016.e00197.

Huang, H., Shao, X., Xie, Y., Wang, T., Zhang, Y., Wang, X., Deng, X., 2019. An integrated genomic regulatory network of virulence-related transcriptional factors in *Pseudomonas aeruginosa*. Nat. Commun. 10, 2931. https://doi.org/10.1038/s41467-019-10778-w.

Joyce, S.A., Watson, R.J., Clarke, D.J., 2006. The regulation of pathogenicity and mutualism in *Photorhabdus*. Curr. Opin. Microbiol. 9, 127–132. https://doi.org/10.1016/j.mib.2006.01.004.

Jurėnas, D., Journet, L., 2021. Activity, delivery, and diversity of Type VI secretion effectors. Mol. Microbiol. 115, 383–394. https://doi.org/10.1111/mmi.14648.

Jurėnas, D., Payelleville, A., Roghanian, M., Turnbull, K.J., Givaudan, A., Brillard, J., Hauryliuk, V., Cascales, E., 2021a. *Photorhabdus* antibacterial Rhs polymorphic toxin inhibits translation through ADP-ribosylation of 23S ribosomal RNA. Nucleic Acids Res 49, 8384–8395. https://doi.org/10.1093/nar/gkab608.

Jurėnas, D., Rosa, L.T., Rey, M., Chamot-Rooke, J., Fronzes, R., Cascales, E., 2021b. Mounting, structure and autocleavage of a type VI secretion-associated Rhs polymorphic toxin. Nat. Commun. 12, 6998. https://doi.org/10.1038/s41467-021-27388-0.

Kapitein, N., Bönemann, G., Pietrosiuk, A., Seyffer, F., Hausser, I., Locker, J.K., Mogk, A., 2013. ClpV recycles VipA/VipB tubules and prevents non-productive tubule formation to ensure efficient type VI protein secretion: Function of the AAA+ protein ClpV in type VI protein secretion. Mol. Microbiol. 87, 1013–1028. https://doi.org/10.1111/mmi.12147.

Lassak, J., Henche, A.-L., Binnenkade, L., Thormann, K.M., 2010. ArcS, the cognate sensor Kinase in an atypical Arc System of *Shewanella oneidensis* MR-1. Appl. Environ. Microbiol. 76, 3263–3274. https://doi.org/10.1128/AEM.00512-10.

Ma, L.-S., Hachani, A., Lin, J.-S., Filloux, A., Lai, E.-M., 2014. *Agrobacterium tumefaciens* deploys a superfamily of type VI secretion DNase effectors as weapons for interbacterial competition in planta. Cell Host Microbe 16, 94–104. https://doi.org/10.1016/j.chom.2014.06.002.

Machado, R.A.R., Wüthrich, D., Kuhnert, P., Arce, C.C.M., Thönen, L., Ruiz, C., Zhang, X., Robert, C.A.M., Karimi, J., Kamali, S., Ma, J., Bruggmann, R., Erb, M., 2018. Whole-genome-based revisit of *Photorhabdus* phylogeny: proposal for the elevation of most *Photorhabdus* subspecies to the species level and description of one novel species *Photorhabdus bodei* sp. nov., and one novel subspecies *Photorhabdus laumondii* subsp. *clarkei* subsp. nov. Int. J. Syst. Evol. Microbiol. 68, 2664–2681. https://doi.org/10.1099/ijsem.0.002820.

Mallik, P., Pratt, T.S., Beach, M.B., Bradley, M.D., Undamatla, J., Osuna, R., 2004. Growth phase-dependent regulation and stringent control of *fis* are conserved processes in enteric bacteria and involve a single promoter (*fisP*) in *Escherichia coli*. J. Bacteriol. 186, 122–135. https://doi.org/10.1128/JB.186.1.122-135.2004.

Mehler, J., Behringer, K.I., Rollins, R.E., Pisarz, F., Klingl, A., Henle, T., Heermann, R., Becker, N.S., Hellwig, M., Lassak, J., 2022. Identification of *Pseudomonas asiatica*

subsp. *bavariensis* str. JM1 as the first N_{ε} -carboxy(m)ethyllysine-degrading soil bacterium. Environ. Microbiol., 1462-2920.16079 https://doi.org/10.1111/1462-2920.16079.

Montenegro Benavides, N.A., Alvarez, B., A., Arrieta-Ortiz, M.L., Rodriguez-R, L.M., Botero, D., Tabima, J.F., Castiblanco, L., Trujillo, C., Restrepo, S., Bernal, A., 2021. The type VI secretion system of *Xanthomonas phaseoli* pv. *manihotis* is involved in virulence and in vitro motility. BMC Microbiol 21, 14. https://doi.org/10.1186/s12866-020-02066-1.

Mougous, J.D., Cuff, M.E., Raunser, S., Shen, A., Zhou, M., Gifford, C.A., Goodman, A.L., Joachimiak, G., Ordoñez, C.L., Lory, S., Walz, T., Joachimiak, A., Mekalanos, J.J., 2006. A virulence locus of *Pseudomonas aeruginosa* encodes a protein secretion apparatus. Science 312, 1526–1530. https://doi.org/10.1126/science.1128393.

Potter, S.C., Luciani, A., Eddy, S.R., Park, Y., Lopez, R., Finn, R.D., 2018. HMMER web server: 2018 update. Nucleic Acids Res 46, W200–W204. https://doi.org/10.1093/nar/gky448.

Pukatzki, S., Ma, A.T., Revel, A.T., Sturtevant, D., Mekalanos, J.J., 2007. Type VI secretion system translocates a phage tail spike-like protein into target cells where it cross-links actin. Proc. Natl. Acad. Sci. 104, 15508–15513. https://doi.org/10.1073/pnas.0706532104.

Pukatzki, S., Ma, A.T., Sturtevant, D., Krastins, B., Sarracino, D., Nelson, W.C., Heidelberg, J.F., Mekalanos, J.J., 2006. Identification of a conserved bacterial protein secretion system in *Vibrio cholerae* using the *Dictyostelium* host model system. Proc. Natl. Acad. Sci. 103, 1528–1533. https://doi.org/10.1073/pnas.0510322103.

Ray, A., Schwartz, N., Souza Santos, M., Zhang, J., Orth, K., Salomon, D., 2017. Type VI secretion system MIX-effectors carry both antibacterial and anti-eukaryotic activities. EMBO Rep. 18, 1978–1990. https://doi.org/10.15252/embr.201744226.

Regaiolo, A., Dominelli, N., Andresen, K., Heermann, R., 2020. The biocontrol agent and insect pathogen *Photorhabdus luminescens* interacts with plant roots. Appl. Environ. Microbiol. 86, e00891-20 https://doi.org/10.1128/AEM.00891-20.

Rodou, A., Ankrah, D.O., Stathopoulos, C., 2010. Toxins and secretion systems of *Photorhabdus luminescens*. Toxins 2, 1250–1264. https://doi.org/10.3390/toxins2061250.

Russell, A.B., LeRoux, M., Hathazi, K., Agnello, D.M., Ishikawa, T., Wiggins, P.A., Wai, S. N., Mougous, J.D., 2013. Diverse type VI secretion phospholipases are functionally plastic antibacterial effectors. Nature 496, 508–512. https://doi.org/10.1038/nature12074.

Russell, A.B., Peterson, S.B., Mougous, J.D., 2014. Type VI secretion system effectors: poisons with a purpose. Nat. Rev. Microbiol. 12, 137–148. https://doi.org/10.1038/nrmicro3185.

Salomon, D., Kinch, L.N., Trudgian, D.C., Guo, X., Klimko, J.A., Grishin, N.V., Mirzaei, H., Orth, K., 2014. Marker for type VI secretion system effectors. Proc. Natl. Acad. Sci. 111, 9271–9276. https://doi.org/10.1073/pnas.1406110111.

Schneider, J.P., Nazarov, S., Adaixo, R., Liuzzo, M., Ringel, P.D., Stahlberg, H., Basler, M., 2019. Diverse roles of TssA-like proteins in the assembly of bacterial type VI secretion systems. EMBO J. 38 https://doi.org/10.15252/embj.2018100825.

Shneider, M.M., Buth, S.A., Ho, B.T., Basler, M., Mekalanos, J.J., Leiman, P.G., 2013. PAAR-repeat proteins sharpen and diversify the type VI secretion system spike. Nature 500, 350–353. https://doi.org/10.1038/nature12453.

Wang, J., Brackmann, M., Castaño-Díez, D., Kudryashev, M., Goldie, K.N., Maier, T., Stahlberg, H., Basler, M., 2017. Cryo-EM structure of the extended type VI secretion system sheath–tube complex. Nat. Microbiol. 2, 1507–1512. https://doi.org/10.1038/s41564-017-0020-7.

Wilkinson, P., Waterfield, N.R., Crossman, L., Corton, C., Sanchez-Contreras, M., Vlisidou, I., Barron, A., Bignell, A., Clark, L., Ormond, D., Mayho, M., Bason, N., Smith, F., Simmonds, M., Churcher, C., Harris, D., Thompson, N.R., Quail, M., Parkhill, J., ffrench-Constant, R.H., 2009. Comparative genomics of the emerging human pathogen *Photorhabdus asymbiotica* with the insect pathogen *Photorhabdus luminescens*. BMC Genom. 10, 302. https://doi.org/10.1186/1471-2164-10-302.

Williams, J.S., Thomas, M., Clarke, D.J., 2005. The gene *stlA* encodes a phenylalanine ammonia-lyase that is involved in the production of a stilbene antibiotic in *Photorhabdus luminescens* TT01. Microbiology 151, 2543–2550. https://doi.org/10.1099/mic.0.28136-0.

Yang, G., Dowling, A.J., Gerike, U., ffrench-Constant, R.H., Waterfield, N.R., 2006. *Photorhabdus* virulence cassettes confer injectable insecticidal activity against the wax moth. J. Bacteriol. 188, 2254–2261. https://doi.org/10.1128/JB.188.6.2254-2261.2006.

Zamora-Lagos, M.-A., Eckstein, S., Langer, A., Gazanis, A., Pfeiffer, F., Habermann, B., Heermann, R., 2018. Phenotypic and genomic comparison of *Photorhabdus luminescens* subsp. *laumondii* TT01 and a widely used rifampicin-resistant *Photorhabdus luminescens* laboratory strain. BMC Genom. 19, 854. https://doi.org/10.1186/s12864-018-5121-z.

Zhang, A., Han, Y., Huang, Y., Hu, X., Liu, P., Liu, X., Kan, B., Liang, W., 2021. *vgrG* is separately transcribed from *hcp* in T6SS orphan clusters and is under the regulation of IHF and HapR. Biochem. Biophys. Res. Commun. 559, 15–20. https://doi.org/10.1016/j.bbrc.2021.04.092.

Zhang, J., Guan, J., Wang, M., Li, G., Djordjevic, M., Tai, C., Wang, H., Deng, Z., Chen, Z., Ou, H.-Y., 2023. SecReT6 update: a comprehensive resource of bacterial Type VI Secretion Systems. Sci. China Life Sci. 66, 626–634. https://doi.org/10.1007/s11427-022-2172-x.

Zimmermann, L., Stephens, A., Nam, S.-Z., Rau, D., Kübler, J., Lozajic, M., Gabler, F., Söding, J., Lupas, A.N., Alva, V., 2018. A Completely Reimplemented MPI Bioinformatics Toolkit with a New HHpred Server at its Core. J. Mol. Biol. 430, 2237–2243. https://doi.org/10.1016/j.jmb.2017.12.007.

Zoued, A., Durand, E., Brunet, Y.R., Spinelli, S., Douzi, B., Guzzo, M., Flaugnatti, N., Legrand, P., Journet, L., Fronzes, R., Mignot, T., Cambillau, C., Cascales, E., 2016. Priming and polymerization of a bacterial contractile tail structure. Nature 531, 59–63. https://doi.org/10.1038/nature17182.

3. The role of the T6SS-3 in insect pathogenicity and bacterial competition in *P. luminescens*

Friederike Pisarz[1], Kira Götz[1], Dhana-Theresa M. Süss[1], Ralf Heermann[1,2], Alice Regaiolo[1]

[1] Johannes Gutenberg University Mainz, Institute of Molecular Physiology, Microbiology and Biotechnology, Hanns-Dieter-Hüsch-Weg 17, 55128 Mainz, Germany

[2] Institute for Biotechnology and Drug Research gGmbH (IBWF), Hanns-Dieter-Hüsch-Weg 17, 55128 Mainz, Germany

3.1 Abstract

The Type VI secretion system (T6SS) is a complex nanomolecular weapon used by Gram-negative bacteria for injecting effectors into target cells. While the T6SS in *Photorhabdus luminescens* is poorly understood, this study explores the role of the T6SS-3 cluster in the strain DJC. Bioinformatic analysis identified missing core components, initially suggesting non-functionality. However, homologues for some components were identified, thus suggesting the T6SS-3 is functional. Subsequent experiments revealed protein-protein interactions between effectors (Tle proteins) and VgrG proteins, indicating that T6SS-3 may deliver a variety of effectors using a heterotrimeric tip structure. Only one effector, Tle4A, was shown do deploy antibacterial activity. Additionally, fluorescence microscopy of mCherry-tagged reporter strains confirmed T6SS-3 expression under stress conditions such as pH changes and high salt concentrations, highlighting its potential role in environmental adaptation and host interaction. Despite the absence of key T6SS components, these findings suggest that the T6SS-3 in *P. luminescens* could function in bacterial competition and environmental stress responses, unveiling a novel subfamily of T6SSs. This study provides new insights into the molecular mechanisms and regulation of T6SS-3, contributing to the broader understanding of bacterial secretion systems and their ecological roles.

3.2 Introduction

The Type VI secretion system is a complex, membrane-bound nanomolecular weapon used by Gram-negative bacteria to inject toxins, so-called effectors, into a neighbouring prokaryotic or eukaryotic target cell (Mougous et al., 2006; Pukatzki et al., 2006; Russell et al., 2014). Structurally, the T6SS resembles a contractile tail structure, similar to bacteriophages (Basler and Mekalanos, 2012). It consists of a membrane bound complex, a baseplate, an inner tube composed of HcP proteins surrounded by a sheath and an effector loaded tip (Russell et al., 2014; Brunet et al., 2015; Durand et al., 2015; Wang et al., 2017). Upon activation of the T6SS, the sheath contracts and propels the inner tube inside the target cell to deliver diverse effectors (Kudryashev et al., 2015; Vettiger et al., 2017; Wang et al., 2017).

To recruit effectors to the T6SS, three different core components- VgrG (valine-glycine repeat protein G), HcP (hemolysin-coregulated protein) and PAAR (proline-alanine-alanine-arginine repeat proteins) but also so-called adaptor proteins are essential (Bondage et al., 2016; Ruiz et al., 2015; Wood et al., 2019). During the assembly of the tube, rings of hexameric arranged HcP proteins placed on top of each other form the tube, with a hollow centre that enables the transport of effectors bound inside this tube (Silverman et al., 2013). However, effector transport along the inner lumen (~ 40 Å) is restricted to small effectors like Tse2 (~ 18 kDa), an effector found in *P. aeruginosa*, whereas larger effectors have to be transported through direct or indirect binding to the tip of the T6SS (Silverman et al., 2013; Mougous et al., 2006; Cherrak et al., 2019). While direct binding of effectors to the VgrG tip is often mediated through a effector binding domain like a transthyretin domain (TTR), indirect binding can be carried out through adaptor proteins belonging to the Eag, Tap or Tla family (Berni et al., 2019; Flaugnatti et al., 2020; Shneider et al., 2013; Unterweger et al., 2017).

Tle (Type VI lipase effector) proteins have been previously described as effectors delivered by the T6SS and bound directly to VgrG or indirectly to Tla3, a cytoplasmic adaptor characterized by a DUF2875 domain (Berni et al., 2019; Flaugnatti et al., 2020). Phylogenetic analysis of the Tle family pointed out five different Tle effectors. Tle1-4 deploy esterase and lipase activity characterized by a catalytic GxSxG motif. In contrary, the class of Tle5 proteins deploy

phospholipase activity and are characterized by a catalytic HxKxxxxD motif (Russell et al., 2013). Initial studies suggested that the effectors of the lipase superfamily mainly play a role in interbacterial competition as it has been observed for $Tle2^{VC}$ of *Vibrio cholerae* (Dong et al., 2013). However, new studies identified: i) the trans-kingdom lipase effector TplE in *P. aeruginosa*, belonging to the Tle4 family and able to target the endoplasmic reticulum as well as ii) the Tle5 family effector PldB, able to foster host cell invasion through phospholipase D activity (Jiang et al., 2016; Jiang et al., 2014).

While the insect pathogenic bacterium *Photorhabdus luminescens* is well described with respect to its insect pathogenicity, toxin-antitoxins as well as PVCs, still many aspects like the role of its T6SSs remain unknown (Brillard et al., 2002; Rodou et al., 2010). First studies identified the antibacterial effector Tre23, which is able to inhibit translation through ADP-ribosylation of 23S ribosomal RNA and binds to the VgrG tip through the interaction with EagR (Jurėnas et al., 2021a; Jurėnas et al., 2021b). To gain insight whether *P. luminescens* also carries Tle effectors, additional bioinformatic analysis and protein activity studies were performed. Additionally, a role of the effectors was studied through fluorescence microscopy and thereby, a better understanding of one of the T6SS found in *P. luminescens* could be achieved. Thus, by understanding the role of T6SS effectors in *P. luminescens*, particularly potential Tle effectors, could not only reveal new insights into the bacterium's interbacterial and host interactions but also pave the way for innovative biotechnological applications, such as developing novel antimicrobial strategies or enhancing symbiotic systems.

3.3 Material and methods

Bioinformatics analyses

Gene and protein sequences of *P. luminescens* subs. *luminescens* strain DJC were retrieved from the NCBI database (https://www.ncbi.nlm.nih.gov/). To identify protein homology, BLASTP analyses were performed (Boratyn et al., 2013). To identify putative protein functionality and protein functional motifs, additional analyses were performed using HHPred, HMMER and NCBI CDD (Wang et al., 2023; Gabler et al., 2020; Zimmermann et al., 2018; Potter et al., 2018). Protein homology alignments were performed with ClustalOmega and visualized with ESPript 3.0 (Madeira et al., 2022; Robert and Gouet, 2014). Structure predictions were performed with AlphaFold2 and visualized with ChimeraX (Jumper et al., 2021; Mirdita et al., 2022; Meng et al., 2023). Predicted alignment error of different protein structure predictions are shown in **Fig. S3.1**.

Bacterial strains and cultivation

P. luminescens strain DJC 1° and 2° wildtype cells were used in this study (Zamora-Lagos et al., 2018). *E. coli* strains DH5α (λ pir), BL21 star, Top10 tnGFP and BTH101 were used for plasmid construction, toxicity assays and BACTH analyses. Unless other stated, bacteria were cultivated under aerobically conditions at 30°C (*P. luminescens*) or 37°C (*E. coli*) in LB medium (1% [w/v] tryptone, 0.5% [w/v] yeast extract, 0.5% [w/v] NaCl) or CASO medium (1.5 % [w/v] peptone, 0.5 % [w/v] peptone from soy, 0.5 % [w/v] NaCl). If required, the media was supplemented with respective antibiotics. For protein expression and repression, 0.1% arabinose or 0.1% glucose were respectively added to the media.

To generate a reporter strain in *P. luminescens* strain DJC 1° and 2° cells, the pNTPs138-R6KT plasmid was used. Briefly, in-frame insertion of *mCherry* in front of *tssC3* was obtained through conjugation and double homologous conjugation as previously described (Lassak et al., 2010).

Generation of plasmids

To perform BACTH analyses, *tle2A, tle2B, tle4A, tle4B, vgrG6, vgrG7 and vgrG8* were cloned into the pKNT25 and pUT18 plasmids. To amplify *tle2A* and *tle2B,* the primer pairs Tle2A-XbaI-B2H + Tle2-BamHI-B2H and Tle2B-XbaI-B2H + Tle2-BamHI-B2H were used and cloned into the pKNT25 plasmid. To generate the plasmids pKNT25::Tle4A and pKNT25::Tle4B, *tle4A* and *tle4B* were amplified using the primer pairs Tle4A-XbaI-B2H + Tle4A-XmaI-B2H and Tle4B-XbaI-B2H + Tle4B-XmaI-B2H. The genes encoding for VgrG6, VgrG7 and VgrG8 were amplified using the primer pairs VgrG6/7-XbaI-B2H + VgrG6-BamHI-B2H, VgrG6/7-XbaI-B2H + VgrG7-BamHI-B2H and VgrG8-PstI-B2H + VgrG8-SalI-B2H and further cloned into the pUT18 and pKNT25 plasmid. Correct insertion was confirmed by PCR using the primers BACTH-check-fwd, pUT18/C-check-rev and pKNT25-check-rev, followed by DNA sequencing. For toxicity assays, genes encoding respective proteins were cloned into the pBAD24 expression plasmid. Genomic *tle2A* was amplified with the primer pair Tle2A-EcoRI-fwd + Tle2-XbaI-rev, genomic *tle2B* with Tle2B-XmaI-fwd + Tle2-XbaI-rev*,* genomic *tle4A* with the primers Tle4A-NcoI-fwd + Tle4A-PstI-rev and *tle4B* with Tle4B-NcoI-fwd + Tle4B-PstI-rev and following cloned into the pBAD24 plasmid. For the expression plasmids of VgrG6-8, genomic *vgrG6* was amplified with the primer pair VgrG6-XmaI-fwd + VgrG6-XbaI-rev, *vgrG7* with the primers VgrG7/8-XbaI-fwd + VgrG7-SalI-rev and *vgrG8* with the primer pair VgrG7/8-XbaI-fwd + VgrG8-SalI-rev Correct insertion was verified by PCR using the pBAD-fwd and pBAD-rev primer pair, followed by DNA sequencing.

To construct reporter strains in *P. luminescens*, the pNTPs138-R6KT plasmid was used. Briefly, *mCherry* was amplified with the primer pair mCherry-EcoRI-fwd + mCherry-EagI-rev, flanking region A (FA) was amplified with the primer pair FA-TssC3-Spe1-fwd + FA-TssC3-mcs-rev and flanking region B (FB) with the primer pair FB-TssC3-mcs-fwd + FB-TssC3-SalI-rev. First the plasmid pNTPs138-R6KT::TssC3-FAB was constructed through restriction and ligation and following the reporter plasmid pNTPs138-R6KT::TssC3-mCherry through restriction and ligation of the *mCherry* fragment in the multiple cloning site of the pNTPs138-R6KT::TssC3-FAB plasmid. Correct insertion was verified using the primer pair pNTPs-check-fwd and

pNTPs-check-rev, followed by DNA sequencing. Oligonucleotides sequences are listed in in the **Table 3.1**.

Table 3.1: **Sequences of primers used for this study.**

Oligo	Sequence 5' – 3'
Tle2-BamHI-B2H	CGTTGGATCCTCATTTCTCAGGCTCCTT
Tle2A-XbaI-B2H	CCTATCTAGAATGTCCGAAATAAAACATCATGA
Tle2B-XbaI-B2H	CGTTTCTAGAATGTCCGAAATAACATATGAAATGA
Tle4A-XbaI-B2H	CTAATCTAGAATGAGTGAGCCGAAAG
Tle4A-XmaI-B2H	TTGACCCGGGTCAATTTTCACCTTTCACC
Tle4B-XbaI-B2H	CGTTTCTAGAATGACTGATTCATCAGAAAAAGT
Tle4B-XmaI-B2H	AACGCCCGGGCTATTCATCGGGATAAGCC
VgrG6/7-XbaI-B2H	CGTTTCTAGAATGACGAACCTAACACC
VgrG6-BamHI-B2H	CCTAGGATCCTTACTCCTCATCTTTTATTTTCAATTG
VgrG7-BamHI-B2H	CGTTGGATCCCTATTTCCTCAAAACAAACCC
VgrG8-PstI-B2H	TTCCTGCAGATGACGAACCTAACACCGATGATCATC
VgrG8-SalI-B2H	TTCGTCGACTCACTCCTTACCTTCTTTTAAATAAAACTTTATTG
Tle2A-EcoRI-fwd	TCTGAATTCATGCATCATCACCACCACCATATGTCCGAAATAAAACATC ATGA
Tle2-XbaI-rev	CTCTCTAGATCATTTCTCAGGCTCCT
Tle2B-XmaI-fwd	TCTCCCGGGATGCATCATCACCACCACCATATGTCCGAAATAACATATG AAATGA
Tle4A-NcoI-fwd	CGTTCCATGGCACCACCACCACCACCACATGAGTGAGCCGAAAG
Tle4A-PstI-rev	GCTTCTGCAGTCAATTTTCACCTTTCACC
Tle4B-NcoI-fwd	CGTTCCATGGCACCACCACCACCACCACATGACTGATTCATCAGAAA AAGT
Tle4B-PstI-rev	GCTTCTGCAGCTATTCATCGGGATAAGCC
VgrG6-XmaI-fwd	CCTCCCGGGATGCATCACCATCACCATCACCATCACCATCACCATCAC ACGAACCTAACACCGAT
VgrG6-XbaI-rev	TTCTCTAGATTACTCCTCATCTTTTATTTTCAATTGACTG
VgrG7/8-XbaI-fwd	TTCTCTAGAATGCATCACCATCACCATCACCATCACCATCACCATCAC ACGAACCTAACACCGAT
VgrG7-SalI-rev	TTCGTCGACCTATTTCCTCAAAACAAACCCTTTCAT
VgrG8-SalI-rev	TTCGTCGACTCACTCCTTACCTTCTTTTAAATAAAACTTTATTG
FA-TssC3-Spe1-fwd	GGTACTAGTAGTCCCGCGATTAACTT
FA-TssC3-mcs-rev	TTCTTACTACTGCAGAGAATTCGCGGCTCGGCCGAACGATAATCCTA TCTCCTGATATATACCG
FB-TssC3-mcs-fwd	TCGTTCGGCCGAGCCGCGAATTCTCTGCAGTAGTAAGAAATGACTGA ACAACAAACCG

FB-TssC3-SalI-rev	TGTGTCGACGAAACTCAGGGTGATGC
mCherry-EcoRI-fwd	CCTGAATTCAAGCTTTTATTTGTATAGTTCATCCAT
mCherry-EagI-rev	ACCCGGCCGATGGCAACTAGCGGC
BACTH-check-fwd	GTGAGCGGATAACAATTTCAC
pUT18/C-check-rev	CTTAACTATGCGGCATCAGAGCAG
pKNT25-check-rev	CTTGCGGCGATACTGCACGGCATAG
pBAD-fwd	GCCGTCACTGCGTCTTTTACTGG
pBAD-rev	CAGAAGTGAAACGCCGTAGCG
pNTPs-check-fwd	TGCTTCCGGCTCGTATG
pNTPs-check-rev	GGACTGGCCGTCGTTTTAC

Bacterial adenylate cyclase two-hybrid (BACTH) assays

To investigate the interaction of the Tle effectors with the different VgrGs, a bacterial adenylate cyclase two-hybrid (BACTH) analysis was performed according to the manufacturer's instructions (Euromedex, Souffelweyersheim). In summary, the genes encoding the proteins of interest (X and Y) were PCR-amplified from the *P. luminescens* DJC genome and subsequently cloned into the plasmids pKNT25 and pUT18. *E. coli* BTH101 cells were co-transformed with these plasmids and cultured on LB agar plates containing 100 µg/ml carbenicillin and 50 µg/ml kanamycin. A 10 µl aliquot of the overnight culture was then spotted onto LB agar plates containing 100 µg/ml carbenicillin, 50 µg/ml kanamycin, 0.5 mM IPTG, and 40 µg/ml X-Gal, followed by incubation at 30°C for 24 hours. The presence of protein interactions was indicated by blue colonies, while the absence of interactions resulted in white colonies. For controls, cells were co-transformed with pUT18C-zip and pKT25-zip as a positive control and with pKT25 and pUT18C as a negative control.

T6SS effector toxicity assays

Following, toxicity of the different Tle's and VgrG's was monitored by performed toxicity assays in bacterial cells as previously published (Pisarz et al., 2024). Briefly, *E. coli* BL21 star cells were transformed with the pBAD24 expression plasmids described and cultivated overnight in media containing the respective antibiotics. The culture OD_{600} was then adjusted to 0.1 and 200 µl of each strain was transferred into a 96-well plate (TC-plate 96 well standard, Sarstedt).

The growth was measured over 7 hours at 30°C with double orbital shaking (amplitude of 1.5 mm, frequency of 180 rpm) in a microplate reader (Tecan). Absorbance at 600 nm was measured every 10 minutes. Protein production was induced or repressed after 2 hours with the addition of 0.1% arabinose or 0.1% glucose, respectively. Addition of ddH_2O served as a control. Each experiment included three biological replicates, each with three technical replicates. Cells containing the empty pBAD24ø plasmid served as control for bacterial growth.

P. luminescens T6SS-3 activity screenings

To determine activity of the T6SS-3 in *P. luminescens,* fluorescence microscopy was performed of 1° and 2° wildtype as well as *tssC3*::*mCherry* reporter strains upon cultivation under different conditions. Briefly, overnight cultures of respective strains cultivated in LB medium were adjusted to an OD_{600} of 0.1 in 5 ml of cultivation medium (**Table 3.2**). The strains were cultivated for 5 h at 30°C unless other stated and following 1.5 ml cells collected and washed 2x in 1x PBS buffer (155 mM NaCl, 2.7 mM Na_2HPO_4 - 7 H_2O, 1.5 mM KH_2PO_4). 10 µl were then spotted on a microscopy slide with an agar pad and covered with a glass coverslip. Fluorescence microscopy was performed with the Leica DMi8 Fluorescence Imaging System with an exposure time of 500 ms and the Texas Red fluorescent filter. For each tested condition five pictures were taken and evaluated with ImageJ by detecting total amount of cells and fluorescent cells. For the preliminary screening, each test was performed once.

Table 3.2: Culture conditions tested in activity screening of the T6SS-3 in *Photorhabdus luminescens*

Condition	Cultivation medium	Cultivation conditions
Control	LB (pH = 7)	5 h, 30°C, 200 rpm
Stationary phase	LB (pH = 7)	24 h, 30°C, 200 rpm
Osmotic stress	LB with 0.5 M NaCl	5 h, 30°C, 200 rpm
	LB without NaCl	5 h, 30°C, 200 rpm
Nutrient limitation	0.1x LB diluted in 1x PBS	5 h, 30°C, 200 rpm
pH	LB (pH = 5)	5 h, 30°C, 200 rpm
	LB (pH = 9)	5 h, 30°C, 200 rpm
Temperature	LB (pH = 7)	5 h, 26°C, 200 rpm
	LB (pH = 7)	5 h, 37°C, 200 rpm
Signalling molecules	LB + 3% PRE (pH = 7)	5 h, 30°C, 200 rpm
	Larvae extract medium	5 h, 30°C, 200 rpm

3.4 Results

Genomic region of the T6SS-3 gene cluster

Initial studies on the genomic organisation of the T6SS in *P. luminescens* strain DJC identified four different gene clusters encoding for structural components (**Fig. 2.1**). The T6SS-3 was identified within the coding region from *PluDJC_16475* to *PluDJC_16665*. T6SS-3 comprises a total of 37 genes encoding for T6SS core components, effectors, immunity proteins, adaptor proteins or proteins of unknown function (hypothetical proteins). A preliminary analysis showed that not all T6SS-structural components were present. However, four different effectors of the lipase family were identified within this cluster, which had not been described before in other bacteria. Therefore, subsequent studies should shed more light on this unique T6SS gene cluster.

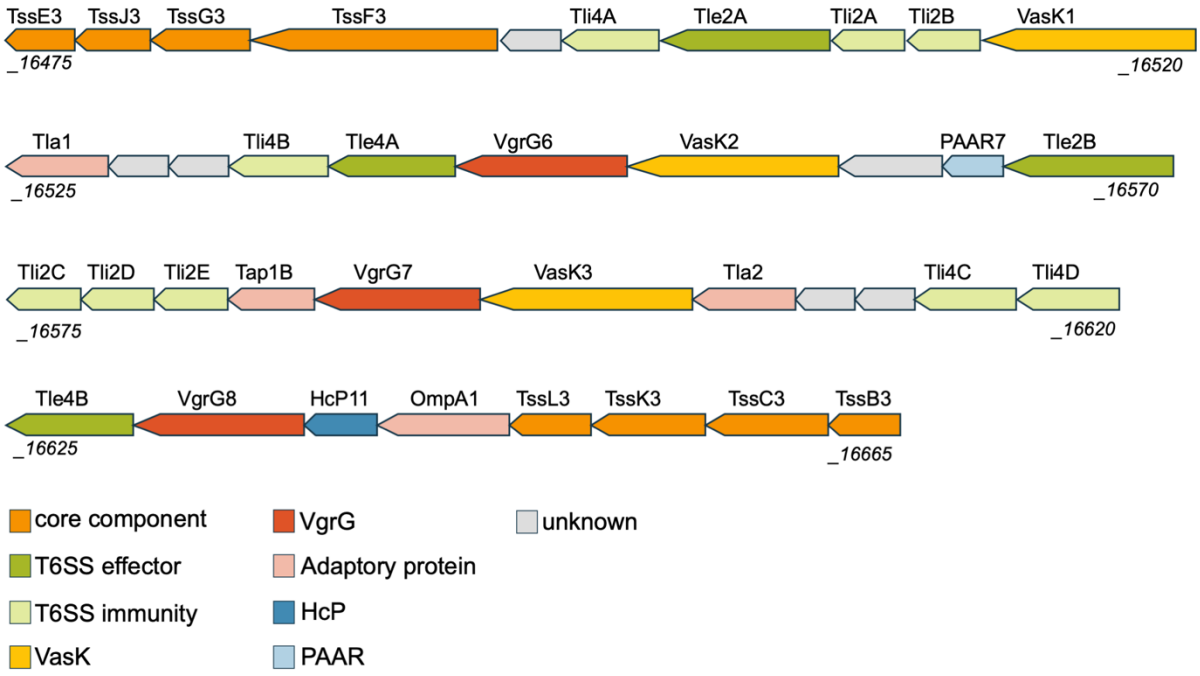

Figure 3.1: The T6SS-3 of *P. luminescens* strain DJC. Genomic organisation of the T6SS-3. Gene numbers are shown below, and protein names are shown above the arrows. Genes encoding core components are shown in orange, genes encoding T6SS effectors in dark green and genes encoding T6SS immunity proteins in light green. Genes encoding VgrG's are shown in dark red and adaptor proteins in light red. HcP encoding genes are shown in dark blue and PAAR proteins in light blue. Genes encoding for unknown proteins are shown in grey.

A first structural operon is found from *PluDJC_16475* – *PluDJC_16490* encoding for the core components TssE3, TssJ3, TssG3 and TssF3, with a second structural operon found from *PluDJC_16650* – *PluDJC_16665* encoding for the core components TssL3, TssK3, TssC3 and TssB3 (**Fig. 3.1**). Between those structural operons, an effector operon is located, encoding for i) the lipase effector Tle2A, Tle2B, Tle4A and Tle4B, ii) the immunity proteins Tli2A-E and Tli4A-D, iii) the adaptor proteins Tap1B, OmpA1, Tla3A and Tla3B, iv) the tip proteins VgrG6-8, PAAR7 and HcP11 and v) 5 hypothetical proteins with unknown functions. Analysis of the hypothetical proteins could not identify a known domain, therefore the question about their role in the T6SS-3 remains open. Additional analysis on the VasK1-3 proteins identified a sequence homology of 91.55 – 97.95 %, and the domains IcmF-related and C-terminally IcmF_C, which were also identified in TssM1 of the T6SS-1 (**Fig. S3.2A**). Yet, the IcmF-related_N domain found in TssM1 is absent in all VasK proteins of the T6SS-3. *PluDJC_16525* and *PluDJC_16600* were described before as proteins with unknown functions. However, a DUF2875 domain was identified, which is also found in the adaptor protein Tla of *P. aeruginosa* and therefore, the proteins were renamed to Tla1 and Tla2, respectively.

Lastly, through additional analyses of the VgrG proteins a C-terminal domain of unknown function could be identified (DUF2345), as well as a C-terminal extension of approx. 30 - 70 amino acids (**Fig. 3.2A**). An overall sequence homology of 80.03% was determined for VgrG6-VgrG7, 79.77% for VgrG7-VgrG8 and 92.87% for VgrG6-VgrG8. Upon comparison of the sequence without the DUF2345 domain and C-terminal extension, a sequence identity of 94 – 98 % was determined. However, comparison of the DUF2345 sequence resulted in a low sequence identity of VgrG6 and VgrG7 with only 32.65% and VgrG7-VgrG8 with 35%, whereas the DUF2345 sequence of VgrG6 and VgrG8 share a 97.97% sequence identity (**Fig. 3.2B**). Lastly, comparison of the C-terminal extension showed an overall low sequence identity, ranging from 15 – 28%. Additional structure predictions of VgrG6-8 indicate the structural similarity of the N-terminal region and the DUF2345 domain, whereas the C-terminal extension differs greatly among the three different VgrGs (**Fig. 3.2C**). While the C-terminal extension of

VgrG7 consists of a single α-helix, a transthyretin-like fold (TTR) was observed for VgrG6 and VgrG8 in the C-terminal extension, similar to VgrG1 from *E. coli* (Flaugnatti et al., 2020).

A

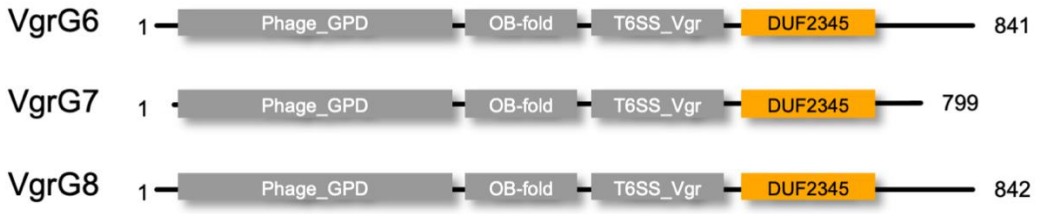

B

	VgrG6	VgrG7	VgrG8
VgrG6	100.00	80.03	92.87
VgrG7	80.03	100.00	79.77
VgrG8	92.87	79.77	100.00

N-term	VgrG6	VgrG7	VgrG8
VgrG6	100.00	95.29	98.71
VgrG7	95.29	100.00	94.48
VgrG8	98.71	94.48	100.00

DUF2345	VgrG6	VgrG7	VgrG8
VgrG6	100.00	32.65	97.97
VgrG7	32.65	100.00	35.00
VgrG8	97.97	35.00	100.00

C-term	VgrG6	VgrG7	VgrG8
VgrG6	100.00	15.62	28.07
VgrG7	15.62	100.00	25.00
VgrG8	28.07	25.00	100.00

C

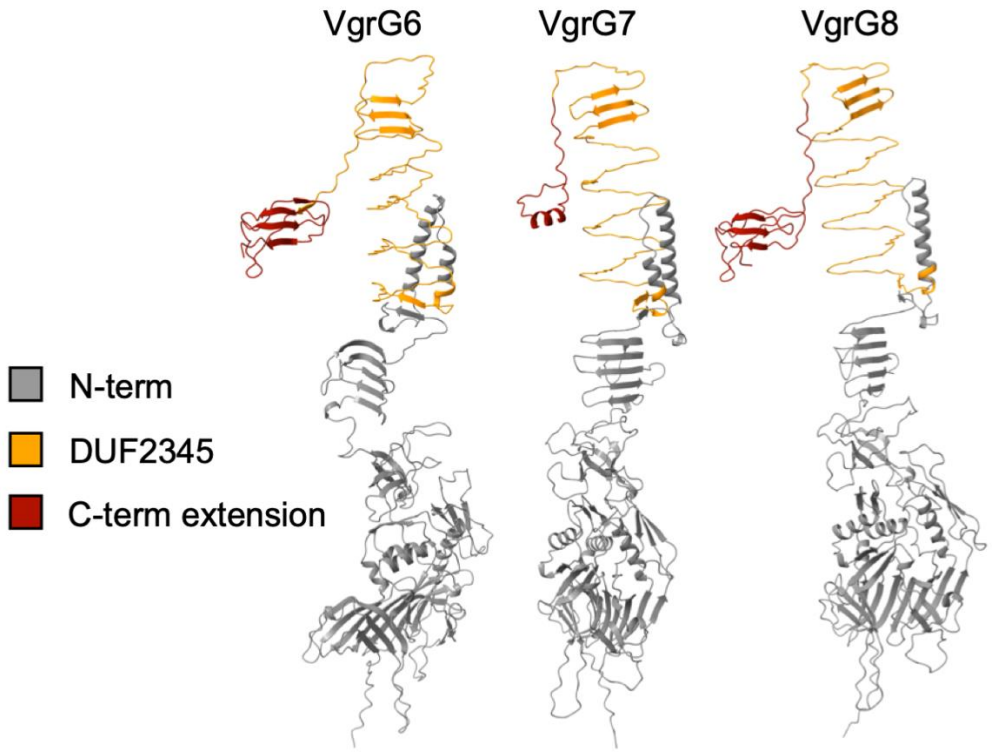

Figure 3.2: Structure prediction and domain organization of VgrG6, VgrG7 and VgrG8. A: Protein sequence of VgrG6, VgrG7 and VgrG8 are shown with the four identified domains Phage_GDP, OB-fold, T6SS_Vgr and DUF2345 (orange). **B**: Sequence homology of the different VgrGs determined through MSA using Clustal Omega. Sequence homology is shown in percent [%] for the complete amino acid sequence, the N-terminal part (Phage_GDP, OB-fold and T6SS_Vgr domains), DUF2345 domain and the C-terminal extension. **C**: Protein structure predictions of VgrG6-8 via AlphaFold2. The DUF2345 domain is shown in orange and the C-terminal extension is shown in red.

Bioinformatic insights into lipase effectors of T6SS-3

In order to gain insights into the role of the different lipase effectors found encoded in the T6SS-3, bioinformatic analysis were performed to determine putative binding sites, domains or putative enzymatic activities.

Screening for known domains via HMMER and HHPred analysis, two DUF2235 domains were identified in the effectors Tle2A and Tle2B, which have been previously described in the class of Tle2 effectors (**Fig. 3.3 and 3.4**). Following, MSA with known Tle effectors identified the conserved catalytic motif GxSxG in the first DUF2235 domain of Tle2A and Tle2B with the conserved amino acids GFSRG. Additional AlphaFold2 predictions of the effectors with consequent structural comparison of Tle1 of *P. aeruginosa* identified the catalytic triad Ser_{245} – Asp_{299} – His_{377} in Tle2A and Ser_{249} – Asp_{303} – His_{381} in Tle2B (**Fig. 3.3**).

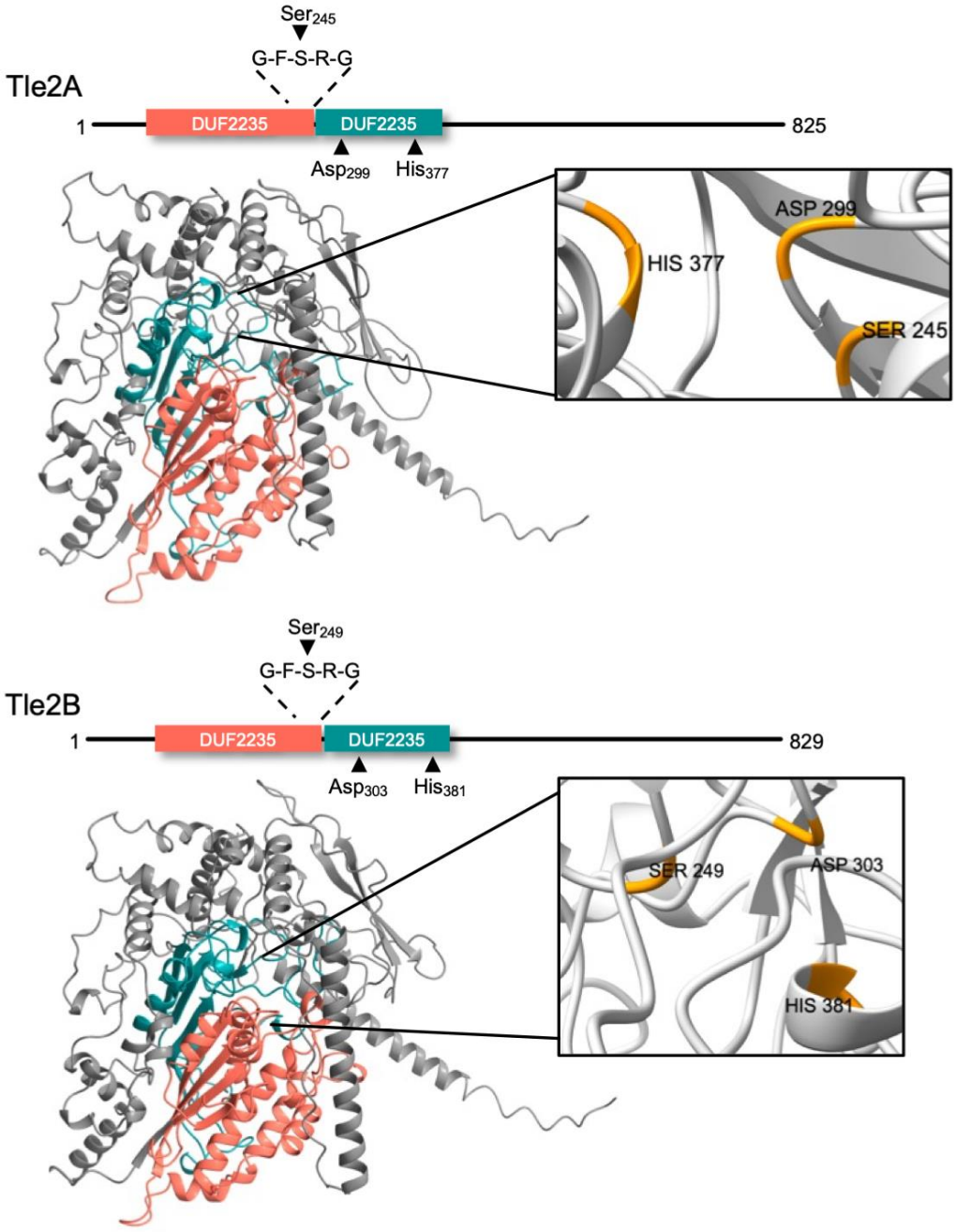

Figure 3.3: Domain organization and structure of the putative lipase effectors Tle2A and Tle2B. Protein sequences are shown with the DUF2235 domains, the conserved motif GFSRG and the catalytic triad Ser-Asp-His is marked by arrows. Protein structure prediction was performed with AlphaFold2, respective domains are coloured as indicated in the protein sequence. The catalytic triad is shown in orange.

Analysis of the effector Tle4A identified a PGAP1 domain (post-glycosylphosphatidylinositol attachment to proteins) and the catalytic motif THSMG localized in the PGAP1 domain (**Fig. 3.4**). In Tle4B, a LCT domain (Lecithin-cholesterol acetyltransferase) was identified along with the catalytic motif THSMG also located in the LCAT domain. AlphaFold2 predictions of the Tle4

effectors along with structural comparison of TplE of *P. aeruginosa* identified the catalytic triad $Ser_{239} – Asp_{478} – His_{503}$ in Tle4A and $Ser_{237} – Asp_{477} – His_{502}$ in Tle4B.

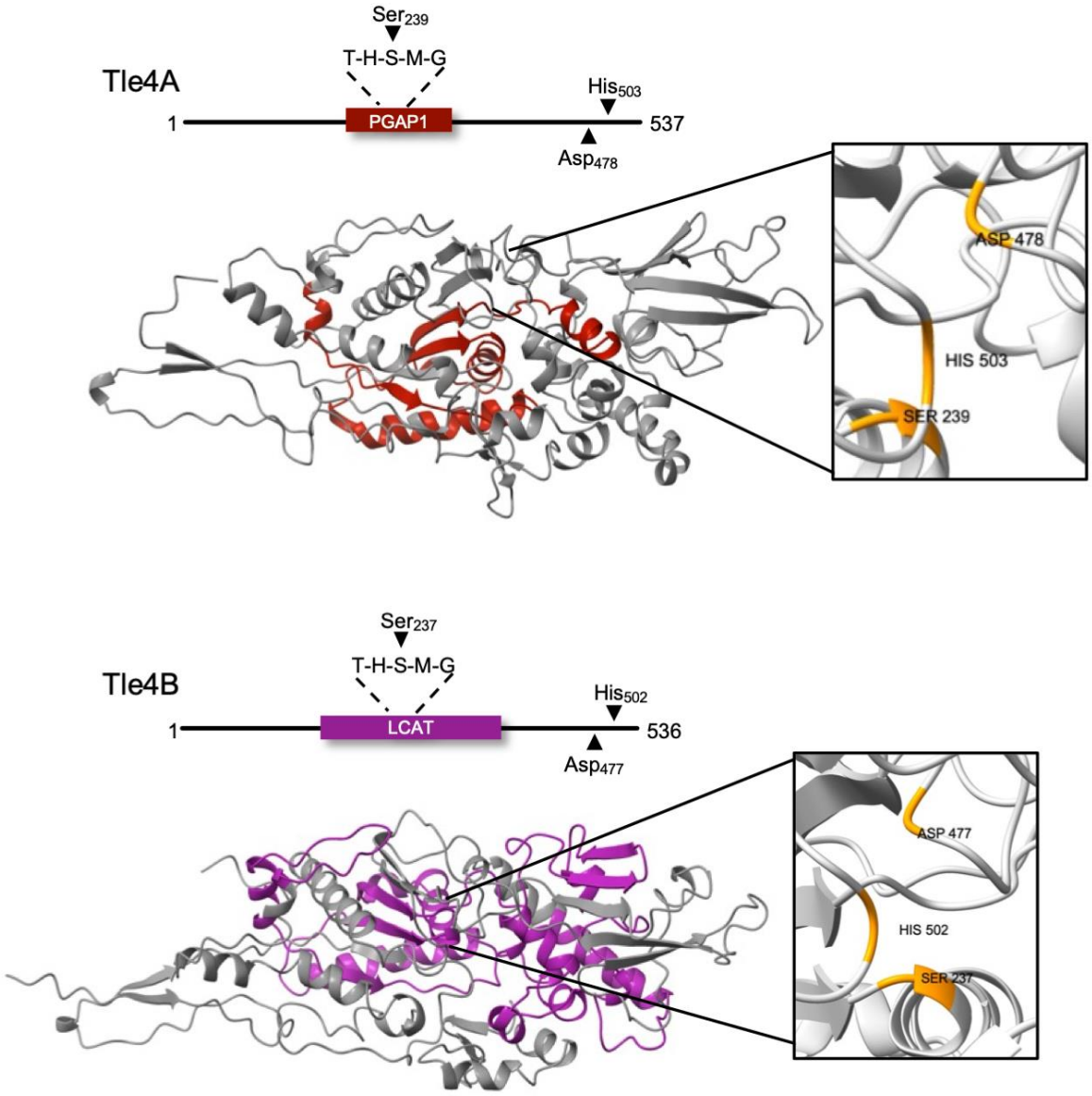

Figure 3.4: Domain organization and structure of the putative lipase effectors Tle4A and Tle4B. Protein sequences are shown with respective PGAP1 or LCAT domain, the conserved motif THSMG and the catalytic triad Ser-Asp-His is marked by arrows. Protein structure prediction was performed with AlphaFold2, respective domains are coloured as indicated in the protein sequence. The catalytic triad is shown in orange.

In summary, this study provides detailed insights into the enzymatic functionalities encoded within the T6SS-3 system, emphasizing the structural determinants and potential biological

roles of identified domains and catalytic motifs in lipase effectors Tle2A, Tle2B, Tle4A, and Tle4B.

BACTH analysis indicate a putative assembly of the T6SS-3 tip

To determine a putative mechanism for the assembly of the T6SS-3 tip, protein-protein interaction studies were performed through BACTH assays. Therefore, a putative interaction between the four different Tle effectors and the three VgrG's of the T6SS-3 as well as a self-interaction of the different VgrG's were analysed (**Fig. 3.5**).

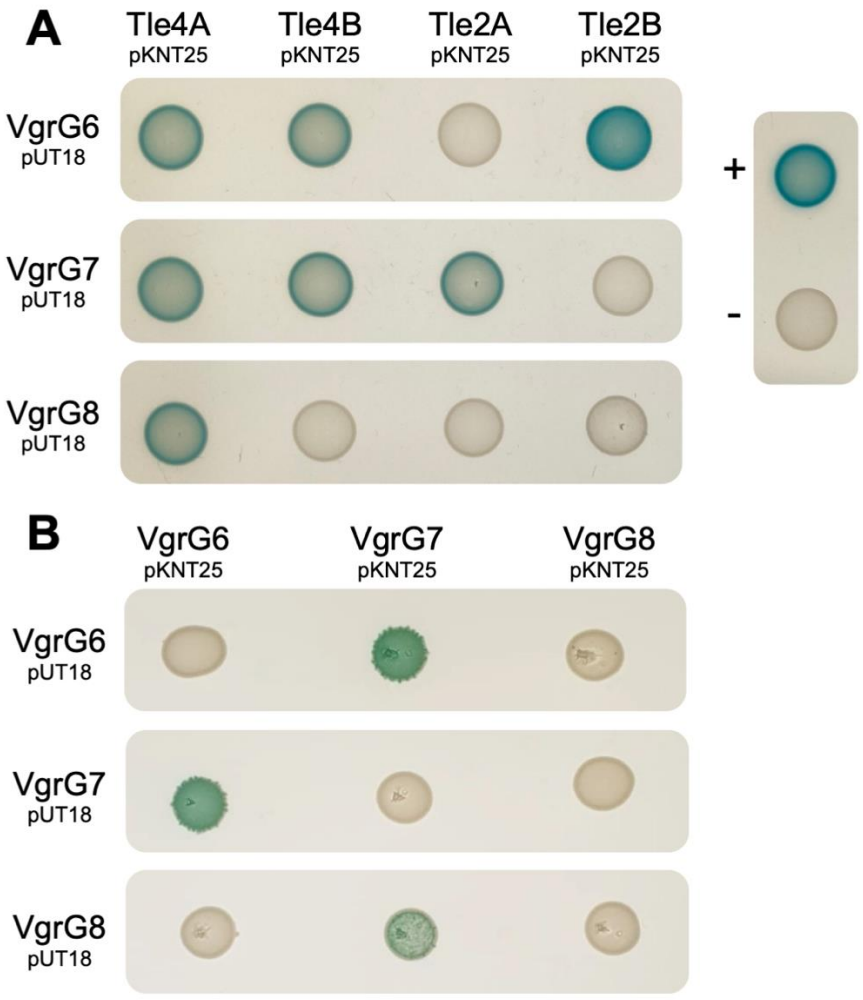

Figure 3.5: BACTH analysis of putative protein-protein interaction of the Tle effectors and VgrG proteins of the T6SS-3. **A:** Interactions of Tle2A, Tle2B, Tle4A and Tle4B of *P. luminescens* DJC cloned into the pKNT25 plasmid and VgrG6, VgrG7 and VgrG8 of *P. luminescens* DJC cloned into the pUT18 plasmid are shown. **B:** Self-interactions of VgrG6, VgrG7 and VgrG8 cloned into the pKNT25 and pUT18 plasmid. Blue colonies indicate an interaction of proteins while white colonies indicate no

interaction. *E. coli* BTH101 cells carrying pKT25-zip + pUT18C-zip (+) and pKNT25 + pUT18 (-) served as controls. Picture of similar outcomes of three biological replicates are shown.

Interestingly, Tle4A was able to interact with all tested VgrGs, whereas interactions of Tle4B only occurred with VgrG6 and VgrG7 but not VgrG8, which is encoded upstream of Tle4B in the gene cluster. In contrary, an interaction was observed for Tle2A and VgrG7 and for Tle2B and VgrG6, with only one interaction observed for the possible Tle2-VgrG interactions (**Fig. 3.5A**). As the T6SS tip is built of trimeric VgrG proteins, we next tested whether the tip is assembled as homo-trimer or hetero-trimer by testing the different possible VgrG interactions (**Fig. 3.5B**). Thereby no self-interaction could be confirmed, indicating the tip of the T6SS-3 is not build up as a homo-trimer. However, an interaction was observed for VgrG6 and VgrG7 as well as VgrG7 and VgrG8, leading to the assumption, a hetero-trimeric tip can be assembled upon T6SS assembly. In conclusion, the BACTH analysis reveals that the T6SS-3 tip likely assembles as a hetero-trimer involving specific interactions between VgrG proteins and Tle effectors.

Expression of Tle effector genes

T6SS effectors of the lipase superfamily have been previously described to deploy antibacterial but also anti-eukaryotic activity (Dong et al., 2013; Jiang et al., 2016). After the characterization of the four Tle effectors via bioinformatic analysis, toxicity assays were performed to determine if the effectors are toxic towards bacterial cells. Briefly, expression of Tle effector proteins were induced in *E. coli* BL21 star cells by the addition of 0.1% arabinose or repressed by the addition of 0.1% glucose and cell growth was measured for 7 h (**Fig. 3.6**).

Upon induction the control (pBAD24ø) and the cells expressing Tle2A or Tle2B showed no impact on the bacterial growth. Similar results were obtained for the effector Tle4B, where no reduction in growth was observed upon induction. However, the induction of Tle4A gene expression led to a reduction in cell growth, indicating that Tle4A is the only effector of the T6SS-3, that deploys antibacterial activity.

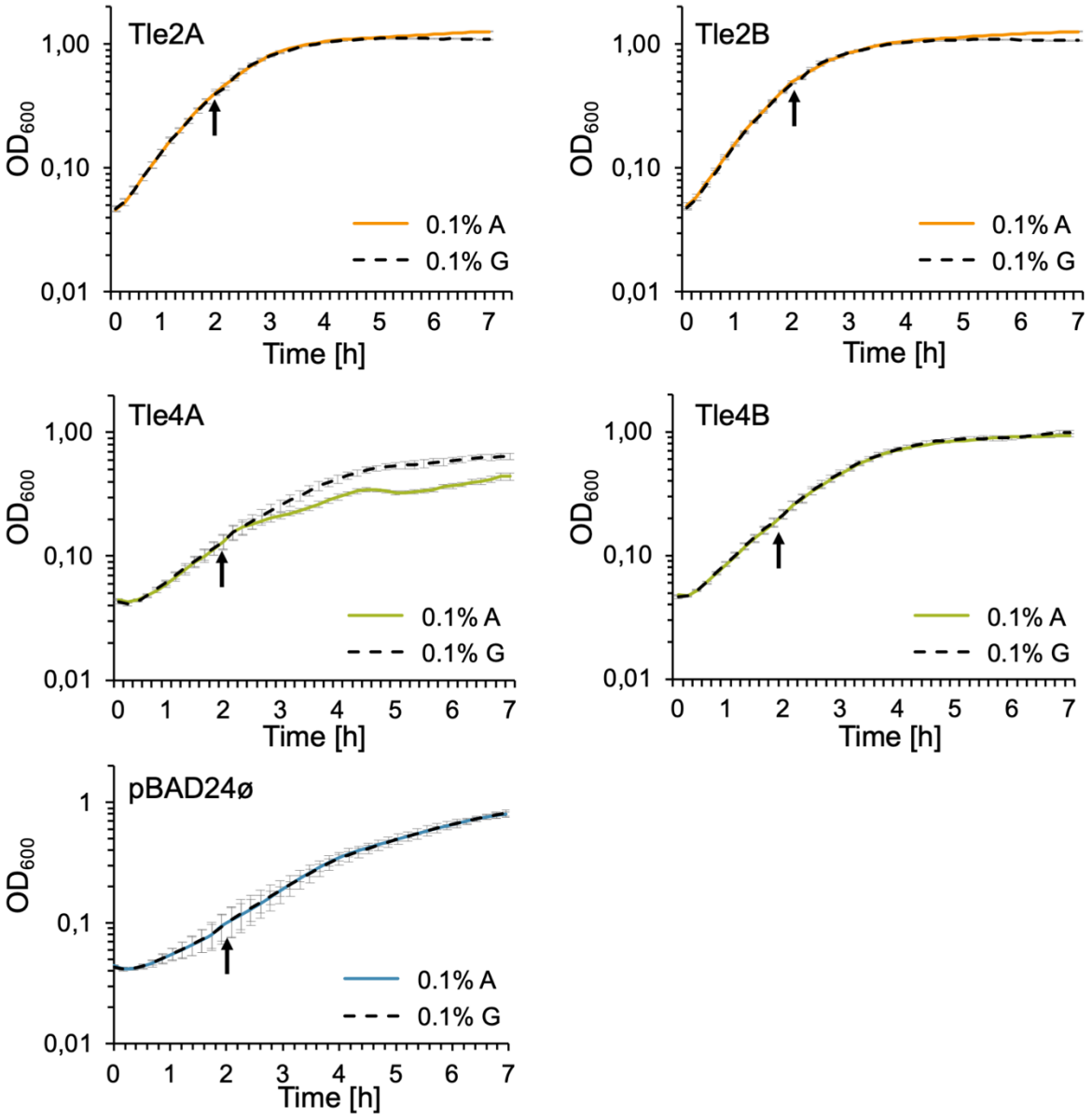

Figure 3.6: Tle4A deploys antibacterial activity. Growth of *E. coli* BL21 star cells transformed with the pBAD24 expression plasmids is shown as OD_{600} (adjusted values to logarithmically) against the time [h]. The T6SS effectors Tle2A, Tle2B, Tle4A and Tle4B of *P. luminescens* DJC were analysed. Growth was measured every 10 minutes in a microplate reader for 7 h, after 2 h the gene expression was either induced with 0.1% arabinose or repressed with 0.1% glucose (indicated with a back arrow). The empty plasmid served as control (pBAD24ø). Values of three independent biological replicates is shown. Error bars indicate standard error.

Since the VgrG proteins of the T6SS-3 all carry a DUF2345 domain, which has also been identified in VgrG4 of *Klebsiella pneumoniae* and was shown to be toxic, additional toxicity assays were performed (**Fig. 3.7**) (Allsopp et al., 2023). Therefore, the genes encoding VgrG6, VgrG7 and VgrG8 were cloned into the pBAD24 plasmid and bacterial growth monitored upon

gene expression induction. The addition of arabinose did not influence the bacterial growth, indicating the different VgrG's of the T6SS-3 are not toxic.

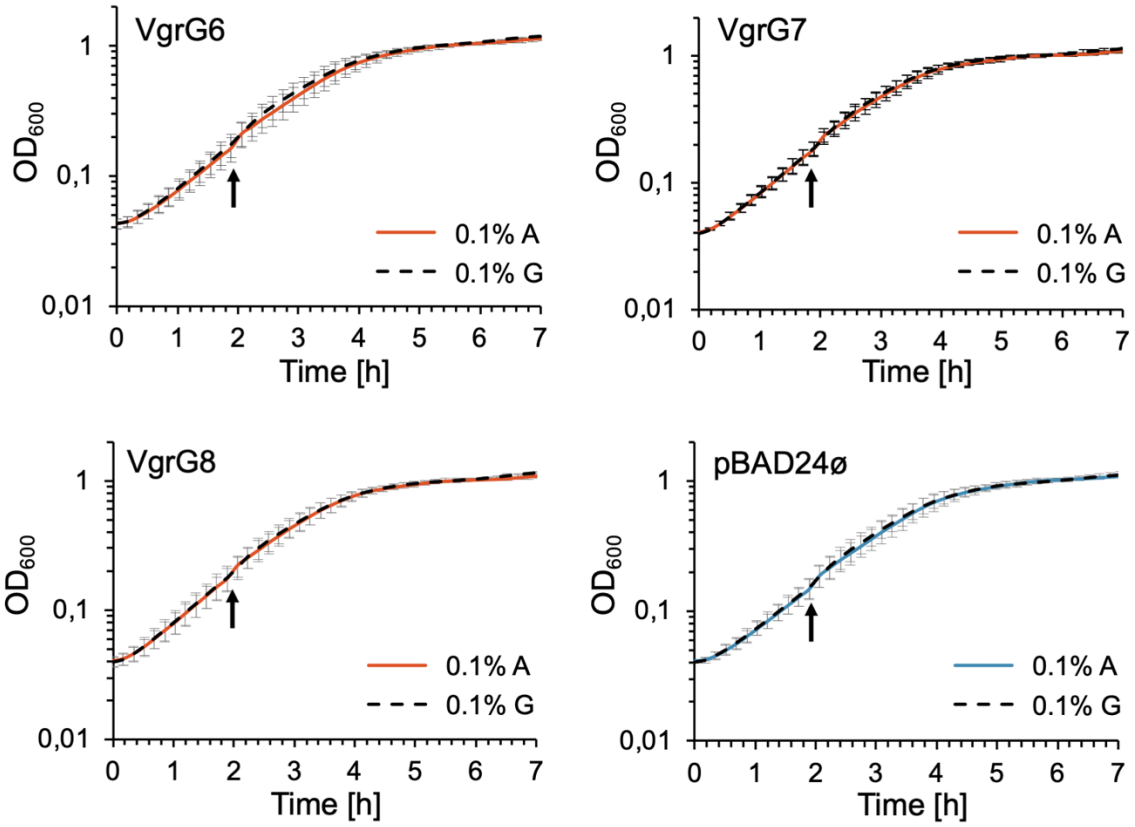

Figure 3.7: The VgrG's of the T6SS-3 have no toxic effect on *E. coli* BL21 star cells. Growth of *E. coli* BL21 star cells containing the pBAD24 expression plasmids is shown as OD_{600} (adjusted values to logarithmically) against the time [h]. The VgrG6, VgrG7 and VgrG8 of the T6SS-3 in *P. luminescens* DJC were analysed. Growth was measured every 10 minutes in a microplate reader for 7 h, after 2 h the gene expression was induced with 0.1% arabinose or repressed with 0.1% glucose (indicated with a black arrow). The empty plasmid served as control (pBAD24ø). Values of three independent biological replicates is shown. Error bars indicate standard error.

Analysis of T6SS-3 expression in *P. luminescens*

The functionality of the *P. luminescens* T6SS-3 remains unclear, as none T6SS operon has been described before to encode for multiple effectors and diverse core components. To gain further insights if the T6SS plays a role in the lifestyle of *P. luminescens*, fluorescence microscopy was performed after cultivation of the different strains under various conditions (**Fig. 3.8 and 3.9**). Therefore, the TssC subunit was tagged with mCherry as the subunit is

crucial for sheath assembly and is present in a high quantity upon assembly, thereby facilitating fluorescence detection.

In 20% of the 2° *tssC3*::*mCherry* strain fluorescence was detected during the exponential phase but not in the 1° *tssC3*::*mCherry* strain (**Fig. 3.8**). Further, $TssC3_{mCherry}$ was detected in the 2° cells when cultivated under nutrient limitation (0.1x LB) and upon changes in the pH. While a pH of 6 led to reduced $TssC3_{mCherry}$ detection compared to the control (LB), a pH of 5 led to an increase. In contrary, after cultivation of the cells in LB pH 8, a similar number of fluorescent cells was observed as in the control whereas a pH of 9 led to reduction in fluorescent cells counts. However, an increase in $TssC3_{mCherry}$ was detected in the 1° *tssC3*::*mCherry* strain when cultivated at pH = 8 compared to the 1° WT strain.

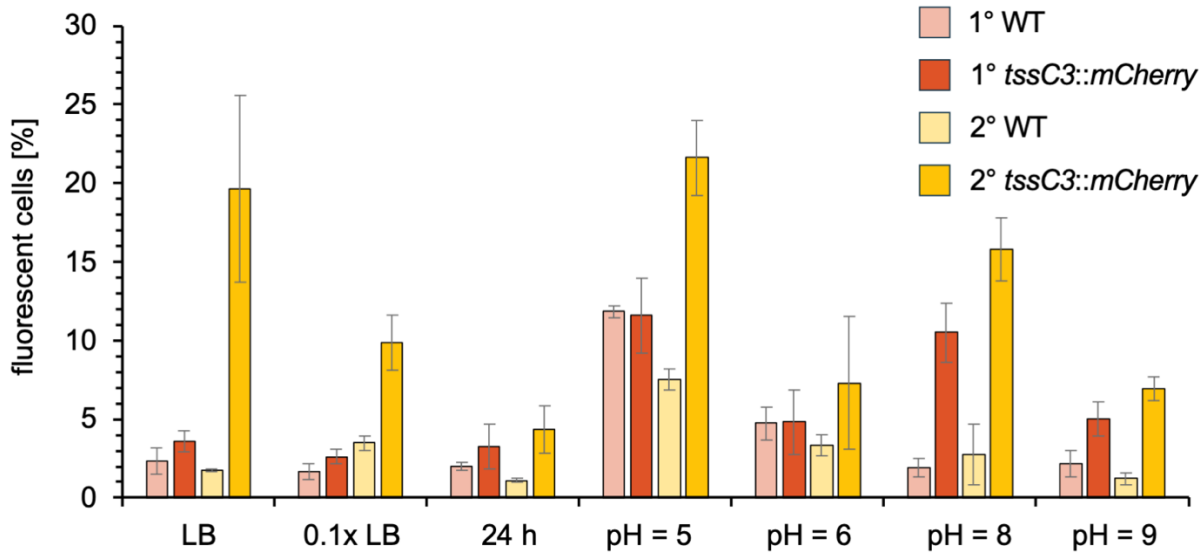

Figure 3.8: Preliminary screening of T6SS-3 activity under diverse conditions. *P. luminescens* 1°/ 2° WT and *tssC3*::*mCherry* strains were cultivated in LB medium under respective conditions. Fluorescence was detected by fluorescence microscopy filtering for mCherry fluorescence. Number of fluorescent cells per total cells is given in percent. Error shows the standard error of five pictures from one trial.

To mimic salt stresses and their influence on the Tss6-3 expression, an increased salt concentration and the lack of salt were tested on the *tssC3*::*mCherry* strains (**Fig. 3.9**). While the increased salt concentration led to an increase of $TssC3_{mCherry}$ detection in 1° cells, no changes were observed for the 2° cells. In contrary, missing salt increased the detection of

fluorescent cells in the 2° *tssC3*::*mCherry* strain, whereas little to no change was observed in the respective 1° cell strain. Studies on temperature stress revealed an increase of fluorescent cells at 37°C in the 1° *tssC3*::*mCherry* cells, whereas the amount of fluorescent cells was reduced in the 2° *tssC3*::*mCherry* cells compared to the LB control. A decrease in temperature to 26°C led to a decrease in fluorescent cells in both, 1° and 2° cells. Final studies of external signals derived by plant root exudates (PRE) or larvae extract showed no fluorescence in the tested strains.

In conclusion, different conditions were identified with an increased number of fluorescent cells, indicating that the T6SS-3 plays a role in the life cycle of *P. luminescens.*

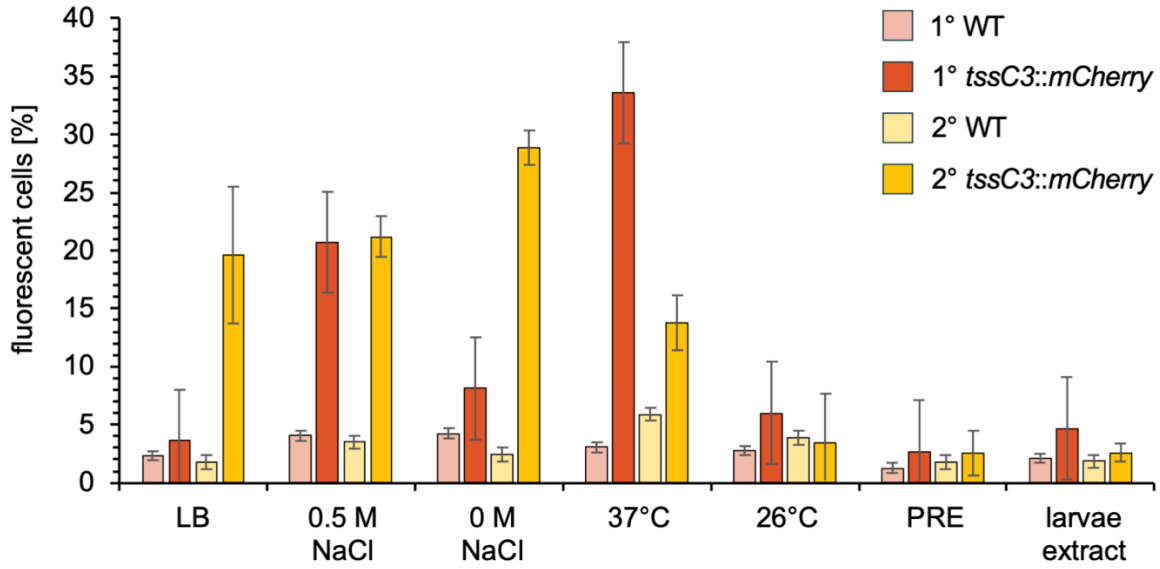

Figure 3.9: Preliminary screening of T6SS-3 activity under diverse conditions. *P. luminescens* 1°/ 2° WT and *tssC3*::*mCherry* strains were cultivated in LB medium under respective conditions. Fluorescence was detected by fluorescence microscopy filtering for mCherry fluorescence. Number of fluorescent cells per total cells is given in percent. Error shows the standard error of five pictures from one trial.

3.5 Discussion

As a nanomolecular weapon the T6SS is utilized by bacteria for interbacterial competition, host manipulation or host colonization, but complex underlying mechanism and regulation remain unclear. In the insect pathogenic bacterium *P. luminescens,* current knowledge on the T6SS is limited to the Rhs-type effector Tre found in the strain TT01 and the influence of plant root exudates on the regulation of genes encoding T6SS core components in the strain DJC (Jurėnas et al., 2021b; Regaiolo et al., 2020). As the initial bioinformatic studies on the *P. luminescens* revealed four gene clusters encoding for T6SS core components, initially the T6SS-3 and T6SS-4 were thought to be not functional as they are lacking genes encoding crucial core components (**Chapter 2**). However, a more in-depth analysis of the T6SS-3 was aiming to determine the role of this gene cluster and whether it could be functional or not.

The previous studies showed that genes encoding TssA, TssH and TssM are missing. However, putative homologues for the missing *tssM* could be identified with *vasK1, vasK2* and *vasK3*, encoding two out of three domains, also identified in *tssM1* of the T6SS-1. VasK has been previously described as a TssM homologue found in the periplasm with a role in translocation of proteins and putatively involved in effector recognition and signal transduction (Shrivastava and Mande, 2008; Cummins et al., 2023). Nevertheless, no homologue was identified for TssA or TssH, two components that were shown to be crucial for T6SS activity (Dix et al., 2018; Asolkar and Ramesh, 2020). Yet, studies in *Amoebophilus* firstly described a T6SS^{VI}, lacking TssH but also the membrane complex TssJLM, resulting in eCIS-like T6SS complexes (Böck et al., 2017).

Therefore, considering that the T6SS-3 could be a functional system, the next aim was to identify the role of the four Tle effectors and the three VgrG proteins. Bioinformatic analysis of the Tle effectors identified the i) unknown domain DUF2235, and ii) PGAP1 and LCAT1, catalytic motifs and the catalytic triad, thereby suggesting those effectors deploy antibacterial activity (Jiang et al., 2016; Lima et al., 2004; Flaugnatti et al., 2016). However, only Tle4A was shown to inhibit bacterial cell growth, whereas the production of Tle2A, Tle2B and Tle4B had no influence (**Fig. 3.6**). As protein production was cytoplasmic, putatively the overproduction

could not lead to intoxication and should rather be performed periplasmic. Similar observations have been made for a Tle1 effector, which was initially overproduced in the cytoplasm with no observed toxicity, yet toxicity was strongly increased in the periplasm (Berni et al., 2019).

C-terminal extension can also enable VgrG proteins to act as toxins and deploy antibacterial activity (Lien and Lai, 2017). As the different VgrG proteins all carry a C-terminal extension with either a DUF2345 domains or a DUF2345 domain plus a TTR-like fold domain, their antibacterial activity was determined (**Fig. 3.7**). Here, no antibacterial activity was observed, suggesting the role of the VgrG proteins is rather in effector binding and transport, which has been described before in *Vibrio cholerae* and *E. coli* (Flaugnatti et al., 2020; Liu et al., 2023). Indeed, interactions were observed between the VgrG proteins and Tle's in BACTH assays. Interestingly, Tle4A interacted with all VgrG proteins, whereas Tle4B was not able to interact with VgrG8 and Tle2A and Tle2B only interacted with one specific VgrG (**Fig. 3.5A**). It has been previously shown, that VgrG proteins specifically interact with Tle effectors depending on the TTR-domain (Wettstadt et al., 2019). However, those VgrG-Tle interactions were commonly observed when the respective genes were on pathogenic islands or only one VgrG-Tle pair encoded within a T6SS gene cluster. In contrary, the T6SS-3 encodes for three different VgrGs, all with different C-terminal extensions and further four Tle proteins. As such a gene cluster has not been described before, it can be hypothesized that the tip of the T6SS-3 consists of a heterotrimer instead of a homodimer and thereby deliver an effector cocktail upon activation. Indeed, BACTH assays showed no self-interaction of the VgrG proteins but interactions with the other VgrG's, supporting this hypothesis (**Fig 3.5B**). Further, the identification of the Tla1 and Tla2 proteins could enable diverse combination, as the class of Tla proteins was previously shown to assist in T6SS effector delivery by binding to the TTR domain of VgrGs and specifically with Tle proteins (Berni et al., 2019). Taken together, the bioinformatic results and protein-protein interaction studies suggest a novel subfamily of T6SSs.

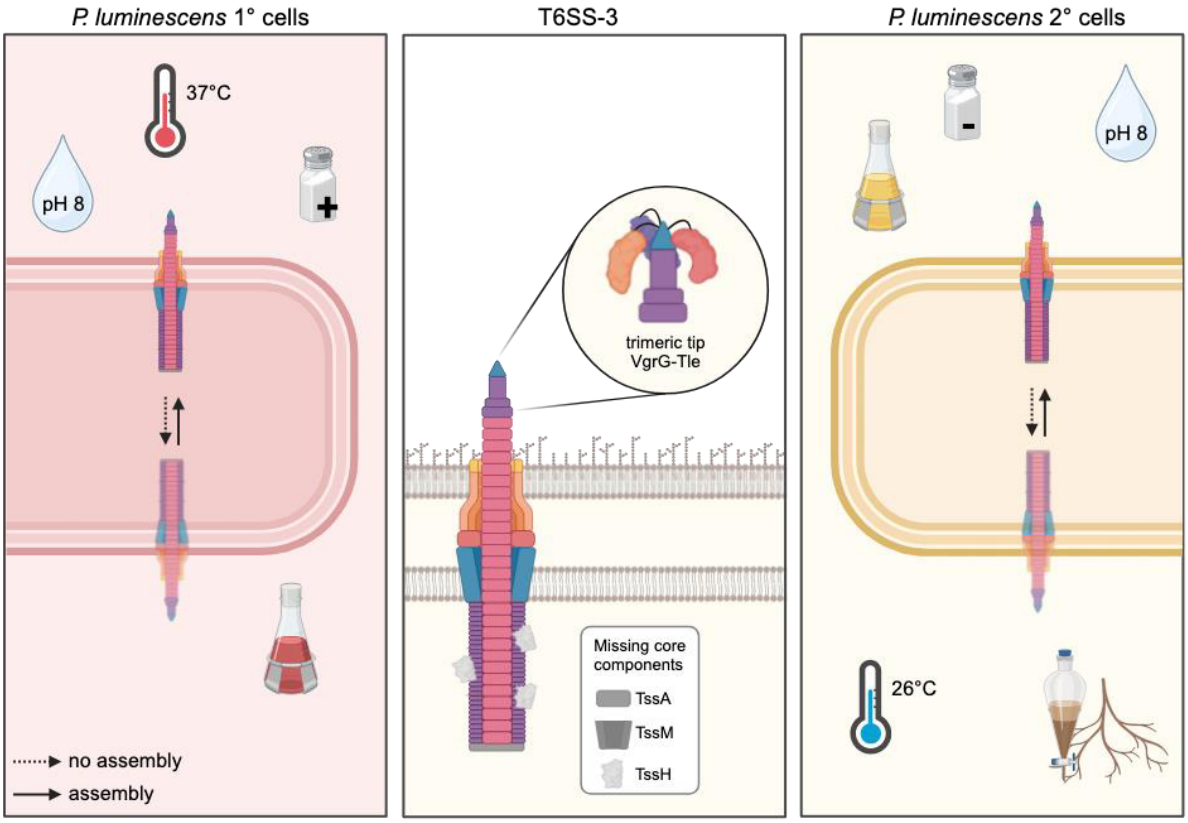

Fig. 3.10: Role of the T6SS-3 in *P. luminescens* 1° and 2° cells. The T6SS-3 is characterized by a trimeric VgrG-tip able to bind four different Tle effectors, namely Tle2A, Tle2B, Tle4A and Tle4B. An antibacterial effect was observed for Tle4A, thus suggesting the T6SS-3 could be involved in interbacterial competition. In the phenotypic different 1° and 2° cell form, expression of the T6SS is differently regulated. High temperature, pH of 8 and high salt concentration lead to T6SS-3 expression in the 1° cells, whereas low salt concentrations, standard laboratory conditions as well as pH 8 lead to expression of the T6SS-3 in the 2° cells. In contrary, the T6SS-3 is not active in 1° cells under standard laboratory conditions, whereas in the 2° cells the T6SS-3 is not active under lower temperatures and upon addition of plant root exudates.

To understand more deeply the role of T6SS-3 and the conditions that could influence its activation, its expression activity was studied through fluorescence microscopy. Contrary to the first assumption, that the T6SS-3 could not operate due to missing core components, the results showed the opposite (**Fig. 3.8 and 3.9**). While in the 2° cells activity was observed under standard laboratory conditions (LB), different external stress factors increased the number of fluorescent cells like pH = 5 or lack of NaCl. The exposure of 2° cells to different stresses in the rhizosphere, like changes in pH and salt concentration or temperature shifts, require the cells to adapt better to the challenging environment and thus the T6SS-3 could be

involved in this adaptation process (Shultana et al., 2022; Hawkins and Oresnik, 2021). In contrary, no T6SS activity was detected under standard laboratory conditions in the 1° cell form, whereas an increase in T6SS-3 mCherry tagged cells was observed at high temperatures, high salt concentrations and a pH of 8. While osmotic stress has been previously described during insect larvae invasion, the T6SS-3 could be important for insect larvae infection and for larvae carcass protection (Crawford et al., 2010). However, these results are limited to preliminary studies, requiring further investigations. In conclusion, the detailed analysis of the T6SS-3 in *P. luminescens* strain DJC reveals a potentially functional system with unique protein-protein interactions and environmental stress responses, suggesting a novel subfamily of T6SSs. These findings underscore the complexity and adaptability of bacterial secretion systems, highlighting the need for further research to fully understand their roles in bacterial ecology and pathogenicity.

3.6 References

Allsopp, Luke P.; Bernal, Patricia (2023): Killing in the name of: T6SS structure and effector diversity. In: *Microbiology (Reading, England)* 169 (7). https://doi.org /10.1099/mic.0.001367.

Asolkar, T., and Ramesh, R. (2020). The involvement of the Type Six Secretion System (T6SS) in the virulence of *Ralstonia solanacearum* on brinjal. 3 Biotech *10*, 324. https://doi.org/10.1007/s13205-020-02311-4.

Basler, M., and Mekalanos, J.J. (2012). Type 6 secretion dynamics within and between bacterial cells. Science (New York, N.Y.) *337*, 815. https://doi.org/10.1126/science.1222901.

Berni, B., Soscia, C., Djermoun, S., Ize, B., and Bleves, S. (2019). A Type VI Secretion System Trans-Kingdom Effector Is Required for the Delivery of a Novel Antibacterial Toxin in *Pseudomonas aeruginosa*. Frontiers in microbiology *10*, 1218. https://doi.org/10.3389/fmicb.2019.01218.

Böck, D., Medeiros, J.M., Tsao, H.-F., Penz, T., Weiss, G.L., Aistleitner, K., Horn, M., and Pilhofer, M. (2017). In situ architecture, function, and evolution of a contractile injection system. Science (New York, N.Y.) *357*, 713-717. https://doi.org/10.1126/science.aan7904.

Bondage, D.D., Lin, J.-S., Ma, L.-S., Kuo, C.-H., and Lai, E.-M. (2016). VgrG C terminus confers the type VI effector transport specificity and is required for binding with PAAR and adaptor-effector complex. Proceedings of the National Academy of Sciences of the United States of America *113*, E3931-40. https://doi.org/10.1073/pnas.1600428113.

Boratyn, G.M., Camacho, C., Cooper, P.S., Coulouris, G., Fong, A., Ma, N., Madden, T.L., Matten, W.T., McGinnis, S.D., and Merezhuk, Y., et al. (2013). BLAST: a more efficient report with usability improvements. Nucleic acids research *41*, W29-33. https://doi.org/10.1093/nar/gkt282.

Brillard, J., Duchaud, E., Boemare, N., Kunst, F., and Givaudan, A. (2002). The PhlA hemolysin from the entomopathogenic bacterium *Photorhabdus luminescens* belongs to the two-partner secretion family of hemolysins. Journal of bacteriology *184*, 3871-3878. https://doi.org/10.1128/JB.184.14.3871-3878.2002.

Brunet, Y.R., Zoued, A., Boyer, F., Douzi, B., and Cascales, E. (2015). The Type VI Secretion TssEFGK-VgrG Phage-Like Baseplate Is Recruited to the TssJLM Membrane Complex via Multiple Contacts and Serves As Assembly Platform for Tail Tube/Sheath Polymerization. PLoS genetics *11*, e1005545. https://doi.org/10.1371/journal.pgen.1005545.

Cherrak, Y., Flaugnatti, N., Durand, E., Journet, L., and Cascales, E. (2019). Structure and Activity of the Type VI Secretion System. Microbiology spectrum *7*. https://doi.org/10.1128/microbiolspec.PSIB-0031-2019.

Crawford, J.M., Kontnik, R., and Clardy, J. (2010). Regulating alternative lifestyles in entomopathogenic bacteria. Current biology : CB *20*, 69-74. https://doi.org/10.1016/j.cub.2009.10.059.

Cummins, E.A., Moran, R.A., Snaith, A.E., Hall, R.J., Connor, C.H., Dunn, S.J., and McNally, A. (2023). Parallel loss of type VI secretion systems in two multi-drug-resistant *Escherichia coli* lineages. Microbial genomics *9*. https://doi.org/10.1099/mgen.0.001133.

Dix, S.R., Owen, H.J., Sun, R., Ahmad, A., Shastri, S., Spiewak, H.L., Mosby, D.J., Harris, M.J., Batters, S.L., and Brooker, T.A., et al. (2018). Structural insights into the function of type

VI secretion system TssA subunits. Nature communications *9*, 4765. https://doi.org/10.1038/s41467-018-07247-1.

Dong, T.G., Ho, B.T., Yoder-Himes, D.R., and Mekalanos, J.J. (2013). Identification of T6SS-dependent effector and immunity proteins by Tn-seq in *Vibrio cholerae*. Proceedings of the National Academy of Sciences of the United States of America *110*, 2623-2628. https://doi.org/10.1073/pnas.1222783110.

Durand, E., van Nguyen, S., Zoued, A., Logger, L., Péhau-Arnaudet, G., Aschtgen, M.-S., Spinelli, S., Desmyter, A., Bardiaux, B., and Dujeancourt, A., et al. (2015). Biogenesis and structure of a type VI secretion membrane core complex. Nature *523*, 555-560. https://doi.org/10.1038/nature14667.

Flaugnatti, N., Le, T.T.H., Canaan, S., Aschtgen, M.-S., van Nguyen, S., Blangy, S., Kellenberger, C., Roussel, A., Cambillau, C., and Cascales, E., et al. (2016). A phospholipase A1 antibacterial Type VI secretion effector interacts directly with the C-terminal domain of the VgrG spike protein for delivery. Molecular microbiology *99*, 1099-1118. https://doi.org/10.1111/mmi.13292.

Flaugnatti, N., Rapisarda, C., Rey, M., Beauvois, S.G., Nguyen, V.A., Canaan, S., Durand, E., Chamot-Rooke, J., Cascales, E., and Fronzes, R., et al. (2020). Structural basis for loading and inhibition of a bacterial T6SS phospholipase effector by the VgrG spike. The EMBO journal *39*, e104129. https://doi.org/10.15252/embj.2019104129.

Gabler, F., Nam, S.-Z., Till, S., Mirdita, M., Steinegger, M., Söding, J., Lupas, A.N., and Alva, V. (2020). Protein Sequence Analysis Using the MPI Bioinformatics Toolkit. Current protocols in bioinformatics *72*, e108. https://doi.org/10.1002/cpbi.108.

Hawkins, J.P., and Oresnik, I.J. (2021). The Rhizobium-Legume Symbiosis: Co-opting Successful Stress Management. Frontiers in plant science *12*, 796045. https://doi.org/10.3389/fpls.2021.796045.

Jiang, F., Wang, X., Wang, B., Chen, L., Zhao, Z., Waterfield, N.R., Yang, G., and Jin, Q. (2016). The *Pseudomonas aeruginosa* Type VI Secretion PGAP1-like Effector Induces Host Autophagy by Activating Endoplasmic Reticulum Stress. Cell reports *16*, 1502-1509. https://doi.org/10.1016/j.celrep.2016.07.012.

Jiang, F., Waterfield, N.R., Yang, J., Yang, G., and Jin, Q. (2014). A *Pseudomonas aeruginosa* type VI secretion phospholipase D effector targets both prokaryotic and eukaryotic cells. Cell host & microbe *15*, 600-610. https://doi.org/10.1016/j.chom.2014.04.010.

Jumper, J., Evans, R., Pritzel, A., Green, T., Figurnov, M., Ronneberger, O., Tunyasuvunakool, K., Bates, R., Žídek, A., and Potapenko, A., et al. (2021). Highly accurate protein structure prediction with AlphaFold. Nature *596*, 583-589. https://doi.org/10.1038/s41586-021-03819-2.

Jurėnas, D., Payelleville, A., Roghanian, M., Turnbull, K.J., Givaudan, A., Brillard, J., Hauryliuk, V., and Cascales, E. (2021a). *Photorhabdus* antibacterial Rhs polymorphic toxin inhibits translation through ADP-ribosylation of 23S ribosomal RNA. Nucleic acids research *49*, 8384-8395. https://doi.org/10.1093/nar/gkab608.

Jurėnas, D., Rosa, L.T., Rey, M., Chamot-Rooke, J., Fronzes, R., and Cascales, E. (2021b). Mounting, structure and autocleavage of a type VI secretion-associated Rhs polymorphic toxin. Nature communications *12*, 6998. https://doi.org/10.1038/s41467-021-27388-0.

Kudryashev, M., Wang, R.Y.-R., Brackmann, M., Scherer, S., Maier, T., Baker, D., DiMaio, F., Stahlberg, H., Egelman, E.H., and Basler, M. (2015). Structure of the type VI secretion system contractile sheath. Cell *160*, 952-962. https://doi.org/10.1016/j.cell.2015.01.037.

Lassak, J., Henche, A.-L., Binnenkade, L., and Thormann, K.M. (2010). ArcS, the cognate sensor kinase in an atypical Arc system of *Shewanella oneidensis* MR-1. Applied and environmental microbiology *76*, 3263-3274. https://doi.org/10.1128/AEM.00512-10.

Lien, Y.-W., and Lai, E.-M. (2017). Type VI Secretion Effectors: Methodologies and Biology. Frontiers in cellular and infection microbiology *7*, 254. https://doi.org/10.3389/fcimb.2017.00254.

Lima, V.L.M., Coelho, Luana C. B. B., Kennedy, J.F., Owen, J.S., and Dolphin, P.J. (2004). Lecithin-cholesterol acyltransferase (LCAT) as a plasma glycoprotein: an overview. Carbohydrate Polymers *55*, 179-191. https://doi.org/10.1016/j.carbpol.2003.09.005.

Liu, M., Wang, H., Liu, Y., Tian, M., Wang, Z., Shu, R.-D., Zhao, M.-Y., Chen, W.-D., Wang, H., and Wang, H., et al. (2023). The phospholipase effector Tle1Vc promotes *Vibrio cholerae* virulence by killing competitors and impacting gene expression. Gut microbes *15*, 2241204. https://doi.org/10.1080/19490976.2023.2241204.

Madeira, F., Pearce, M., Tivey, A.R.N., Basutkar, P., Lee, J., Edbali, O., Madhusoodanan, N., Kolesnikov, A., and Lopez, R. (2022). Search and sequence analysis tools services from EMBL-EBI in 2022. Nucleic acids research *50*, W276-W279. https://doi.org/10.1093/nar/gkac240.

Meng, E.C., Goddard, T.D., Pettersen, E.F., Couch, G.S., Pearson, Z.J., Morris, J.H., and Ferrin, T.E. (2023). UCSF ChimeraX: Tools for structure building and analysis. Protein science : a publication of the Protein Society *32*, e4792. https://doi.org/10.1002/pro.4792.

Mirdita, M., Schütze, K., Moriwaki, Y., Heo, L., Ovchinnikov, S., and Steinegger, M. (2022). ColabFold: making protein folding accessible to all. Nature methods *19*, 679-682. https://doi.org/10.1038/s41592-022-01488-1.

Mougous, J.D., Cuff, M.E., Raunser, S., Shen, A., Zhou, M., Gifford, C.A., Goodman, A.L., Joachimiak, G., Ordoñez, C.L., and Lory, S., et al. (2006). A virulence locus of *Pseudomonas aeruginosa* encodes a protein secretion apparatus. Science (New York, N.Y.) *312*, 1526-1530. https://doi.org/10.1126/science.1128393.

Pisarz, F., Glatter, T., Süss, D.-T.M., Heermann, R., and Regaiolo, A. (2024). The Type VI secretion systems of the insect pathogen *Photorhabdus luminescens* are involved in interbacterial competition, motility and secondary metabolism. The Microbe *3*, 100067. https://doi.org/10.1016/j.microb.2024.100067.

Potter, S.C., Luciani, A., Eddy, S.R., Park, Y., Lopez, R., and Finn, R.D. (2018). HMMER web server: 2018 update. Nucleic acids research *46*, W200-W204. https://doi.org/10.1093/nar/gky448.

Pukatzki, S., Ma, A.T., Sturtevant, D., Krastins, B., Sarracino, D., Nelson, W.C., Heidelberg, J.F., and Mekalanos, J.J. (2006). Identification of a conserved bacterial protein secretion system in *Vibrio cholerae* using the *Dictyostelium* host model system. Proceedings of the National Academy of Sciences of the United States of America *103*, 1528-1533. https://doi.org/10.1073/pnas.0510322103.

Regaiolo, A., Dominelli, N., Andresen, K., and Heermann, R. (2020). The Biocontrol Agent and Insect Pathogen *Photorhabdus luminescens* Interacts with Plant Roots. Applied and environmental microbiology *86*. https://doi.org/10.1128/AEM.00891-20.

Robert, X., and Gouet, P. (2014). Deciphering key features in protein structures with the new ENDscript server. Nucleic acids research *42*, W320-4. https://doi.org/10.1093/nar/gku316.

Rodou, A., Ankrah, D.O., and Stathopoulos, C. (2010). Toxins and secretion systems of *Photorhabdus luminescens*. Toxins *2*, 1250-1264. https://doi.org/10.3390/toxins2061250.

Ruiz, F.M., Santillana, E., Spínola-Amilibia, M., Torreira, E., Culebras, E., and Romero, A. (2015). Crystal Structure of Hcp from Acinetobacter baumannii: A Component of the Type VI Secretion System. PLOS ONE *10*, e0129691. https://doi.org/10.1371/journal.pone.0129691.

Russell, A.B., LeRoux, M., Hathazi, K., Agnello, D.M., Ishikawa, T., Wiggins, P.A., Wai, S.N., and Mougous, J.D. (2013). Diverse type VI secretion phospholipases are functionally plastic antibacterial effectors. Nature *496*, 508-512. https://doi.org/10.1038/nature12074.

Russell, A.B., Peterson, S.B., and Mougous, J.D. (2014). Type VI secretion system effectors: poisons with a purpose. Nature reviews. Microbiology *12*, 137-148. https://doi.org/10.1038/nrmicro3185.

Shneider, M.M., Buth, S.A., Ho, B.T., Basler, M., Mekalanos, J.J., and Leiman, P.G. (2013). PAAR-repeat proteins sharpen and diversify the type VI secretion system spike. Nature *500*, 350-353. https://doi.org/10.1038/nature12453.

Shrivastava, S., and Mande, S.S. (2008). Identification and functional characterization of gene components of Type VI Secretion system in bacterial genomes. PloS one *3*, e2955. https://doi.org/10.1371/journal.pone.0002955.

Shultana, R., Zuan, A.T.K., Naher, U.A., Islam, A.K.M.M., Rana, M.M., Rashid, M.H., Irin, I.J., Islam, S.S., Rim, A.A., and Hasan, A.K. (2022). The PGPR Mechanisms of Salt Stress Adaptation and Plant Growth Promotion. Agronomy *12*, 2266. https://doi.org/10.3390/agronomy12102266.

Silverman, J.M., Agnello, D.M., Zheng, H., Andrews, B.T., Li, M., Catalano, C.E., Gonen, T., and Mougous, J.D. (2013). Haemolysin coregulated protein is an exported receptor and chaperone of type VI secretion substrates. Molecular cell *51*, 584-593. https://doi.org/10.1016/j.molcel.2013.07.025.

Unterweger, D., Kostiuk, B., and Pukatzki, S. (2017). Adaptor Proteins of Type VI Secretion System Effectors. Trends in microbiology *25*, 8-10. https://doi.org/10.1016/j.tim.2016.10.003.

Vettiger, A., Winter, J., Lin, L., and Basler, M. (2017). The type VI secretion system sheath assembles at the end distal from the membrane anchor. Nature communications *8*, 16088. https://doi.org/10.1038/ncomms16088.

Wang, J., Brackmann, M., Castaño-Díez, D., Kudryashev, M., Goldie, K.N., Maier, T., Stahlberg, H., and Basler, M. (2017). Cryo-EM structure of the extended type VI secretion system sheath-tube complex. Nature microbiology *2*, 1507-1512. https://doi.org/10.1038/s41564-017-0020-7.

Wang, J., Chitsaz, F., Derbyshire, M.K., Gonzales, N.R., Gwadz, M., Lu, S., Marchler, G.H., Song, J.S., Thanki, N., and Yamashita, R.A., et al. (2023). The conserved domain database in 2023. Nucleic acids research *51*, D384-D388. https://doi.org/10.1093/nar/gkac1096.

Wettstadt, S., Wood, T.E., Fecht, S., and Filloux, A. (2019). Delivery of the *Pseudomonas aeruginosa* Phospholipase Effectors PldA and PldB in a VgrG- and H2-T6SS-Dependent Manner. Frontiers in microbiology *10*, 1718. https://doi.org/10.3389/fmicb.2019.01718.

Wood, T.E., Howard, S.A., Wettstadt, S., and Filloux, A. (2019). PAAR proteins act as the 'sorting hat' of the type VI secretion system. Microbiology *165*, 1203-1218. https://doi.org/10.1099/mic.0.000842.

Zamora-Lagos, M.-A., Eckstein, S., Langer, A., Gazanis, A., Pfeiffer, F., Habermann, B., and Heermann, R. (2018). Phenotypic and genomic comparison of *Photorhabdus luminescens* subsp. *laumondii* TT01 and a widely used rifampicin-resistant *Photorhabdus luminescens* laboratory strain. BMC genomics *19*, 854. https://doi.org/10.1186/s12864-018-5121-z.

Zimmermann, L., Stephens, A., Nam, S.-Z., Rau, D., Kübler, J., Lozajic, M., Gabler, F., Söding, J., Lupas, A.N., and Alva, V. (2018). A Completely Reimplemented MPI Bioinformatics Toolkit with a New HHpred Server at its Core. Journal of molecular biology *430*, 2237-2243. https://doi.org/10.1016/j.jmb.2017.12.007.

3.7 Supplementary material

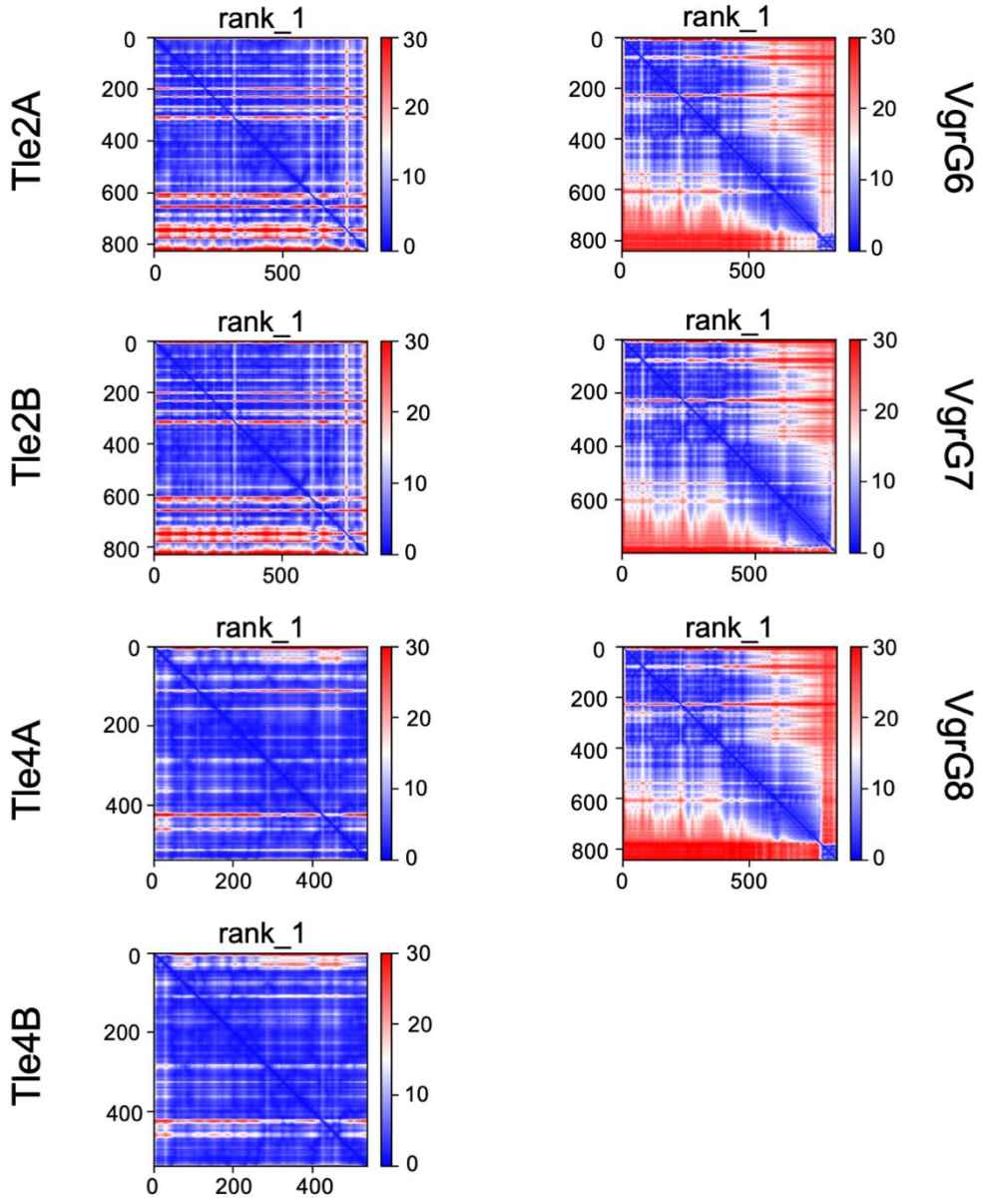

Figure S3.1: AlphaFold2 protein structure predictions of Tle2A, Tle2B, Tle4A, Tle4B, VgrG6, VgrG7 and VgrG8. Predicted alignment error (PAE) plots for best model is shown (rank 1 – rank 5).

A

	TssM1	TssM2	VasK1	VasK2	Vask3
TssM1	**100.00**	21.71	20.77	20.88	20.88
TssM2	21.71	**100.00**	16.07	17.03	16.19
VasK1	20.77	16.07	**100.00**	91.55	97.95
VasK2	20.88	17.03	91.55	**100.00**	91.82
VasK3	20.88	16.19	97.95	91.82	**100.00**

B

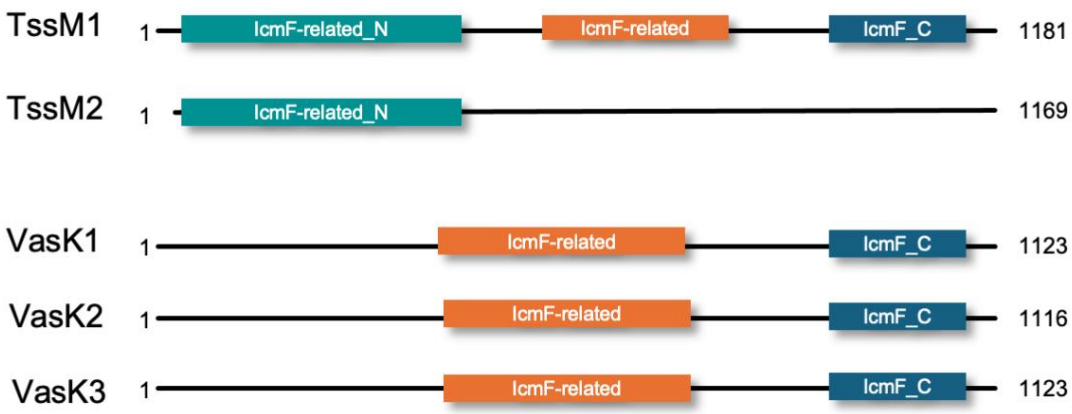

Figure S3.2: Bioinformatics analysis of the TssM homologous VasK1-3. A: Sequence homology of the TssM1, TssM2, VasK1, VasK2 and Vask3 determined through MSA with Clustal Omega. **B**: Protein sequence of TssM1, TssM2, VasK1, VasK2 and VasK3 showing the domains IcmF-related_N (turquoise), IcmF-related (orange) and IcmF_C (blue).

4. Characterization of T6SS Pore Forming Effectors Tme1 in *Photorhabdus luminescens*: Mechanisms of Interbacterial Competition and Immunity

Friederike Pisarz[1], Luca Rabbachin[1], Melanie Hoos[1], Ralf Heermann[1,2]*, Alice Regaiolo[1*]

[1] Johannes Gutenberg University Mainz, Institute of Molecular Physiology, Microbiology and Biotechnology, Hanns-Dieter-Hüsch-Weg 17, 55128 Mainz, Germany

[2] Institute for Biotechnology and Drug Research gGmbH (IBWF), Hanns-Dieter-Hüsch-Weg 17, 55128 Mainz, Germany

4.1 Abstract

Bacteria inhabit complex ecosystems, requiring diverse mechanisms for survival and competition, including symbiosis, antibiotic production, and biofilm formation. The type VI secretion system (T6SS) is a notable nanomolecular weapon found in Gram-negative bacteria that delivers antibacterial and anti-eukaryotic effectors into target cells. This study investigates two T6SS membrane-disrupting effectors, Tme1A and Tme1B, in the insect pathogenic bacterium *Photorhabdus luminescens* strain DJC. *P. luminescens* exhibits phenotypic heterogeneity, differentiating into primary (1°) and secondary (2°) cell forms. We identified *tme1A* and *tme1B* in auxiliary gene clusters of the *P. luminescens* DJC genome. Bacterial Adenylate Cyclase Two-Hybrid (BACTH) analysis confirmed interactions between Tme1 effectors and various HcP tube homologues, indicating a putative transport mechanism for the effector proteins. AlphaFold2 predictions suggested that Tme1A forms a pore. Here supported Time-lapse microscopy supported the prediction as heterologous overexpression of *tme1A* showed rapid cell lysis. Furthermore, BACTH analysis confirmed Tme1A-Tme1A self-interaction. Co-expression of the effector-immunity proteins showed Tme1 cross-neutralization by non-cognate immunity proteins. Moreover, a conserved C-terminal loop in the immunity proteins (Tmi1) was identified, which is essential for neutralizing Tme1 effectors, preventing their oligomerization and pore formation. Promoter activity in luminescence-based reporter assay revealed different *tme1A* and *tme1B* expression patterns during bacterial growth. The different promoter activity of P_{tme1A} during exponential growth suggested a putative role in bacterial competition under specific environmental conditions. Tme1A was particularly active in 1° cells, potentially aiding competition during nematode symbiosis or in insect pathogenicity. In summary, we could demonstrate that the Tme1A and Tme1B of the insect pathogen *P. luminescens* are antibacterial effectors that can be neutralized by Tmi1 immunity proteins. Finally, we were able to identify a conserved Tmi1 motif found in DUF1240 proteins, which is crucial for effector neutralization.

4.2 Author summary

The type VI secretion systems (T6SS) are found in Gram-negative bacteria and function as membrane bound molecular weapons, which inject toxins into target cells. The insect pathogen *P. luminescens* harbours multiple gene clusters encoding T6SSs as well as above 20 effectors, but none has been proved to deploy antibacterial activity yet. Our findings confirm two T6SS membrane disrupting effectors (Tme) in *P. luminescens* deploying antibacterial activity. As cognate immunity proteins are important to avoid self-intoxication, we could show that the *P. luminescens* Tme immunity proteins (Tmi) can provide cross-neutralization to Tme effectors. Moreover, we were able to identify a conserved motif in Tmi proteins crucial for neutralization, which builds a C-terminal loop and interacts with the Tme protein. Finally, we aimed to understand the role of the Tme effectors in the life cycle of *P. luminescens* by performing luminescence-based reporter assays. Thereby, we could show how future promoter activity analyses of T6SS effector genes could provide a first hint on their role in the lifestyle of the bacteria.

4.3 Introduction

Bacteria live in complex ecosystems in which they are forced to interact with other microorganisms and also eukaryotes [1, 2]. Therefore, bacteria have developed various mechanisms to survive in these environments, e.g. undergoing symbioses with their hosts, producing antibiotics to kill concurrent microorganisms or organising in biofilms being well protected against toxic environmental conditions [3–5]. One notable mechanism are secretion systems designed to actively fight against competitors, such as the type VI secretion system (T6SS) [6]. The T6SS is a nanomolecular weapon found in Gram-negative bacteria belonging to the family of contractile injection systems (CIS) [7]. Upon contraction of the multiprotein complex, the needle-like structure is injected into a target cell, delivering anti-bacterial or anti-eukaryotic effectors [8, 9]. The broad diversity of secreted T6SS effectors enables the T6SS to play a role in both, interbacterial but also interkingdom competition [10]. Genes encoding for T6SS core components can be found in around 25% of Gram-negative bacteria such as *Vibrio* spec., *Burkholderia* spec. or *Pseudomonas* spec. [11–13].

The T6SS is membrane-bound and consists of 13 core components, divided into the membrane complex, baseplate, tube, sheath and the tip [14–18]. The membrane complex anchors the syringe-like structure in the membrane, allowing the complex to span through the whole cell [15]. While the inner tube is build up by hexameric hemolysin-coregulated proteins (HcPs), it is wrapped by a sheath and topped by a trimeric tip consisting of valine-glycine repeat protein G (VgrG) [19, 20]. The spike which is required to perforate the target cell wall, is sharpened by a proline-alanine-alanine-arginine repeat protein (PAAR) to enhance the puncturing [21]. Upon activation of the T6SS, the contraction of the sheath leads to a conformation change, which propels the inner tube out of the cell into a neighbouring target cell [22]. Thereby, the HcP-VgrG-PAAR tip punctures the membrane and allows the delivery of specific T6SS toxins, so-called effectors [23, 24]. While the T6SSs core components are mostly encoded in gene clusters, effector proteins can be encoded either in such gene cluster or in auxiliary clusters found spread in the bacterial genome [14].

The effector arsenal allows the T6SS harbouring bacteria (T6SS$^+$) to tackle different components of the target cell such as the membrane, the cell wall or the DNA/RNA [14, 25, 26]. Those effectors can deploy antibacterial or anti-eukaryotic activities upon functioning as DNases, lipases, peptidases or through the formation of pores [11, 27–29]. To counteract self-intoxication or intoxication of sister cells upon producing the T6SS-effectors, cognate immunity proteins can directly bind to the effectors and thereby neutralize them [30]. The genes encoding those effector-immunity pairs (E-I pair) are found in genomic neighbourhood and are often found in diverse bacteria as result of horizontal gene transfer event [31]. While the identification of T6SS E-I pairs in bacteria has increased throughout the last years, many questions remain open regarding the physiological role of those effectors. One recently identified effector family is the Tme toxin family (Type VI membrane-disrupting effector) found almost exclusively in T6SS$^+$ bacteria [11]. A first study showed the toxic effect of Tme proteins found in *Vibrio parahaemolyticus* towards *E. coli* cells, leading to a reduction in membrane potential and disruption of the cell membrane [11]. These effector proteins are characterised by a DxxK motif and C-terminal transmembrane helix (TMH), providing the effector to integrate into the membrane [11].

Recently, multiple gene clusters encoding for T6SS core components and remote satellite islands (auxiliary clusters) have been identified in the insect pathogenic bacterium *Photorhabdus luminescens* subsp. *luminescens* strain DJC [32], also classified as *P. laumondii* subsp*. luminescens* [33]. This particular bacterium is characterised by phenotypic heterogeneity, which differentiates between i) primary (1°) cell form which lives in symbiosis with entomopathogenic nematodes and ii) the secondary (2°) cell form, which colonizes and protects plants against phytopathogenic fungi [34–36]. Initial studies showed that the T6SSs play a role in interbacterial competition, motility and in the secondary metabolism of *P. luminescens* DJC, but no toxic effector was confirmed experimentally [32]. Furthermore, these studies were limited to the 1° cell form of *P. luminescens* and to date no studies on T6SSs have been performed in bacteria characterised by phenotypic heterogeneity.

Therefore, we aimed to investigate the function of two Tme-like effectors in the *P. luminescens* DJC 1° and 2° cell form through in vivo and in vitro analysis as the complex lifestyle of this bacterium includes diverse interactions with eukaryotes and microorganisms, which makes it a perfect model organism to study the roles of its weaponry. Here we demonstrate that *P. luminescens* DJC harbours two T6SS effectors (Tme1) with antibacterial activity, which can be neutralized through their cognate immunity proteins Tmi1. Moreover, we identified a conserved motif in Tmi1 proteins at the C-terminal end, which is crucial to neutralize the respective Tme1 effector.

4.4 Results

Photorhabdus luminescens DJC harbours two Tme-like effectors

By analysing T6SS effectors in the genome of *P. luminescens* DJC we could identify two Aux clusters (Aux2 and Aux6) harbouring Tme-like effectors (**Fig. 4.1A**). The Aux2 cluster encodes the Tme effector Tme1A (*PluDJC_01980)* and three putative cognate immunity proteins Tmi1 (Tmi1A-C; *PluDJC_01985* – *PluDJC_10995*). Furthermore, a gene encoding the structural component HcP (HcP3, *PluDJC_01970)* was identified downstream of Tme1A, yet in reverse complement direction. Another gene encoding a Tme-like effector was found in the Aux6 cluster, which encodes the E-I pair Tme1B (*PluDJC_05765*) and Tmi1D-F (*PluDJC_05760* – *PluDJC_05750*), yet no carrier protein like VgrG or HcP could be detected in the genomic neighbourhood.

Subsequent *in silico* analysis of the protein sequences revealed two transmembrane regions in the Tme1A C-terminal end and Tme1B as well as a conserved DxxK motif, which has been previously described for a family of Tme effectors (**Fig. 4.1B**) [11]. The two predicted transmembrane regions (TM) in Tme1A range from Phe 192 – Ile 213 and Val 219 – Leu 245, while the DxxK motif was found in the first TM at position Asp 199 – Lys 202. In Tme1B, the transmembrane region was predicted from Ala 152 – Phe 170 and Val 176 – Leu 194, whereas the DxxK motif was in front of the first TM, at position Asp 148 – Lys151. Following AlphaFold2 predictions of the Tme1A and Tme1B protein structure indicated the Tme proteins consist of four α-helical structures (α1, α2, α3 and α4), which are aligned adjacent to each other (**Fig. 4.1C**). While the AlphaFold2-prediction of the first 100 AA in Tme1A and the first 50 AA in Tme1B showed a lower confidence, the transmembrane helices (TMH) could be predicted with a high confidence for both effectors, Tme1A and Tme1B (**Fig. S4.1**). Taken together, our genome analysis of *P. luminescens* DJC confirmed the Tme1-Tmi1 as an E-I pair.

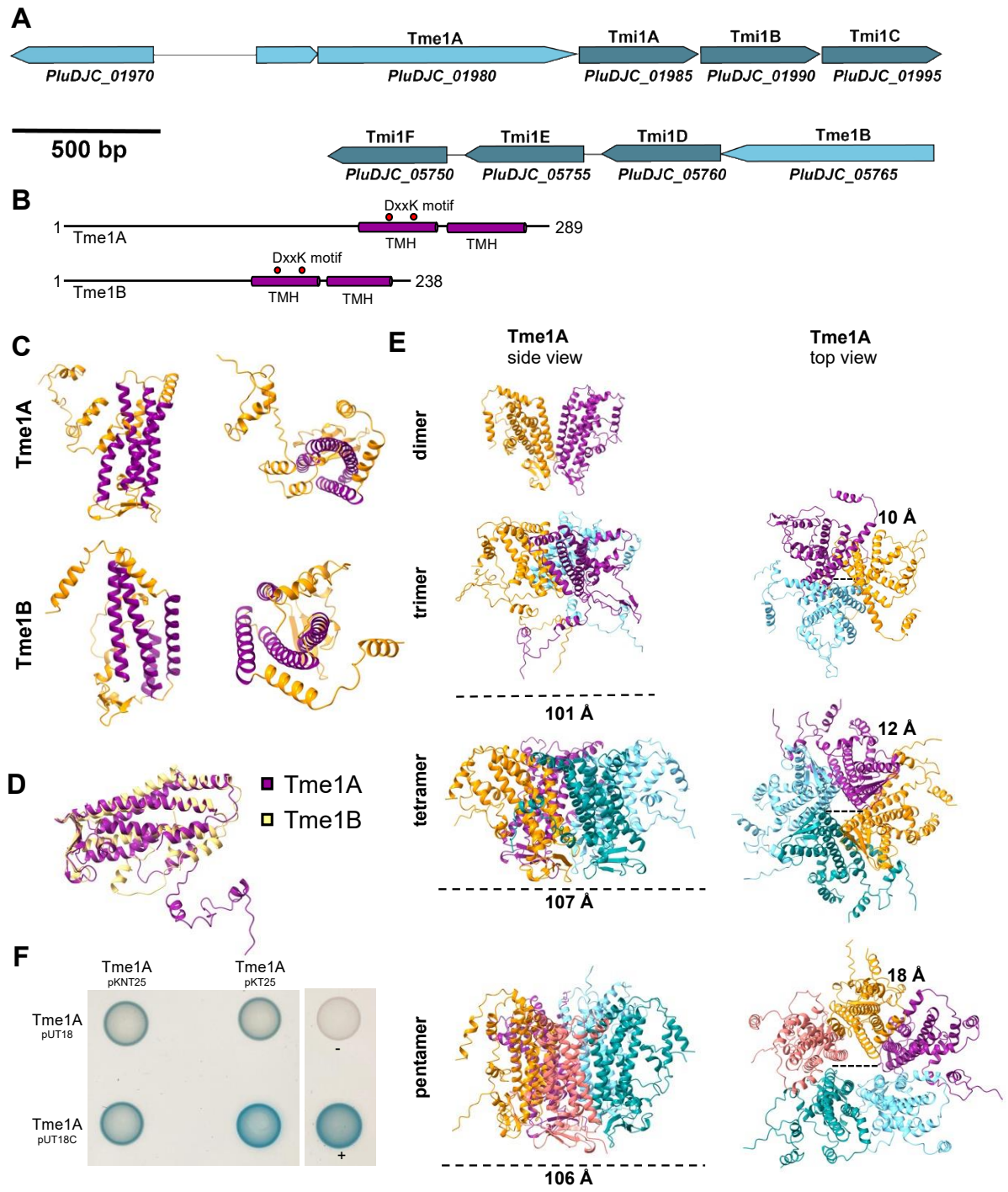

Fig 4.1. *In silico* analysis of the *Photorhabdus luminescens* T6SS effector Tme1A and Tme1B. **A,** Genomic organisation of the auxiliary cluster 2 and auxiliary cluster 6 in *P. luminescens* strain DJC. **B,** Secondary structure predictions of Tme1A and Tm1B including the DxxK motif and transmembrane helices (TMH) predicted by HMMER. **C** AlphaFold2 predicted structures of Tme1A and Tme1B. Purple regions indicate the α-helical structures. **D** Protein structure alignment of Tme1A and Tme1B performed with ChimeraX. **E** Multimer predictions of Tme1A performed with AlphaFold2 as dimer, trimer, tetramer and pentamer. Different colors indicate the monomers of Tme1A, model images are generated with ChimeraX. **F** BACTH analysis of Tme1A-Tme1A self-interaction. Blue colonies indicate an interaction, white colonies show no interaction. *E. coli* BTH101 cells carrying pKT25-zip +

pUT18C-zip and pKNT25 + pUT18 were used as controls. Pictures of similar outcomes of three biological replicates are shown.

Multimeric Tme1A assembles to a pore

Next, to investigate i) the structural properties of Tme1A and Tme1B, ii) their putative multimerization and iii) pore-forming complexes potential; multimer AlphaFold2-predictions were performed. The AlphaFold2-protein structure alignments of Tme1A and Tme1B indicated a high similarity of the TM region and the α-helices, whereas the N-terminal and C-terminal region were rather diverse (**Fig. 4.1D**). Subsequently, we conducted multimer predictions for Tme1A and Tme1B to evaluate their potential to form a pore within a target membrane. These studies were prompted by previous findings that indicated Tme-like effectors acting as membrane-disrupting agents [11]. Given this, we aimed to perform detailed protein structure predictions of multimers to determine whether these proteins could indeed form a pore, thereby confirming their role as membrane-disrupting effectors. By that, Tme1A could be assembled into a trimer, tetramer and pentamer which resemble a pore-forming complex (**Fig. 4.1E**). Upon assembly to a multimer, the two α-helices located in the C-terminal end (α3 and α4) face towards the inner lumen of the pore. Furthermore, the inner lumen size expands significantly when Tme1A is predicted to form a pentamer as opposed to a trimer. While the Tme1A-trimer has a predicted outer diameter of 101 Å and an inner lumen with around 10 Å, the Tme1A pentamer was predicted with a size of 106 Å of the outer diameter and an inner diameter of 18 Å. Similar observations were made upon AlphaFold2-predictions of Tme1B as a multimer (**Fig. S4.2)**. Unlikely to the Tme1A pentamer, the predicted Tme1B pentamer indicates a bigger inner lumen with an outer diameter of 86 Å and an inner diameter of 23 Å (**Fig. S4.2**). The pLDDT and PAE plots for all AlphaFold2 predictions are shown in **Fig. S4.1**. Additionally, *in vivo* protein interaction studies were performed to test whether Tme1A can interact with itself (**Fig. 4.1F**). BACTH assays showed a Tme1A self-interaction in all tested combinations. However, the strongest interaction was observed for T25-Tme1A and T18-Tme1A, when the T25 or T18 fragment were fused N-terminally to Tme1A. Indicating fusion to the C-terminal end

could affect the self-interaction. These data point out that the Tme-like effectors in *P. luminescens* DJC can self-assemble to a pore and putatively disrupt a target cell membrane. Further, first *in vivo* studies indicated that Tme1A can self-interact.

Tme1 effectors interact with the tube protein HcP

Since the gene encoding HcP3 is located in in the Tme1A genomic neighbourhood, we attempted to examine whether Tme1A or Tme1B interact with the tube core component HcP. For that purpose, we cloned the genes encoding the different HcP proteins of *P. luminescens* DJC into the pUT18 plasmid and performed BACTH analyses with the respective pUT25 derviatives harboring the Tme effector coding genes. HcP4 and HcP5 have a premature stop codon and were therefore not considered for BACTH analyses. No interaction was observed for Tme1A and HcP3, but with HcP8 as well as HcP9, which are both encoded in the auxiliary clusters 8 and 9 (**Fig. 4.2A**). Furthermore, a slight interaction of Tme1A was observed with HcP12, which is encoded in the T6SS-4gene cluster. Contrarily, an interaction between Tme1B and HcP2 (which is encoded in the T6SS-1 gene cluster) was observed, indicating that Tme1B is secreted by the T6SS-1 of *P. luminescens* (**Fig. 4.2B**). Slight interactions were also observed between Tme1B and HcP6, HcP7 and HcP8. While HcP6 is not genetically linked with any effector gene, HcP7 is encoded in the T6SS-2 gene cluster. In summary, these data indicate that Tme1A and Tme1B interact with different HcP proteins, suggesting a possible HcP-mediated Tme1A and Tme1B effector transport into the respective target cell.

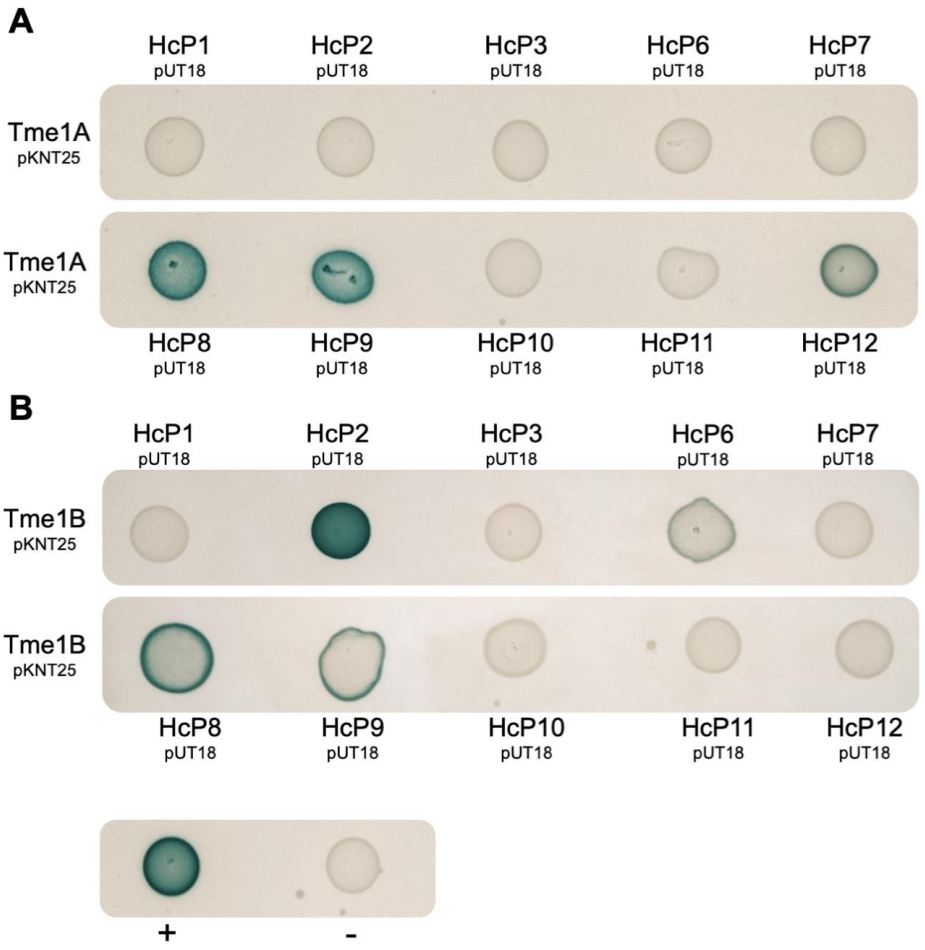

Fig 4.2. Interaction of Tme1A and Tme1B with different HcP tube proteins of *P. luminescens*. BACTH analysis of **A** Tme1A and **B** Tme1B with HcP1-3 and HcP6-12 of *P. luminescens* strain DJC are shown. Genes encoding the respective effector proteins were cloned in the pKNT25 vector and genes encoding the respective HcP tube proteins in the pUT18 vector. Blue colonies indicate an interaction, white colonies show no interaction. *E. coli* BTH101 cells carrying pKT25-zip + pUT18C-zip and pKNT25 + pUT18 were used as controls. Pictures of similar outcomes of three biological replicates are shown.

Antibacterial activity of Tme1 can be cross-neutralized by Tmi1 immunity proteins

Following, we aimed to confirm the antibacterial effect of the *P. luminescens* T6SS effectors Tme1A and Tme1B as it has been shown for respective homologues in other bacteria. Thereby, we expressed genes encoding the respective effectors via the expression plasmid pBAD24 and induced or repressed their transcription with either arabinose or glucose. Here, we considered the FoldChange, which displays the change of bacterial growth during the exponential growth by comparing the repressed (glucose treated) to the induced groups

(arabinose treated). As shown in **Fig. 4.3A**, bacterial growth was impaired when the bacteria overproduced Tme1A or Tme1B, confirming their antibacterial effect. While the expression of *tme1A* in *E. coli* induced with 0.1 % arabinose led to a reduction in bacterial growth by 0.46 FoldChange compared to the glucose control, expression of *tme1B* decreased the bacterial growth by a 0.73 FoldChange, indicating a stronger toxicity compared to Tme1A.

To test whether expression of the T6SS effector genes impairs the bacterial growth and/or leads to cell death, we performed time-lapse microscopy of *E. coli* cells overproducing Tme1A. While the pBAD24 vector control was not impaired in cell growth, the addition of 0.1 % arabinose to the *tme1A* overexpressing strain led to cell rounding, followed by cell lysis within 15 minutes (**Fig. 4.3B**; **Fig. S4.3**).

Previous findings of Tme-Tmi1 E-I pairs in *V. parahaemolyticus* identified one cognate immunity protein encoded in the genomic neighbourhood of the effector, which was not sufficient to provide cross-protection [11]. Unlike in *V. parahaemolytcus*, three genes encoding putative cognate immunity proteins were identified in the genomic neighbourhood of *tme1A* as well as *tme1B* (**Fig. 4.1A**). To determine whether each immunity protein is sufficient to neutralize the Tme1A and Tme1B antibacterial effect, we co-expressed the Tmi proteins along with the effectors. The co-expression of Tme1A and Tmi1A resulted in a complete restored growth upon induction, neutralizing the Tme1A effector (**Fig. 4.3C**). We next co-expressed the cognate immunity proteins Tmi1B and Tmi1C of the Aux2 cluster together with the respective effector Tme1A. While the toxic effect was neutralized partly after 7 h of incubation, yet bacterial growth restored completely and resulted in a growth FoldChange of 0.12 for Tmi1B and 0.19 FoldChange for Tmi1C (**Fig. 4.3C**). We next analysed whether the immunity proteins of the Aux6 cluster could cross-neutralize the Tme1A effector. While co-expression of Tmi1F enabled neutralization of the toxic effect similar to Tmi1C (0.2 FoldChange), the co-expression of Tmi1D and Tmi1E was not sufficient to restore the bacterial growth (**Fig. 4.3C**). Similar to Tme1A, all immunity proteins were tested whether they are able to neutralize the antibacterial effect of Tme1B and were therefore co-expressed and the growth monitored. While Tmi1A (0.19 FoldChange), Tmi1D (0.14 FoldChange), Tmi1E (0.19 FoldChange) and Tmi1F (0.19

FoldChange) partially neutralised the toxic effect; Tmi1B had the strongest neutralization ability (0.06 FoldChange) (**Fig. 4.3D**). In contrary to the previous results, co-expression of Tmi1C was not sufficient to provide cross-protection against Tme1B, leading to a significant decrease in bacterial growth (0.52 FoldChange). These results collectively show, that Tme1A and Tme1B are T6SS effectors of *P. luminescens* deploying antibacterial activity, which can be neutralized by their cognate immunity proteins and partially be cross-neutralized.

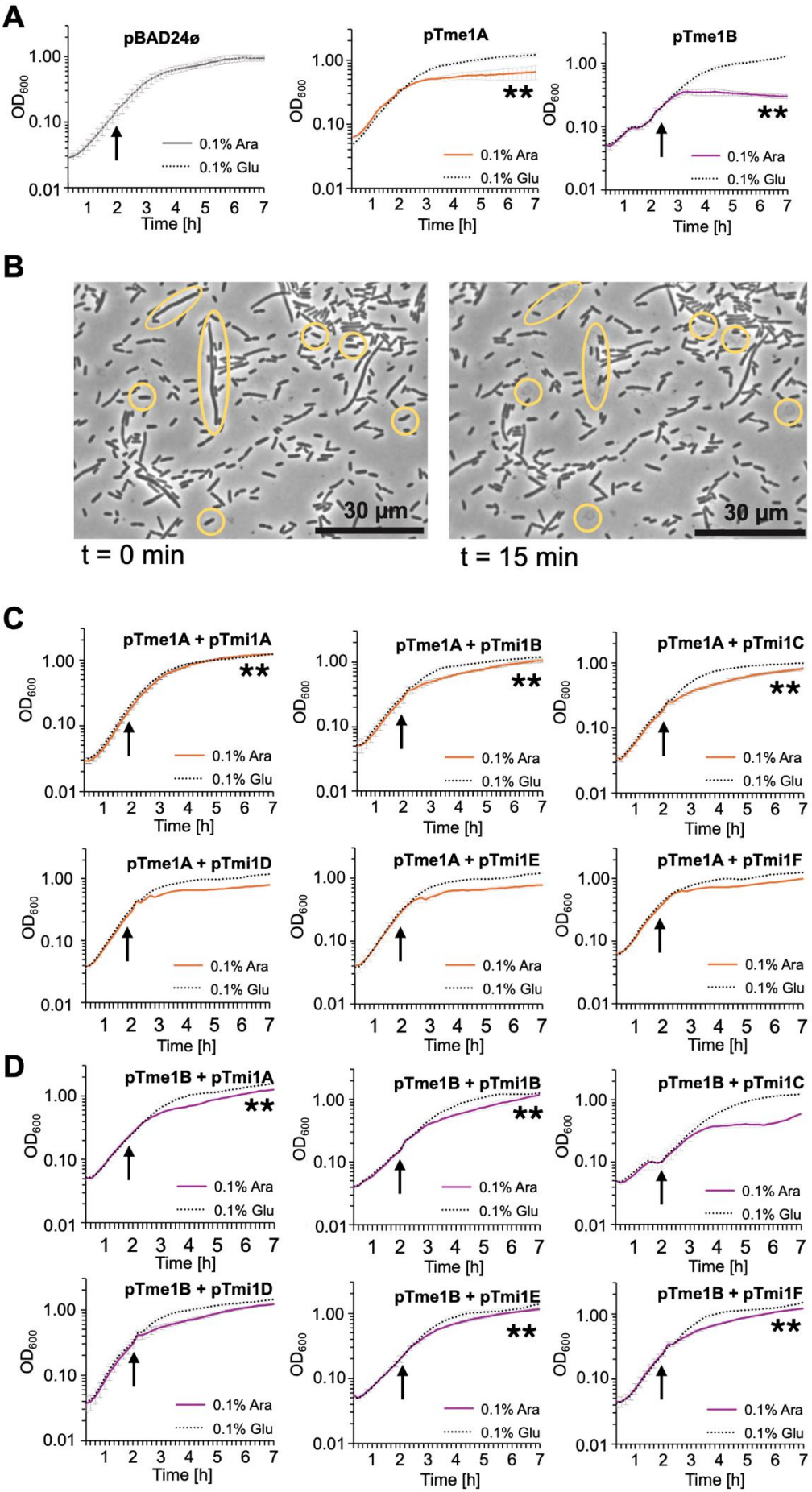
A
pBAD24ø
pTme1A
pTme1B
OD600
Time [h]
0.1% Ara
0.1% Glu
**
B
30 µm
t = 0 min
t = 15 min
C
pTme1A + pTmi1A
pTme1A + pTmi1B
pTme1A + pTmi1C
pTme1A + pTmi1D
pTme1A + pTmi1E
pTme1A + pTmi1F
D
pTme1B + pTmi1A
pTme1B + pTmi1B
pTme1B + pTmi1C
pTme1B + pTmi1D
pTme1B + pTmi1E
pTme1B + pTmi1F

Fig 4.3. Cell protection through Tmi1's against Tme1A and Tme1B. A Expression of *tme1A* and *tme1B* in *E. coli* BL21 star cells induced with 0.1% arabinose (continuous coloured line) or repressed with 0.1% glucose (black dotted line) after 2 h of growth. Growth of *E. coli* was monitored for 7 h. Cells carrying the empty vector were used as control. Arrows indicate the time point arabinose or glucose was added. **B** Time-lapse microscopy of *E. coli* BL21 cells overproducing Tme1A. Disrupting cells are indicated with yellow circles. **C – D** Co-expression of *tme1A* or *tme1B* with the cognate and non-cognate immunity proteins Tmi1A-F. Genes encoding the effector proteins were cloned into pBAD24 and genes encoding the immunity proteins were cloned into pBAD33 vector. Growth of *E. coli* was monitored for 7 h and gene expression resulting in protein overproduction induced with either 0.1% arabinose (continuous colored line) or repressed with 0.1% glucose (black dotted line). Arrows indicate the time point arabinose or glucose was added. The OD_{600} is plotted against the time. Data represent the mean ± standard error of three independent experiments with each technical triplicate. *P* values below 0.05 are indicated in the respective graphs with asterisks (**).

The C-terminal loop of Tmi1 is required for Tme1 protection

Previously was shown that the class of Tme immunity proteins harbours DUF1240 or DUF1240-like domains, yet no specific domain crucial to provide immunity has been identified yet [11]. Considering our previous outcomes by analysing the ability of the immunity proteins to protect the cells, we subsequently performed sequence analysis and multiple sequence alignments. Initial *in silico* analysis of the six Tmi1 protein homologues identified three transmembrane helices and a DUF1240 domain, yet the overall sequence identity was rather low (**Fig. S4.4**). While the immunity proteins encoded by the Aux6 cluster share a sequence similarity of 64 - 84%, the immunity proteins in the Aux2 cluster shared only a sequence identity ranging from 53 – 61% (**Fig. S4.4**). To determine conserved regions, multiple sequence alignments on the amino acid sequences of *P. luminescens* DJC Tmi1 protein was performed. While no conserved region was identified in the N-terminal region, a high conserved region in the C-terminal end (~ 20 amino acids) was found (**Fig. 4.4A**). Following AlphaFold2-predictions indicated the respective conserved region assembles a loop found at the C-terminal end with a high structure similarity (**Fig. 4.4B**, **S4.4**). Respective PAE of AlphaFold2 predictions are shown in **Fig. S4.6**. In order to determine whether the C-terminal loop is involved in the interaction with the effector protein Tme1, AlphaFold2 predictions of Tme1A-Tmi1A interaction were performed (**Fig. 4.4C**). Interestingly, the prediction suggested that the C-terminal loop is

found in proximity of the α3 and α4-helices of Tme1A, which are directed towards the inner lumen upon multimeric pore assembly. Heterodimer predictions of Tme1A and Tme1B with the diverse *P. luminescens* DJC Tmi1 proteins (~ 2500 DUF1240 and DUF1240-like proteins were analysed) showed identical interactions of Tme1 and Tmi1 via the C-terminal loop (**Fig. S4.5**). Thus, this suggests that the C-terminal loop is crucial to provide protection against the Tme1 effectors. The analysis highlighted a conserved motif consisting of an invariant CxxxxW followed by an CxxW (**Fig. 4.4D**). In accordance with the *in silico* analyses, Tmi1C was unable to neutralise Tme1B, which might be caused by an amino acid substitution from tryptophan to leucine within the conserved amino acid motif (**Fig. 4.4C and 4.4D**). To confirm the role of the conserved motif, we generated a plasmid to express a truncated version of *tmi1A* coding for a TmiA derivative lacking the amino acids from position 112 to position 132 ($Tmi1A_{112V}$). While the co-expression of Tme1A and Tmi1A led to a protection of the cells against the effector, co-expression of $Tmi1A_{112V}$ was no sufficient to protect the cells against Tme1A (**Fig. 4.4E**). Therefore, we can conclude that the C-terminal loop is crucial to provide neutralization of the Tme1 effectors and suggest, that the conserved motif is a characteristic feature found in the family of Tmi1 immunity proteins.

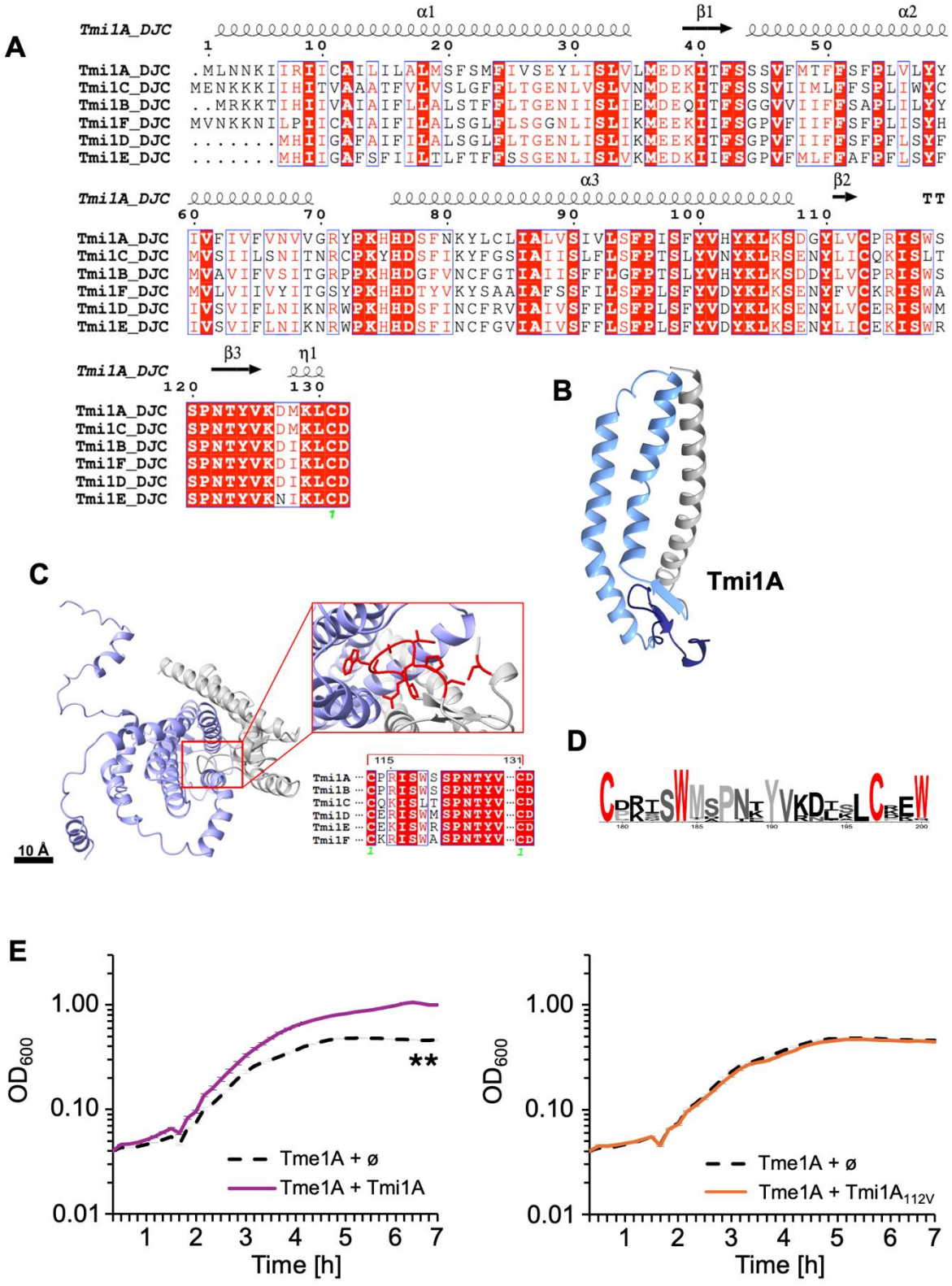

Fig 4.4. Identification of Tmi1 conserved motif in DUF1240 domain containing proteins. A Multiple sequence alignment of Tmi1A-F performed with Clustal Omega and visualized with ESpript 3.0. **B** AlphaFold2 structure prediction of Tmi1A, light blud indicates DUF1240 domain and dark blud C-terminal loop. **C** AlphaFold2 structure prediction of Tme1A-Tmi1A heterooligomer with focused image of

putative interaction side (indicated in red). **D** Conserved amino acid motif found in the C-terminal region of DUF1240 domain containing proteins, illustrated with WebLogo 3 based on multiple sequence alignment. Conserved amino acids are indicated in red. **E** Co-expression of Tme1A-Tmi1A and Tme1A-Tmi1A$_{112V}$ lacking the C-terminal loop. Gene expression was induced after 2 h with either 0.1% arabinose (continuous colored line) or repressed with 0.1% glucose (black dashes line). OD_{600} is plotted against the time. Data represent the mean ± standard error of three independent experiments with each technical triplicate. *P* values below 0.05 are indicated in the respective graphs with asterisks (**).

The promoter of *tme1A* (P_{tme1A}) is active in the exponential growth phase

Finally, to determine how the T6SS-effectors Tme1A and Tme1B contribute to the bacteria's viability, we performed luminescence-based reporter assays in the reporter strain *P. luminescens* DJC Δ*lux*. Briefly, the promoter regions downstream of *tme1A* and upstream of *tme1B* were cloned into the reporter plasmid pBBR1-lux and analysed for bioluminescence. As reported previously, T6SS activity can depend on the presence of bacteria harbouring T6SSs. We therefore tested *Klebsiella pneumoniae* as T6SS$^+$ and *E. coli* Top10 as T6SS$^-$ competitors [37]. Furthermore, since the T6SS is active at different time points during bacterial growth, we monitored the activity of the respective promoters over 24 h. Wheareas in the control groups, reporter strains harbouring pBBR1-lux ø, no luminescence was detected, a signal for P_{tme1A} activity was observed in the *P. luminescens* DJC Δ*lux* strains test group (**Fig. 4.5A**). No activity was observed within the first 9 h, however, the P_{tme1A} and P_{tme1B} promoter activities increased throughout the exponential phase and was then reduced in the stationary phase in both *P. luminescens* DJC 1° and 2° Δ*lux* cells. Using the T6SS$^-$ *E. coli* strain as competitor, a reduction on P_{tme1A} activity was observed in the *P. luminescens* DJC 1° Δ*lux* but not in the 2° Δ*lux* cells. When monitoring the competition with the T6SS$^+$ *K. pneumoniae* strain, an overall reduction in P_{tme1A} activity was detected. Interestingly, no activity for P_{tme1B} was detected in the *P. luminescens* DJC 1° and 2° Δ*lux* cells under the tested conditions. The P_{tme1A} activity and the absence P_{tme1B} activity indicates that Tme1A plays a crucial role in the lifestyle of *P. luminescens* DJC cells.

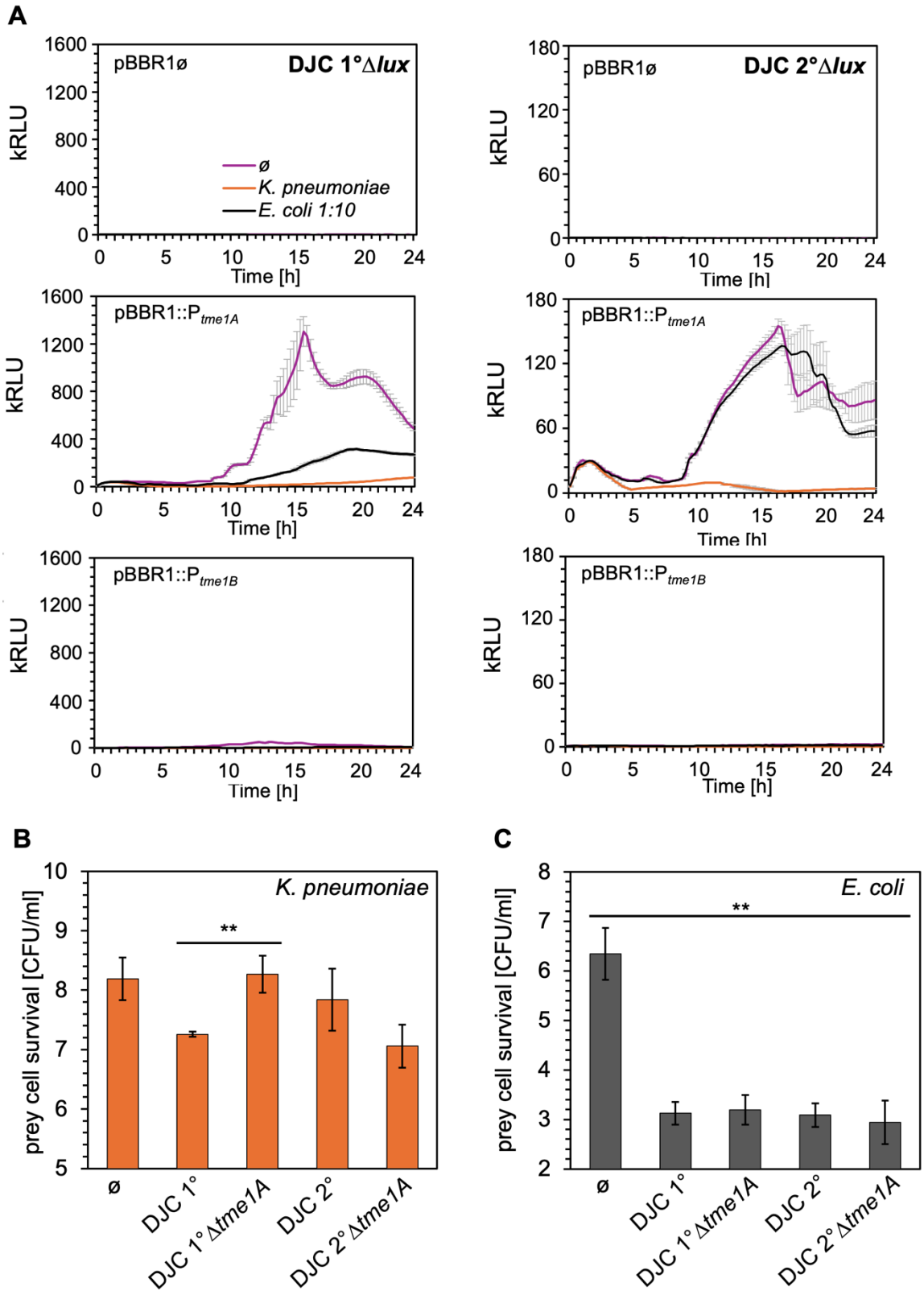

Fig 4.5. Role of Tme1A and Tme1B for the biology of the insect pathogen *P. luminescens*. A Luminescence signal during luminescence-based reporter assays performed with *P. luminescens* 1° and 2°Δ*lux* strains carrying the reporter plasmids pBBR1-luxø, pBBR1-lux::P_{tme1A} and pBBR1-lux::P_{tme1B}.

Prey organisms *E. coli* Top10 and *K. pneumoniae* were added in a 1:10 ratio (prey : hunter) after 2 h of cultivation. Luminescence was measured every 10 minutes for 24 h. Data represent mean ± standard error of three independent experiments with each technical triplicate. Interbacterial competition assay with **B** *K. pneumoniae* and **C** *E. coli* Top10 as prey and *P. luminescens* 1°/2° WT and Δ*tme1A* strains as hunter strains. Prey and hunter were mixed in a 1:10 ratio and co-cultivated for 9 h. Surviving prey cells were quantified of colony forming units (CFU/ml) upon selection on antibiotic resistance. Mean ± standard error of three independent experiments is shown. Asterisk indicates significance according to t-test.

Tme1A is crucial for interbacterial competition

Next, we investigated whether the observed promoter activation of P_{tme1A} in the stationary growth phase reflects a crucial time point in the *P. luminescens* DJC interbacterial competition. For that purpose, we performed interbacterial competition assays using the $T6SS^+$ and $T6SS^-$ strains described above as preys and *P. luminescens* DJC WT and Δ*tme1A* as target strains (**Fig. 4.5B and 4.5C**). Respective *P. luminescens* Δ*tme1B* mutants were not taken in context as no promoter activity was observed in the above-described experiment.

While the prey cells survival rate decreased for both, *K. pneumoniae* and *E. coli* Top10, when competing with *P. luminescens* DJC 1° cells, a significant increase in surviving prey cells could be observed when *P. luminescens* DJC 1°Δ*tme1A* and *K. pneumoniae* competed. On the contrary, competition of *K. pneumoniae* and *P. luminescens* DJC 2°Δ*tme1A* resulted in a decreased amount of surviving prey cells compared to the DJC 2° WT. Interestingly, although the promoter of *tme1A* was active when tested against *E. coli* Top10, no differences were observed in the prey cell survival despite the lack of *tme1A* in *P. luminescens* DJC. However, these results indicate, that the T6SS effector Tme1A plays an important role in interbacterial competition and is crucial for *P. luminescens* DJC when competing with *K. pneumoniae* (a $T6SS^+$ strain).

4.5 Discussion

The diversity of bacteria in terms of their lifestyles requires different mechanisms to maintain their population size and to compete with other microorganisms. The type VI secretion system (T6SS) resembles such a competition mechanism and is found in diverse Gram-negative bacteria [6, 38]. The ability of bacteria to intoxicate a target cell through the T6SS with a broad spectrum of antibacterial or anti-eukaryotic effectors makes it an interesting molecular weapon to study [29, 39]. However, many details about the effectors and their role in bacteria's viability remain unknown. In this study, we have given further insights into the class of T6SS membrane disrupting effectors (Tme) and analysed them with respect to the biological importance for the insect pathogenic bacterium *Photorhabdus luminescens*.

Our bioinformatics analysis on the family of Tme like effectors identified the two effectors Tme1A and Tme1B. The corresponding genes are located within auxiliary gene clusters in the genome of *P. luminescens* strain DJC (**Fig. 4.1A**). Both effectors harbour the Tme conserved motif, however, no further domain such as MIX or PAAR could be identified, which have been previously described to be found in the Tme effector family [11]. Therefore, there is no hint from the homology how the toxins are secreted by the T6SS into a target cell. Yet, the presence of an HcP encoding gene in the genomic neighbourhood of *tme1A* indicates that the Tme1 effectors could be transported within the lumen by hexameric HcP's (**Fig. 4.1A**). The BACTH analyses revealed that Tme1A and Tme1B are indeed able to interact with different HcPs, although Tme1A was not able to interact with HcP3 (**Fig. 4.2A**). As well, the pore-forming T6SS toxins Tse1-4 of *Pseudomonas aeruginosa* have been shown to interact with HcP1, but not HcP2 or HcP3, indicating that the HcP-effector interactions are very unique [40]. Yet, a limiting factor for the transport of toxins through the HcP lumen is the size of the toxin, as the inner lumen of the HcP tube has a size of ~ 40 Å [38]. Nevertheless, Tme1A and Tme1B have a molecular weight of 26 - 32 kDa, therefore, their size is not a restriction and support the hypothesis that Tme is transported along the Hcp tube inside of a target cell.

The BATCH analysis further showed that Tme1A was able to interact with itself, which supports the multimeric AlphaFold2-predictions of a pore formation upon predicting multimers of Tme1A (**Fig. 4.1E and 4.1F**). While these results are mostly based on *in silico* analyses, previous studies showed how Tme of *V. parahaemolyticus* led to membrane disruption and loss of membrane potential similarly to the well-studied VasX effector of *V. cholerae*, which resembles the pore-forming colicins [28, 41, 42]. In addition, our time-lapse microscopy supports the hypothesis of a pore formation, as the Tme1A effector can intoxicate a target cell and thereby disrupt the cell membrane within 15 minutes (**Fig. 4.3B and Fig. S4.3**). However, further biochemical studies are required to confirm the pore formation of the Tme proteins and their mode of action to disrupt a targets cell membrane.

Previous studies showed that DUF1240 proteins can provide immunity against their cognate Tme effectors but cannot provide cross-protection [11]. Unlikely, our results show that the non-cognate immunity proteins can neutralise other Tme effectors, although not with equal efficiency as the cognate immunity proteins (**Fig. 4.3C and 4.3D**). Furthermore, we propose a conserved motif for the Tmi protein family, which is found at the C-terminal end and forms a loop. This is supported by the finding that the absence of the loop results in the toxin no longer being neutralised (**Fig. 4.4E**). Moreover, the C-terminal loop of Tmi1 interacts with the α3- and α4-helices of Tme1, which are located towards the inner lumen of the pore. Therefore, we suggest that neutralization through the Tmi immunity family could rely on the interaction of both proteins. Due to the interaction, the immunity proteins might prevent the hetero-oligomerization of the effector to a pore, similarly to the E-I pairs Tle4-Tli4 and Tse3-Tsi3 of *P. aeruginosa* [43, 44]. Additionally, our findings show that Tmi1C is capable to neutralize Tme1B, while it is the only of the immunity proteins with an amino acid substitution from tryptophan to leucine in the conserved motif (**Fig. 4.3D and 4.4C**). In summary, these results collectively indicate that the C-terminal loop of T6SS immunity proteins is essential to provide neutralization as previously observed in *P. aeruginosa* and here in *P. luminescens.*

Finally, we performed first studies of the T6SS in a bacterium that is characterized by distinct phenotypic heterogeneity. Thereby we aimed to understand the role of Tme1A and Tme1B in

the viability of *P. luminescens* by studying the promoter activity when the bacteria compete against others. While we could not determine under which extracellular or environmental signals Tme1B is essential, Tme1A emerged to be active when the cells enter the exponential growth phase (**Fig. 4.5A and 4.B**). Interestingly, the increased P_{tmeA1} promoter activity in the *P. luminescens* DJC 1° cells goes along with increased survival of *K. pneumoniae* prey cells, when *tme1A* is lacking (**Fig. 4.5C**). This indicates that the T6SS is active under these conditions, and that the effectors are differently used in the two phenotypic different cell forms, which leads us to hypothesize that Tme1A could play a role in competition with other bacteria during nematode symbiosis or in the insect larvae.

Concluding, our study provides new insights on the Tmi1 immunity proteins, indicating that these proteins can neutralize a broader range of Tme1 effectors, albeit varying in their efficiency. Thereby, the C-terminal loop of the Tmi1 proteins is critical for neutralization, as it likely prevents the oligomerization of Tme1 pore formation. To summarize, we propose a model of action on how the Tme1 is T6SS-transferred into the target cells and how the Tme1-Tmi1 pairs is working in *Photorhabdus* (**Fig. 7.2**). Identification of the Tme1-Tmi1 complex by cryo-electron microscopy could help to understand the role of the C-terminal loop in the effector neutralization. Overall, our findings provide new insights into the T6SS function of *P. luminescens* strain DJC, highlighting its importance for bacterial competition within the lifecycle of this biotechnological relevant bacterium.

4.6 Material and methods

Bioinformatics analysis of Tme1-Tmi1 pairs in *P. luminescens*

DNA and protein sequences were obtained from the NCBI database (https://www.ncbi.nlm.nih.gov/). The NCBI CDD was used to obtain information on conserved domains together with HHpred protein analyses [45–47]. Protein structure modelling of monomers and multimers were performed using AlphaFold2 [48, 49]. ChimeraX was used for visualization and structural alignments [50]. Multiple sequence alignments were performed with Clustal Omega and further visualized with ESpript 3.0 [51, 52].

Identification of DUF1240-domain containing proteins

Five iterations of PSI-BLAST against the reference protein *P. luminescens* DJC Tmi1A (WP_011144793.1) were performed to identify proteins containing the DUF1240 domain along with NCBI CDD [45, 46, 53, 54]. Subsequently, protein sequences and accession were retrieved from the NCBI database. DUF1240 domain containing proteins were aligned using Clustal Omega and following illustrated using the WebLogo3 server [51, 55].

Bacterial strains and cultivation

Escherichia coli strains DH5α (λ pir), BL21 star, Top10 tnGFP and BTH101 were grown in LB medium (1% [w/v] tryptone, 0.5% [w/v] yeast extract, 0.5% [w/v] NaCl) supplemented with or without respective antibiotics under aerobic conditions at 37°C. *E. coli* strains DH5α (λ pir) were used for plasmid construction. *E. coli* BL21 star was used for toxicity assays and protein production, and *E. coli* BTH101 was used for bacterial two-hybrid assays. For induction and repression of the genes of interest, 0.1% [w/v] arabinose or 0.1% [w/v] glucose was added to the media. For in vitro assays, *Photorhabdus luminescens* subsp. *luminescens* strain DJC [56] and *Klebsiella pneumoniae* were cultivated aerobically at 30°C in CASO medium (1.5 % [w/v] peptone, 0.5 % [w/v] peptone from soy, 0.5 % [w/v] NaCl).

Generation of plasmids

For arabinose inducible effector gene expression, plasmid pBAD24 was used. To generate pBAD24::Tme1A and pBAD24::Tme1B, genomic *tme1A* was amplified by PCR using the primer pair XmaI-Tme1A-fwd + XbaI-Tme1A-rev and genomic *tme1B* using the primer pair XmaI-Tme1B-fwd and XbaI-Tme1B-rev. The fragment was cloned into pBAD24 plasmid downstream of the P_{ara} promoter, utilizing the introduced restriction sites. To generate the plasmids for immunity protein production, plasmid pBAD33 was used. For amplification of genomic *tmi1A*, the primer pair XbaI-Tmi1A-fwd + HindIII-Tmi1A-rev and for genomic *tmi1B* the primer pair XmaI-Tmi1B-fwd + XbaI-Tmi1B-rev was used. To amplify genomic *tmi1C* and *tmi1D*, the primer pairs XbaI-Tmi1C-fwd + HindIII-Tmi1C-rev and XbaI-Tmi1D-fwd + HindIII-Tmi1D-rev were used. For genomic *tmi1E* and *tmi1F* amplification, the primer pairs XbaI-Tmi1E-fwd + HindIII-Tmi1E-rev and XbaI-Tmi1F-fwd + HindIII-Tmi1F-rev were used. The fragments were then cloned into the pBAD33 plasmid downstream of the P_{ara} promoter, utilizing the respective restriction enzymes. Correct insertion was verified by PCR using the pBAD-fwd and pBAD-rev primer pair, followed by DNA sequencing.

To generate the reporter plasmids pBBR1-lux::P_{tme1A} and pBBR1-lux::P_{tme1B}, the promoter regions of *tme1A* and *tme1B* were cloned into pBBR1-lux plasmid with the respective restriction enzymes. To amplify the promoter of *tme1A*, the primer pair Ptme1A-XbaI + Ptme1A-HindIII and for the promoter of *tme1B* the primer pair Ptme1B-XbaI + Ptme1B-HindIII was used. Correct insertion was confirmed using the primers pBBR1-check-fwd + pBBR1-check-rev, followed by DNA sequencing.

For the generation of BACTH plasmids carrying *tme1A*, the genomic region was amplified by PCR using the primer pair Tme1A-XbaI-B2H + Tme1A-XmaI-B2H. The fragment was cloned into pUT18, pUT18C, pKT25 and pKNT25 (Euromedex, Souffelweyersheim) to generate the plasmids pUT18::Tme1A, pUT18C::Tme1A, pKNT25::Tme1A and pKT25::Tme1A using the restriction enzymes XbaI and XmaI. The plasmid pKNT25::Tme1B was generated by amplification of *tme1B* with the primer pair Tme1B-XbaI-B2H + Tme1B-XmaI-B2H. The amplicon was cloned into pKNT25 using the respective restriction enzymes. BACTH plasmids

carrying the immunity proteins were generated in plasmid pUT18 utilizing the respective restriction enzymes. Genomic *tmi1A* was amplified using the primer pair Tmi1A-XbaI-B2H + Tmi1A-XmaI-B2H, genomic *tmi1B* using the primer pair Tmi1B-XbaI-B2H + Tmi1B-XmaI-B2H, genomic *tmi1C* with the primer pair Tmi1C-XbaI-B2H + Tmi1C-XmaI-B2H, genomic *tmi1D* using the primers Tmi1D-XbaI-B2H + Tmi1D-XmaI-B2H, genomic *tmi1E* with the primers Tmi1E-XbaI-B2H + Tmi1E-XmaI-B2H and genomic *tmi1F* using the primer pair Tmi1F-XbaI-B2H + Tmi1F-XmaI-B2H. To test interactions of Tme1 with the different HcPs, respective pUT18 plasmids were constructed and amplicons inserted using the restriction enzymes XbaI and XmaI. Amplification of *hcP1* was performed by PCR using the primer pair HcP1-XbaI-B2H + HcP1-XmaI-B2H. For genomic *hcP2*, the primer pair HcP2-XbaI-B2H + HcP2-XmaI-B2H was used. Genomic *hcP3* was amplified using the primers HcP3-XbaI-B2H + HcP3-XmaI-B2H and for *hcP6*, the primers HcP6-XbaI-B2H + HcP6-XmaI-B2H. The primers HcP7-XbaI-B2H + HcP7-XmaI-B2H were used to amplify *hcP7*, HcP8-XbaI-B2H + HcP8-XmaI-B2H to amplify *hcP8* and HcP9-XbaI-B2H + HcP9-XmaI-B2H to amplify *hcP9*. Genomic *hcP10* was amplified using the primers HcP10-XbaI-B2H + HcP10-XmaI-B2H, *hcP11* with the primers HcP11-XbaI-B2H + HcP11-XmaI-B2H and *hcP12* with the primer pair HcP12-XbaI-B2H + HcP12-XmaI-B2H. Correct insertion was confirmed by PCR using the primers BACTH-check-fwd, pUT18/C-check-rev, pKNT25-check-rev and pKT25-check-rev, followed by DNA sequencing.

To generate the reporter plasmids pBBR1-lux::P_{tme1A} and pBBR1-lux::P_{tme1B}, the promoter regions of *tme1A* and *tme1B* were inserted into pBBR1-lux plasmid with the respective restriction enzymes. To amplify the promoter of *tme1A*, the primer pair Ptme1A-XbaI + Ptme1A-HindIII and for the promoter of *tme1B* the primer pair Ptme1B-XbaI + Ptme1B-HindIII was used. Correct insertion was confirmed using the primers pBBR1-check-fwd + pBBR1-check-rev, followed by DNA sequencing.

For the generation of plasmids pNTPs::Tme1A and pNTPS::Tme1B for in-frame deletion mutants, 300 bp up- and downstream of genomic *tme1A* and *tme1B* were amplified. To amplify the flanking regions of genomic *tme1A*, the primer pairs FA-Tme1A-BamHI + FA-Tme1A-ovl and FB-Tme1A-ovl + FB-Tme1A-EagI were used. The flanking regions were then fused by

overlap extension PCR using the primer pair FA-Tme1A-BamHI + FB-Tme1A-EagI. For amplification of the flanking regions of genomic *tme1B*, the primer pairs FA-Tme1B-BamHI + FA-Tme1B-ovl and FB-Tme1B-ovl + FB-Tme1B-EagI were used. For fusion of the amplicons by overlap extension PCR, the primer pair FA-Tme1B-BamHI + FB-Tme1B-EagI was used. The resulting fragments were cloned into the pNTPs138-R6KT plasmid using the respective restriction enzymes. Correct insertion was verified using the primer pair pNTPs-check-fwd and pNTPs-check-rev, followed by DNA sequencing. Oligonucleotides sequences are listed in in the supplementary material **Table S4.1**.

Generation of genomic gene deletions in *P. luminescens* and generation of reporter strains

For *tme1A* and *tme1B* deletion in the genome of *P. luminescens* DJC 1° and 2° cells, the plasmids pNTPs::Tme1A and pNTPs::Tme1B were used. Deletion of genes occurred through double homologous recombination as previously described [57]. Briefly, the respective plasmids were conjugated from *E. coli* ST18 cells into *P. luminescens* 1° and 2° cells and selected for Km^R. The pNTPs138-R6KT plasmids carries the *sacB* gene and therefore, a second selection was performed on Sac^R Km^S. Successful deletion was confirmed by PCR using the primer pair FA-Tme1A-BamHI + FB-Tme1A-EagI or FA-Tme1B-BamHI + FB-Tme1B-EagI, followed by DNA sequencing. To generate the *P. luminescens* 1° and 2° reporter strains, the respective plasmids pBBR1-luxø, pBBR1-lux::P_{tme1A} and pBBR1-lux::P_{tme1B} were conjugated from *E. coli* ST18 to 1° and 2° cells. Selection of successful plasmid transfer was ensured for testing the cells on Gm^R.

Effector-immunity protein toxicity assays

To determine the toxic effect of Tme1A and Tme1B, bacterial growth was monitored after effector production. Briefly, *E. coli* BL21 cells were transformed with pBAD24 effector plasmids (pBAD24::effector) and cultivated in LB medium supplemented with carbenicillin and 0.1% [w/v] glucose to repress the P_{ara} promoter. Cultures were adjusted to OD_{600} = 0.01 and 200 µl were transferred into a 96-well plate in technical triplicates. Samples were then incubated for

7 h at 37°C under shaking (135 rpm) and the OD_{600} was measured every 10 minutes using a Spark microplate reader (Tecan, Salzburg). After 2 h, heterologous protein production was started by induction of gene expression using 0.1% [w/v] arabinose, or it was repressed using 0.1% [w/v] glucose. Three biological replicates were performed. *E. coli* BL21 star cells containing the empty pBAD24 vector served as control.

Neutralization of the toxic effectors was determined by co-expression of the effector genes located on the pBAD24 derivatives with the respective immunity genes located on pBAD33 (pBAD33::immunity). Both plasmids contain compatible origins of replication and are therefore stable in *E. coli*. *E. coli* BL21 cells were co-transformed with the respective pBAD24::effectors and pBAD33::immunity plasmid derivatives and cultivated in LB medium containing carbenicillin, chloramphenicol and 0.1% [w/v] glucose. Experiments were performed as described above, except that addition of chloramphenicol was further added to the growth media. Three biological replicates were performed. *E. coli* BL21 star cells containing the pBAD24 and pBAD33 empty vectors served as control. The mean of three independent biological replicates and three technical replicates was calculated and the respective standard error. Statistical analysis was performed through linear regression of logarithmically transformed data.

Time-lapse microscopy

To monitor cells after production of Tme1A, time-lapse microscopy was performed. Briefly, an overnight cultures of *E. coli* BL21 cells containing the pBAD24::Tme1A or pBAD24ø plasmid was inoculated in new medium with OD_{600} = 0.2 and cultivated for another 2 h. Gene expression was induced by the addition of 0.1% [w/v] arabinose. After 15 min, 10 µl were pipetted on a specimen slide and visualized by phase-contrast microscopy with the 100x magnitude (Leica Dmi8 Fluorescence Imaging System). Pictures were taken for 5 minutes in 5 second intervals.

Bacterial adenylate cyclase two-hybrid (BACTH) assays

To understand the delivery mechanism of Tme1A and Tme1B into a target cell, bacterial adenylate cyclase two-hybrid BACTH analysis were performed according to the manufacturer's protocol (Euromedex, Souffelweyersheim). Briefly, genes encoding proteins of interest (X and Y) were amplified by PCR from the *P. luminescens* DJC genome and inserted into the pKNT25 and pUT18 plasmids. *E. coli* BTH101 cells were co-transformed with the respective plasmids and cultivated on LB plates containing carbenicillin (100 µl/ml) and kanamycin (50 µg/ml). 10 µl of an overnight culture were spotted onto a LB plate containing carbenicillin (100 µl/ml), kanamycin (50 µg/ml), IPTG (0.5 M) and X-Gal (40 µg/ml) and incubated for 24 h at 30°C. The interaction was monitored by visual blue colonies, whereas no interaction was indicated by white colonies. As a positive control, cells co-transformed with pUT18C-zip and pKT25-zip were used, and cells co-transformed and with pKT25 and pUT18C served as negative control.

Interbacterial competition assays

P. luminescens strains were tested in interbacterial competition against $T6SS^+$ and $T6SS^-$ bacteria. Streptomycin resistant *E. coli* Top10 tnGFP was used as $T6SS^-$ strain and *Klebsiella pneumoniae* as $T6SS^+$ strain. Competition assays were performed as previously described [32]. Briefly, overnight cultures of *P. luminescens*, *E. coli* and *K. pneumoniae* were mixed in a OD_{600} ratio of 10:1 (hunter : prey), and 100 µl spotted onto a pre-heated CASO agar plate. The cells were co-incubated for 9 h at 30°C and afterwards resuspended in 1 ml sterile PBS buffer pH 7.4 [137 mM NaCl; 2.7 mM KCl; 10 mM 10 mM Na_2HPO_4; 1.8 mM KH_2PO_4]. A serial dilution of the co-culture was spotted onto CASO plates containing the respective antibiotics and then incubated at 30°C. Three biological replicates were performed, and the respective hunter strains alone served as a control.

Luminescence-based reporter assays

To investigate the activity of the *tme1A* and *tme1B* promoter region, luminescence-based reporter assays were performed. Briefly, *P. luminescens* Δ*lux* reporter strains were cultivated

in a black 96-well microtiter plate with a starting OD_{600} = 0.1. After 2 h of incubation at 30°C, *E. coli* Top10 or *K. pneumoniae* were added in a 1:10 ratio (hunter : prey) and cultivated for another 22 h. Blank media served as control. OD_{600} and luminescence was recorded every 30 minutes in a luminescence microplate reader (Tecan, Salzburg) in at least three biological and three technical replicates.

Acknowledgements

We thank Kirsten Schaubruch for excellent technical assistance.

Funding

A.R. received funding by the “Inneruniversitäre Forschungsförderung” of the JGU (Stufe I).

Author Contributions

Conceptualization: Alice Regaiolo

Formal analysis: Friederike Pisarz

Investigation: Friederike Pisarz, Luca Rabbachin, Melanie Hoos, Alice Regaiolo

Resources: Ralf Heermann

Supervision: Alice Regaiolo; Ralf Heermann

Writing - original draft: Friederike Pisarz, Alice Regaiolo

Writing – review and editing: Ralf Heermann, Alice Regaiolo

4.7 References

1. Dunny GM, Brickman TJ, Dworkin M. Multicellular behavior in bacteria: communication, cooperation, competition and cheating. Bioessays. 2008;30:296–8. doi:10.1002/bies.20740.

2. Weiland-Bräuer N. Friends or Foes-Microbial Interactions in Nature. Biology (Basel) 2021. doi:10.3390/biology10060496.

3. Peterson E, Kaur P. Antibiotic Resistance Mechanisms in Bacteria: Relationships Between Resistance Determinants of Antibiotic Producers, Environmental Bacteria, and Clinical Pathogens. Front Microbiol. 2018;9:2928. doi:10.3389/fmicb.2018.02928.

4. Stanley NR, Lazazzera BA. Environmental signals and regulatory pathways that influence biofilm formation. Mol Microbiol. 2004;52:917–24. doi:10.1111/j.1365-2958.2004.04036.x.

5. Sasakawa C, Hacker J. Host-microbe interaction: bacteria. Curr Opin Microbiol. 2006;9:1–4. doi:10.1016/j.mib.2005.12.015.

6. Pukatzki S, McAuley SB, Miyata ST. The type VI secretion system: translocation of effectors and effector-domains. Curr Opin Microbiol. 2009;12:11–7. doi:10.1016/j.mib.2008.11.010.

7. Boyer F, Fichant G, Berthod J, Vandenbrouck Y, Attree I. Dissecting the bacterial type VI secretion system by a genome wide in silico analysis: what can be learned from available microbial genomic resources? BMC Genomics. 2009;10:104. doi:10.1186/1471-2164-10-104.

8. Durand E, Cambillau C, Cascales E, Journet L. VgrG, Tae, Tle, and beyond: the versatile arsenal of Type VI secretion effectors. Trends Microbiol. 2014;22:498–507. doi:10.1016/j.tim.2014.06.004.

9. Hachani A, Wood TE, Filloux A. Type VI secretion and anti-host effectors. Curr Opin Microbiol. 2016;29:81–93. doi:10.1016/j.mib.2015.11.006.

10. Jurėnas D, Journet L. Activity, delivery, and diversity of Type VI secretion effectors. Mol Microbiol. 2021;115:383–94. doi:10.1111/mmi.14648.

11. Fridman CM, Keppel K, Gerlic M, Bosis E, Salomon D. A comparative genomics methodology reveals a widespread family of membrane-disrupting T6SS effectors. Nat Commun. 2020;11:1085. doi:10.1038/s41467-020-14951-4.

12. Bernal P, Allsopp LP, Filloux A, Llamas MA. The *Pseudomonas putida* T6SS is a plant warden against phytopathogens. ISME J. 2017;11:972–87. doi:10.1038/ismej.2016.169.

13. Klonowska A, Melkonian R, Miché L, Tisseyre P, Moulin L. Transcriptomic profiling of *Burkholderia phymatum* STM815, *Cupriavidus taiwanensis* LMG19424 and *Rhizobium mesoamericanum* STM3625 in response to *Mimosa pudica* root exudates illuminates the molecular basis of their nodulation competitiveness and symbiotic evolutionary history. BMC Genomics. 2018;19:105. doi:10.1186/s12864-018-4487-2.

14. Russell AB, Peterson SB, Mougous JD. Type VI secretion system effectors: poisons with a purpose. Nat Rev Microbiol. 2014;12:137–48. doi:10.1038/nrmicro3185.

15. Durand E, van Nguyen S, Zoued A, Logger L, Péhau-Arnaudet G, Aschtgen M-S, et al. Biogenesis and structure of a type VI secretion membrane core complex. Nature. 2015;523:555–60. doi:10.1038/nature14667.

16. Brunet YR, Zoued A, Boyer F, Douzi B, Cascales E. The Type VI Secretion TssEFGK-VgrG Phage-Like Baseplate Is Recruited to the TssJLM Membrane Complex via Multiple Contacts and Serves As Assembly Platform for Tail Tube/Sheath Polymerization. PLoS Genet. 2015;11:e1005545. doi:10.1371/journal.pgen.1005545.

17. Shneider MM, Buth SA, Ho BT, Basler M, Mekalanos JJ, Leiman PG. PAAR-repeat proteins sharpen and diversify the type VI secretion system spike. Nature. 2013;500:350–3. doi:10.1038/nature12453.

18. Wang J, Brackmann M, Castaño-Díez D, Kudryashev M, Goldie KN, Maier T, et al. Cryo-EM structure of the extended type VI secretion system sheath-tube complex. Nat Microbiol. 2017;2:1507–12. doi:10.1038/s41564-017-0020-7.

19. Ruiz FM, Santillana E, Spínola-Amilibia M, Torreira E, Culebras E, Romero A. Crystal Structure of Hcp from Acinetobacter baumannii: A Component of the Type VI Secretion System. PLOS ONE. 2015;10:e0129691. doi:10.1371/journal.pone.0129691.

20. Bondage DD, Lin J-S, Ma L-S, Kuo C-H, Lai E-M. VgrG C terminus confers the type VI effector transport specificity and is required for binding with PAAR and adaptor-effector complex. Proc Natl Acad Sci U S A. 2016;113:E3931-40. doi:10.1073/pnas.1600428113.

21. Wood TE, Howard SA, Wettstadt S, Filloux A. PAAR proteins act as the 'sorting hat' of the type VI secretion system. Microbiology. 2019;165:1203–18. doi:10.1099/mic.0.000842.

22. Brunet YR, Espinosa L, Harchouni S, Mignot T, Cascales E. Imaging type VI secretion-mediated bacterial killing. Cell Rep. 2013;3:36–41. doi:10.1016/j.celrep.2012.11.027.

23. Cianfanelli FR, Alcoforado Diniz J, Guo M, Cesare V de, Trost M, Coulthurst SJ. VgrG and PAAR Proteins Define Distinct Versions of a Functional Type VI Secretion System. PLOS Pathogens. 2016;12:e1005735. doi:10.1371/journal.ppat.1005735.

24. Cianfanelli FR, Monlezun L, Coulthurst SJ. Aim, Load, Fire: The Type VI Secretion System, a Bacterial Nanoweapon. Trends Microbiol. 2016;24:51–62. doi:10.1016/j.tim.2015.10.005.

25. Russell AB, Hood RD, Bui NK, LeRoux M, Vollmer W, Mougous JD. Type VI secretion delivers bacteriolytic effectors to target cells. Nature. 2011;475:343–7. doi:10.1038/nature10244.

26. Burkinshaw BJ, Liang X, Wong M, Le ANH, Lam L, Dong TG. A type VI secretion system effector delivery mechanism dependent on PAAR and a chaperone-co-chaperone complex. Nat Microbiol. 2018;3:632–40. doi:10.1038/s41564-018-0144-4.

27. Hu H, Zhang H, Gao Z, Wang D, Liu G, Xu J, et al. Structure of the type VI secretion phospholipase effector Tle1 provides insight into its hydrolysis and membrane targeting. Acta Crystallogr D Biol Crystallogr. 2014;70:2175–85. doi:10.1107/S1399004714012899.

28. Jana B, Fridman CM, Bosis E, Salomon D. A modular effector with a DNase domain and a marker for T6SS substrates. Nat Commun. 2019;10:3595. doi:10.1038/s41467-019-11546-6.

29. Ray A, Schwartz N, Souza Santos M de, Zhang J, Orth K, Salomon D. Type VI secretion system MIX-effectors carry both antibacterial and anti-eukaryotic activities. EMBO Rep. 2017;18:1978–90. doi:10.15252/embr.201744226.

30. Yang X, Long M, Shen X. Effector–Immunity Pairs Provide the T6SS Nanomachine its Offensive and Defensive Capabilities. Molecules 2018. doi:10.3390/molecules23051009.

31. Thomas J, Watve SS, Ratcliff WC, Hammer BK. Horizontal Gene Transfer of Functional Type VI Killing Genes by Natural Transformation. mBio 2017. doi:10.1128/mbio.00654-17.

32. Pisarz F, Glatter T, Süss D-TM, Heermann R, Regaiolo A. The Type VI secretion systems of the insect pathogen *Photorhabdus luminescens* are involved in interbacterial competition, motility and secondary metabolism. The Microbe. 2024;3:100067. doi:10.1016/j.microb.2024.100067.

33. Machado RAR, Wüthrich D, Kuhnert P, Arce CCM, Thönen L, Ruiz C, et al. Whole-genome-based revisit of *Photorhabdus* phylogeny: proposal for the elevation of most *Photorhabdus* subspecies to the species level and description of one novel species *Photorhabdus bodei* sp. nov., and one novel subspecies *Photorhabdus laumondii* subsp. *clarkei* subsp. nov. Int J Syst Evol Microbiol. 2018;68:2664–81. doi:10.1099/ijsem.0.002820.

34. Forst S, Nealson K. Molecular biology of the symbiotic-pathogenic bacteria *Xenorhabdus* spp. and *Photorhabdus* spp. Microbiol Rev. 1996;60:21–43. doi:10.1128/mr.60.1.21-43.1996.

35. Dominelli N, Platz F, Heermann R. The Insect Pathogen *Photorhabdus luminescens* Protects Plants from Phytopathogenic *Fusarium graminearum* via Chitin Degradation. Appl Environ Microbiol. 2022;88:e0064522. doi:10.1128/aem.00645-22.

36. Regaiolo A, Dominelli N, Andresen K, Heermann R. The Biocontrol Agent and Insect Pathogen *Photorhabdus luminescens* Interacts with Plant Roots. Appl Environ Microbiol 2020. doi:10.1128/AEM.00891-20.

37. Basler M, Ho BT, Mekalanos JJ. Tit-for-tat: type VI secretion system counterattack during bacterial cell-cell interactions. Cell. 2013;152:884–94. doi:10.1016/j.cell.2013.01.042.

38. Mougous JD, Cuff ME, Raunser S, Shen A, Zhou M, Gifford CA, et al. A virulence locus of *Pseudomonas aeruginosa* encodes a protein secretion apparatus. Science. 2006;312:1526–30. doi:10.1126/science.1128393.

39. Mariano G, Trunk K, Williams DJ, Monlezun L, Strahl H, Pitt SJ, Coulthurst SJ. A family of Type VI secretion system effector proteins that form ion-selective pores. Nat Commun. 2019;10:5484. doi:10.1038/s41467-019-13439-0.

40. Howard SA, Furniss RCD, Bonini D, Amin H, Paracuellos P, Zlotkin D, et al. The Breadth and Molecular Basis of Hcp-Driven Type VI Secretion System Effector Delivery. mBio. 2021;12:e0026221. doi:10.1128/mBio.00262-21.

41. Miyata ST, Kitaoka M, Brooks TM, McAuley SB, Pukatzki S. *Vibrio cholerae* requires the type VI secretion system virulence factor VasX to kill *Dictyostelium discoideum*. Infect Immun. 2011;79:2941–9. doi:10.1128/iai.01266-10.

42. Miyata ST, Unterweger D, Rudko SP, Pukatzki S. Dual expression profile of type VI secretion system immunity genes protects pandemic *Vibrio cholerae*. PLoS Pathog. 2013;9:e1003752. doi:10.1371/journal.ppat.1003752.

43. Lu D, Shang G, Zhang H, Yu Q, Cong X, Yuan J, et al. Structural insights into the T6SS effector protein Tse3 and the Tse3-Tsi3 complex from *Pseudomonas aeruginosa* reveal a calcium-dependent membrane-binding mechanism. Mol Microbiol. 2014;92:1092–112. doi:10.1111/mmi.12616.

44. Lu D, Zheng Y, Liao N, Wei L, Xu B, Liu X, Liu J. The structural basis of the Tle4-Tli4 complex reveals the self-protection mechanism of H2-T6SS in *Pseudomonas aeruginosa*. Acta Crystallogr D Biol Crystallogr. 2014;70:3233–43. doi:10.1107/S1399004714023967.

45. Wang J, Chitsaz F, Derbyshire MK, Gonzales NR, Gwadz M, Lu S, et al. The conserved domain database in 2023. Nucleic Acids Res. 2023;51:D384-D388. doi:10.1093/nar/gkac1096.

46. Gabler F, Nam S-Z, Till S, Mirdita M, Steinegger M, Söding J, et al. Protein Sequence Analysis Using the MPI Bioinformatics Toolkit. Curr Protoc Bioinformatics. 2020;72:e108. doi:10.1002/cpbi.108.

47. Zimmermann L, Stephens A, Nam S-Z, Rau D, Kübler J, Lozajic M, et al. A Completely Reimplemented MPI Bioinformatics Toolkit with a New HHpred Server at its Core. J Mol Biol. 2018;430:2237–43. doi:10.1016/j.jmb.2017.12.007.

48. Jumper J, Evans R, Pritzel A, Green T, Figurnov M, Ronneberger O, et al. Highly accurate protein structure prediction with AlphaFold. Nature. 2021;596:583–9. doi:10.1038/s41586-021-03819-2.

49. Mirdita M, Schütze K, Moriwaki Y, Heo L, Ovchinnikov S, Steinegger M. ColabFold: making protein folding accessible to all. Nat Methods. 2022;19:679–82. doi:10.1038/s41592-022-01488-1.

50. Meng EC, Goddard TD, Pettersen EF, Couch GS, Pearson ZJ, Morris JH, Ferrin TE. UCSF ChimeraX: Tools for structure building and analysis. Protein Sci. 2023;32:e4792. doi:10.1002/pro.4792.

51. Madeira F, Pearce M, Tivey ARN, Basutkar P, Lee J, Edbali O, et al. Search and sequence analysis tools services from EMBL-EBI in 2022. Nucleic Acids Res. 2022;50:W276-W279. doi:10.1093/nar/gkac240.

52. Robert X, Gouet P. Deciphering key features in protein structures with the new ENDscript server. Nucleic Acids Res. 2014;42:W320-4. doi:10.1093/nar/gku316.

53. Altschul SF, Madden TL, Schäffer AA, Zhang J, Zhang Z, Miller W, Lipman DJ. Gapped BLAST and PSI-BLAST: a new generation of protein database search programs. Nucleic Acids Res. 1997;25:3389–402. doi:10.1093/nar/25.17.3389.

54. Altschul SF, Wootton JC, Gertz EM, Agarwala R, Morgulis A, Schäffer AA, Yu Y-K. Protein database searches using compositionally adjusted substitution matrices. FEBS J. 2005;272:5101–9. doi:10.1111/j.1742-4658.2005.04945.x.

55. Schneider TD, Stephens RM. Sequence logos: a new way to display consensus sequences. Nucleic Acids Res. 1990;18:6097–100. doi:10.1093/nar/18.20.6097.

56. Zamora-Lagos M-A, Eckstein S, Langer A, Gazanis A, Pfeiffer F, Habermann B, Heermann R. Phenotypic and genomic comparison of *Photorhabdus luminescens* subsp. *laumondii* TT01 and a widely used rifampicin-resistant *Photorhabdus luminescens* laboratory strain. BMC Genomics. 2018;19:854. doi:10.1186/s12864-018-5121-z.

57. Lassak J, Henche A-L, Binnenkade L, Thormann KM. ArcS, the cognate sensor kinase in an atypical Arc system of *Shewanella oneidensis* MR-1. Appl Environ Microbiol. 2010;76:3263–74. doi:10.1128/AEM.00512-10.

4.8 Supplementary Information

Table 4.S1: Oligo nucleotides used in this study

Name	Oligo sequence 5' – 3'
XmaI-Tme1A-fwd	TCTCCCGGGATGCATCATCACCACCACCATATGACATATAAAAAATACAACCCCT
XbaI-Tme1A-rev	CTCTCTAGATTATTTAACATATCTCCCCCAATTA
XmaI-Tme1B-fwd	TCTCCCGGGATGCATCATCACCACCACCATTTGCTATCCTTAGAGGAAGC
XbaI-Tme1b-rev	CTCTCTAGATTATTTACCATAATTCCCCCAG
XbaI-Tmi1A-fwd	CCTATCTAGAATGCATCATCACCACCACCATATGTTAAATAATAAAATAATACGTATTATTTGC
HindIII-Tmi1A-rev	CGTTAAGCTTTCAATCACATAGCTTCATATC
XmaI-Tmi1B-fwd	CCTACCCGGGATGCATCATCACCACCACCATATGAGAAAAAAAACTA
XbaI-Tmi1B-rev	CGTTTCTAGATCAATCACATAGTTTAATA
XbaI-Tmi1C-fwd	CCTATCTAGAATGCATCATCACCACCACCATATGGAAAATAAAAAAAAAGATTATACATATCA
HindIII-Tmi1C-rev	CGTTAAGCTTTCAATCACATAGCTTCATATC
XbaI-Tmi1D-fwd	CCTATCTAGAATGCATCATCACCACCACCATATGCATATCATCGGCG
HindIII-Tmi1D-rev	CGTTAAGCTTTTAATCACATAGTTTAATATCTTTTACATAG
XbaI-Tmi1E-fwd	CCTATCTAGAATGCATCATCACCACCACCATATGCATATTATAGGAGCTTTTTC
HindIII-Tmi1E-rev	CGTTAAGCTTTTAATCACATAGCTTAATGTTTTT
XbaI-Tmi1F-fwd	CCTATCTAGAATGCATCATCACCACCACCATATGGTAAATAAGAAAAATATCTTACC
HindIII-Tmi1F-rev	CGTTAAGCTTTTAATCACATAGCTTAATATCTTTTACATA
Ptme1A-Xba1	GTCATCTAGAGGTACGACCTTAACACC
Ptme1A-HindIII	GTAGAAGCTTACGGCTAACCCCATTA
Ptme1B-Xba1	TACTTCTAGACCGATGTGACGACTTTTG
Ptme1B-HindIII	AGTCAAGCTTCGCAATATACGTTGTATTCTCG
Tme1A-XbaI-B2H	CGTTTCTAGAATGACATATAAAAAATACAACCCCT
Tme1A-XmaI-B2H	CGTTCCCGGGTTATTTAACATATCTCCCCCAATTA
Tme1B-XbaI-B2H	CGTTTCTAGATTGCTATCCTTAGAGGAAG
Tme1B-XmaI-B2H	CGTTCCCGGGTTATTTACCATAATTCCCCCAG

Tmi1A-XbaI-B2H	CCTATCTAGAATGTTAAATAATAAAATAATAC
Tmi1A-XmaI-B2H	CGTTCCCGGGATCACATAGCTTCATATCTTTCAC
Tmi1B-XbaI-B2H	CCTATCTAGAATGAGAAAAAAAACTA
Tmi1B-XmaI-B2H	CGTTCCCGGGATCACATAGTTTAATA
Tmi1C-XbaI-B2H	CCTATCTAGAATGGAAAATAAAAAAAAGAT
Tmi1C-XmaI-B2H	CGTTCCCGGGTCAATCACATAGCTTCATATCTTTTACATA
Tmi1D-XbaI-B2H	CGTTTCTAGAATGCATATCATCGGCGCTTT
Tmi1D-XmaI-B2H	CCTACCCGGGCGAATCACATAGTTT
Tmi1E-XbaI-B2H	CGTTTCTAGAATGCATATTATAGG
Tmi1E-XmaI-B2H	CCTACCCGGGCGAATCACATAGCTTAATAT
Tmi1F-XbaI-B2H	CGTTTCTAGAATGGTAAATAAGAAAA
Tmi1F-XmaI-B2H	CGTTCCCGGGATGGTAAATAAGAAAA
HcP1-XbaI-B2H	CGTTTCTAGAATGGCTGACATGATTTACA
HcP1-XmaI-B2H	CGTTCCCGGGTTAATAAATTCTGTCATCCCAAATA
HcP2-XbaI-B2H	CGTTTCTAGAATGCCAACTCCATGTTATAT
HcP2-XmaI-B2H	CGTTCCCGGGTCAGGCAACAATAGGTG
HcP3-XbaI-B2H	CGTTTCTAGAATGTCACATATAAT
HcP3-XmaI-B2H	CCTACCCGGGATAAATTCTATCAT
HcP6-XbaI-B2H	CGTTTCTAGAATGGCTATTCCTTTATATATGTAC
HcP6-XmaI-B2H	CGTTCCCGGGTTATACCTTTTCAGCCCAA
HcP7-XbaI-B2H	CGTTTCTAGAATGAGTTCTTCAATCTTTTTACAA
HcP7-XmaI-B2H	CGTTCCCGGGTTATTGTTTTTTGTTCTCGATAAGA
HcP8-XbaI-B2H	CGTTTCTAGAATGGCAAATATGATTTA
HcP8-XmaI-B2H	CCTACCCGGGTCAATAAACCATCT
HcP9-XbaI-B2H	CGTTTCTAGAATGGCGAATATAATCTATT
HcP9-XmaI-B2H	CCTACCCGGGTCAGTAAACGTTGTCTTCCCATAT
HcP10-XbaI-B2H	CGTTTCTAGATTGGCTGACTTAATCTATCT
HcP10-XmaI-B2H	CGTTCCCGGGTTAATATACCGTATCTTCCCA

HcP11-XbaI-B2H	CGTTTCTAGAATGGCGATTCCCG
HcP11-XmaI-B2H	CGTTCCCGGGTTACGCCGTCGTG
HcP12-XbaI-B2H	CGTTTCTAGAATGGCAATCCCTGC
HcP12-XmaI-B2H	CGTTCCCGGGTTACGCCTGACTGC
Tmi1A-118V-XbaI	CGTTAAGCTTTACTAAATAGCCATCACTTTTTAAC
FA-Tme1A-BamHI	CCTAGGATCCTGTAATATAGTGCTATCTTCGAATTC
FA-Tme1A-ovl	CGTCAGTAGATCCGTGAAACCCTTTCCA
FB-Tme1A-ovl	GATCTACTGACGTAAAATAATACGTATTATTTGCGCAAT
FB-Tme1A-EagI	CGTTCGGCCGTTATAATGCACATAGAAAGATATGGG
FA-Tme1B-BamHI	CCTAGGATCCTAATCCACATAAAAAGATAAAGGAAAA
FA-Tme1B-ovl	CGTCAGTAGATCGAAAAATATCTTACCAATAATCTGTGC
FB-Tme1B-ovl	GATCTACTGACGCGCAATATACGTTGTATTCTC
FB-Tme1B-EagI	CGTTCGGCCGATGCGTTGCGCTTATC
pBAD-check-fwd	GCCGTCACTGCGTCTTTTACTGG
pBAD-check-rev	CAGAAGTGAAACGCCGTAGCG
pNTPs-check-fwd	TGCTTCCGGCTCGTATG
pNTPs-check-rev	GGACTGGCCGTCGTTTTAC
pBBR1-check-fwd	GTAATGACTCTCTAGCTTGAG
pBBR1-check-rev	TCATCACTTTCGGGAAAG
BACTH-check-fwd	GTGAGCGGATAACAATTTCAC
pUT18/C-check-rev	CTTAACTATGCGGCATCAGAGCAG
pKNT25-check-rev	CTTGCGGCGATACTGCACGGCATAG
pKT25-check-rev	GATGTGCTGCAAGGCGATTAAG

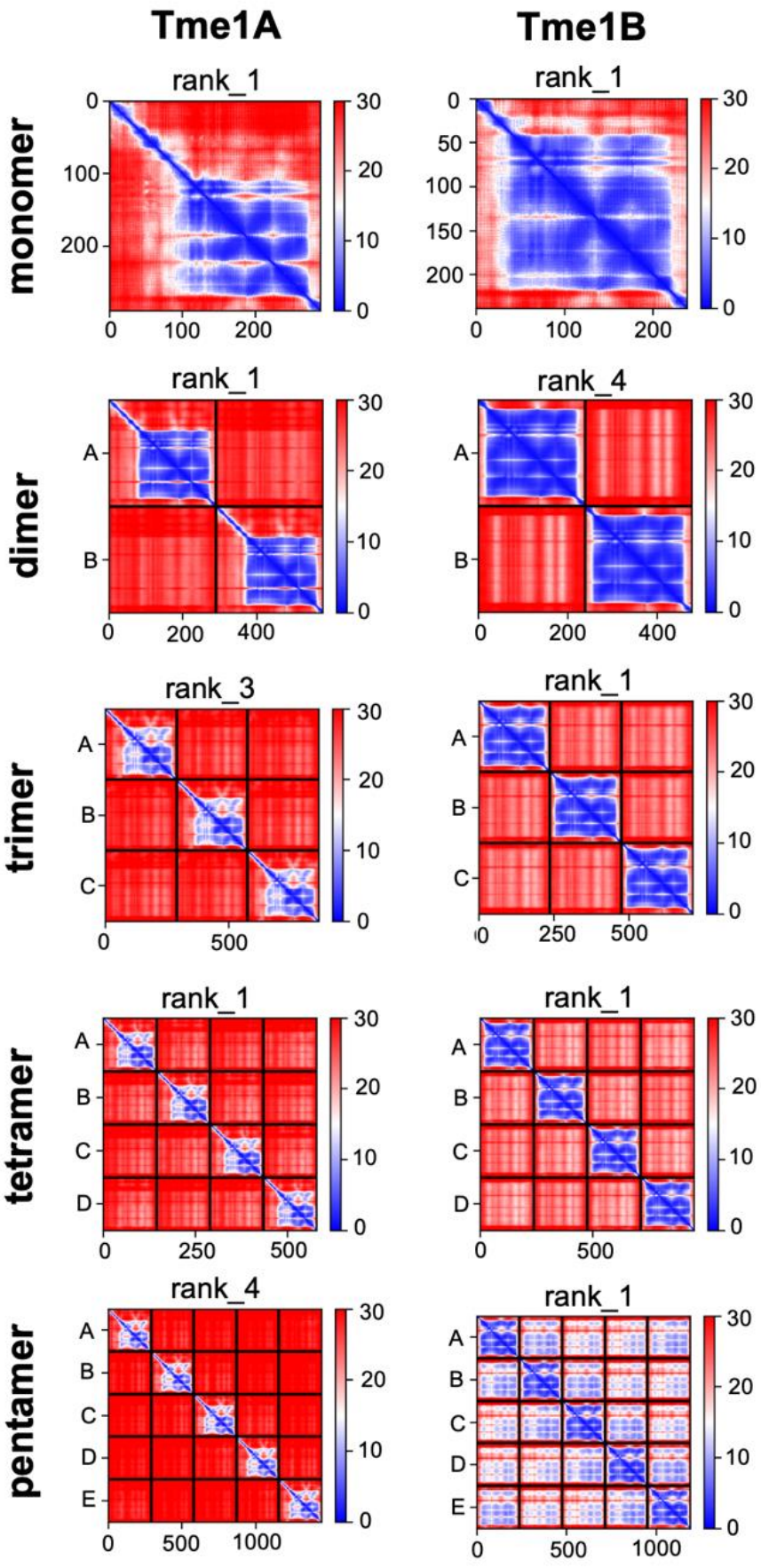

Fig S4.1. AlpaFold2 structure predictions of Tme1A and Tme1B monomer and multimers.

Predicted alignment error (PAE) plots for best model (rank 1 – rank 5).

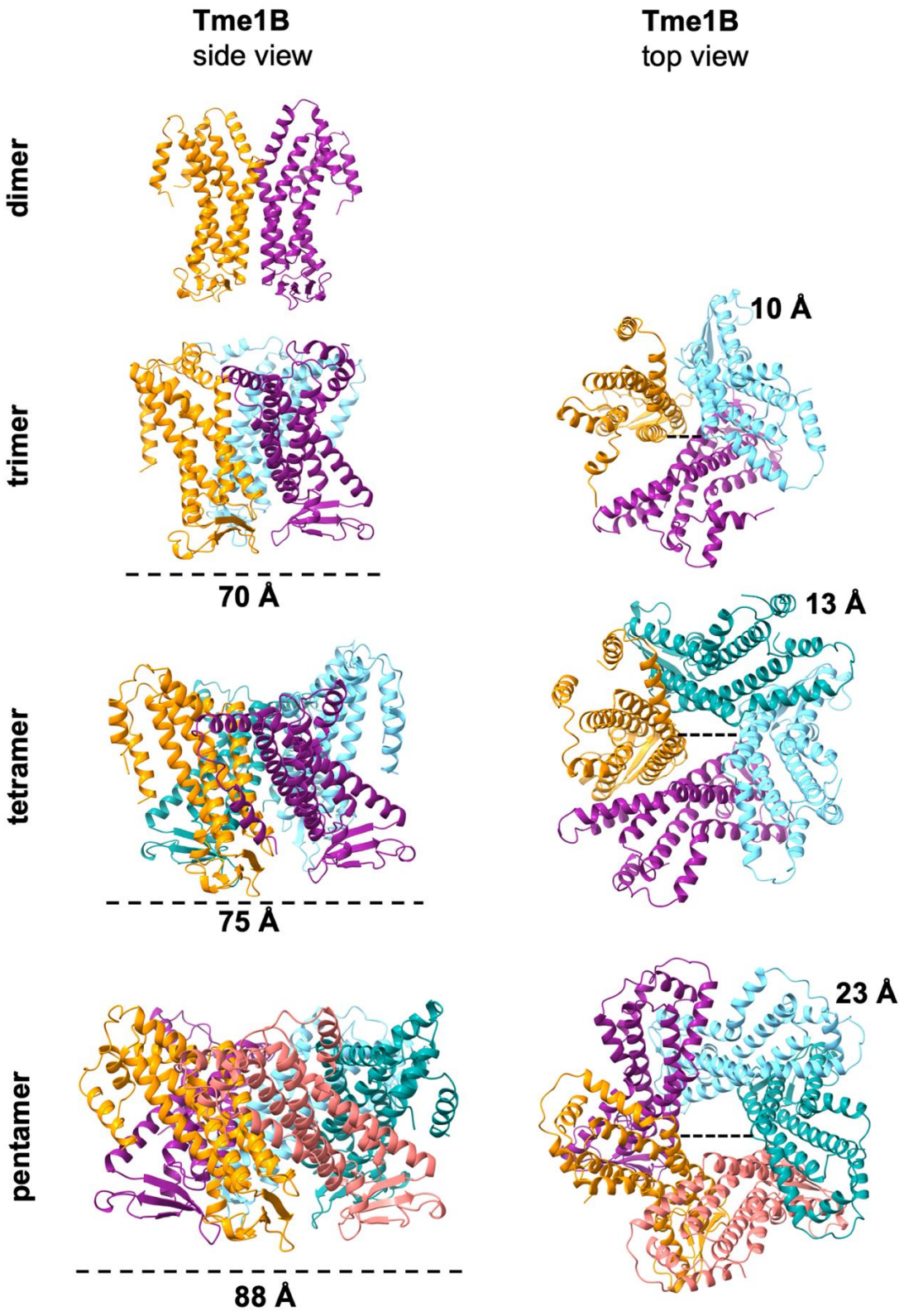

Fig S4.2. Multimer predictions of Tme1B. AlphaFold2 predictions of Tme1B as dimer, trimer, tetramer and pentamer. Different colours indicate monomers of Tme1B. Model images are generated with ChimeraX.

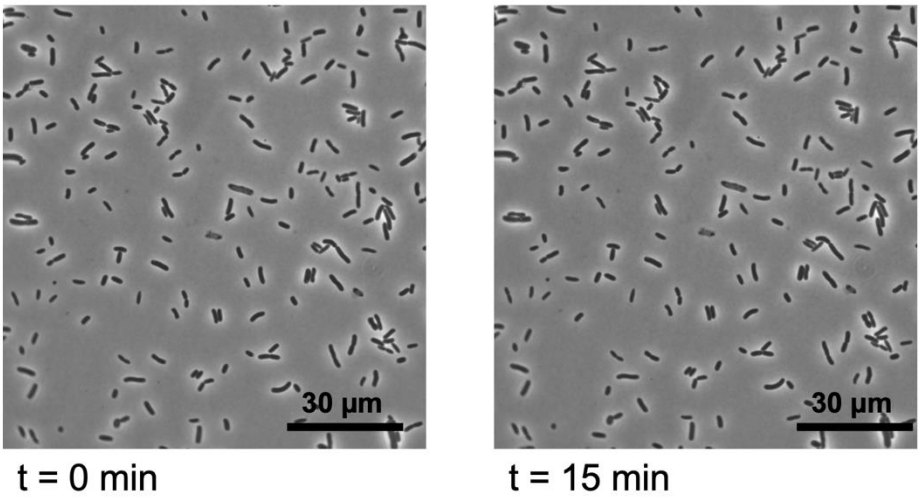

Fig S4.3. Time-lapse microscopy of *E. coli* BL21 cells. Overexpression of *E. coli* BL21 cells carrying the pBAD24 empty plasmid. Expression was induced with 0.1% arabinose and cells following incubated at 30°C for 15 min. Following time-lapse was performed for additional 15 minutes, pictures were taken in 5 second intervals.

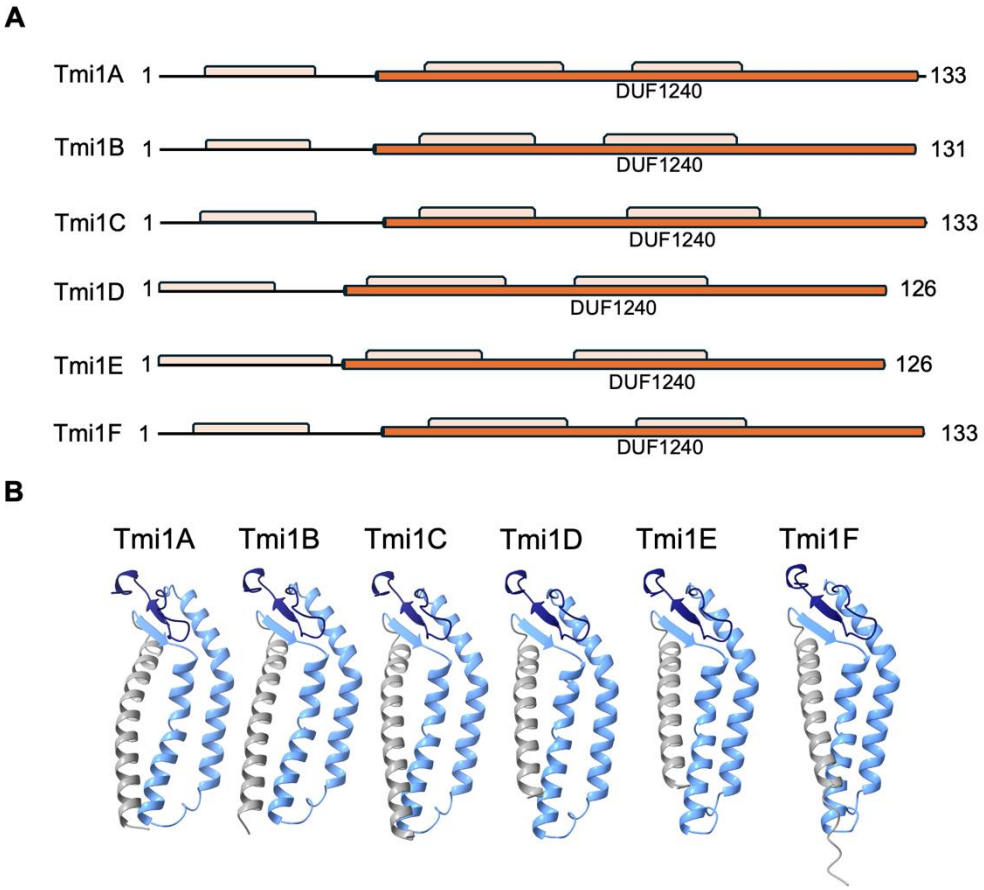

Fig S4.4. Amino acid sequences and AlphaFold2 predictions of the *P. luminescens* Tmi1 immunity proteins. A Amino acid sequence of Tmi1A, Tmi1B, Tmi1C, Tmi1D, Tmi1E, and Tmi1F. The DUF1240 domain is shown in orange and transmembrane helices in beige. **B** AlphaFold2 prediction of Tmi1A, Tmi1B, Tmi1C, Tmi1D, Tmi1E, and Tmi1F. Light blue colour highlights the DUF1240 domain while dark blue highlights the C-terminal loop.

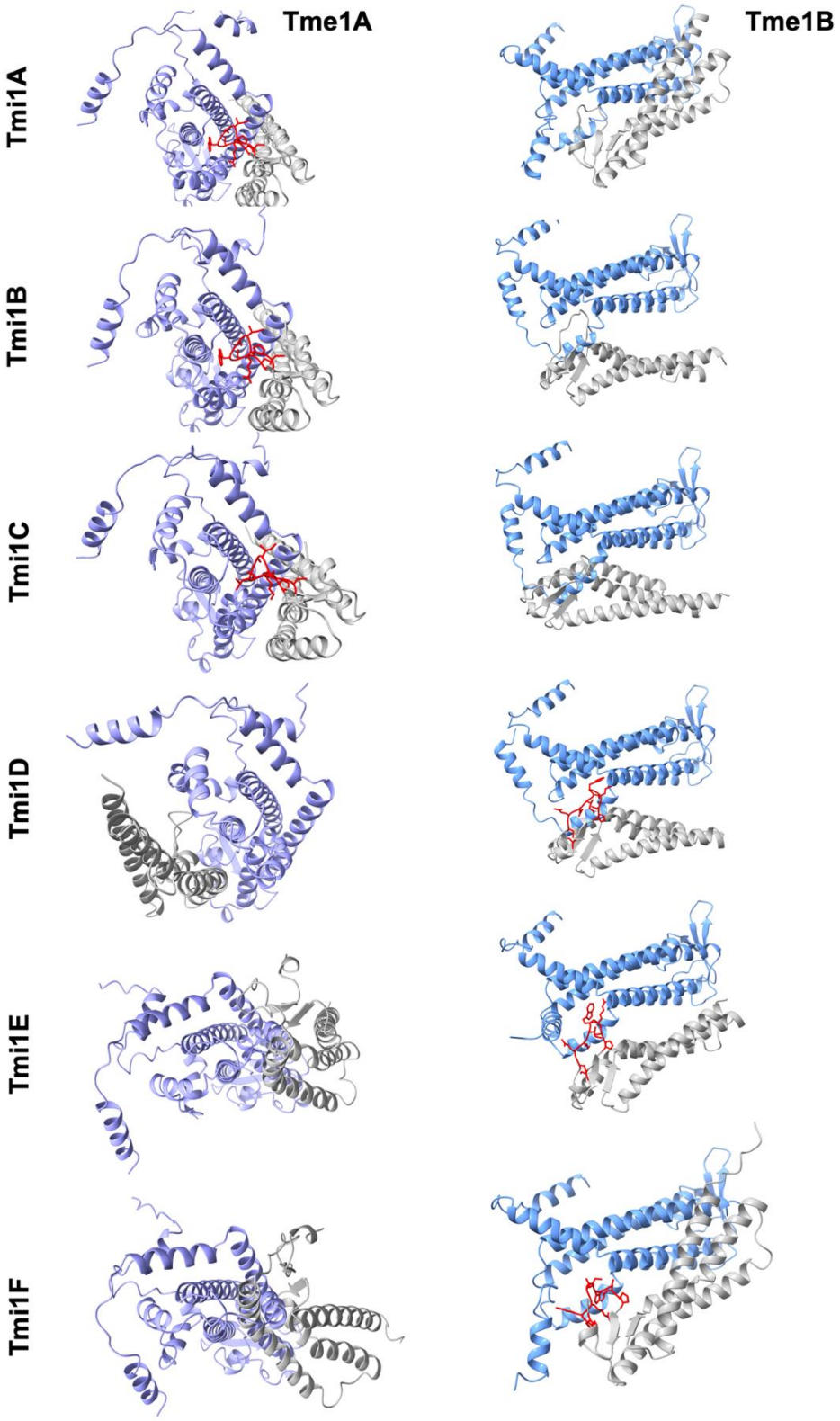

Fig S4.5. AlpfaFold2 predictions of Tme1-Tmi1 interactions. Tme1A and Tme1B are highlighted in blue, Tmi1 proteins is showed in grey. The C-terminal loop of cognate immunity proteins is red-coloured.

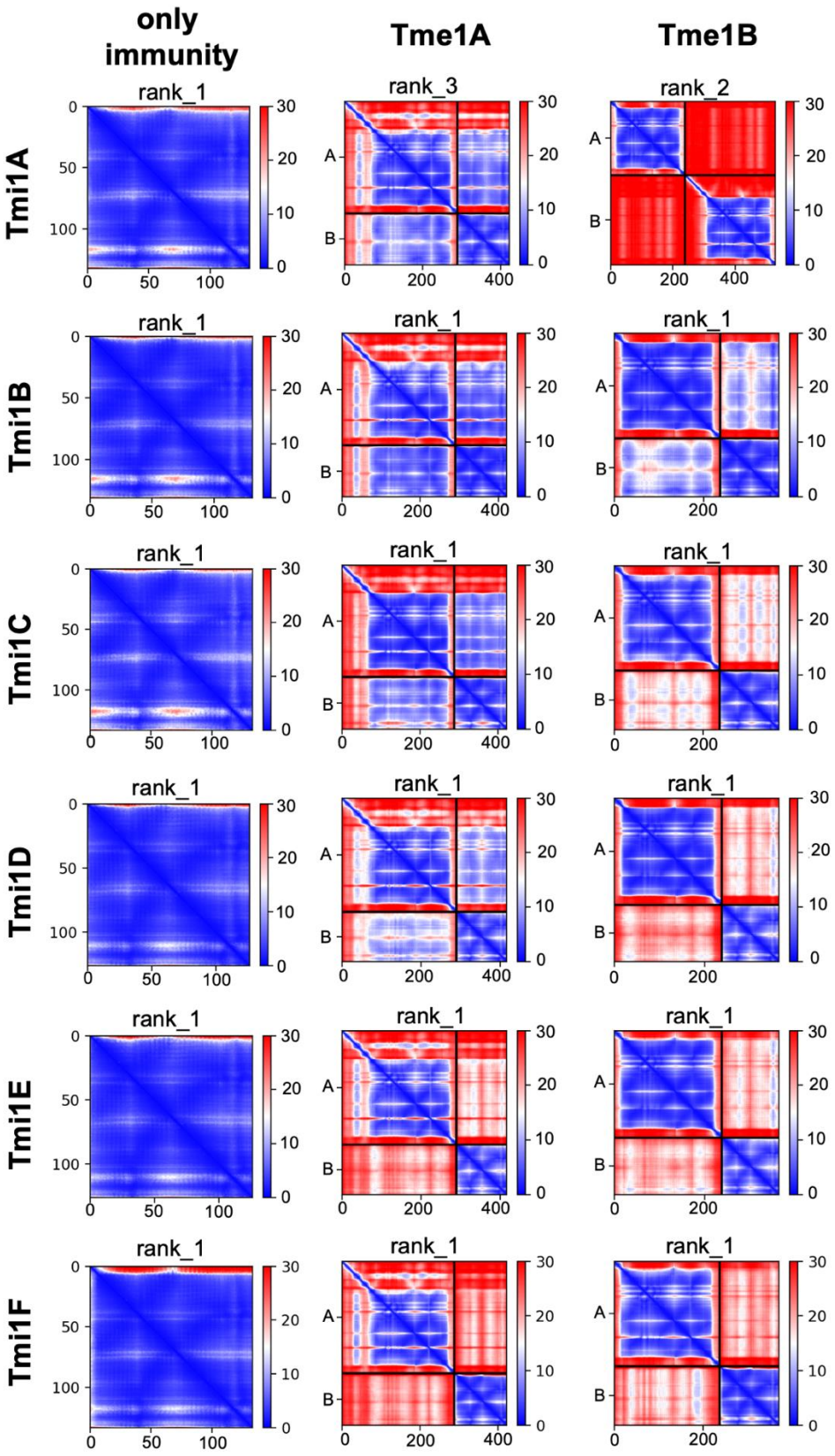

Fig S4.6. AlphaFold2 protein structure predictions of monomeric Tmi1A, Tmi1B, Tmi1C, Tmi1D, Tmi1E, and Tmi1F as well as the Tme1-Tmi1 heterodimers. Predicted alignment error (PAE) plots for best model (rank 1 – rank 5).

5. Lights off – Role of bioluminescence for the biology of the biocontrol agent *Photorhabdus luminescens*

Friederike Pisarz, Luca Rabbachin, Fabio Platz, Alice Regaiolo, Ralf Heermann (2024).

Lights off - Role of bioluminescence for the biology of the biocontrol agent *Photorhabdus luminescens.*

iScience (2024) https://doi.org/10.1016/j.isci.2024.110977

Full-text article:

https://www.cell.com/iscience/fulltext/S2589-0042(24)02202-8

iScience

CellPress
OPEN ACCESS

Article

Lights off - Role of bioluminescence for the biology of the biocontrol agent *Photorhabdus luminescens*

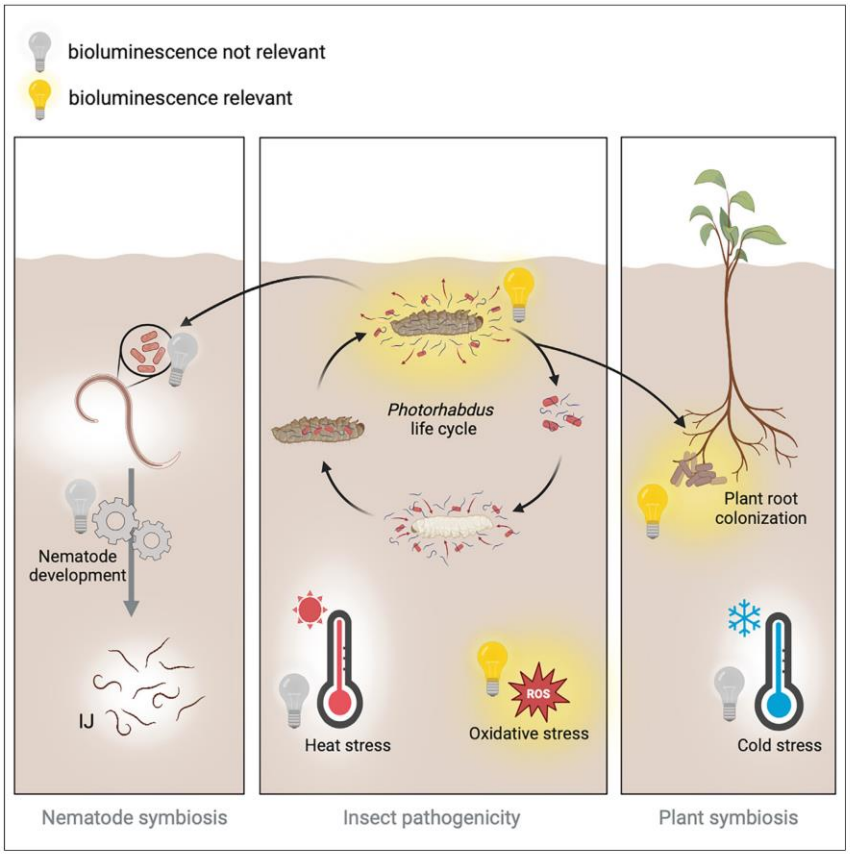

Friederike Pisarz, Luca Rabbachin, Fabio Platz, Alice Regaiolo, Ralf Heermann

aregaiol@uni-mainz.de (A.R.)
heermann@uni-mainz.de (R.H.)

Highlights

Inactivation of the *luxCDABDE* operon in *P. luminescens* results in a dark phenotype

Bioluminescence impacts biotic interactions and stress response of *P. luminescens*

P. luminescens Δ*lux* mutants can be used for bioluminescence-based reporter assays

Pisarz et al., iScience 27, 110977
October 18, 2024
https://doi.org/10.1016/j.isci.2024.110977

iScience

CellPress
OPEN ACCESS

Article

Lights off - Role of bioluminescence for the biology of the biocontrol agent *Photorhabdus luminescens*

Friederike Pisarz,[1] Luca Rabbachin,[1] Fabio Platz,[1] Alice Regaiolo,[1,*] and Ralf Heermann[1,2,3,*]

SUMMARY

Bioluminescence is found across various organisms having crucial functions for biotic interactions and stress adaptation. The only known terrestrial bioluminescent bacteria are entomopathogenic bacteria of the genus *Photorhabdus*. However, the reason why these bacteria produce light is not understood. *P. luminescens* exists in two cell forms called primary (1°) and secondary (2°) cells. The 1° cells colonize the nematode symbiosis partner and produce bright light, whereas 2° cells colonize plant roots only emitting weak light. Here we show that bioluminescence is important but not essential for the biology of the bacteria. Deletion of the *luxCDABE* operon in 1° cells impaired insect pathogenicity and nematode interaction. The complete loss of light of 2° cells resulted in enhanced plant root colonization, enhanced haemolysis, and reduced oxidative stress adaptation. Since bioluminescence is not essential for the survival of the bacteria, *P. luminescens* Δ*lux* 1° and 2° emerged as useful tools for bioluminescence-based reporter assays.

INTRODUCTION

Bacterial bioluminescence has attracted much attention since its first discovery. During the chemical reaction light is emitted, whereby the luciferase LuxAB catalyses the oxidation from $FMNH_2$ under the consumption of oxygen.[1] To date, all known bioluminescent bacteria are Gram-negative and most are found in a marine environment.[2] The biological functions can reach from defense, prey attraction, communication to counterillumination or symbiosis with i.e., fish or squids.[3–5] However, the terrestrial bacterium *Photorhabdus luminescens* is also bioluminescent due to expression of the *luxCDABE* operon.[6] Whilst in marine bacteria such as *Vibrio fischeri* bioluminescence plays an important role for establishing bacterial-host interactions and is relevant for the formation of the squid light organ.[7] Yet, even though many studies have been performed, no direct role for bioluminescence could be assigned for *P. luminescens*, the only terrestrial bacterium found to date deploying bioluminescence.[8,9] *Photorhabdus luminescens* subsp. *luminescens* strain DJC is a Gram-negative entomopathogenic bacterium characterized by insect pathogenicity, plant protection, phenotypic heterogeneity, and name-giving bioluminescence.[10–12] The two phenotypic different cell forms are designated as primary (1°) and secondary (2°) cells. The 1° cells live in mutualistic symbiosis with nematodes of the genus *Heterorhabditidae bacteriophora* and are highly pathogenic toward insects.[13] In addition, there are other properties well-known to *P. luminescens* 1°, such as the production of stilbene and anthraquinones.[14,15] All these phenotypic traits including bioluminescence are highly repressed or absent from 2° cells, respectively. In contrast, 2° cells can colonize and protect plant roots through the production of a chitinase against phytopathogens such as *Fusarium graminearum*.[10,16]

The role of bioluminescence for the physiology and ecology of *P. luminescens* is not yet understood. Previous studies have shown low bioluminescence in *P. luminescens* 1° cells in the exponential growth phase, but very high in the late logarithmic growth phase.[17] However, no potential reason could be defined why bioluminescence decreases in the stationary phase. One of the Patterson's hypotheses is the attraction of uninfected larvae to an already infected larva, which reduces the distance of the nematodes to a new host and therefore supports the nematode-bacteria symbiosis.[18] Another hypothesis suggests that bioluminescence is an event of horizontal gene transfer.[8] Furthermore, it has been suggested that bioluminescence in *P. luminescens* has a simple physiological importance, i.e., reducing the oxidizing conditions in the insect hemolymph when the bacteria reach their high growth rates after infection using the oxygen-dependent luciferase.[19] According to Clarke, dark mutants of *P. temperata* are not able to support nematode development and therefore stated, bioluminescence underlies environmental selection.[20] However, the role of bioluminescence in *P. luminescens* DJC has not been investigated yet, and the importance of the biology of the bacteria is unclear. Yet, the complexity of the *P. luminescens* life cycle, involving multiple eukaryotic interactions, makes the bacterium an interesting candidate as a biocontrol agent. Therefore, extensive studies are essential to determine the various aspects of *P. luminescens* on e.g., the role of the bioluminescence, the microflora of plants, and the optimal environmental conditions to exploit its

[1]Johannes Gutenberg University Mainz, Institute of Molecular Physiology, Microbiology and Biotechnology, Hanns-Dieter-Hüsch-Weg 17, 55128 Mainz, Germany
[2]Institute for Biotechnology and Drug Research gGmbH (IBWF), Hanns-Dieter-Hüsch-Weg 17, 55128 Mainz, Germany
[3]Lead contact
*Correspondence: aregaiol@uni-mainz.de (A.R.), heermann@uni-mainz.de (R.H.)
https://doi.org/10.1016/j.isci.2024.110977

full potential. Reporter assays, using fluorescent proteins or bioluminescence, are one way of investigating gene expression or cellular events of bacteria.[21] While fluorescent proteins have high stability, indicating gene activity, the long half-time of fluorophores cannot reflect accurately the on- and off-phase of the respective genes.[22] Furthermore, a high fluorescence background is often detected depending on the autofluorescence of media compounds or different secondary metabolites produced by the bacteria.[14] In contrast, luminescence-based reporter assays are more sensitive and enable the study of gene activity in bacteria during symbiosis with other organisms without external interfering factors or false positives.[23] Thus, the *P. luminescens luxCDABE* operon has been used for more than 20 years to monitor gene expression in Gram-negative bacteria.[14] To date, luminescence-based reporter assays could not be performed in *P. luminescens* due to its intrinsic luminescence. Therefore, we aimed to shed light on the role of bioluminescence in *P. luminescens* and further establish a luminescence-based reporter assay. Thereby, we generated a *P. luminescens* DJC Δ*lux* mutant in 1° as well as in 2° cells and analyzed various phenotypes that are important for the life cycle of the bacteria. As light production was not essential for growth of *P. luminescens* in both cell variants, we demonstrate that bioluminescence can therefore be perfectly used as a reporter in the engineered *P. luminescens* DJC Δ*lux* 1° and 2° variants.

RESULTS

The role of bioluminescence in the growth of *P. luminescens*

To determine whether bioluminescence plays a functional role in *P. luminescens* DJC such as its growth as well as its adaptation to various environmental changes, we generated mutant strains of *P. luminescens* strain DJC 1° and 2° cells lacking the complete *lux* operon (genes *luxCDABE*; *PluDJC_11100 – PluDJC_11120*). These mutants are further referred to as Δ*lux*. In the initial phase of the study, growth tests were carried out by comparing the growth rate of the *P. luminescens* wildtype 1° and 2° variants compared to the isogenic Δ*lux* mutants in different culture media (Figure 1). No significant differences were observed in bacterial growth when cultivated in either CASO medium (Figure 1A), LB medium (Figure 1B) or M9 medium (Figure 1C). As expected, no luminescence was detected in the *P. luminescens* Δ*lux* strains, whereas a high luminescence was detected in *P. luminescens* 1° cells in CASO or LB medium, after 2 h of cultivation and in the stationary phase. In summary, the deletion of the *lux* operon did not impair bacterial growth and therefore these results showed no correlation between the absence of bioluminescence and bacterial growth when cultivated under standard laboratory conditions.

The role of bioluminescence for stress response and enzymatic activities in *P. luminescens*

We further investigated whether the lack of bioluminescence affects enzymatic activities such as proteolysis or hemolysis or whether it plays a crucial role in stress adaptation mechanisms, which are important for the biology of *P. luminescens*. Therefore, as the second step the growth rate and colony development of the *P. luminescens* Δ*lux* 1° and 2° cells were evaluated in comparison to the respective wildtype. Accordingly, we exposed the bacteria to osmotic salt and sugar stress, oxidative stress and different temperatures measured the $OD_{600,}$ and monitored their ability to form colony forming units. Thereby, we could identify possible correlations between bioluminescence and the bacterial response to environmental stresses (Figure 2A). Surprisingly, the *P. luminescens* 1°Δ*lux* mutant showed a similar fold change of growth rates compared to the isogenic wildtype, however, colony growth was absent in both *P. luminescens* 1° and 1°Δ*lux* cells under most conditions besides salt stress, where colony formation was observed. In contrast, the *P. luminescens* 2°Δ*lux* strain showed a significant decrease in growth and was no longer able to form colonies after the addition of 3% (v/v) H_2O_2, while the *P. luminescens* 2° wildtype was still able to form colonies. Nonetheless, no distinctive pattern could be identified in which the deletion of the *lux* operon plays a crucial role in stress-coping in both, *P. luminescens* 1° and 2° cells.

Next, to test the proteolytic and hemolytic activity semi-quantitative phenotypic assays were performed. For that purpose, the bacteria were plated on caseinate and sheep blood agar, respectively. No significant change in proteolytic activity was observed for the Δ*lux* strains compared to the respective wild type. Only a slight increase in proteolysis was observed for the *P. luminescens* 2°Δ*lux* cells (Figure 2B). However, a significant shift was observed for hemolytic activity in both, *P. luminescens* 1°Δ*lux* and 2°Δ*lux* cells. While a decrease of haemolysis was observed for the *P. luminescens* 1°Δ*lux* strain compared to its wildtype, a significant increase was observed for the *P. luminescens* 2°Δ*lux* cells, with an almost 50% increase in hemolytic activity (Figure 2C). In summary, the absence of bioluminescence due to the deletion of the *lux* operon in the *P. luminescens* 1° cell form did not affect the adaptation to stress as well as the tested enzymatic activity. However, the increased hemolysis observed in *P. luminescens* 2°Δ*lux* cells was accompanied by an impaired ability to adapt to high oxidative stress, suggesting a correlation of bioluminescence with the underlying mechanisms.

Influence of bioluminescence on the interaction of *P. luminescens* with eukaryotic hosts

We then addressed our focus on a comprehensive investigation of the relevance of bioluminescence in the context of the interactions of *P. luminescens* DJC with its eukaryotic hosts that are important at different stages of their life cycle. For that purpose, we investigated insect pathogenicity, nematode colonization as well as plant root colonization of *P. luminescens* DJC 1° as well as 2° cells and the respective mutants lacking their ability to produce light.

First, the insect pathogenicity of *P. luminescens* wildtype and Δ*lux* strains was determined by infecting *Galleria mellonella* larvae by injecting 2.000 cells of the respective bacteria, and mortality was monitored over 48 h (Figure 3A). The *P. luminescens* 1° wildtype showed a lower pathogenicity toward the insect larvae, the mortality of the larvae in the presence of the bacteria was reduced to 35% after 24 h, whereas *P. luminescens* 1°Δ*lux* pathogenicity was reduced by 20%. A reduction in mortality of the larvae was also observed for the *P. luminescens* 2°Δ*lux* strain, with a 30% reduction in mortality of the insect larvae. Additionally, the infected insect larvae were monitored 24 h post-infection

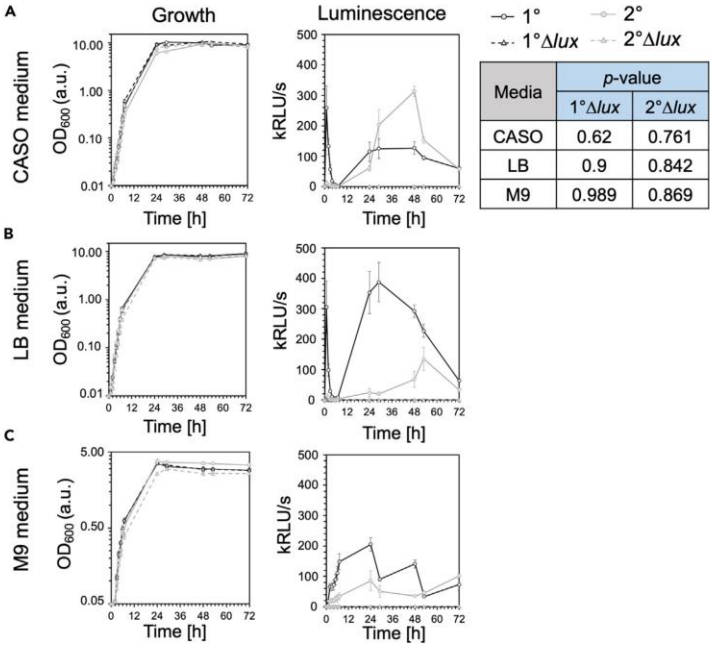

Media	*p*-value	
	1°Δ*lux*	2°Δ*lux*
CASO	0.62	0.761
LB	0.9	0.842
M9	0.989	0.869

Figure 1. Growth and bioluminescence of *P. luminescens* DJC wildtype and Δ*lux* mutants

Growth was monitored over 3 days in CASO medium (A), LB medium (B) and M9 medium (C). Y axis shows the OD_{600} representing logarithmic bacterial growth or the luminescence as relative luminescence (kRLU/s) and the X axis the time in hours. Values are means of three independent biological replicates; error bars represent the standard deviation. The *p*-value using linear regression of OD_{600} was calculated to examine growth differences of the different strains in the same media.

regarding bioluminescence produced by *P. luminescens*, and indeed, luminescent larvae, dead or alive, were observed after infection with *P. luminescens* 1° and 2° wildtype, but not with the respective Δ*lux* cells variants. However, after 48 h the pathogenicity was restored in the *P. luminescens* 2°Δ*lux* cells, while the pathogenicity of the *P. luminescens* 1°Δ*lux* cells was still decreased by 25%. This indicates that the bioluminescence could play a role in the insecticidal activity of *P. luminescens* after insect infection as the loss of bioluminescence led to a reduced insect larvae mortality in the first stages after infection.

Then, we tested whether the *P. luminescens* 1°Δ*lux* cells were still able to re-associate with nematodes and if *P. luminescens* 2° cells were still unable to engage in nematode symbiosis. For that purpose, we counted the number of infective juveniles (IJs) emerging after 21 days of feeding of 50 hermaphrodites on the respective bacterial strain. Approximately 120.000 developed after co-cultivation with the *P. luminescens* 1° wildtype with the hermaphrodites. A slight decrease of 25% IJs was developed compared to the wildtype (Figure 3B). As expected, a significantly lower number of IJs (approximately 20.000) developed on the *P. luminescens* 2° cells. However, the number of IJs developed on the *P. luminescens* 2°Δ*lux* strain was comparable to the wild type. In conclusion, bioluminescence is important for nematode symbiosis of *P. luminescens*, however, is not essential for successful nematode reproduction and development as the luminescent deficient strain was still able to promote nematode development.

It could be demonstrated before that *P. luminescens* 2° cells specifically colonize plant roots.[16] Although bioluminescence is strictly reduced in 2° cells, we nevertheless tested the role of the remaining light of *P. luminescens* for plant interaction by analyzing the colonization of *P. luminescens* DJC 2° Δ*lux* strains with *Arabidopsis thaliana*. For that purpose, *A. thaliana* Col-0 seedlings were co-cultivated with the respective strains for 14 days. Then, the colonization of the roots by the presence of surrounding bacteria or those saddled on the roots were analyzed by microscopy (Figure 3C). As expected, *P. luminescens* 2° wildtype cells could be detected accumulating to the plant roots as well as in the surroundings of the roots. However, the accumulation of cells was also observed with *P. luminescens* 2°Δ*lux* cells, whereby an increased number of cells attached to the roots became visible when microscopically analyzed. This analysis indicates a positive effect on the interaction of *P. luminescens* Δ*lux* 2° cells with plant roots compared to the wild type.

In summary, the deletion of the *luxCDABE* operon and therefore the loss of bioluminescence had slight effects on the *P. luminescens*-host interactions, however, it was not essential for the interaction with the different eukaryotic hosts under the conditions tested. While the *P. luminescens* 1°Δ*lux* strain is impaired to promote nematode development and reduced insect pathogenicity, the *P. luminescens* 2°Δ*lux*

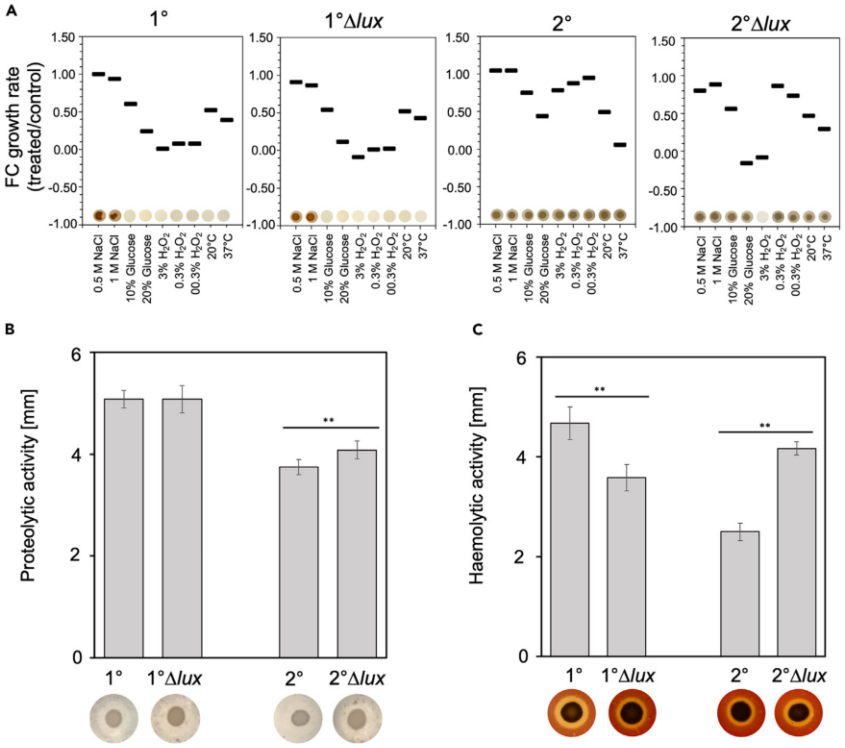

Figure 2. Phenotypical characterization of the *P. luminescens* DJC 1° and 2° wildtype and the respective Δ*lux* strains

(A) Bacterial growth and ability to form colonies tested under different stress conditions. Bacterial growth was measured for 3 h after stress induction, and the growth rate (μ) was calculated in the linear growth phase within the 3 h after stress treatment or without treatment in the same time frame. Displayed is the Fold-change of the treated group against the control group. Colony formation on solid media after stress induction is indicated in the pictures below.

(B) Analysis of proteolytic activity on caseinate agar plates after 2 days.

(C) Secreted hemolytic activity of wildtype and Δ*lux* strains on sheep blood agar plates after 5 days. Errors bars represent the standard deviation of three independently performed experiments. Representative pictures of one trial are displayed. Statistical significance ($p \leq 0.05$) was calculated using a t-test and is indicated with **.

strain showed an enhanced colonization of plant roots, suggesting a less crucial role of the bioluminescence in the *P. luminescens* 2° cells than for the 1° cells.

Using the *lux* operon for bio luminescence-based reporter assays in *P. luminescens*

Fluorescence-based reporter assays are commonly used to detect the activity of bacterial promoters monitoring gene expression. However, the production of secondary metabolites by *P. luminescens* as well as the culture medium can cause background noise and therefore generate false positive results. Since bioluminescence was not observed to be essential for the biology of *P. luminescens*, we tested whether the *P. luminescens* DJC Δ*lux* 1° and 2° cells could be used for bioluminescence-based reporter assays. First, we tested the background signal representing the fluorescence channels used for the detection of various fluorophores (e.g., mCherry, CYA3, YFP, GFP), representing the condition if no expression of these fluorophores is present in the cells. In *P. luminescens* DJC, background noises due to e.g., secondary metabolite production were detected over a time span of 24 h with significant variations in signal strength depending on the culture media, whereas background noises detected for *E. coli* are significantly less (Figure 4). To monitor gene regulation *in vivo* in *P. luminescens*, it is therefore more suitable to apply luminescence-based reporter assays, as no background noise was observed in the initial growth tests performed of the *P. luminescens* 1° and 2°Δ*lux* strains (Figure 1). Therefore, a luminescence-based reporter assay can improve the precision and lower false positives due to the high background fluorescence of *P. luminescens* while examining promoter activities *in vitro*. First, we transformed *P. luminescens* DJC 1°Δ*lux* and 2°Δ*lux* with the pBBR1-*lux* plasmid carrying the *P. luminescens luxCDABE* operon under the control of the *pcfA*, *antA*, or *ftsQ* promoter regions, respectively, and measured bioluminescence in different growth phases of the bacteria over 24 h

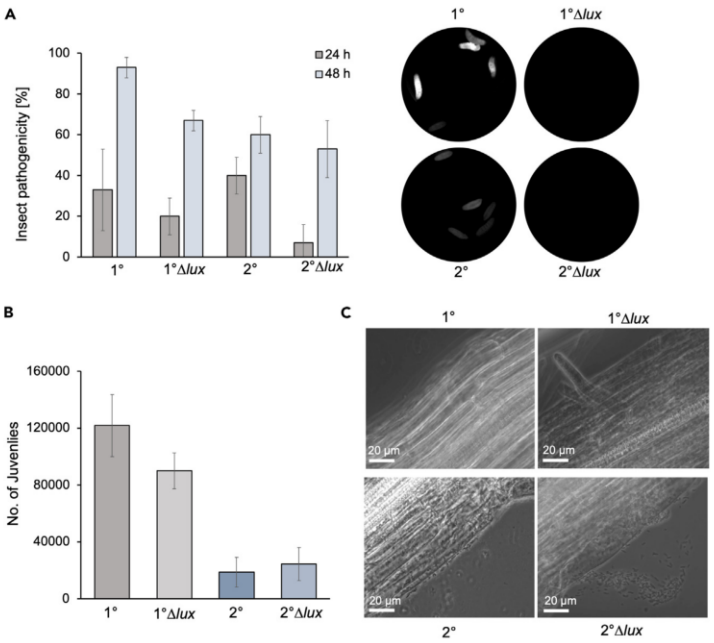

Figure 3. Bacteria-host interactions of *P. luminescens* 1° and 2° Δ*lux* strains

(A) Insect pathogenicity of *P. luminescens* toward *Galleria mellonella* larvae. Five larvae were injected with 2.000 cells and mortality was observed over 48 h. Larvae are shown 24 after infection with 2.000 cells of the respective strains. Luminescence was detected with the Bio-Rad Gel Doc XR$^+$ Gel Documentation System.

(B) Nematode bioassays are performed with *Heterorhabditis bacteriophora* on the respective *P. luminescens* wildtype and Δ*lux* strains. Number of infected juveniles after 21 days is shown.

(C) Phase contrast microscopy of *Arabidopsis thaliana* roots after 14 days of co-cultivation with *P. luminescens* wildtype and Δ*lux* strains. The pictures represent one characteristic of three independent biological replicates. Errors bars represent the standard deviation of three independently performed experiments. Statistical significance is indicated by the t-test (**, $p \leq 0.05$).

(Figure 5). While the promoter of *pcfA* and *antA* have already been shown to be active in the exponential phase in *P. luminescens* 1° cells, activity of the *ftsQ* promoter should be detected in the exponential growth phase, as the protein is crucial for cell division.[24–27] The empty reporter plasmid served as control to rule out the possibility of background luminescence. While no bioluminescence could be detected in the controls, activity of the *pcfA* promoter in the *P. luminescens* 1° cells was observed in the late exponential phase, followed by a significant increase after 20 h in the stationary phase. Similar to the promoter activity of *pcfA*, the *antA* promoter activity increased with the stationary phase in *P. luminescens* 1°Δ*lux* cells but not in *P. luminescens* 2°Δ*lux* cells. However, a significant difference between the culture media could be observed, where the activity of the *antA* promoter was significantly higher in CASO than in the LB medium. In contrast, the *ftsQ* promoter was active in the exponential growth phase in both *P. luminescens* 1°Δ*lux* and 2°Δ*lux* cells and not in the stationary growth phase. In summary, we could observe the expected promoter activities of the different reporter strains as expected from previous results. Furthermore, these results show that the deletion of the *luxCDABE* operon can be complemented in 1° as well as in 2° cells *in trans*. In conclusion, we could highlight that a bioluminescence-based reporter assay is functional in *P. luminescens* and is, therefore, a versatile tool for investigating promoter activities alternatively to the less-sensitive and fluorescence-based reporter assays.

DISCUSSION

Bioluminescence, a phenomenon found in various kingdoms attracted much research since its first observations. Bacterial bioluminescence is mostly found in marine bacteria, where it plays a role in symbiosis with marine fish or squids. However, bacteria of the *Photorhabdus* species live in terrestrial habitats and no role of bioluminescence has been assigned yet.[14,28] With our study, we aimed to clarify the role of the bioluminescence in the insect pathogen *P. luminescens* DJC, an entomopathogenic bacterium previously proposed as a very useful biocontrol agent due to its high bioinsecticide activity as well as plant-growth promoting and antifungal properties.[10,16] Thereby, we were able to generate *P. luminescens* mutants lacking the *luxCDABE* operon, which harbors the crucial genes encoding bacterial luciferase. First, we could show that the lack of bioluminescence does not affect the vitality of *P. luminescens* DJC, i.e., that the inactivation of the corresponding genes

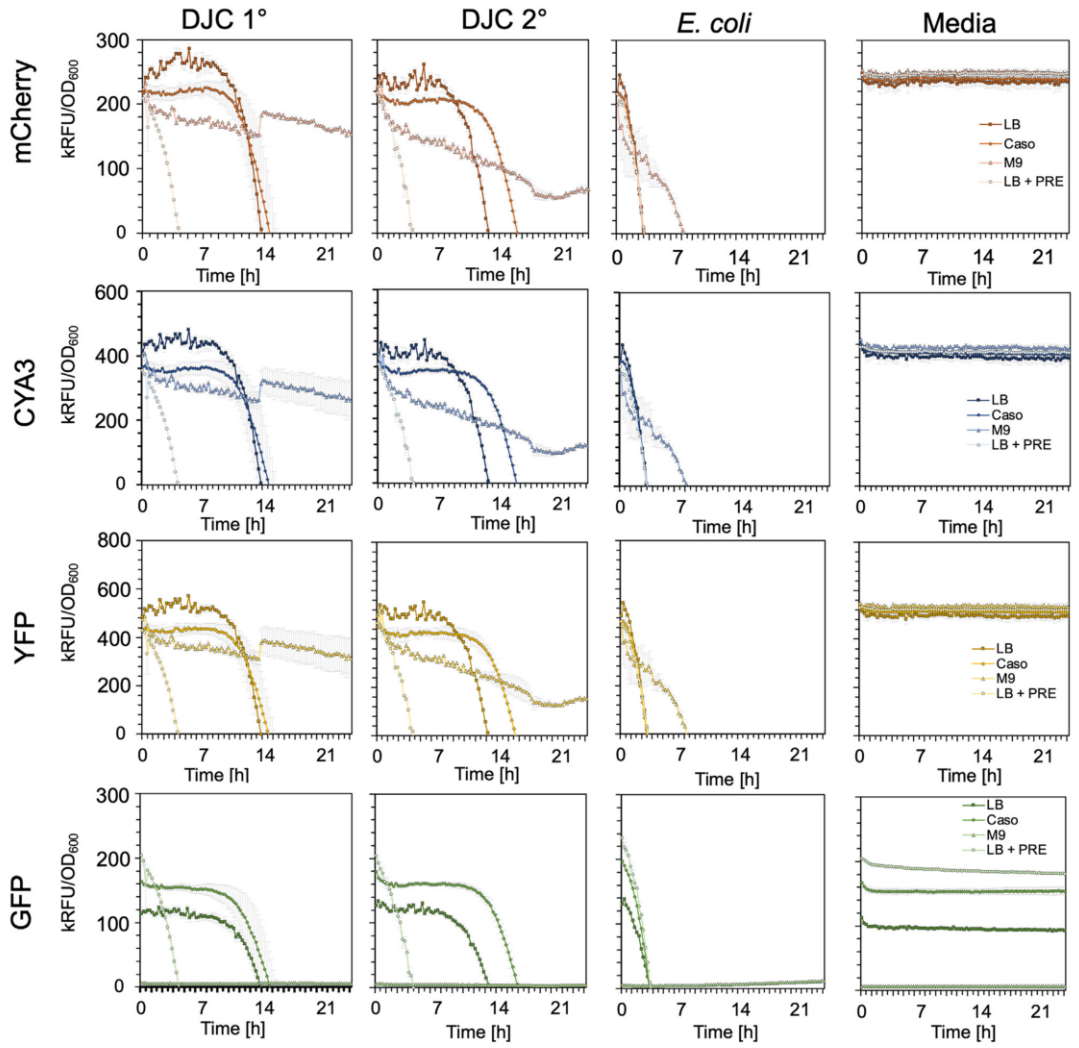

Figure 4. Fluorescence background detected in *P. luminescens* 1° and 2° cells and *E. coli* DH5α λ*pir*

P. luminescens 1° and 2° cells, as well as E. coli, were cultivated in LB, CASO, M9, and LB + 3% PRE at 30°C for 24 h, and OD_{600} as the fluorescence was measured (GFP = excitation/emission 485/535 nm, YFP = excitation/emission 513/530 nm, CYA3 = excitation/emission 579/591 nm, mCherry = excitation/emission 587/610 nm). The respective growth media served as blank controls. The normalized fluorescence with the OD_{600} was plotted against the time. Three biological replicates were performed, and error bars represent the standard deviation of three biological trials.

is not lethal for the bacteria. Furthermore, we could show that light production is important for the interaction with the eukaryotic hosts, yet not crucial to establish these interactions. Based on these results, the *lux*-mutants became accessible for use as putative bioluminescence-base reporter strains through a plasmid-based reporter system, which can be subsequently used to study the phenotypical heterogeneity at gene expression level in both cell variants, the 1° as well as the 2° cells. This offers a more sensitive approach than a fluorescence-based reporter system due to high background fluorescence probably due to the production of a high subset of secondary metabolites by the cells.

Bioluminescence can consume up to 20% of cell energy, making it a highly energy-intensive process.[29] To determine whether the lack of bioluminescence promotes bacterial growth, respective growth assays were performed. However, in the absence of bioluminescence, no increase or decrease in bacterial growth was observed. Therefore, we can conclude that bioluminescence is not related to bacterial growth

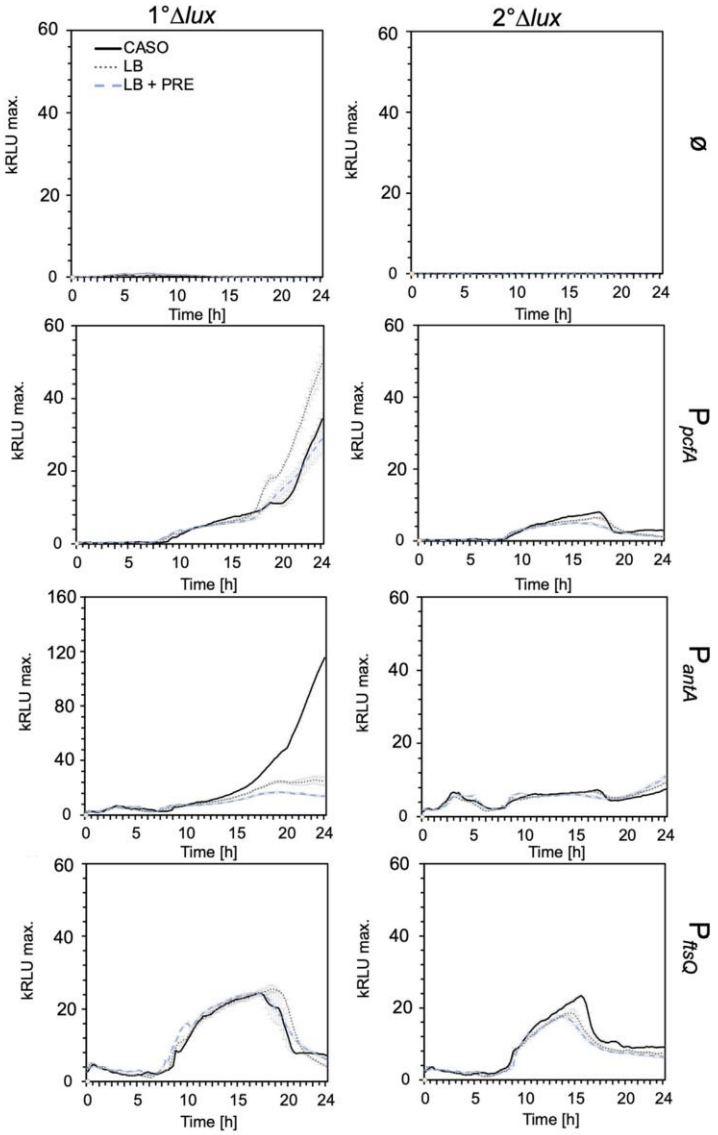

Figure 5. Bioluminescence-based reporter assays in *P. luminescens*

P. luminescens 1°Δ*lux* and 2°Δ*lux* carrying the reporter plasmids pBBR1-luxP_{pfcA}, pBBR1-luxP_{antA} and pBBR1-luxP_{ftsQ} were cultivated in CASO, LB, and LB medium with or without the addition of 3% plant root exudates (PRE) for 24 h. OD_{600} and luminescence were measured in a microplate reader. The y axis indicates the relative luminescence and the x axis the time in hours. *P. luminescens* 1°Δ*lux* and 2°Δ*lux* carrying the empty pBBR1-lux plasmid served as control (ø). Errors bars represent the standard deviation of three independently performed experiments.

under standard laboratory conditions. Therefore, bioluminescence-based reporter assays can be performed without being affected by negative cell growth. Yet, upon the induction of oxidative stress through the addition of 3% H_2O_2, the reduced bacterial growth and the lack of colony formation in *P. luminescens* 2°Δ*lux* cells show that bioluminescence also plays an important physiological role. In the process of bioluminescence, the luciferase LuxAB catalyzes the oxidation of reduced flavin ($FMNH_2$) to oxidized flavin (FMN) under the consumption of O_2 and

it was previously suggested, that bioluminescence protects *P. luminescens* against reactive oxygen species, for example under highly oxidizing conditions in insect hemolymph.[28,30] However, cell death was only observed in *P. luminescens* 2°Δ*lux* cells at high concentrations of hydroperoxide, as it has also been observed for *Vibrio harveyi* Δ*luxA* and Δ*luxB* mutant, suggesting that bioluminescence plays a supporting but not a vital role in adaptation to oxidative stress.[31]

Further analyses of the *P. luminescens* Δ*lux* mutants showed that the lack of bioluminescence does not influence the proteolytic activity, but hemolytic activity with a significant increase in the *P. luminescens* 2° cells and reduction in the *P. luminescens* 1° cells. Presumably, the lack of bioluminescence in the *P. luminescens* 2°Δ*lux* cells could provide energy for other cellular processes such as hemolysis. Indeed, an increase in *P. luminescens* 2°Δ*lux* cells attached and close to the plant roots could also be observed, which suggests similar benefits upon bioluminescence absence although bioluminescence is highly repressed in 2° cells compared to 1° wildtype cells. Previous studies suggested that the lack of bioluminescence is a benefit for the bacteria due to the lower energy costs and that dark mutants could outcompete the luminescent strains.[32,33] However, studies of O'Grady showed, that dark mutants are rather rare and do not bring evolutionary advantage compared to the wildtypes.[34] A further argument against this conclusion is the results of the analyses of the *P. luminescens* 1°Δ*lux* mutant, which is impaired in interacting with nematodes, reduced promotion of the reproduction of IJs, and showed a reduced insect pathogenicity. Therefore, we can conclude that the bioluminescence of the 1° cell form of *P. luminescens* is an advantage in the interaction with the eukaryotic hosts, but it is not essential. However, bioluminescence deficiency in *P. luminescens* DJC 1°Δ*lux* appears to be associated with reduced pathogenicity toward insect larvae, probably by a lack of oxidative stress response in the insect cadaver as previously suggested.[35] Defense mechanisms of the insect larvae could be dependent on the availability of reactive oxygen species, which would be depleted by luciferase activity.[35] Thus, the absence of luciferase could result in the larvae's defense mechanism remaining intact, causing reduced pathogenicity of the bacteria.

In conclusion, the absence of bioluminescence had different effects on the different cell forms of *P. luminescens*. While *P. luminescens* 1° cells are impaired in their interaction with their eukaryotic hosts, *P. luminescens* 2° cells benefit from the absence of luminescence, leading to the increased colonization of plant roots and increased hemolysis. The results again highlight the significant differences between *P. luminescens* 1° and 2° cells, which need to be further investigated to enable the future use of *P. luminescens* as a potent biocontrol agent. The application of bacteria as BCA demands studies of various characteristics, including the interaction with other microorganisms. To elucidate unresolved characteristics between the 1° and 2° cell forms, luminescence-based reporter assays can be used to uncover the underlying gene regulatory mechanisms that lead to the colonization of plant roots with 2° cells on the one hand and to a symbiosis of 1° cells and nematodes on the other. We therefore first tested luminescence-based reporter assays as a further step to optimize the analysis of the two distinct phenotypes as fluorescence-based reporter assays are often not suitable in *P. luminescens*. For this purpose, the promoter activity of P_{pcfA}, P_{antA}, and P_{ftsQ} was examined over a period of 24 h in different media. The expression of the *pcf* gene cluster leads to cell clumping and increased virulence, especially in the *P. luminescens* 1° cells[25,26]. This is also consistent with the results of the *lux*-reporter assays carried out here, where we detected a slight increase in promoter activity in the late exponential phase and a significant increase in the early stationary phase. Furthermore, an altered reporter activity was detected when plant root exudates were added to the medium. Moreover, the activity of P_{antA}, the promoter for the synthesis of anthraquinone, a pigment present in the 1° cell form of *P. luminescens*,[27] was found to increase upon entry into the stationary phase in the CASO medium. In contrast, in the *P. luminescens* 2° cells, only P_{ftsQ} activity was detected in the exponential growth phase, which is also consistent with the expected activity, as FtsQ is a low abundance protein essential for cell division. While studies on promoter activities have been performed before, we can provide here a more detailed study on the promoter activities *in vivo*, monitoring promoter activities over a longer time period without the influence of culture media or secondary metabolites.

Conclusion

Here we could shed light on the role of bioluminescence in the biology of *P. luminescens* DJC. In particular, the reduced pathogenicity and impaired interaction with nematodes in the *P. luminescens* 1° cells caused by the incapability of the bacteria to produce light are of interest, as bioluminescence is generally higher in 1° cells and therefore plays a more important role in the life cycle of the 1° compared to the 2° cells. However, a role of bioluminescence could be assigned in the *P. luminescens* 2° cells as well, supporting the role of light production as adaptation mechanism for oxidative stress in the future. Therefore, transcriptome analyses could unravel the link between bioluminescence and oxidative stress by identifying unknown or further investigating known gene regulation pathways in *P. luminescens*. Finally, the re-introduction of the *lux* genes via a plasmid-based created a versatile reporter system that can be used to investigate bacterial-host interactions in depth over a prolonged time in the future. Overall, this work provides further insights into the complex life cycle as well as into the biology of *P. luminescens* and supports understanding the role of bioluminescence in terrestrial bacteria.

Limitations of the study

Our study demonstrates that the bioluminescence of *P. luminescens* has an impact on the biology of the bacteria, affecting biotic interactions to the three eukaryotic hosts as well as the oxidative stress response. However, it remains unclear whether light emission itself has direct impact on the biology of the bacteria and is sensed by specific receptors, or if light influences other physicochemical parameters within the cell thereby having an indirect effect on the bacterial physiology. It could also be possible that the bacterial light is sensed by the eukaryotic host, i.e., insects, nematodes as well as plants, thereby affecting the biotic interactions with the bacteria. Finally, there are also some limitations for the application of the *P. luminescens* Δ*lux* mutants for bioluminescence-based reporter gene assays. It is not recommended to perform those assays with promoters of genes that are involved in the physiology of the bacteria affected by bioluminescence as those assays are not performed in wildtype backgrounds.

RESOURCE AVAILABILITY

Lead contact

Further information and requests for resources should be directed to and will be fulfilled by the lead contact, Ralf Heermann (heermann@uni-mainz.de).

Material availability

The bacterial strains, plasmids and all new materials described in this study will be shared upon reasonable request from the lead contact.

Data and code availability

- This article does not report the original code.
- Any data reported in this article is available from the lead contact upon request.
- Any additional information reported in this article is available from the lead contact upon request.

ACKNOWLEDGMENTS

Research was funded by the "Inneruniversitäre Forschungsförderung ("Stufe I")," Johannes Gutenberg University of Mainz, Germany, to A.R. We thank Kirsten Schaubruch (JGU) for excellent technical assistance.

AUTHOR CONTRIBUTIONS

Fr.P and L.R. performed the molecular biological and microbiological experiments and analyzed the data. Fa.P. performed the nematode bioassays. Fr.P. and R.H. designed, and R.H. and A.R. supervised the experiments. Fr.P., A.R., and R.H. wrote the article. All authors participated in the scientific discussion and in writing, read and approved the final version of the article.

DECLARATION OF INTERESTS

The authors declare no competing interests.

STAR★METHODS

Detailed methods are provided in the online version of this paper and include the following:

- KEY RESOURCES TABLE
- EXPERIMENTAL MODEL AND STUDY PARTICIPATION DETAILS
- METHOD DETAILS
  - Bacterial strains and cultivation
  - Generation of plasmids
  - Generation of *P. luminescens* mutant and reporter strains
  - Growth assays
  - Insect pathogenicity assays
  - Protease bioassays
  - Haemolysis bioassays
  - Plant root colonization assays
  - Nematode bioassays
  - Extraction of plant root metabolites
  - Bioluminescence-based reporter assays
- QUANTIFICATION AND STATISTICAL ANALYSIS

Received: March 20, 2024
Revised: May 17, 2024
Accepted: September 13, 2024
Published: September 17, 2024

REFERENCES

1. Ulitzur, S., and Hastings, J.W. (1979). Evidence for tetradecanal as the natural aldehyde in bacterial bioluminescence. Proc. Natl. Acad. Sci. USA *76*, 265–267. https://doi.org/10.1073/pnas.76.1.265.
2. Brodl, E., Winkler, A., and Macheroux, P. (2018). Molecular mechanisms of bacterial bioluminescence. Comput. Struct. Biotechnol. J. *16*, 551–564. https://doi.org/10.1016/j.csbj.2018.11.003.
3. Widder, E.A. (2010). Bioluminescence in the ocean: origins of biological, chemical, and ecological diversity. Science *328*, 704–708. https://doi.org/10.1126/science.1174269.
4. Haddock, S.H.D., Moline, M.A., and Case, J.F. (2010). Bioluminescence in the sea. Ann. Rev. Mar. Sci *2*, 443–493. https://doi.org/10.1146/annurev-marine-120308-081028.
5. Dunlap, P.V. (2009). Bioluminescence, microbial. In Encyclopedia of Microbiology (Elsevier), pp. 45–61.
6. Dunlap, P. (2014). Biochemistry and genetics of bacterial bioluminescence. Adv. Biochem. Eng. Biotechnol. *144*, 37–64. https://doi.org/10.1007/978-3-662-43385-0_2.
7. Visick, K.L., Foster, J., Doino, J., McFall-Ngai, M., and Ruby, E.G. (2000). *Vibrio fischeri lux* genes play an important role in colonization and development of the host light organ. J. Bacteriol. *182*, 4578–4586. https://doi.org/10.1128/JB.182.16.4578-4586.2000.
8. Peat, S.M., Ffrench-Constant, R.H., Waterfield, N.R., Marokházi, J., Fodor, A., and Adams, B.J. (2010). A robust phylogenetic framework for the bacterial genus *Photorhabdus* and its use in studying the evolution and maintenance of bioluminescence: a case for 16S, *gyrB*, and *glnA*. Mol. Phylogenet. Evol. *57*, 728–740. https://doi.org/10.1016/j.ympev.2010.08.012.
9. Daborn, P.J., Waterfield, N., Blight, M.A., and ffrench-Constant, R.H. (2001). Measuring virulence factor expression by the pathogenic

bacterium *Photorhabdus luminescens* in culture and during insect infection. J. Bacteriol. *183*, 5834–5839. https://doi.org/10.1128/JB.183.20.5834-5839.2001.

10. Dominelli, N., Platz, F., and Heermann, R. (2022). The insect pathogen *Photorhabdus luminescens* protects plants from phytopathogenic *Fusarium graminearum* via chitin degradation. Appl. Environ. Microbiol. *88*, e0064522. https://doi.org/10.1128/aem.00645-22.
11. Rajagopal, R., and Bhatnagar, R.K. (2002). Insecticidal toxic proteins produced by *Photorhabdus luminescens akhurstii*, a symbiont of *Heterorhabditis indica*. J. Nematol. *34*, 23–27.
12. Eckstein, S., Dominelli, N., Brachmann, A., and Heermann, R. (2019). Phenotypic heterogeneity of the Insect pathogen *Photorhabdus luminescens*: insights into the fate of secondary cells. Appl. Environ. Microbiol. *85*, e01910-19. https://doi.org/10.1128/AEM.01910-19.
13. Forst, S., and Nealson, K. (1996). Molecular biology of the symbiotic-pathogenic bacteria *Xenorhabdus* spp. and *Photorhabdus* spp. Microbiol. Rev. *60*, 21–43. https://doi.org/10.1128/mr.60.1.21-43.1996.
14. Winson, M.K., Swift, S., Hill, P.J., Sims, C.M., Griesmayr, G., Bycroft, B.W., Williams, P., and Stewart, G.S. (1998). Engineering the *luxCDABE* genes from *Photorhabdus luminescens* to provide a bioluminescent reporter for constitutive and promoter probe plasmids and mini-Tn5 constructs. FEMS Microbiol. Lett. *163*, 193–202. https://doi.org/10.1111/j.1574-6968.1998.tb13045.x.
15. Brachmann, A.O., Joyce, S.A., Jenke-Kodama, H., Schwär, G., Clarke, D.J., and Bode, H.B. (2007). A type II polyketide synthase is responsible for anthraquinone biosynthesis in *Photorhabdus luminescens*. Chembiochem *8*, 1721–1728. https://doi.org/10.1002/cbic.200700300.
16. Regaiolo, A., Dominelli, N., Andresen, K., and Heermann, R. (2020). The biocontrol agent and insect pathogen *Photorhabdus luminescens* interacts with plant roots. Appl. Environ. Microbiol. *86*, e00891-20. https://doi.org/10.1128/AEM.00891-20.
17. Schmidt, T.M., Kopecky, K., and Nealson, K.H. (1989). Bioluminescence of the insect pathogen *Xenorhabdus luminescens*. Appl. Environ. Microbiol. *55*, 2607–2612. https://doi.org/10.1128/aem.55.10.2607-2612.1989.
18. Patterson, W. (2015). Attractant Role of bacterial bioluminescence of *Photorhabdus luminescens* on a *Galleria mellonella* model. AJLS *3*, 290. https://doi.org/10.11648/j.ajls.20150304.16.
19. Zavilgelsky, G.B., and Shakulov, R.S. (2018). Mechanisms and origin of bacterial biolumenescence. Mol. Biol. *52*, 812–822. https://doi.org/10.1134/S0026893318060183.
20. Clarke, D.J. (2014). The genetic basis of the symbiosis between *Photorhabdus* and its invertebrate hosts. In Advances in Applied Microbiology (Elsevier), pp. 1–29.
21. Naylor, L.H. (1999). Reporter gene technology: the future looks bright. Biochem. Pharmacol. *58*, 749–757. https://doi.org/10.1016/s0006-2952(99)00096-9.
22. Heng, Y.C., and Foo, J.L. (2022). Development of destabilized mCherry fluorescent proteins for applications in the model yeast *Saccharomyces cerevisiae*. Biotechnol. Notes *3*, 108–112. https://doi.org/10.1016/j.biotno.2022.12.001.
23. Gregor, C., Gwosch, K.C., Sahl, S.J., and Hell, S.W. (2018). Strongly enhanced bacterial bioluminescence with the *i-lux* operon for single-cell imaging. Proc. Natl. Acad. Sci. USA *115*, 962–967. https://doi.org/10.1073/pnas.1715946115.
24. Kureisaite-Ciziene, D., Varadajan, A., McLaughlin, S.H., Glas, M., Montón Silva, A., Luirink, R., Mueller, C., den Blaauwen, T., Grossmann, T.N., Luirink, J., and Löwe, J. (2018). Structural analysis of the interaction between the bacterial cell division proteins FtsQ and FtsB. mBio *9*, e01346-18. https://doi.org/10.1128/mBio.01346-18.
25. Brameyer, S., Kresovic, D., Bode, H.B., and Heermann, R. (2014). LuxR solos in *Photorhabdus* species. Front. Cell. Infect. Microbiol. *4*, 166. https://doi.org/10.3389/fcimb.2014.00166.
26. Brameyer, S., Kresovic, D., Bode, H.B., and Heermann, R. (2015). Dialkylresorcinols as bacterial signaling molecules. Proc. Natl. Acad. Sci. USA *112*, 572–577. https://doi.org/10.1073/pnas.1417685112.
27. Heinrich, A.K., Glaeser, A., Tobias, N.J., Heermann, R., and Bode, H.B. (2016). Heterogeneous regulation of bacterial natural product biosynthesis via a novel transcription factor. Heliyon *2*, e00197. https://doi.org/10.1016/j.heliyon.2016.e00197.
28. Welham, P.A., and Stekel, D.J. (2009). Mathematical model of the Lux luminescence system in the terrestrial bacterium *Photorhabdus luminescens*. Mol. Biosyst. *5*, 68–76. https://doi.org/10.1039/b812094c.
29. Ziegler, M.M., and Baldwin, T.O. (1981). Biochemistry of bacterial bioluminescence. In Current Topics in Bioenergetics (Elsevier), pp. 65–113.
30. Rees, J.F., de Wergifosse, B., Noiset, O., Dubuisson, M., Janssens, B., and Thompson, E.M. (1998). The origins of marine bioluminescence: turning oxygen defence mechanisms into deep-sea communication tools. J. Exp. Biol. *201*, 1211–1221. https://doi.org/10.1242/jeb.201.8.1211.
31. Szpilewska, H., Czyz, A., and Wegrzyn, G. (2003). Experimental evidence for the physiological role of bacterial luciferase in the protection of cells against oxidative stress. Curr. Microbiol. *47*, 379–382. https://doi.org/10.1007/s00284-002-4024-y.
32. Kenyan, A., and Hastings, J.W. (1961). The isolation and characterization of dark mutants of luminescent bacteria. Biol. Bull. *121*, 375–378.
33. Stabb, E. (2005). Shedding light on the bioluminescence "paradox". ASM News *71*, 223–229.
34. O'Grady, E.A., and Wimpee, C.F. (2008). Mutations in the *lux* operon of natural dark mutants in the genus *Vibrio*. Appl. Environ. Microbiol. *74*, 61–66. https://doi.org/10.1128/AEM.01199-07.
35. Waterfield, N.R., Ciche, T., and Clarke, D. (2009). *Photorhabdus* and a host of hosts. Annu. Rev. Microbiol. *63*, 557–574. https://doi.org/10.1146/annurev.micro.091208.073507.
36. Zamora-Lagos, M.-A., Eckstein, S., Langer, A., Gazanis, A., Pfeiffer, F., Habermann, B., and Heermann, R. (2018). Phenotypic and genomic comparison of *Photorhabdus luminescens* subsp. *laumondii* TT01 and a widely used rifampicin-resistant *Photorhabdus luminescens* laboratory strain. BMC Genom. *19*, 854. https://doi.org/10.1186/s12864-018-5121-z.
37. Brachmann, A.O., Brameyer, S., Kresovic, D., Hitkova, I., Kopp, Y., Manske, C., Schubert, K., Bode, H.B., and Heermann, R. (2013). Pyrones as bacterial signaling molecules. Nat. Chem. Biol. *9*, 573–578. https://doi.org/10.1038/nchembio.1295.
38. Brameyer, S. (2015). Cell-cell Communication via LuxR Solos in *Photorhabdus* Species. Doctoral Thesis (Ludwig-Maximilians-Universität München).
39. Thoma, S., and Schobert, M. (2009). An improved *Escherichia coli* donor strain for diparental mating. FEMS Microbiol. Lett. *294*, 127–132. https://doi.org/10.1111/j.1574-6968.2009.01556.x.
40. Lassak, J., Henche, A.-L., Binnenkade, L., and Thormann, K.M. (2010). ArcS, the cognate sensor kinase in an atypical Arc system of *Shewanella oneidensis* MR-1. Appl. Environ. Microbiol. *76*, 3263–3274. https://doi.org/10.1128/AEM.00512-10.

STAR★METHODS

KEY RESOURCES TABLE

REAGENT or RESOURCE	SOURCE	IDENTIFIER
Bacterial and virus strains		
Photorhabdus luminescens subsp. *luminescens* DJC 1°	Zamora-Lagos et al.[36]	DJC 1°
Photorhabdus luminescens subsp. *luminescens* DJC 2°	Zamora-Lagos et al.[36]	DJC 2°
Photorhabdus luminescens DJC 1°Δ*lux*	This study	1°Δ*lux*
Photorhabdus luminescens DJC 2°Δ*lux*	This study	2°Δ*lux*
Biological samples		
Galleria mellonella	Reared in our lab	N/A
Arabidopsis thaliana Col-O	Grown in our lab	N/A
Heterorhabditis bacteriophora	Reared in our lab	N/A
Oligonucleotides		
CTAACTGCAGTTTGTATATAAAGAAGAGCTTGAT	This study	FA_lux_operon_PstI
CGTCAGTAGATCATTAGCCATCCATTTAATGG	This study	FA_lux_operon_ovl
GATCTACTGACGTATACTCTATGGATTTTAAGATGC	This study	FB_lux_operon_ovl
GACCGGATCCGAACATGAATAAAGTGATACTTCT	This study	FB_lux_operon_BamHI
Recombinant DNA		
pNTPs138-R6KT::lux	This study	N/A
pBBR1-*lux*-P_{pcfA}	Brachmann et al.[37]	N/A
pBBR1-*lux*-P_{antA}	Heinrich et al.[27]	N/A
pBBR1-*lux*-P_{ftrsQ}	Brameyer et al.[38]	N/A
Software and algorithms		
CGGC: Compare groups of growth curves	Walter and Eliza Hall Institute of Medical Research	https://bioinf.wehi.edu.au/software/compareCurves/

EXPERIMENTAL MODEL AND STUDY PARTICIPATION DETAILS

Key resources table contains a list of all strains used or generated in this study. All tested strains were cultivated in liquid medium at 30°C unless other stated in the method details section. Strains that needed to be preserved were stored in 60% glycerol at −80°C.

Arabidopsis thaliana seeds were surface sterilized using 50% bleach (v/v), rinsed with sterile water five times, and sown on MS agar plates (0.4% [w/v] MS Basal Salt moisture, 3% [w/v] Sucrose, 0.8% [w/v] agar). The agar plates were transferred to a growth chamber and incubated at 24°C under a 16-h-light/8-h-dark time period for up to 14 days.

METHOD DETAILS

Bacterial strains and cultivation

Escherichia coli strain ST18[39] were cultivated in LB medium (1% [w/v] tryptone, 0.5% [w/v] yeast extract, 0.5% [w/v] NaCl) at 37°C, shaking under aerobic conditions. *Photorhabdus luminescens* subsp. *luminescens* strain DJC[36] was aerobically cultivated at 30°C in CASO medium (1.5% [w/v] peptone, 0.5% [w/v] peptone from soy, 0.5% [w/v] NaCl).

Generation of plasmids

To generate the plasmid pNTPs138-R6KT::lux, 300 bp upstream (FA) and downstream (FB) of the *lux* operon (*PluDJC_11100* to *PluDJC_11120*) were amplified by PCR using the primer pairs FA_lux_operon_PstI + FA_lux_operon_ovl and FB_lux_operon_ovl + FB_lux_operon_BamHI, introducing a PstI and BamHI restriction side. PCR products were fused by overlap extension PCR and cloned into the pNTPs::138-R6KT plasmid. Correct insertion was confirmed by PCR using the primers check-pNTPs fwd and check-pNTPs-rev, followed by DNA sequencing.

Generation of *P. luminescens* mutant and reporter strains

For in-frame deletion strains *P. luminescens* Δ*lux*, conjugation and double homologous recombination was performed as previously described.[40] Therefore, the respective plasmid was conjugated from *E. coli* strain ST18 into *P. luminescens* 1° and 2° cells and screened for kanamycin resistance. As the pNTPs138-R6KT plasmid contains the *sacB* gene, a second screening was performed to isolate clones with Suc^R Km^S phenotype. Successful deletion of the *luxCDABE* operon was confirmed by PCR using the primer pair FA_lux_operon_PstI + FB_lux_operon_BamHI, followed by DNA sequencing.

For construction of *P. luminescens* 1° and 2° reporter strains, the respective plasmids pBBR1-*lux*-P_{pcfA},[37] pBBR1-*lux*-P_{antA},[27] pBBR1-*lux*-P_{ftrsQ}[38] and pBBR1-luxø were transferred into *E. coli* ST18 cells via transformation. Plasmids were transferred through conjugation and selection on Gm^R.

Growth assays

To determine whether deletion of the *luxCDABE* affects the cell growth of *P. luminescens*, growth was monitored under different conditions. Therefore, 50 mL of CASO or LB medium were inoculated with the bacteria at OD_{600} = 0.01 and 50 mL of M9 medium was inoculated at OD_{600} = 0.05. Cultures were grown under aerobic conditions at 30°C for 72 h. OD_{600} and luminescence was measured every hour until 7 h and following every 24 h. Three biological replicates were performed. Statistical analyses were performed through linear regression of logarithmically transformed data.

For stress tests, *P. luminescens* cells were grown overnight in CASO medium and following adjusted to OD_{600} = 0.1. At OD_{600} = 1, stress was induced upon adding stock solutions of different solutions to a final concentration of i) 0.5 M or 1 M NaCl, ii) 3%, 0.3% or 0.03% H_2O_2 or iii) incubation temperature adjusted to 16°C or 37°C. After further cultivation for 3 h, serial dilutions were spotted on agar plates and growth on solid medium was analyzed. Growth rates were calculated within a 3 h the time after stress treatment. Respective fold changes of the growth rates (μ) treated group versus the control group were calculated to display differences in bacterial growth.

Insect pathogenicity assays

Insect pathogenicity assays were performed as previously described.[36] Larvae of *Galleria mellonella* (reared in our lab) were numbed on ice and surface sterilized with 80% [v/v] ethanol. With a sterile Hamilton syringe (1702 RN, 25 μL, Hamilton), 2 x 10^3 cells of the *P. luminescens* wildtype or Δ*lux* cells were injected into the hemocoel and the larvae following incubated at 30°C for 48 h. After 24 h and 48 h, mortality was determined, and luminescence visualized (Bio-Rad Gel Doc XR^+ Gel Documentation System). Sterile medium was injected into the larvae as control, three biological replicates were performed with 5 larvae.

Protease bioassays

Semi-quantitative proteolytic activity was determined on caseinate agar plates (1% [w/v] skim milk, 0.3% [w/v] yeast extract, 1.2% [w/v] agar). Briefly, overnight cultures of *P. luminescens* wildtype and Δ*lux* strains were adjusted to OD_{600} = 1 and 50 μL spotted on the mid of a skim-milk agar plate. Plates were incubated for 2 days at 30°C. Three biological replicates were performed.

Haemolysis bioassays

Haemolysis was semi-quantitative determined on sheep blood agar (0.5% [w/v] NaCl, 1.0% [w/v] meat extract, 1.0% [w/v] peptone, 0.5% [v/v] sheep blood, 1% [w/v] agar, pH 7.5). Overnight cultures of *P. luminescens* WT and Δ*lux* strains were adjusted to OD_{600} = 1 and 50 μL spotted on the mid of a haemolysis agar plate. Plates were incubated for 4 days at 30°C. Three biological replicates were performed.

Plant root colonization assays

To determine the ability of *P. luminescens* to colonize plant roots, a root colonization assay was performed as previously described.[16] Briefly, *Arabidopsis thaliana* Col-0 seedlings were cultivated on MS agar plates (0.4% [w/v] MS Basal Salt moisture, 3% [w/v] Sucrose, 0.8% [w/v] agar) for 7 days at 24°C with 16 light and 8 h dark regime. *P. luminescens* DJC wildtype and Δ*lux* strains were grown overnight at 30°C and washed with 10 mM $MgSO_4$. Then, 120 μL of OD_{600} = 0.02 were spotted on the seedling root tip and visualized by phase-contrast microscopy with the 100x magnitude after 7 and 14 days, respectively (Leica Dmi8 Fluorescence Imaging System). 10 mM $MgSO_4$ served as control, three independent biological replicates were performed.

Nematode bioassays

To determine the ability of *P. luminescens* to promote the development of *Heterorhabditis bacteriophora*, nematode bioassays were performed. First, 50 μL of *P. luminescens* overnight cultures adjusted to OD_{600} = 1 were spread as a Z onto lipid agar plates (1% [v/v] corn syrup, 0.5% [w/v] yeast extract, 5% [v/v] cod liver oil, 2% [w/v] MgCl2 6xH2O, 2.5% [w/v] Difco nutrient agar [Becton, Dickinson, Heidelberg, Germany]) and incubated for 72 h at 30°C. Then, 50 surface-sterilized axenic *H. bacteriophora* injective juveniles were added and following incubated at RT for up to 21 days. The nematode recovery was monitored after 7 days, 14 days and 18 days by counting the number of infective juveniles (IJs).

Extraction of plant root metabolites

Plant root exudates were extracted as previously described.[16] Briefly, exudates were collected from *Pisum sativum* variant *Arvica*, grown for 2 weeks at 24°C with 16 light and 8 h dark regime in vermiculite. Then, roots of 75 plants were collected and stirred in 250 mL 50% ethanol or 100% methanol for 12 h. Exudates were sterilized through an 0.22 μm sterile-filter and stored at −20°C until further use.

Bioluminescence-based reporter assays

To determine bioluminescence as well as background fluorescence in different media, reporter assays were performed in a Tecan Spark microplate reader (Tecan, Salzburg, Austria). Briefly, overnight cultures of *P. luminescens* 1°, 2° and *E. coli* DH5α λ*pir* were washed with 1x PBS-buffer and OD_{600} adjusted to 0.05 in the respective media. Respective media were used as negative control and blank zero points. Then, 200 μL of the cultures were transferred in a black 96-well plate with transparent bottom and incubated for 24 h at 30°C, measuring the OD_{600}, luminescence and fluorescence (GFP = excitation/emission 485/535 nm, YFP = excitation/emission 513/530 nm, CYA3 = excitation/emission 579/591 nm, mCherry = excitation/emission 587/610 nm). Values were normalized by using the formula (sample signal – negative control signal)/OD_{600}. Three biological replicates were performed.

QUANTIFICATION AND STATISTICAL ANALYSIS

Unless otherwise stated, at least three biological independent experiments were performed for each of the assays. Values shown represent the mean ± standard error. Additionally, t-tests were performed to analyze significance (marked with **). To analyze the significance of bacterial growth curves, linear regression of logarithmically transformed data was performed.

6. Identification of *Pseudomonas asiatica* subsp. *bavariensis* str. JM1 as the first Nε-carboxy(m) ethyllysine-degrading soil bacterium

Judith Mehler[1], Kim Ina Behringer[2,3], Robert Ethan Rollins[4], Friederike Pisarz[5], Andreas Klingl[6], Thomas Henle[7], Ralf Heermann[5], Noémie S. Becker[4], Michael Hellwig[2,3], Jürgen Lassak[1]

[1] Division of Microbiology, Faculty of Biology, Ludwig-Maximilians-Universität München, Planegg/Martinsried, Germany

[2] Chair of Special Food Chemistry, Technische Universität Dresden, D-01062, Dresden, Germany

[3] Technische Universität Braunschweig – Institute ofFood Chemistry, Braunschweig, Germany.

[4] Division of Evolutionary Biology, Faculty of Biology, Ludwig-Maximilians-Universität München, Planegg/Martinsried, Germany

[5] Institute of Molecular Physiology, Microbiology and Wine Research, Johannes Gutenberg University Mainz, Mainz, Germany

[6] Division of Botany, Faculty of Biology, Ludwig-Maximilians-Universität München, Planegg/Martinsried, Germany

[7] Chair of Food Chemistry, Technische Universität Dresden, D-01062, Dresden, Germany

environmental microbiology

Environmental Microbiology (2022) **24**(7), 3229–3241 doi:10.1111/1462-2920.16079

Identification of *Pseudomonas asiatica* subsp. *bavariensis* str. JM1 as the first N_ε-carboxy(m)ethyllysine-degrading soil bacterium

Judith Mehler[1], **Kim Ina Behringer**[2,3], **Robert Ethan Rollins**[4], **Friederike Pisarz**[5], **Andreas Klingl**[6], **Thomas Henle**[7], **Ralf Heermann**[5], **Noémie S. Becker**[4], **Michael Hellwig**[2,3*] **and Jürgen Lassak**[1*]

[1]*Division of Microbiology, Faculty of Biology, Ludwig-Maximilians-Universität München, Planegg/Martinsried, Germany.*

[2]*Chair of Special Food Chemistry, Technische Universität Dresden, D-01062, Dresden, Germany.*

[3]*Technische Universität Braunschweig – Institute of Food Chemistry, Braunschweig, Germany.*

[4]*Division of Evolutionary Biology, Faculty of Biology, Ludwig-Maximilians-Universität München, Planegg/Martinsried, Germany.*

[5]*Institute of Molecular Physiology, Microbiology and Wine Research, Johannes Gutenberg University Mainz, Mainz, Germany.*

[6]*Division of Botany, Faculty of Biology, Ludwig-Maximilians-Universität München, Planegg/Martinsried, Germany.*

[7]*Chair of Food Chemistry, Technische Universität Dresden, D-01062, Dresden, Germany.*

Summary

Thermal food processing leads to the formation of advanced glycation end products (AGE) such as N_ε-carboxymethyllysine (CML). Accordingly, these non-canonical amino acids are an important part of the human diet. However, CML is only partially decomposed by our gut microbiota and up to 30% are excreted via faeces and, hence, enter the environment. In frame of this study, we isolated a soil bacterium that can grow on CML as well as its higher homologue N_ε-carboxyethyllysine (CEL) as sole source of carbon. Bioinformatic analyses upon whole-genome sequencing revealed a subspecies of *Pseudomonas asiatica*, which we named '*bavariensis*'. We performed a metabolite screening of *P. asiatica* subsp. *bavariensis* str. JM1 grown either on CML or CEL and identified *N*-carboxy methylaminopentanoic acid and *N*-carboxyethylamino pentanoic acid respectively. We further detected α-aminoadipate as intermediate in the metabolism of CML. These reaction products suggest two routes of degradation: While CEL seems to be predominantly processed from the α-C-atom, decomposition of CML can also be initiated with cleavage of the carboxymethyl group and under the release of acetate. Thus, our study provides novel insights into the metabolism of two important AGEs and how these are processed by environmental bacteria.

Received 17 November, 2021; revised 18 May, 2022; accepted 19 May, 2022. *For correspondence. E-mail michael.hellwig@tu-dresden.de; juergen.lassak@lmu.de. Tel. +4935146332006; Fax: +49351 46334138.

Introduction

Glycation is one of the physiologically most important non-enzymatic post-translational modification reactions (Hellwig and Henle, 2014; Lassak *et al*., 2019; Lassak *et al*., 2022). It is a specific case of the common amino-carbonyl reactions and mainly refers to the reaction of reducing sugars and their degradation products with amino and guanidino compounds (Ulrich and Cerami, 2001). First, Schiff bases are formed at the amino termini of free amino acids, peptides, or proteins, or the ε-amino groups of lysine residues (Hellwig and Henle, 2014; Graf von Armansperg *et al*., 2021). These Schiff bases rearrange very fast into the more stable Amadori or Heyns products (Heyns and Noack, 1962). Thermodynamically not stable, Amadori and Heyns products are subject to degradation with the production of reactive dicarbonyl compounds, and further reactions lead to the formation of so-called advanced glycation end products (AGEs) (Fig. 1) (Hellwig and Henle, 2014; Henning and Glomb, 2016). In the century since its first description in 1912 by Maillard (1912a) and Maillard (1912b), the reaction was found to be responsible not only for the flavour, taste and appearance of thermally processed foods (Hellwig and Henle, 2014) but also as a protein degradation reaction in living systems. The formation of fructosamine or the glycated haemoglobin variant

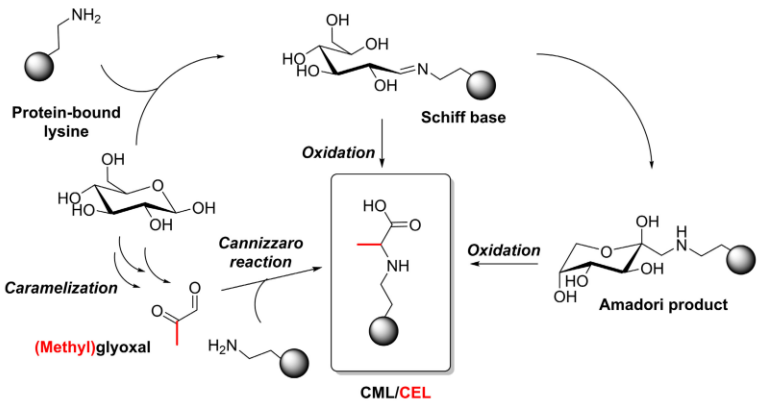

Fig. 1. Formation of Nε-carboxy methyllysine (CML) and CEL in proteins.

HbA1C is well-known examples of *in vivo* glycation, which increases under diabetic conditions. One of the most important glycated amino acids is the alkylated lysine derivative N_ε-carboxymethyllysine (CML) (Wadman *et al*., 1975; Ahmed *et al*., 1986). This compound can be formed by oxidation of Schiff bases and Amadori compounds, but also by reaction of lysine with glyoxal (Fig. 1) in foods and under physiological conditions. In food, CML is present as a protein-bound amino acid (Hegele *et al*., 2008), and it has been quantified in dairy, bakery and meat products at concentrations ranging from 10 to 60 mg kg^{-1} protein, while extreme concentrations of up to 560 mg kg^{-1} protein have been detected in heavily heat-treated products such as bread crust or evaporated milk (Assar *et al*., 2009). From foods, a daily exposure of 2.1–11.3 mg CML has been estimated (Birlouez-Aragon *et al*., 2010; Delgado-Andrade *et al*., 2012; Scheijen *et al*., 2018; Hellwig *et al*., 2019). The metabolic fate of CML has been studied intensely over the past decade. Recently, CML has been shown to be degraded by the human colonic microbiota (Bui *et al*., 2019; Hellwig *et al*., 2019). The gut microbiota of different individuals metabolizes CML quite differently, pointing to highly specialized microorganisms that may find a niche in the human intestine as dependent on the dietary habits of the host (Bui *et al*., 2019; Hellwig *et al*., 2019). Thus, up to 30% of the ingested CML enters the environment upon excretion (Somoza *et al*., 2006; Delgado-Andrade *et al*., 2012; Alamir *et al*., 2013; Roncero-Ramos *et al*., 2013; Roncero-Ramos *et al*., 2014). The metabolic fate of CML in the environment, however, remains enigmatic. In this study we describe for the first time a soil bacterium being capable of degrading CML as well as its higher homologue N_ε-carboxyethyllysine (CEL). Whole-genome sequencing and extensive phenotypic characterization identified a new subspecies of *Pseudomonas asiatica*, which we named '*bavariensis*'. Metabolite analyses of *P. asiatica* subsp. *bavariensis* JM1 (hereafter JM1) either grown on CML or CEL indicate for distinct degradation routes.

Experimental procedures

Bacterial strains and culture conditions

Strains and primers are listed in Tables S1 and S2. For growth on surfaces lysogeny broth (LB) (Bertani, 1951) according to Miller modification supplemented with 1.5% (wt./vol.) agar was used. When grown in liquids, strains were cultured aerobically at 30°C (pseudomonads) or 37°C (*Escherichia coli*) in either LB, modified super optimal broth (SOB) (Hanahan, 1983) or M9 minimal medium (Studier, 2005). Media supplements and carbon sources were added as indicated.

Phenotypic characterization

To assess the cell morphology and quantify cell size of the isolate we used light microscopy. Cells were inoculated in SOB or M9 medium and samples were taken during logarithmic growth phase. The cells were placed onto a 2% agarose (wt./vol.) disc and imaged with differential interference contrast (DIC) microscopy using a Leica DMI6000B fluorescence microscope (Leica, Bensheim, Germany) and the application LAS AF software (Leica). The cell wall type was examined via Gram staining and a potassium hydroxide test. Flagellation was investigated performing a swimming assay (Paulick *et al*., 2009): SOB agar [0.25% (wt./vol.)] plates were poured, dried for a few hours and 2 µl of overnight culture in SOB were spotted onto the agar plate. The plates were incubated overnight under aerobic conditions at 30°C and imaged with a gel documentation system from PEQLAB. Flagellation was also assessed using transmission electron microscopy (TEM). For this, cells were negative stained as described

previously (Lassak *et al*., 2012). In more detail, freshly grown cells were harvested via centrifugation. The resulting cell pellet was resuspended in 50 µl of medium and 5 µl was applied to glow-discharged carbon-coated copper grids before negative staining with 2% uranyl acetate for 20 s. Electron microscopy was carried out using a ZEISS EM912 (ZEISS, Oberkochen, Germany) with an integrated OMEGA filter, operated at 80 kV in the zero-loss mode. For image acquisition we used a 2k × 2k slow-scan CCD camera (TRS Tröndle Restlichtverstärkersysteme, Moorenweis, Germany). To determine the temperature range and optimum, cells were cultivated in SOB. Per approach 50 µl of bacterial suspension was inoculated in a thermocycler at temperatures ranging from 4°C to 55°C. To determine the optimal temperature for growth, the optical density at 600 nm (OD_{600nm}) was determined after 4 h of growth. Production of a fluorescent pigment was evaluated using cetrimide agar plates (Sigma Aldrich). The strains were cultivated overnight on the selective medium and the fluorescence was visualized with UV light. To determine the pH optimum, cells were cultured in SOB. Growth was monitored over 24 h at 30°C. The pH of the medium was adjusted using citrate buffer (pH 3–5.5), phosphate buffer (pH 6–7), Tris HCl buffer (pH 7.5–9), carbonate/bicarbonate buffer (pH 10), phosphate buffer (pH 11) or potassium chloride/sodium hydroxide (pH 12–13). To test the assimilation of carbon and nitrogen sources, the strains were precultured in M9 minimal medium with 10 mM of glucose as source of carbon, washed three times and incubated with 10 mM of the respective substrate in a 96 well plate at 30°C for 72 h. Growth was recorded in a ClarioStar Plus plate reader with orbital shaking (600 rpm).

Entomopathogenicity assays

Larvae of *Galleria mellonella* (reared in JGU Mainz, Heermann lab) were numbed on ice and surface sterilized with 80% (vol./vol.) ethanol. Then, the larvae were infected with 2×10^4 and 2×10^3 *Pseudomonas asiatica subssp. bavariensis str.* JM1, *Photorabdus luminescens* DJC 1° and *Pseudomonas putida* KT2440 cells respectively, using a sterilized microlight syringe (1702 RN, 25 µl, Hamilton). Numbers were calculated from turbidity measurements OD_{600nm} of the cell culture. Infected larvae were incubated at 30°C and larvae mortality was monitored by counting dead larvae after 24 and 48 h. The experiment was performed three times, 10 larvae were infected for each trial.

Plant root colonization assays

Bacterium plant root colonization assays on 8-day-old *Arabidopsis thaliana* Col-0 seedlings cultivated in MS agar plates [0.4% (wt./vol.) MS Basal Salt moisture, 3% (wt./vol.) Sucrose, 0.8% (wt./vol.) agar] for 8 days at 24°C with 16 h light/8 h dark regime were performed as reported previously (Regaiolo *et al*., 2020). Briefly, JM1, DJC 1° and KT2440 were grown at 30°C overnight. Cells were collected by centrifugation, washed with 10 mM $MgSO_4$ and 120 µl (OD_{600nm} = 0.02) spotted on the seedling root tip. After 7 and 14 days, roots were visualized by phase-contrast microscopy with the 100× magnitude (Leica Dmi8 Fluorescence Imaging System). 10 mM $MgSO_4$ served as control. The experiment was performed in three independent biological replicates.

16S rRNA gene analysis

Amplification of 16S rRNA genes from bacterial colonies was achieved using GoTaq® Green Master Mix (Promega) and the primer pair UNI8f 5′-AGAGTTTGATCCTGGCTCAG-3′ and uni 1492r 5′-GGTTACCTTGTTACGACTT-3′ (Weisburg *et al*., 1991) using the following program: 95°C 5′ – 80° 5′ – 10× [94°C 30″ – 59°C 50 s – 72°C 1′] – 25× [94°C 30″ – 55°C 50 s – 72°C 1′] – 72°C 10′. After purification with the Hi Yield® Gel/PCR DNA fragment extraction kit (Süd-Laborbedarf GmbH) according to the manufacturer's instructions, the amplicons were sequenced by the LMU Sequencing Service performing Sanger sequencing. Blast analysis was carried out using the NCBI information hub. Multiple sequence alignment was carried out via Clustal X 2.1 (Higgins and Sharp, 1988; Larkin *et al*., 2007). The phylogenetic tree was designed with the aid of the online tool iTOL (Letunic and Bork, 2021).

Genomic DNA extraction and sequencing

Genomic DNA (gDNA) was isolated according to the modified standard procedure established by Pospiech and Neumann (1995). The cells were precultured in SOB overnight at 30°C. Subsequently, harvested cells were resolved in SET buffer (75 mM NaCl, 25 mM EDTA, 20 mM Tris, pH 7.5) containing 100 µg ml^{-1} RNAseA (Thermo Fisher Scientific). A spatula tip of lysozyme from chicken egg white (Sigma Aldrich) was added and the suspension was incubated for 1 h at 37°C. Then SDS and proteinase K (Sigma Aldrich) were added to final concentration of 1% (wt./vol.) and 100 µg ml^{-1} respectively followed by incubation overnight at 55°C. Separation of proteins and nucleic acids was performed using a mixture of Phenol:Chloroform:Isoamyl alcohol (PCI; Roth). The phenolic phase, as well as the protein-containing interface, was discarded. DNA in the aqueous phase was precipitated with 50% (vol./vol.) isopropyl alcohol (final concentration) and washed twice with 70% ethanol. The DNA pellet was re-suspended in water and

the isolated gDNA was sent to StarSEQ GmbH (Mainz, Germany) for whole-genome sequencing: Paired-end sequencing, read length 150 nt on the Illumina NextSeq 2000™ platform, read depth 100×.

Genome reconstruction

Raw reads were assembled using SPAdes v. 3.9.0 (Bankevich *et al*., 2012) using default parameters. Genome closing using multiple references was performed using MeDuSa v. 1.6 (Bosi *et al*., 2015) using as references the closest genomes found in GenBank *Pseudomonas asiatica* C3 (NZ_CP061848.1), *Pseudomonas putida* DLLE4 (NZ_CP007620.1), *Pseudomonas putida* HB3267 (NC_019905.1) and *Pseudomonas putida* S16 (NC_015733.1). REAPR pipeline v. 1.0.18 (Hunt *et al*., 2013) with default parameters was next used for assembly correction and filtering scaffolds shorter than 1000 bp. Remaining adaptor sequences were identified using NCBI VecScreen and trimmed. Finally, summary statistics and assembly quality were assessed using QUAST v. 5.0.2 (Gurevich *et al*., 2013) and the final assembly was annotated using the RAST server v. 2.0 (Aziz *et al*., 2008; Overbeek *et al*., 2014; Brettin *et al*., 2015). This final genome assembly was deposited in the NCBI database and can be accessed under BioProject number PRJNA772912. Based on average nucleotide identity (ANI) (Federhen *et al*., 2016; Ciufo *et al*., 2018), NCBI defined *Pseudomonas inefficax* JV551A3 (ANI: 97.258%; coverage: 89.8%) as the type strain and deposited our isolate under *P. inefficax* strain JM1 (TaxID: 2078786). The seeming contradiction in species specification is a result of the simultaneous description of *P. asiatica* (Tohya *et al*., 2019) and *P. inefficax* (Keshavarz-Tohid *et al*., 2019). Due to extensive misclassifications within the *Ps putida* group, we decided to follow the most recent phylogenetic analysis and nomenclature (Passarelli-Araujo *et al*., 2021), and thus named our isolate *P. asiatica*.

Multi-locus sequence typing analysis and phylogenetic reconstruction

We used PubMLST (Jolley *et al*., 2018) to extract the sequences of the eight MLST from the *P. putida* scheme (Ogura and Kanesaki, 2018) from the assembled SPAdes scaffolds. New identified MLST sequence types were submitted to PubMLST.

To compare our new isolate to other members of the *P. putida* group, we downloaded all available complete *P. putida* as well as all genomes belonging to the *P. putida* group as described by Ogura and Kanesaki (2018) and from the *P. putida* clade in Peix *et al*. (2018) resulting in 45 genomes (see Table S5 for accessions numbers). We added as outgroups the genomes of *Pseudomonas aeruginosa* reference strain PAO1 and *Pseudomonas fluorescens* reference strain ATCC13525. From these 48 genomes (including ours) potential phage sequences were identified using the PHASTER (Zhou *et al*., 2011; Arndt *et al*., 2016) online platform and removed from the genomes with custom scripts.

A set of genes orthologous between all 48 isolates was selected as described by Becker *et al*. (2016) starting from the list of 5254 total coding sequences (CDS) from *Pseudomonas putida* reference strain KT2440 (NC_021505.1). Briefly, BLAST v. 2.8.1 (Altschul *et al*., 1990) (algorithm blastn) was used to search for all KT2440 genes in each of the 47 other genomes and genes were kept only if they had one and only one hit in each isolate with at least 80% identity over 50% of its length. The hits in each genome were then blasted again against the KT2440 reference using the same criteria. The remaining 358 orthologous genes were aligned using MUSCLE v. 3.8.1551 (Edgar, 2004) with default parameters.

Mash v. 2.3 (Ondov *et al*., 2016) with default settings was used for estimating the genomic distance between our isolate and the most closely related strains *P. asiatica* C3 and *P. putida* DLL-E4, HB3267 and S16.

A phylogeny based on the 358 identified orthologous genes over 48 genomes was reconstructed with MrBayes v.3.2.6 (Ronquist and Huelsenbeck, 2003) using a GTR model with inverse gamma rate variation and ploidy set to haploid. The phylogeny was run as a partitioned analysis where each gene was viewed as their own data partition but had the same settings. Three independent runs were launched and ran for 3.5 million generations at which point convergence of parameters was checked with Tracer v. 1.7.1. (Rambaut *et al*., 2018). Consensus trees were built using the sumt command from MrBayes using a relative burn-in of 25%. Convergence to a single topology in all three independent runs was checked manually in FigTree v. 1.4.4 (http://tree.bio.ed.ac.uk/software/figtree/) which was also used to plot the tree shown in Fig. S1. The tree was rooted on the branch leading to the *P. aeruginosa* reference strain PAO1 outgroup.

Acetate colourimetric assay

A preculture in M9 minimal medium containing 10 mM L-lysine as sole carbon source was incubated at 30°C overnight and subsequently washed. M9 containing 10 mM Lysine, CML or CEL as sole carbon source was inoculated to an OD_{600nm} of 0.01 and incubated for further 24 h at 30°C. 100 µl of samples were taken at timepoints 0, 4, 8 and 24 h. To assess the production of

the metabolite acetate, the Acetate Colorimetric Assay Kit (Sigma Aldrich) was used according to the manufacturer's instructions. The absorbance at the wavelength of 450 nm was measured using a ClarioStar Plus plate reader.

In vivo *AGE degradation*

The used strains were precultured in M9 medium, harvested and washed three times. M9 minimal medium containing 10 mM Lysine, CML or CEL as sole carbon source was inoculated to an OD_{600nm} of 0.05 and incubated at 30°C while shaking (600 rpm). 200 µl samples were collected at timepoints 0, 0.5, 1, 2, 4, 6, 8 and 24 h. The samples were immediately stored at −20°C to stop any further metabolism. For quantification of CML, CEL and lysine, 10 µl of samples were diluted with 90 µl of water, and 150 µl 0.1 M sodium carbonate solution, as well as 200 µl of a solution of dansyl chloride in acetone (0.5%, wt./vol.), were added. After incubation in a water bath (40°C, 1 h), 10 µl of 3 M HCl was added. After shaking, 540 µl of 0.1% aqueous formic acid was added. The solutions were centrifuged (10 000*g*, 10 min, 4°C), and the supernatants were transferred to HPLC vials. An aliquot (20 µl) was injected into an HPLC system from Knauer (Berlin, Germany) equipped with a diode array detector (DAD 2.1l) that operated at $\lambda = 254$ nm. As solvent A, 0.1% formic acid in water was used, and 0.1% formic acid in a mixture of acetonitrile and water (90/10, vol./vol.) as solvent B. Separations were performed at 40°C on a C-18 column (Eurospher-100, 250 × 4.6 mm, 5 µm, Knauer) with an integrated guard column (5 × 4.6 mm) of the same material. The flow rate was 1 ml min^{-1}, and a gradient was used (0 min, 20% B; 17 min, 67% B; 25 min, 100% B).

For the analysis of metabolites, 10 µl of samples were diluted with 90 µl of acetonitrile and membrane filtered (0.2 µm) into an HPLC vial, and 1 µl was injected into the UHPLC system Infinity 1290 (Agilent, Waldbronn, Germany) that was connected to the mass spectrometer TIMS-TOF (Bruker, Bremen, Germany). As solvent A, 10 mM acetic acid in MS grade water was used, and pure acetonitrile as solvent B. Separations were performed at 25°C on a HILIC column (ZIC-HILIC, 3.5 µm, 100 Å, 2.1 × 100 mm, Merck KGaA, Darmstadt, Germany). The flow rate was 0.2 ml min^{-1}, and a gradient was used (0 min, 90% B; 2 min, 90% B; 20 min, 50% B). The mass spectrometer operated in the Scan mode (*m/z* 20–1300; positive mode, scan time, 500 ms; dry gas flow, 10 L nitrogen min^{-1}; dry temperature, 220°C; nebulizer pressure, 2.2 bar; capillary voltage, 4500 V).

CM-CAD and CE-CAD were analysed as published previously (Hellwig *et al*., 2019). 15 µl of samples were diluted with 135 µl of 10 mM nonafluoropentanoic acid (NFPA). After centrifugation (10 000*g*, 10 min, RT), the supernatant was transferred to an HPLC vial and 5 µl was injected into the HPLC system 1200 that was connected to the mass spectrometer Triple Quad 6410 (both from Agilent). As solvent A, 10 mM NFPA in double-distilled water was used, and 10 mM NFPA in acetonitrile as solvent B. Separations were performed at 35°C on a C-18 column (Zorbax 300 SB-C18, 2.1 × 50 mm). The flow rate was 0.25 ml min^{-1}, and a gradient was used (0 min, 10% B; 15 min, 66% B). The mass spectrometer operated in the scan mode (*m/z* 80–250; positive mode, scan time, 500 ms; gas flow, 11 L nitrogen min^{-1}; gas temperature, 350°C; nebulizer pressure, 35 psi; capillary voltage, 4000 V).

Pre-column derivatization was applied for the determination of organic acids similar to the approach of Liao *et al*. (2021) but using a different derivatizing agent. Methanol (420 µl) was added to samples (60 µl), and the mixtures were shaken for 5 min followed by centrifugation (10 000*g*, 10 min, 4°C). To 120 µl of the supernatant was added 60 µl 0.2 M pentafluorophenylhydrazine (dissolved in methanol/water, 60/40, vol./vol.) and 60 µl 0.12 M 1-Ethyl-3-(3-dimethylaminopropyl)-carbodiimide (dissolved in methanol), and the mixtures were incubated in a water bath at 40°C for 20 min. After cooling and short centrifugation, 30 µl methanol was added, the mixtures were centrifuged again after mixing (10 000*g*, 10 min, 4°C), and membrane filtered (0.2 µm) before UHPLC analysis (injection volume, 1 µl) with the same device and TIMS-TOF detector as stated above. Separations were performed at 30°C on an RP column (Eurospher II, 100–3, 2 × 50 mm, Knauer, Berlin, Germany). The flow rate was 0.2 ml min^{-1}, and a gradient was used (0 min, 30% B; 4 min, 30% B; 20 min, 90% B). As solvent A, 0.2% acetic acid in MS grade water was used, and pure methanol as solvent B.

Results

Isolation of a CML utilizing soil bacterium

To study the metabolism of CML by environmental microorganisms, near-surface soil samples (rhizosphere) were taken from a meadow in front of the Biocenter of the Ludwig-Maximilians-Universität München in Planegg-Martinsried (Bavaria) (Fig. 2A). Microorganisms from about 20 g of soil were enriched and then plated onto M9 minimal agar (Studier, 2005) containing 10 mM CML as the sole carbon source (Fig. 2B). After 72 h of incubation at 30°C plenty of colonies had emerged. Those

showing robust growth with CML as sole carbon source all belonged to the same colony morphotype with round shape, an entire margin and convex elevation. Further phenotyping unveiled Gram-negative, fluorescent (Fig. 2C), rod-shaped (Fig. 2D) bacteria with 2–3 μm in length and 0.5–1 μm in width (Fig. 2D–F) being motile (Fig. S2A) via lophotrichous flagella (Fig. 2E and F). The bacterium tolerates an external pH >5 and <9 but grows optimally only between pH 6 and 8 (Fig. S2B). It can be cultivated at temperatures ranging from 11°C to 40°C and at T_{opt} = 35°C (Fig. S2C). Our isolate doubles every 30–40 min in rich media and needs around 110 min in minimal media with glucose as sole carbon source (Fig. S2D). Growth on cetrimide agar (Fig. 2C) suggests the bacterium belongs to the pseudomonad family. We confirmed this through 16S rRNA gene sequencing and comparison to other sequences, which indicated that the bacterium belongs phylogenetically to the *P. putida* group (Fig. 2G). The isolated pseudomonad is clearly distinguishable from the intensively studied reference strain *P. putida* KT2440 [recently proposed to be renamed in *Pseudomonas alloputida* KT2440 (Keshavarz-Tohid *et al*., 2019, Passarelli-Araujo *et al*., 2021)] but closely related to *P. asiatica* as well as a *Pseudomonas plecoglossicida* strain (Fig. 2G). *P. plecoglossicida* has been reported to be entomopathogenic (Danismazoglu *et al*., 2012). Therefore, we examined whether our pseudomonad isolate has insecticidal activity towards *G. mellonella* larvae (Fig. 3A and B) and compared it to *P. putida* KT2440 (KT2440) and *P. luminescens* DJC primary cell variant 1° (DJC 1°), which is known to be highly pathogenic towards insects (Zamora-Lagos *et al*., 2018). For that purpose, we injected 20 000 and 2000 cells of the respective bacteria per insect, and monitored larvae mortality after 24 and 48 h. When injecting 20 000 cells the insect mortality of the pseudomonad isolate was nearly comparable to the mortality caused by DJC 1°; however, the mortality was decreased to approximately 20% compared to DJC 1° after 48 h when injecting 10-fold less cells (Fig. 3A). KT2440 was used as control and showed no insect pathogenicity. As expected, dead larvae killed by the isolate did not turn red as it is the case for DJC 1° due to anthraquinone pigment production (Fig. 3B). These data clearly show that our

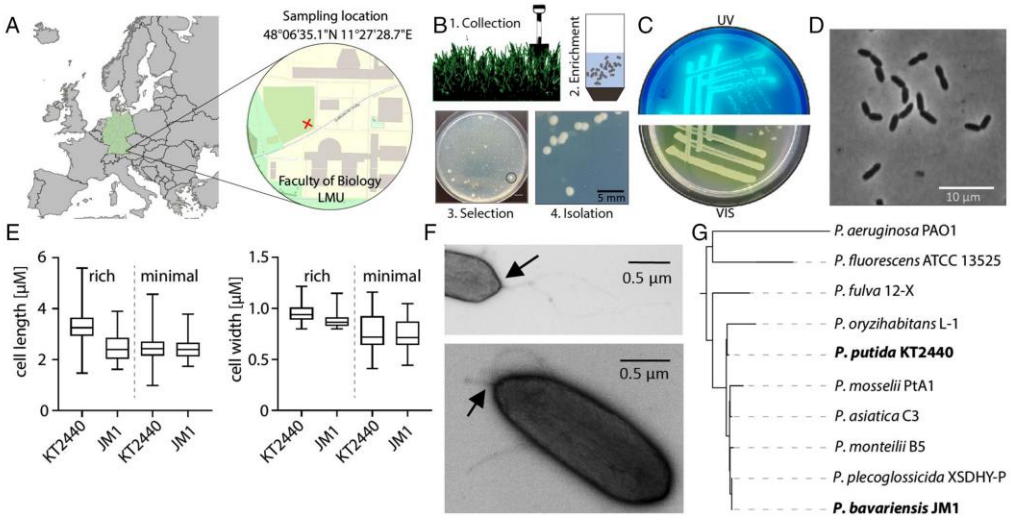

Fig. 2. Isolation and initial characterization of a CML-degrading soil bacterium.
A. Sampling location (The maps were obtained from OpenStreetMap).
B. Isolation and colony-morphotyping: 1. Near surface soil was collected. 2. Bacteria were enriched by filtration and centrifugation. 3. Selection was done on M9 minimal agar containing 10 mM of CML as sole carbon source. 4. Selected colonies (round circle) were streaked out again to exclude contamination by other species.
C. Growth on cetrimide agar and visualization under UV-light (UV) or visible light (VIS).
D. Shown is a differential interference contrast (DIC) image of exponentially grown cells cultivated in rich medium.
E. Measures of cell length and width of the isolate JM1 in comparison to *P. putida* KT2440.
F. TEM micrographs of the isolate. Arrows depict lophotrichous flagella.
G. Phylogenetic analysis based on the 16S rRNA gene. Depicted in bold are the isolate – *P. asiatica* subsp. bavariensis JM1 – and *P. putida* KT2440. *P. aeruginosa* PAO1 and *P. fluorescens* ATCC 13525 served as outgroup.

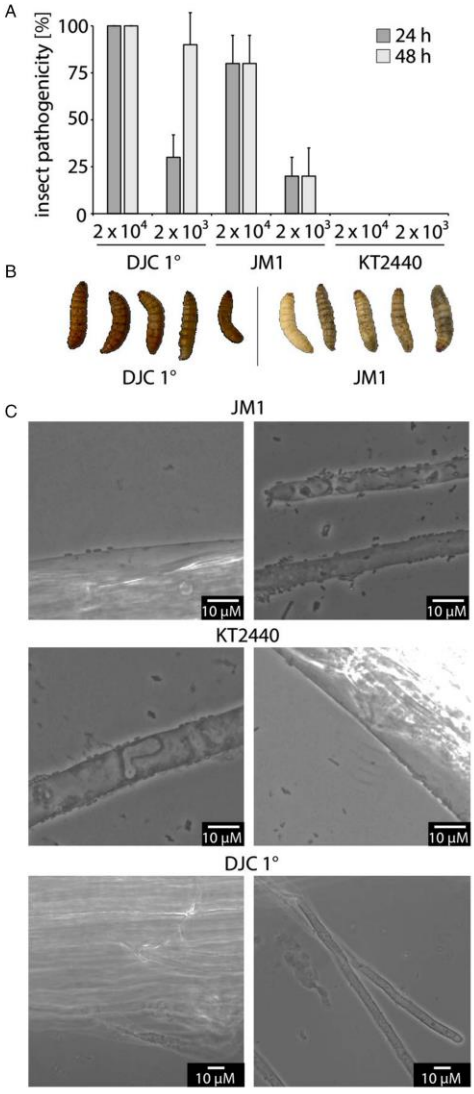

Fig. 3. Insect pathogenicity and plant root colonization of *P. asiatica* subsp. *bavariensis* JM1.
A. Insect pathogenicity of JM1 towards *G. mellonella* larvae in comparison to *P. luminescens* DJC 1° (positive control) and *P. putida* KT2440 (negative control). Error bars represent standard deviation of three independently performed experiments.
B. *G. mellonella* larvae after 48 h infected with 20 000 cells of *P. luminescens* 1° cells DJC 1° (left panel) and JM1 (right panel). The picture shows five representative infected larvae from the experiments shown in (A).
C. Phase contrast microscopy of *Arabidopsis thaliana* roots colonized by JM1, KT2440 (positive control) and DJC 1° (negative control) after 7 days (left picture) and 14 days (right picture). The pictures represent each one characteristic of three independently performed experiments.

pseudomonad displays high pathogenicity against insects. Furthermore, pseudomonads are known as plant root colonizers (Kim and Anderson, 2018). To test whether the isolate also colonizes plant roots, a plant root colonization assay on *A. thaliana* seedlings was performed. Therefore, the seedlings were co-cultured for 14 days with JM1 and KT2440 (positive control) as well as DJC 1° (negative control) for comparison. Upon 7 days and 14 days of co-cultivation, both pseudomonads but not DJC 1° colonized the plant root (Fig. 3C). Accordingly, and as other related pseudomonads (Vacheron *et al*., 2016; Keshavarz-Tohid *et al*., 2019) JM1 seems to be perfectly adapted to a rhizosphere environment, where the microbe was isolated from.

Phylogenetic assignment as new subspecies Pseudomonas asiatica *subsp.* bavariensis *JM1*

We next conducted a whole-genome sequencing and assembled the genome into 769 scaffolds using SPAdes (Bankevich *et al*., 2012) and attempted to close the genome using MeDuSa (Bosi *et al*., 2015) and REAPR (Hunt *et al*., 2013) resulting in a final assembly of 57 scaffolds longer than 1000 bp with a total length of 5 639 629 bp and an N50 of 223 868 bp. GC content was 63.07% and annotation with RAST (Aziz *et al*., 2008; Overbeek *et al*., 2014; Brettin *et al*., 2015) identified 5327 ORFs including 5262 protein-encoding genes, six rRNAs or rRNA subunits and 59 tRNAs. The sequences of the *P. putida* multi-locus sequence typing (MLST) scheme were extracted from this genome data using PubMLST (Jolley *et al*., 2018; Ogura and Kanesaki, 2018). For six out of eight genes, our isolate had the exact same sequence as ST14 (*P. asiatica*), the two remaining genes (*ppsA* and *rpoD*) showed three and five single nucleotide changes with respect to ST14 (new PubMLST types *ppsA* 107 and *rpoD* 110) which was the closest sequence present in the database. Hence our isolate was found to have *P. asiatica* as its closest relative based on MLST. In accordance with our initial assumption derived from the 16S rRNA gene analysis we placed our isolate into the phylogeny of the *P. putida* group using 358 orthologous genes identified in 47 *Pseudomonas* genomes (see Experimental procedures) (Fig. S1). The phylogeny, reconstructed with MrBayes (Ronquist and Huelsenbeck, 2003), showed that one *P. putida* isolate (JBC17) was more closely related to *P. fluorescens*. The rest of the *P. putida* group was monophyletic with *P. alkylphenolica* being the most basal species of the group. Within the group, however, the species for which we had more than one isolate were not monophyletic (*P. putida*, *Pseudomonas entomophila* and *Pseudomonas parafulva*) except for *Pseudomonas mosselii*. Our isolate was found to be closely related but distinct from a group

formed by *P. asiatica* strain C3 and three *P. putida* isolates (DLL-E4, HB3267 and S16).

Following Passarelli-Araujo *et al*. (2021) we used Mash (Ondov *et al*., 2016) to estimate the genomic distance between our isolate and the most closely related strains (Passarelli-Araujo *et al*., 2021). The authors used 0.05 as a threshold for defining a new species. We found that our isolate had distances ranging between 0.048 and 0.051 with the four other strains belonging to the *P. asiatica* group showing that it can be classified as belonging to this species (Table S3). However, the four other strains have lower distances between each other (0.008–0.026). We thus propose that our isolate belongs to a new subspecies of *P. asiatica* and name it *P. asiatica* subsp. *bavariensis* JM1 in reference to the region in Germany it was isolated from.

The distinction is further supported as neither nicotine nor p-nitrophenol served as nutrient source (Table S4) in contrast to what was reported for the closely related strains *P. putida* S16 and *P. putida* DLL-E4 respectively (Yu *et al*., 2011; Chen *et al*., 2016). Despite this lack of metabolic activity towards the latter compounds, JM1 is highly versatile and not only grows on most of the 20 canonical amino acids but also on CEL, the higher homologue of CML (Table S4; Fig. 4A).

CML degradation by P. asiatica *subsp.* bavariensis *JM1 occurs from the carboxymethyl group as well as from the* α*-C-atom*

Having phenotypically characterized JM1, we were curious about the metabolic fate of CML and CEL. Based on the selection criteria we know that both AGEs can be utilized by JM1 as sole carbon source (Fig. 4A). We now tested whether CML and CEL can also be used as sole source of nitrogen. Accordingly, we inoculated bacterial cells in minimal medium lacking any further N-source but containing either 10 mM of CML or CEL instead. Regardless of both AGEs were used as sole C- or N-source, JM1 could grow but with significant differences in growth rate. Whereas exponentially growing bacteria double around every hour with CML as carbon source, doubling time (t_d) increased to about 2.5 h when used as nitrogen source. Similarly, t_d with CEL increased from 90 min (C-source) to almost 8 h (N-source). We note that the slow division rates in media with the two AGEs as sole nitrogen source rationalize why we used different time scales for the growth curves presented in the two diagrams of Fig. 4A and which account for the differences in the maximum optical density. Overall, our growth analyses suggest that both CML and CEL are rather preferred as source of carbon compared to their use as nitrogen source and which might be attributed to the initial selection regime (Fig. 2B). This could also account for the differences in growth rate between CML and CEL (Fig. 4A).

We next analysed CML/CEL degradation over time and compared it to lysine as reference by using HPLC with UV-detection after dansylation (Fig. 4B) (Thompson *et al*., 2019). Within 24 h, lysine as well as CML and CEL were almost completely decomposed. Thus JM1 is an efficient degrader of these AGEs and might have a major impact on the decomposition of CML and CEL in the environment. A closer look at the curves revealed differences in the degradation of the three analysed compounds: After 8 h of incubation over 90% of CEL and lysine had remained intact, whereas already almost 40% of CML was degraded. Thus, degradation of CML is more efficient than decomposition of CEL which is in line with the observed differences in growth on the two AGEs. Either JM1 has a specialized metabolism for CML with certain promiscuity towards CEL. Alternatively, the two AGEs might be degraded by distinct pathways. To test which of the hypothesized scenarios is the most plausible, we conducted a metabolomic study and determined the fate of CML and CEL by HILIC coupled to time-of-flight mass spectrometry. The identities of the peaks were assessed by their chromatographic behaviour and interpretation of the mass spectra (Figs S3–S7). The formation of *N*-carboxymethylaminopentanoic acid (CM-APA) was observed at *m/z* 176.0917 when CML had been offered to the cells (Fig. S4). The mass spectrum, as well as the MS/MS spectrum of CM-APA (Fig. S7), was in accordance with the data previously published (Hellwig *et al*., 2019). The compound may be formed by the route outlined in Fig. 5 by decarboxylation and transamination of the resulting amine (Hellwig *et al*., 2019). When analysing the HILIC-TOF-MS data of JM1 grown on CEL, we observed a strong abundance of the ion *m/z* 190.1074 at the retention time that one would expect for the higher homologue of CM-APA – carboxyethylaminopentanoic acid (CE-APA) (Fig. 4E, Fig. S7): The observed increase by 14.016 in the molecular weight of several MS/MS fragments (*m/z* 144, *m/z* 126, *m/z* 98) matches exactly the difference in the monoisotopic molecular masses of CM-APA and CE-APA which is equivalent to a methylene group. We note that CE-APA will have to be independently synthesized in the future to complete the assignment. Together our data suggest that there is a common reaction cascade for degrading both CML and CEL which is similar to what was reported previously in *E. coli* and other gut microorganisms (Bui *et al*., 2019; Hellwig *et al*., 2019). Interestingly and in contrast to cultures of JM1 incubated with lysine or CEL we further detected a significant increase by 15- to 20-fold in the concentration of α-aminoadipate when CML was utilized as sole source

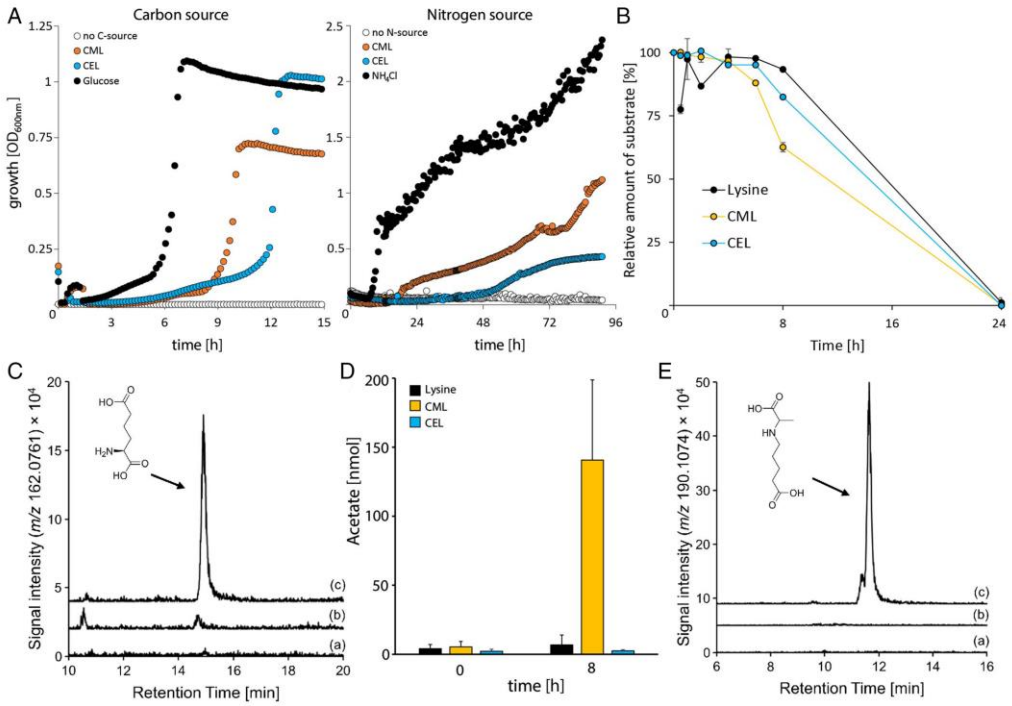

Fig. 4. Analysis of CML/CEL metabolism of *P. asiatica* subsp. *bavariensis* JM1.
A. Growth on 10 mM CML and CEL as sole carbon or nitrogen source: Main cultures in M9 minimal medium containing the respective compound (starting OD600nm = 0.05) were incubated at 30°C. Growth was recorded over maximally 72 h with measures every 10 min. Depicted are the averages derived from three independent biological replicates.
B. *In vivo* degradation of lysine, CML and CEL by *P. asiatica* subsp. *bavariensis* JM1. Cells were cultivated in M9 minimal medium containing either 10 mM lysine, CML or CEL (starting OD600nm = 0.05) and were incubated at 30°C for 24 h. Samples were taken at designated timepoints and substrate concentrations were quantified relative to the maximum at time point 0 h = 100% using HPLC-UV after dansylation.
C. Formation of α-aminoadipic acid in the culture supernatants as measured by HILIC-TOF-MS in the Scan mode; extracted ion chromatograms for *m/z* 162.0761 ± 0.005 (protonated molecular ion of α-aminoadipic acid) are shown for (a) the cultures with lysine, (b) the cultures with CEL and (c) the cultures with CML after 24 h of incubation.
D. *P. asiatica* subsp. *bavariensis* JM1 was cultivated in M9 minimal medium containing 10 mM lysine, CML, or CEL. External acetate was quantified and is given in nmol as the average from three independent replicates.
E. Formation of N-carboxyethylaminopentanoic acid in the culture supernatants as measured by HILIC-TOF-MS in the Scan mode; extracted ion chromatograms for *m/z* 190.1074 ± 0.005 (protonated molecular ion of N-carboxyethylaminopentanoic acid) are shown for (a) the cultures with lysine, (b) the cultures with CML and (c) the cultures with CEL after 24 h of incubation.

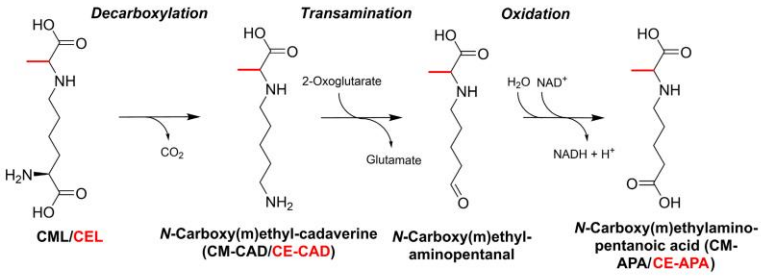

Fig. 5. Proposed pathway for CML/CEL degradation by *P. asiatica* subsp. *bavariensis* JM1.

of carbon (Fig. 4C and S6). Its emergence strongly suggests for an additional alternative route of degradation that starts with the removal of the carboxymethyl group. This in turn might lead to the formation of acetate. If so, acetate will, in turn, be excreted in a process termed overflow metabolism (Wolfe, 2005) and can then easily be quantified colourimetrically. Accordingly, we analysed supernatants of JM1 cultures grown on CML as sole carbon source and used lysine and CEL as control substrates (Fig. 4D). Strikingly, with CML, acetate levels were more than 20 times higher compared to what we found with lysine or CEL. The data were corroborated after RP-HPLC-TOF-MS measurements of carboxylic acids derivatized to the respective pentafluorphenylhydrazones: An increase in the concentration of acetate was observed only in culture supernatants after incubation with CML (data not shown). If CEL would be processed analogously propionate should be generated instead of acetate. As propionate is processed via the 2-methylcitric acid cycle (Ewering *et al*., 2006), we looked simultaneously for increased pyruvate concentrations. However, neither of the two organic acids could be detected. This in turn indicates a thus far unknown AGE metabolism in JM1 being rather unique to CML (Fig. 6). Parallel processing of CML from both the α-C-atom and the ε-amino group might also explain the observed differences in growth compared to CEL, which seems to be processed predominantly from C_{α}.

Regardless of which of the two putative routes JM1 uses to decompose CML or CEL, the metabolic velocity exceeds by far everything reported for bacteria of the human intestine. Here even within several days of incubation, a large proportion of CML is left intact while the rest is only partially digested, as can be concluded from the fraction of intermediates that could be detected (Bui *et al*., 2019; Hellwig *et al*., 2019).

Concluding remarks

In this study, we isolated the first CML/CEL-degrading soil bacterium as new subspecies of *P. asiatica* and belonging to the *Pseudomonas putida* group. Metabolic profiling suggests CML/CEL processing by first decarboxylation followed by transamination and oxidation (Fig. 5) in a reaction cascade being reminiscent of what was suggested for CML degradation by *E. coli* and other gut microorganisms (Bui *et al*., 2019, Hellwig *et al*., 2019). The proposed pathway is analogous to the one of lysine decomposition (Thompson *et al*., 2019) which also starts with a decarboxylation reaction followed by a transamination, in which glutamate is formed from oxalacetate as byproduct, and an oxidation accompanied by the reduction of NAD^+ to NADH + H^+. The fact that we did not find the expected biogenic amines derived from CML and CEL decarboxylation, carboxymethylcadaverine (CM-Cad) and carboxyethylcadaverine (CE-Cad) respectively (Figs S3 and S5) does not exclude them as metabolites. We rather hypothesize that processing beyond CM-APA and CE-APA is rate limiting in the decomposition process. Further downstream processing might involve removal of the carboxy(m)ethyl group and a second decarboxylation reaction to finally yield α-ketoglutarate and succinate both of which are part of central carbon metabolism. As CEL is degraded almost as fast as CML and together with the chemical similarity of both compounds we think that one and the same pathway is used with enzymes being promiscuous towards both AGEs. Future studies have to reveal these biocatalysts and clarify whether they are involved in both CML and CEL metabolism.

Equally important will be the identification of enzymes mediating CML processing that starts at the ε-amino group and finally leads to the formation of α-aminoadipate (Fig. 4C). We hypothesize that this metabolite is generated by first decarboxymethylation – an apparently simple but chemically difficult abstraction, hence demanding for enzymes that are able to oxidize the C-N bond. An example of such biocatalysts is fructosamine oxidases, which act on Amadori products that incorporate the α-amino group of amino acids. Both of the C-N bonds adjacent to the secondary amino group can be oxidized enzymatically in Amadori compounds (Horiuchi, 1989; Gerhardinger *et al*., 1995). The imine intermediate resulting from the CML decarboxymethylation reaction is further hydrolyzed first to allysine and subsequently oxidized to α-aminoadipate (Fig. 6). The latter oxidation was found to be NAD^+-

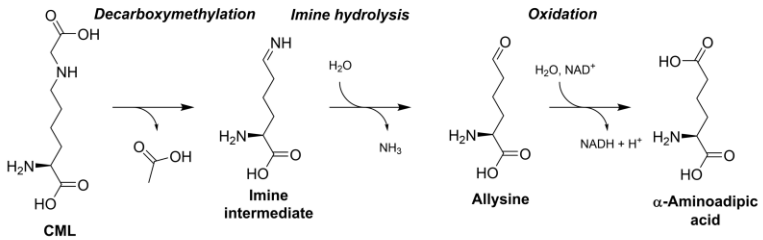

Fig. 6. Proposed pathway for CML degradation by *P. asiatica* subsp. *bavariensis* JM1.

dependent in a *Pseudomonas* strain (Calvert and Rodwell, 1966). α-Aminoadipate on the other hand is a metabolite in the lysine catabolism of pseudomonads and is further processed via α-oxoadipate and α-hydroxyglutarate to α-ketoglutarate (Thompson *et al*., 2019).

Acknowledgements

We thank Jannis Brehm for technical assistance with the insect pathogenicity experiments and the Deutsche Forschungsgemeinschaft for their contribution to the applied MS/MS device (DFG Major Research Instrumentation Programme grant INST 188/521-1 FUGG). Open Access funding enabled and organized by Projekt DEAL.

Author Contributions

J.M. isolated and characterized the CML degrading isolate unless indicated otherwise. She also initially classified the bacterium as pseudomonad of the *P. putida* group. All other bioinformatic analyses were done by R.E.R. and N.S.B. A.K. performed electron microscopy experiments. F.P. and R.H. performed entomopathogenicity assays and analysed plant root colonization. K.I.B. and M.H. synthesized CML/CEL and analysed their degradation and metabolic derivatives. J.L. and M.H. wrote the manuscript with contributions from all other authors. The study was designed by J.L. and M.H. with contributions from all other authors.

References

Ahmed, M.U., Thorpe, S.R., and Baynes, J.W. (1986) Identification of N_ε-carboxymethyllysine as a degradation product of fructoselysine in glycated protein. *J Biol Chem* **261**: 4889–4894.

Alamir, I., Niquet-Leridon, C., Jacolot, P., Rodriguez, C., Orosco, M., Anton, P.M., and Tessier, F.J. (2013) Digestibility of extruded proteins and metabolic transit of N_ε-carboxymethyllysine in rats. *Amino Acids* **44**: 1441–1449.

Altschul, S.F., Gish, W., Miller, W., Myers, E.W., and Lipman, D.J. (1990) Basic local alignment search tool. *J Mol Biol* **215**: 403–410.

Arndt, D., Grant, J.R., Marcu, A., Sajed, T., Pon, A., Liang, Y., and Wishart, D.S. (2016) PHASTER: a better, faster version of the PHAST phage search tool. *Nucleic Acids Res* **44**: W16–W21.

Assar, S.H., Moloney, C., Lima, M., Magee, R., and Ames, J. M. (2009) Determination of N_ε-carboxymethyllysine in food systems by ultra performance liquid chromatography-mass spectrometry. *Amino Acids* **36**: 317–326.

Aziz, R.K., Bartels, D., Best, A.A., DeJongh, M., Disz, T., Edwards, R.A., *et al*. (2008) The RAST server: rapid annotations using subsystems technology. *BMC Genomics* **9**: 75.

Bankevich, A., Nurk, S., Antipov, D., Gurevich, A.A., Dvorkin, M., Kulikov, A.S., *et al*. (2012) SPAdes: a new genome assembly algorithm and its applications to single-cell sequencing. *J Comput Biol* **19**: 455–477.

Becker, N.S., Margos, G., Blum, H., Krebs, S., Graf, A., Lane, R.S., *et al*. (2016) Recurrent evolution of host and vector association in bacteria of the *Borrelia burgdorferi* sensu lato species complex. *BMC Genomics* **17**: 734.

Bertani, G. (1951) Studies on lysogenesis. I. The mode of phage liberation by lysogenic *Escherichia coli*. *J Bacteriol* **62**: 293–300.

Birlouez-Aragon, I., Saavedra, G., Tessier, F.J., Galinier, A., Ait-Ameur, L., Lacoste, F., *et al*. (2010) A diet based on high-heat-treated foods promotes risk factors for diabetes mellitus and cardiovascular diseases. *Am J Clin Nutr* **91**: 1220–1226.

Bosi, E., Donati, B., Galardini, M., Brunetti, S., Sagot, M.F., Lió, P., *et al*. (2015) MeDuSa: a multi-draft based scaffolder. *Bioinformatics* **31**: 2443–2451.

Brettin, T., Davis, J.J., Disz, T., Edwards, R.A., Gerdes, S., Olsen, G.J., *et al*. (2015) RASTtk: a modular and extensible implementation of the RAST algorithm for building custom annotation pipelines and annotating batches of genomes. *Sci Rep* **5**: 8365.

Bui, T.P.N., Troise, A.D., Fogliano, V., and de Vos, W.M. (2019) Anaerobic degradation of N_ε-carboxymethyllysine, a major glycation end-product, by human intestinal bacteria. *J Agric Food Chem* **67**: 6594–6602.

Calvert, A.F., and Rodwell, V.W. (1966) Metabolism of pipecolic acid in a *Pseudomonas* species. 3. L-α-aminoadipate δ-semialdehyde:nicotinamide adenine dinucleotide oxidoreductase. *J Biol Chem* **241**: 409–414.

Chen, Q., Tu, H., Luo, X., Zhang, B., Huang, F., Li, Z., *et al*. (2016) The regulation of para-nitrophenol degradation in *Pseudomonas putida* DLL-E4. *PLoS One* **11**: e0155485.

Ciufo, S., Kannan, S., Sharma, S., Badretdin, A., Clark, K., Turner, S., *et al*. (2018) Using average nucleotide identity to improve taxonomic assignments in prokaryotic genomes at the NCBI. *Int J Syst Evol Microbiol* **68**: 2386–2392.

Danismazoglu, M., Demir, İ., Sevim, A., Demirbag, Z., and Nalcacioglu, R. (2012) An investigation on the bacterial flora of Agriotes lineatus (Coleoptera: Elateridae) and pathogenicity of the flora members. *Crop prot* **40:** 1–7.

Delgado-Andrade, C., Tessier, F.J., Niquet-Leridon, C., Seiquer, I., and Pilar Navarro, M. (2012) Study of the urinary and faecal excretion of N_ε-carboxymethyllysine in young human volunteers. *Amino Acids* **43**: 595–602.

Edgar, R.C. (2004) MUSCLE: multiple sequence alignment with high accuracy and high throughput. *Nucleic Acids Res* **32**: 1792–1797.

Ewering, C., Heuser, F., Benölken, J.K., Brämer, C.O., and Steinbüchel, A. (2006) Metabolic engineering of strains of *Ralstonia eutropha* and *Pseudomonas putida* for biotechnological production of 2-methylcitric acid. *Metab Eng* **8**: 587–602.

Federhen, S., Rossello-Mora, R., Klenk, H., Tindall, B.J., Konstantinidis, K.T., Whitman, W.B., *et al*. (2016) Meeting report: GenBank microbial genomic taxonomy workshop (12–13 May, 2015). *Stand Genomic Sci* **11**: 15.

Gerhardinger, C., Marion, M.S., Rovner, A., Glomb, M., and Monnier, V.M. (1995) Novel degradation pathway of glycated amino acids into free fructosamine by a *Pseudomonas* sp. soil strain extract. *J Biol Chem* **270**: 218–224.

Graf von Armansperg, B., Koller, F., Gericke, N., Hellwig, M., Jagtap, P.K.A., Heermann, R., *et al*. (2021) Transcriptional regulation of the Nε-fructoselysine metabolism in *Escherichia coli* by global and substrate-specific cues. *Mol Microbiol* **115**: 175–190.

Gurevich, A., Saveliev, V., Vyahhi, N., and Tesler, G. (2013) QUAST: quality assessment tool for genome assemblies. *Bioinformatics* **29**: 1072–1075.

Hanahan, D. (1983) Studies on transformation of *Escherichia coli* with plasmids. *J Mol Biol* **166**: 557–580.

Hegele, J., Buetler, T., and Delatour, T. (2008) Comparative LC-MS/MS profiling of free and protein-bound early and advanced glycation-induced lysine modifications in dairy products. *Anal Chim Acta* **617**: 85–96.

Hellwig, M., Auerbach, C., Müller, N., Samuel, P., Kammann, S., Beer, F., *et al*. (2019) Metabolization of the advanced glycation end product N_{ε}-carboxymethyllysine (CML) by different probiotic *E. coli* strains. *J Agric Food Chem* **67**: 1963–1972.

Hellwig, M., and Henle, T. (2014) Baking, ageing, diabetes: a short history of the Maillard reaction. *Angew Chem Int Ed Engl* **53**: 10316–10329.

Henning, C., and Glomb, M.A. (2016) Pathways of the Maillard reaction under physiological conditions. *Glycoconj J* **33**: 499–512.

Heyns, K., and Noack, H. (1962) Die Umsetzung von D-Fructose mit L-Lysin und L-Arginin und deren Beziehung zu nichtenzymatischen Bräunungsreaktionen. *Chem Ber-Recl* **95**: 720–727.

Higgins, D.G., and Sharp, P.M. (1988) CLUSTAL: a package for performing multiple sequence alignment on a microcomputer. *Gene* **73**: 237–244.

Horiuchi, T. (1989) Purification and properties of N-acyl-d-hexosamine oxidase from *Pseudomonas* sp. 15-1. *Agric Biol Chem* **53**: 361–368.

Hunt, M., Kikuchi, T., Sanders, M., Newbold, C., Berriman, M., and Otto, T.D. (2013) REAPR: a universal tool for genome assembly evaluation. *Genome Biol* **14**: R47.

Jolley, K.A., Bray, J.E., and Maiden, M.C.J. (2018) Open-access bacterial population genomics: BIGSdb software, the PubMLST.org website and their applications. *Wellcome Open Res* **3**: 124.

Keshavarz-Tohid, V., Vacheron, J., Dubost, A., Prigent-Combaret, C., Taheri, P., Tarighi, S., *et al*. (2019) Genomic, phylogenetic and catabolic re-assessment of the *Pseudomonas putida* clade supports the delineation of *Pseudomonas alloputida* sp. nov., *Pseudomonas inefficax* sp. nov., *Pseudomonas persica* sp. nov., and *Pseudomonas shirazica* sp. nov. *Syst Appl Microbiol* **42**: 468–480.

Kim, Y.C., and Anderson, A.J. (2018) Rhizosphere pseudomonads as probiotics improving plant health. *Mol Plant Pathol* **19**: 2349–2359.

Larkin, M.A., Blackshields, G., Brown, N.P., Chenna, R., McGettigan, P.A., McWilliam, H., *et al*. (2007) Clustal W and Clustal X version 2.0. *Bioinformatics* **23**: 2947–2948.

Lassak, J., Koller, F., Krafczyk, R., and Volkwein, W. (2019) Exceptionally versatile – arginine in bacterial post-translational protein modifications. *Biol Chem* **400**: 1397–1427.

Lassak, J., Sieber, A., and Hellwig, M. (2022) Exceptionally versatile take II: post-translational modifications of lysine and their impact on bacterial physiology. *Biol Chem*.

Lassak, K., Neiner, T., Ghosh, A., Klingl, A., Wirth, R., and Albers, S.V. (2012) Molecular analysis of the crenarchaeal flagellum. *Mol Microbiol* **83**: 110–124.

Letunic, I., and Bork, P. (2021) Interactive Tree Of Life (iTOL) v5: an online tool for phylogenetic tree display and annotation. *Nucleic Acids Res* **49**: W293–w296.

Liao, H.Y., Wang, C.Y., Lee, C.H., Kao, H.L., Wu, W.K., and Kuo, C.H. (2021) Development of an efficient and sensitive chemical derivatization-based LC-MS/MS method for quantifying gut microbiota-derived metabolites in human plasma and its application in studying cardiovascular disease. *J Proteome Res* **20**: 3508–3518.

Maillard, L.C. (1912a) The action of amino acids on sugar; the formation of melanoidin by a methodic route. *C R Hebd Séances Acad Sci* **154**: 66–68.

Maillard, L.C. (1912b) General reaction of amino acids on sugars: its biological consequences. *C R Séances Soc Biol Ses Fil* **72**: 599–601.

Ogura, M., and Kanesaki, Y. (2018) Newly identified nucleoid-associated-like protein YlxR regulates metabolic gene expression in *Bacillus subtilis*. *mSphere* **3**: e00501-18.

Ondov, B.D., Treangen, T.J., Melsted, P., Mallonee, A.B., Bergman, N.H., Koren, S., and Phillippy, A.M. (2016) Mash: fast genome and metagenome distance estimation using MinHash. *Genome Biol* **17**: 132.

Overbeek, R., Olson, R., Pusch, G.D., Olsen, G.J., Davis, J. J., Disz, T., *et al*. (2014) The SEED and the rapid annotation of microbial genomes using subsystems technology (RAST). *Nucleic Acids Res* **42**: D206–D214.

Passarelli-Araujo, H., Jacobs, S.H., Franco, G.R., and Venancio, T.M. (2021) Phylogenetic analysis and population structure of *Pseudomonas alloputida*. *Genomics* **113**: 3762–3773.

Paulick, A., Koerdt, A., Lassak, J., Huntley, S., Wilms, I., Narberhaus, F., and Thormann, K.M. (2009) Two different stator systems drive a single polar flagellum in *Shewanella oneidensis* MR-1. *Mol Microbiol* **71**: 836–850.

Peix, A., Ramírez-Bahena, M.H., and Velázquez, E. (2018) The current status on the taxonomy of *Pseudomonas* revisited: an update. *Infect Genet Evol* **57**: 106–116.

Pospiech, A., and Neumann, B. (1995) A versatile quick-prep of genomic DNA from Gram-positive bacteria. *Trends Genet* **11**: 217–218.

Rambaut, A., Drummond, A.J., Xie, D., Baele, G., and Suchard, M.A. (2018) Posterior summarization in Bayesian phylogenetics using Tracer 1.7. *Syst Biol* **67**: 901–904.

Regaiolo, A., Dominelli, N., Andresen, K., Heermann, R., and Schaffner, D.W. (2020) The biocontrol agent and insect pathogen *Photorhabdus luminescens* interacts with plant roots. *Appl Environ Microbiol* **86**: e00891-00820.

Roncero-Ramos, I., Delgado-Andrade, C., Tessier, F.J., Niquet-Leridon, C., Strauch, C., Monnier, V.M., and Navarro, M.P. (2013) Metabolic transit of N_{ε}-carboxymethyllysine after consumption of AGEs from bread crust. *Food Funct* **4**: 1032–1039.

Roncero-Ramos, I., Niquet-Leridon, C., Strauch, C., Monnie, V.M., Tessier, F.J., Navarro, M.P., and Delgado-Andrade, C. (2014) An advanced glycation end product (AGE)-rich diet promotes N_{ε}-carboxymethyllysine

accumulation in the cardiac tissue and tendons of rats. *J Agric Food Chem* **62**: 6001–6006.
Ronquist, F., and Huelsenbeck, J.P. (2003) MrBayes 3: Bayesian phylogenetic inference under mixed models. *Bioinformatics* **19**: 1572–1574.
Scheijen, J., Hanssen, N.M.J., van Greevenbroek, M.M., Van der Kallen, C.J., Feskens, E.J.M., Stehouwer, C.D.A., and Schalkwijk, C.G. (2018) Dietary intake of advanced glycation endproducts is associated with higher levels of advanced glycation endproducts in plasma and urine: the CODAM study. *Clin Nutr* **37**: 919–925.
Somoza, V., Wenzel, E., Weiss, C., Clawin-Radecker, I., Grubel, N., and Erbersdobler, H.F. (2006) Dose-dependent utilisation of casein-linked lysinoalanine, N_ε-fructoselysine and N_ε-carboxymethyllysine in rats. *Mol Nutr Food Res* **50**: 833–841.
Studier, F.W. (2005) Protein production by auto-induction in high-density shaking cultures. *Protein Expr Purif* **41**: 207–234.
Thompson, M.G., Blake-Hedges, J.M., Cruz-Morales, P., Barajas, J.F., Curran, S.C., Eiben, C.B., *et al*. (2019) Massively parallel fitness profiling reveals multiple novel enzymes in *Pseudomonas putida* lysine metabolism. *mBio* **10**: e02577-02518.
Tohya, M., Watanabe, S., Teramoto, K., Uechi, K., Tada, T., Kuwahara-Arai, K., *et al*. (2019) *Pseudomonas asiatica sp*. *nov*., isolated from hospitalized patients in Japan and Myanmar. *Int J Syst Evol Microbiol* **69**: 1361–1368.
Ulrich, P., and Cerami, A. (2001) Protein glycation, diabetes, and aging. *Recent Prog Horm Res* **56**: 1–21.
Vacheron, J., Moënne-Loccoz, Y., Dubost, A., Gonçalves-Martins, M., Muller, D., and Prigent-Combaret, C. (2016) Fluorescent *pseudomonas* strains with only few plant-beneficial properties are favored in the maize rhizosphere. *Front Plant Sci* **7**: 1212.
Wadman, S.K., De Bree, P.K., Van Sprang, F.J., Kamerling, J. P., Haverkamp, J., and Vliegenthart, J.F. (1975) N_ε-carboxymethyllysine, a constituent of human urine. *Clin Chim Acta* **59**: 313–320.
Weisburg, W.G., Barns, S.M., Pelletier, D.A., and Lane, D.J. (1991) 16S ribosomal DNA amplification for phylogenetic study. *J Bacteriol* **173**: 697–703.
Wolfe, A.J. (2005) The acetate switch. *Microbiol Mol Biol Rev* **69**: 12–50.
Yu, H., Tang, H., Wang, L., Yao, Y., Wu, G., and Xu, P. (2011) Complete genome sequence of the nicotine-degrading *Pseudomonas putida* strain S16. *J Bacteriol* **193**: 5541–5542.
Zamora-Lagos, M.A., Eckstein, S., Langer, A., Gazanis, A., Pfeiffer, F., Habermann, B., and Heermann, R. (2018) Phenotypic and genomic comparison of *Photorhabdus luminescens subsp*. *laumondii* TT01 and a widely used rifampicin-resistant *Photorhabdus luminescens* laboratory strain. *BMC Genomics* **19**: 854.
Zhou, Y., Liang, Y., Lynch, K.H., Dennis, J.J., and Wishart, D.S. (2011) PHAST: a fast phage search tool. *Nucleic Acids Res* **39**: W347–W352.

Supporting Information

Additional Supporting Information may be found in the online version of this article at the publisher's web-site:

Table S1. Strains used in this study.

Table S2. Primers used in this study

Table S3. Mash distances.

Table S4. Genotypic and phenotypic characteristics of *P. asiatica subsp. bavariensis strain*JM1 in comparison to *P. putida* KT2440.

Table S5. Sequences for phylogenetics.

Fig. S1. Phylogenetic classification of the *Pseudomonas* isolate performed in MrBayes v.3.2. (Ronquist and Huelsenbeck, 2003) using a GTR model with inverse gamma rate variation and ploidy set to haploid. Trees were run in triplicate for 3.5 million generations and with a respective burn-in of 25%. All nodes have a posterior probability of one.

Fig. S2. Phenotypic analysis of *Pseudomonas asiatica subsp. bavariensis strain JM1* A) Swimming behaviour of *E. coli* BW25113 and its isogenic deletion strain Δ*fliC* in comparison to *P. putida* KT2440 and *P. asiatica subsp. bavariensis* JM1 on soft agar plates. B) Growth behaviour of KT2440 and JM1 at different pH values. Shown is the optical density at 600 nm (OD 600 nm) after 24 h growth in SOB at 30°C. C) Growth behaviour of KT2440 and JM1 at different temperatures. Shown is the optical density at 600 nm (OD 600 nm) after 24 h growth in rich medium (lysogeny broth). D) Generation times of KT2440 and JM1 logarithmically grown either in SOB (rich) or M9 (minimal) medium.

Fig. S3. Investigation of the formation of *N*-carboxymethylcadaverine (CM-CAD) in the culture supernatants as measured by RP-HPLC–MS/MS in the Scan mode; extracted ion chromatograms for m/z 161 (protonated molecular ion of CM-CAD) are shown for (a) the cultures with CEL, (b) the cultures with lysine, (c) the cultures with CML, (d) the medium with CML after 24 h of incubation. CM-CAD elutes at 12.9 min in this system.

Fig. S4. Investigation of the formation of *N*-carboxymethylaminopentanoic acid (CM-APA) in the culture supernatants as measured by HILIC-MS-TOF in the Scan mode; extracted ion chromatograms for m/z 176.0917 ± 0.005 (protonated molecular ion of CM-APA) are shown for (a) the cultures with lysine, (b) the cultures with CEL, and (c) the cultures with CML after 24 h of incubation. For spectra, see Fig. S7.

Fig. S5. Investigation of the formation of *N*-carboxyethylcadaverine acid (CE-CAD) in the culture supernatants as measured by RP-HPLC–MS/MS in the Scan mode; extracted ion chromatograms for m/z 175 (protonated molecular ion of CE-CAD) are shown for (a) the cultures with CML, (b) the cultures with lysine, (c) the cultures with CEL, (d) the medium with CEL after 24 h of incubation. CE-CAD elutes after 14.5 min in this system.

Fig. S6. (A) Spectrum of the peak eluting at 14.8 min in the supernatant of a culture of *P. asiatica subsp. bavariensis*JM1 that had been incubated with CML for 24 h (chromatogram, see Fig. 4C in the main text), (B) spectrum of a commercially available standard of α-aminoadipic acid.

Fig. S7. (A) Spectrum of the peak eluting at 12.6 min in the supernatant of a culture of *P. asiatica subsp. bavariensis* JM1 that had been incubated with CML for 24 h, (B) MS/MS spectrum of m/z 176.0917 (C) Spectrum of the peak eluting at 11.6 min in the supernatant of a culture of *P. asiatica subsp. bavariensis* JM1 that had been incubated with CEL for 24 h, (D) MS/MS spectrum of m/z 190.1074.

7. Concluding discussion

In recent years, biotechnology has gained prominence as a vital field for addressing critical challenges across medicine, agriculture and environmental sustainability. While traditional methods, such as chemical treatments, have been effective, they often lead to unintended consequences, including pollution, resource depletion and increased resistance in pathogens (Rathore and Singh 2022; Jurick II 2022). For example, in medicine, overreliance on synthetic drugs has contributed to the emergence of antibiotic-resistant bacteria, while in agriculture, chemical pesticides can disrupt soil ecosystems and lead to resistant pest strains (Lamichhane et al. 2018). Consequently, there is a need for more efficient, precise and sustainable biotechnological approaches that address these limitations while minimizing ecological impact (Villadsen 2007; Ghosh et al. 2019).

Bacterial secretion systems, with their ability to transport proteins directly into the extracellular environment, present a promising alternative for advancing sustainable biotechnological applications. In addition to simplifying downstream processing and reducing host cell toxicity, these systems are highly specialized, allowing for targeted protein delivery with minimal impact on surrounding organisms. Such capabilities make bacterial secretion systems valuable for applications in medicine, agriculture, and industry, where precision and sustainability are crucial. In this context, studying the Type VI Secretion System (T6SS) in *P. luminescens* is of particular importance. The T6SS plays a central role in bacterial interaction with other microbes and hosts, making it an ideal model for understanding competitive mechanisms and interspecies interactions. By exploring the T6SS in *P. luminescens*, this study aims to uncover the role of the T6SS in this bacterium and further, how bacterial systems can be repurposed for targeted applications.

In this study, whole-cell proteomics revealed the role of T6SS-1 and T6SS-2 in the lifestyle of *P. luminescens*, identifying their association with various fitness factors essential to the bacterium. This investigation also demonstrated the importance of the T6SS in interbacterial competition, though it found no significant role for T6SSs in interkingdom interactions. Through

examining the T6SS-3, the study identified external factors influencing its activation, alongside discovering a novel T6SS operon structure. Additionally, this study explored bioluminescence as a response to oxidative stress, providing initial insights into its adaptive function for *P. luminescens*. Further, a luminescence-based reporter platform was established in *P. luminescens*, which was then used to confirm the activity of the T6SS effector Tme1 in *in vivo* competition assays. The subsequent analysis of Tme1 revealed its antibacterial properties and offered new insights into its neutralization mechanism through its cognate immunity protein. Together, these findings deepen the understanding of the T6SS in *P. luminescens* and highlight its potential applications in biotechnology for targeted microbial interactions and antibacterial strategies.

7.1 The roles of T6SSs in *Photorhabdus luminescens*: Competition and pathogenicity

The complex life cycle of *P. luminescens*, which ranges from insect pathogenicity to symbiosis with nematodes and plants, calls for a diverse array of interbacterial and interkingdom defence and symbiosis mechanisms. In the past, studies on the T6SS in different bacteria showed its role in the most diverse interbacterial or host-pathogen interactions, like the virulence of *Ralstonia solanacearum* on eggplants or the contribution to insect pathogenicity in *Pseudomonas protegens* (Asolkar und Ramesh 2020; Vacheron et al. 2019). Yet, current research on the T6SS in *P. luminescens* is limited to one T6SS effector (Rhs1) found in the strain TTO1, which deploys antibacterial activity by deploying a GTPase activity (Jurėnas et al. 2021). Comparative bioinformatics of the *P. luminescens* strains DJC and TTO1 showed a high-level conservation of T6SS structural genes, which is also reported in other T6SS harbouring bacteria like *Acinetobacter* spp. (Pisarz et al. 2024; Sun et al. 2024) **Chapter 2, Fig. 2.1**). However, while no transposons or integrons were identified in the DJC strain, multiple transposases were found in T6SS gene loci in the strain TTO1, indicating an event of horizontal gene transfer (HGT), a tool to enhance the bacterial virulence (Thomas et al. 2017). Moreover, the previously described effector Rhs1 is not present in the genome of *P. luminescens* DJC,

indicating it is not essential for this bacterium's fitness. Acquisition of T6SS encoding genes, especially T6SS effectors, through HGT occurs frequently and was previously described for various *V. cholerae* strains, were a novel effector-immunity pair was functionally transferred through HGT to a new *V. cholerae* strain, resulting in increased bacterial fitness (Thomas et al. 2017; Barret et al. 2011). Given the possibility to introduce new T6SS-delivered toxins through HGT into *P. luminescens* to enhance its fitness, opens new possibilities for biotechnological innovations like targeted delivery of antimicrobial peptides.

Although T6SS elements can be gained by HGT, still the functionality and activity of the T6SS is required to know but difficult to determine. Previous studies aimed to categorize the role and functionality of different T6SS gene loci based on phylogenetic groups, resulting in five cluster families (Boyer et al. 2009). However, the ability of the T6SS to be virulent against a wide range of organisms, including insects, plants, bacteria, fish and fungi, makes the spectrum of activity and classification of the system based on phylogenetic analysis difficult (Hood et al. 2010; Asolkar und Ramesh 2020; Vacheron et al. 2019; Trunk et al. 2018; Wang et al. 2009). Thus, although four different T6SS gene loci were identified in *P. luminescens* (Pisarz et al. 2024) **Chapter 2, Fig. 2.1**), the classification of those T6SSs in the different phylogenetic groups could not provide new insights into the role and functionality of those systems. But the presence of multiple T6SS clusters in *P. luminescens* suggest diverse roles for the bacterial cells similar to *V. parahaemolyticus*, where two T6SSs are important for interbacterial competition, whereas the other two T6SSs were found important for anti-eukaryotic activity by inducing inflammasome-mediated cell death in macrophages (Ray et al. 2017; Cohen et al. 2022; Salomon et al. 2013; Fridman et al. 2020). Thus, another feature that can help identify the role of the T6SS for the bacterial virulence are the effectors encoded within the gene locus like in *Pseudomonas putida*, where an antibacterial effector is encoded in the T6SS-K1 gene loci and the T6SS is found essential for interbacterial competition (Bernal et al. 2017). Building on the bioinformatic identification of four distinct T6SS clusters in *P. luminescens*, each system may contribute to specialized roles within the bacterium's lifecycle according to the encoded effectors. However, as no effectors are present in either T6SS-1 or T6SS-2 and no initial

function could be assigned, those systems were analysed whether they are constitutively expressed by whole-cell proteomics (Pisarz et al. 2024) (**Chapter 2, Fig. 2.4, Tab. 2.1**). Constitutive expression of the T6SS can give a competitive advantage over other bacteria and also eukaryotes as observed in *V. cholerae* (Unterweger et al. 2012). There, deletion of a T6SS gene abolished the killing of bacteria which could be restored after complementation and thus, the constitutive T6SS expression provides the *V. cholerae* cells with an enhanced survival in their environmental niche (Unterweger et al. 2012). Indeed, also in *P. luminescens* the T6SSs were found constitutively expressed in whole-cell proteomics, with multiple proteins of the T6SS-1, T6SS-3 and T6SS-4 detected in high protein levels in 1° WT cells (Pisarz et al. 2024); **Chapter 2, Tab. 2.1, Tab 2.S2**). In accordance, interbacterial competition assays showed, that *P. luminescens* 1° cells can outcompete *E. coli* cells and further, deletion of *tssA*2 resulted in a reduction of the killing capacity of *P. luminescens* (**Chapter 2, Fig. 2.2B**). Thus, a role of the T6SS-2 in interbacterial competition is most likely. Interestingly, the reduced killing was accompanied by an increase in the abundance of T6SS-1 proteins, pointing to a possible co-regulation between the T6SS-1 and T6SS-2. However, no T6SS effector was detected in higher abundance along with a decreased killing capacity and therefore it is most likely that the T6SS-1 is not crucial for interbacterial competition. Indeed, despite the increased presence of T6SS-1 proteins, no significant change in bacterial competitive ability was observed when *tssA1b* was deleted, suggesting that the T6SS-1 is not involved in interbacterial competition. However, also external signals such as salt stress can initiate the assembly and activation of T6SSs, whereby different T6SSs can be regulated differentially in a single organism and thus, further conditions need to be investigated (Salomon et al. 2013).

In *Acinetobacter baumannii* and *Pseudomonas protegens* it was observed that an impaired T6SS can reduce the bacterial virulence towards insect larvae like *Galleria mellonella* (Repizo et al. 2015; Vacheron et al. 2019). *P. luminescens* is a highly insect pathogenic bacterium and diverse mechanisms like PVCs or toxin-antitoxins were identified as crucial to maintain the pathogenicity (Yang et al. 2006; Ffrench-Constant et al. 2007). However, when analysing the insect pathogenicity of T6SS-1 and T6SS-2 deficient *P. luminescens* strains, no reduction in

insect pathogenicity was observed, thereby indicating those T6SSs are not crucial for the pathogenicity towards insect larvae (Pisarz et al. 2024); **Fig. 2.S3**). In contrary to those observations, diverse proteins related to virulence mechanisms like S-type pyocins, PVCs or T3SS were detected in higher abundance in the 1° *tssA*1b strain (Pisarz et al. 2024) **Chapter 2; Table 2.2**). While the insect pathogenicity was not increased although those proteins were detected in higher abundance, these indicates the presence of a master regulator for different virulence mechanisms in *P. luminescens* including the T6SSs. In *P. aeruginosa* multiple master regulator were identified involved in the co-regulatory process of virulence factors like quorum sensing, T3SS and T6SS (Huang et al. 2019). However, subsequent studies are required to identify such a master regulator in *P. luminescens*. Identifying a potential master regulator in *P. luminescens* that coordinates various virulence mechanisms, including the T6SSs, could not only enhance the understanding of its complex pathogenicity network but also offer valuable targets for biotechnological and therapeutic applications, such as the development of precise antimicrobial interventions or bioengineering strategies for pest control.

Besides interbacterial and interkingdom competition, the T6SS can be intricately connected to diverse phenotypic traits such as motility, proteolysis or biofilm formation (Li et al. 2020). Indeed, the comparative proteomics revealed a higher abundance of proteins required for bacterial motility, such as FliA (a transcriptional regulator for flagellar filament synthesis) in the T6SS-deficient *P. luminescens* strains (Liu und Matsumura 1994). Consequent motility assays showed increased motility of the T6SS-deficient *P. luminescens* strains, although the 1° cell form is reported as not motile (Eckstein et al. 2019; Pisarz et al. 2024); **Chapter 2, Fig. 2.2C**). However, a correlation between T6SS activity and motility has also been previously reported in *Ralstonia solanacearum*, where deletion of *tssB* reduced motility and led to a downregulation of genes required for motility (Zhang et al. 2014). In contrary, motility can be an escape mechanism for bacteria to encounter eukaryotic predators as previously described in *V. cholerae* (Wettstadt 2020). Thus, it could be demonstrated, that motility increases along with a higher abundance of proteins involved in motility, when the T6SS-1 or T6SS-2 is impaired, enabling the *P. luminescens* cells to outcompete competitors. In addition to motility, the

production of secondary metabolites is also part of bacteria's ability to increase their fitness, e.g. through the production of antibiotics (Joyce et al. 2011). In particular, *P. luminescens* 1° cells produce several secondary metabolites with antifungal activity such as anthraquinone and hydroxystilbene (Li et al. 1995). Interestingly, proteins of the anthraquinone metabolism were found in higher levels and indeed, a shift in the secondary metabolism of *P. luminescens* 1° cells was observed upon T6SS-deficiency (Pisarz et al. 2024) **Chapter 2, Tab. 2.2, Fig. 2.2B**). However, no correlation between secondary metabolism and T6SS activity was reported before, although it has been discussed that the secretion system may play a role in biocontrol agents to deliver antibacterial or antifungal compounds (Lucke et al. 2020). Overall, these findings highlight the connection between T6SS activity, bacterial motility, and secondary metabolite production, showing new mechanisms of adaptation and survival of *P. luminescens* in different environments.

In conclusion, by performing comparative proteomics of *P. luminescens* 1° WT cells and respective T6SS-1 and T6SS-2 deficient strains, first insights into the role of the T6SSs in the insect pathogen *P. luminescens* were obtained. The data suggest a role of the T6SS-2 in interbacterial competition, whereas no clear role could be assigned to the T6SS-1 (**Fig. 7.2**). In addition, a correlation between the different fitness factors like T6SS, motility and secondary metabolism was observed along with increased abundance of PVC, T3SS and R-type pyocin proteins. However, the regulatory mechanism leading to the activity of different virulence and fitness factors remains unknown. Future investigations into the regulatory mechanisms between T6SSs, motility, and secondary metabolism in *P. luminescens* could provide deeper insights into its pathogenicity and fitness strategies, potentially uncovering novel biotechnological applications or targets for managing insect-borne diseases.

7.2 The novel structure and potential functionality of the T6SS-3 in *P. luminescens*

Many bacteria harbouring T6SSs are characterize by multiple T6SS gene clusters, i.e., three clusters are found in *P. aeruginosa*, four in *Yersinia pseudotuberculosis* and six in *Burkholderia pseudomallei* (Filloux et al. 2008; Shalom et al. 2007; Zhang et al. 2021). While most T6SSs are not constitutively assembled but rather need environmental factors like marine conditions in *V. cholerae*, to trigger their expression and assembly; the external factors leading to expression and assembly of many T6SSs are still unknown (Salomon et al. 2013). The initial studies identified four T6SS gene clusters in *P. luminescens* DJC, but the absence of genes encoding core components in the T6SS-3 and T6SS-4 clusters initially suggested that these T6SSs were not functional (Pisarz et al. 2024); **Chapter 2, Fig. 2.1**). However, the comparative proteomics revealed multiple proteins in higher levels belonging to these T6SSs in the *P. luminescens* 1° cells under standard laboratory conditions, raising the question of whether these systems might be functional (**Chapter 2, Tab. 2.1**).

To elucidate the role of the T6SS-3, in-depth analyses were performed to determine if homologous proteins of the missing core components are present in the T6SS-3 gene loci. Thereby three homologous for the missing core component TssM were identified with VasK1-3 (**Chapter 3; Fig. S3.2**). Yet, the core components TssA, crucial to stabilize the T6SS during assembly and TssH, crucial for disassembly of the T6SS are still missing (Bernal et al. 2021; Kapitein et al. 2013). However, previous studies identified a new subfamily of T6SSs in *Amoebophilues* spp., were unlike in other T6SSs, TssH is missing along with the TssJLM complex, which is found in the membrane and was previously described to be essential for the T6SS (Böck et al. 2017; Durand et al. 2015). While the T6SS is a membrane bound complex in contrary to extracellular contractile injection systems like R-type pyocins or Afps, the T6SS^{VI} subfamily found in *Amoebophilus* spp. is hypothesized to be evolutionary closer to eCIS systems mediating interactions with animal larvae (Böck et al. 2017). Further, the presence of multiple genes encoding for VgrG and T6SS effectors present in one T6SS gene loci was not

described before, thus questioning whether the T6SS-3 of *P. luminescens* represents a new subfamily of T6SSs, with a yet undescribed genetic structure (**Chapter 3, Fig. 3.1 and 3.2**). Unlike the T6SS-1 and T6SS-2, the gene loci of the T6SS-3 and T6SS-4 encode for multiple candidate effectors, thus providing first insights into the putative roles of those T6SSs. However, the three unknown effectors Tme_{Pl} found in the T6SS-4 loci were found to not deploy antibacterial activity and thus, consequent studies were focused on the T6SS-3, encoding four effectors belonging to the lipase superfamily, namely Tle2 and Tle4 (**Chapter 2, Fig. 2.1, S2 and S3; Chapter 3, Fig. 3.1**). Effectors of the lipase superfamily are often linked to antibacterial activities but are also found deploying anti-eukaryotic activity, as seen in *Pseudomonas aeruginosa* (Russell et al. 2013; Jiang et al. 2014; Jiang et al. 2016). Thus, the T6SS-3 could be involved in interbacterial or trans-kingdom interactions and indeed, the phospholipase Tle4A was found to deploy antibacterial activity and reduce bacterial growth (**Chapter 3, Fig. 3.6**). In contrast, no antibacterial activity was observed for the other lipase effectors of the T6SS-3, although they share structural and domain similarity with known antibacterial T6SS effectors like Tle4 or TplE of *P. aeruginosa* (**Chapter 3, Fig. 3.3, 3.4, 3.6**; (Russell et al. 2013; Jiang et al. 2016; Jiang et al. 2014). Nevertheless, toxicity of the lipase effectors was tested upon overproduction in the cytoplasm which needs to be repeated upon periplasmic overproduction as the effectors target the membrane and cause membrane destruction (Russell et al. 2013). Indeed, Tle1 found in *P. aeruginosa* only showed toxicity upon overproduction in the periplasm rather than in the cytoplasm (Berni et al. 2019). However, given the antibacterial activity of Tle4A, it can be concluded that the T6SS-3 is involved in interbacterial competition. Yet, the antibacterial activities of other structurally similar effectors remain inconclusive and may require further testing to rule out whether those effectors also deploy antibacterial activity or in contrast, could play a role in trans-kingdom competition.

Delivery of those effectors can occur through direct or indirect binding to the VgrG tip or the HcP tube. Effectors belonging to the lipase superfamily are commonly found to interact with VgrG through a specific C-terminal sequence which can also enable the VgrG protein to deploy antibacterial activity (Bondage et al. 2016; Flaugnatti et al. 2016; Lien und Lai 2017). The

presence of three genes encoding for VgrG's in the T6SS-3 loci questioned, whether one of those VgrGs harbours such a C-terminal extension and thus, deploys antibacterial activity. Indeed, the VgrGs of the T6SS-3, VgrG6, VgrG7 and VgrG8, all harbour a C-terminal extension after the DUF2345 domain of 30 – 70 amino acids (**Chapter 3, Fig. 3.2**). However, toxicity assays revealed, that the VgrGs are not antibacterial and therefore it is most likely that the VgrGs are only involved in binding and delivery of the Tle effectors (**Chapter 2, Fig. 3.7**). Previously, a 1:1 stoichiometry for VgrG and Tle1 of *E. coli* has been reported, allowing the translocation of three Tle effectors from the cell to a target cell (Flaugnatti et al. 2020). Thereby, the N-terminal part of Tle1 directly binds to the C-terminal TTR-domain of VgrG without an additional adaptor or PAAR protein (Flaugnatti et al. 2020). The presence of a TTR domain in VgrG6 and VgrG8 thus indicates a similar effector binding and delivery mechanism, but no such domain was identified in VgrG7, indicating an adaptor protein is necessary for effector binding (**Chapter 3, Fig. 3.2**). Interestingly, bacterial two hybrid protein-protein interaction studies showed complex interaction patterns between the different Tle and VgrG proteins (**Chapter 3, Fig. 3.5A**). Moreover, it was shown that the VgrGs are not capable to interact with themselves but rather with other VgrGs, thereby indicating the VgrG tip of the T6SS-3 is build up as a heterotrimer, putatively able to deliver a lipase effector cocktail inside a target cell (**Chapter 3, Fig. 3.5B**). In addition to the three VgrGs, two adaptor proteins, Tla1 and Tla2, were identified that are homologous to Tla3, a cytoplasmic adaptor protein in *P. aeruginosa* (Berni et al. 2019). It was previously shown that Tla3 specifically interacts with the TTR domain and specifically binds Tle3 but not Tle4, thus supporting the transport of specified effector proteins (Berni et al. 2019). Given the presence of the two adaptor proteins and one PAAR protein in the T6SS-3, indirect binding of the different Tle-VgrG proteins which could not be identified by BACTH are therefore possible. In conclusion, the results suggest that although the VgrGs of the T6SS-3 do not possess antibacterial activity themselves, they could facilitate the binding and delivery of various lipase effectors, likely forming a heterotrimeric tip and interact with adaptor proteins to effectively translocate effector cocktails into target cells, which could be bacterial of eukaryotic host cells. This would represent a novel assembly of a T6SS

tip, which has not been reported before and could offer a novel tool for targeted delivery of multiple proteins.

Although the bioinformatic and toxicity assays suggest that the T6SS-3 could be functional and is involved in interbacterial competition in *P. luminescens*, the question remained when the T6SS-3 plays a role in the bacteria's lifestyle. Thus, expression of the T6SS-3 was analysed through fluorescence microscopy under various environmental stress factors, similar to the environment of *P. luminescens* is found in, as the activity of T6SSs can be influenced through the presence of competing bacteria, eukaryotic hosts or through environmental stress factors like changes in salt concentrations (Salomon et al. 2013). Indeed, in alignment with the observations of whole-cell proteomics, expression of the T6SS-3 was observed under standard laboratory conditions. Further, the results indicated that the T6SS-3 activates under acidic and alkaline conditions in the 2° cells, as well as in response to changes in salt concentration. The expression of the T6SS-3 under acidic, alkaline, and varying salt concentrations in the 2° cells found in the rhizosphere indicates that this system could be involved in the bacterium's ability to withstand challenging environmental conditions. Such activation implies that the T6SS-3 enhances the bacterium's adaptability, allowing it to thrive and compete effectively in the dynamic and nutrient-variable rhizosphere. Also in *Acinetobacter baumanii* T6SS-dependent killing of bacterial cells under alkaline conditions was increased with enhanced activity of the effector Tse4 (Le et al. 2021). Although a reduction in T6SS-3 activity was observed in addition of PRE , based on the previously shown activity of the effector Tle4A against bacteria, it is very likely that the T6SS-3, similar to the T6SS-2, could be involved in *P. luminescens* 2° cells interbacterial competition. In contrary, a differential regulation of T6SS-3 was observed in the *P. luminescens* 1° cells with enhanced assembly at 37°C, under alkaline and under high salt concentrations (**Chapter 3, Fig. 3.9**). Thus, the T6SS-3 could be active and assembled in 1° cells during the infection of insect larvae as osmotic stress was previously described as a stress factor inside the insect larvae carcass (Crawford et al. 2010). In accordance to that, similarly to the effector PdlB in *P. aeruginosa*, a phospholipase effector crucial during infection of human epithelial cells, the phospholipase effectors Tle2 and Tle4 could play an important

role during the invasion of insect larvae (Jiang et al. 2014). However, those hypotheses are limited to preliminary results obtained from fluorescence microscopy and requires additional studies.

In conclusion, several T6SS gene clusters have been identified in different bacteria, with different roles in different species. In *P. luminescens* DJC, besides the T6SS-2 also the T6SS-3 appears to be involved in interbacterial competition, through the Tle4A effector, despite the absence of certain core components. The system is activated under different environmental conditions, such as acidic, alkaline and high salt concentrations, suggesting that it enhances the bacterium's adaptability in challenging environments such as the rhizosphere. However, further studies are needed to fully understand its assembly, the functional implications and regulatory mechanisms of T6SS-3 in *P. luminescens.* Thus, not only the contribution of the T6SS-3 to the bacterial environmental adaptability and interbacterial competition could be elucidated, but also new opportunities for biotechnological applications in fields such as agriculture and microbial ecology could be uncovered.

7.3 Membrane-disrupting T6SS effectors and their role in antibacterial activity in *P. luminescens*

The T6SS effectors exhibit a wide range of activities, including those associated with lipases, DNases, membrane pore formation and antifungal properties (Flaugnatti et al. 2016; Ma et al. 2014; Fridman et al. 2020; Trunk et al. 2018). The class of membrane-disrupting effectors (Tme) was recently described in *V. parahaemolyticus* and is found in many bacteria belonging to the *Proteobacterial* class (Fridman et al. 2020). Those effectors deploy antibacterial activity, leading to a decrease in membrane potential and thus, to a disruption of the bacterial cell membrane (Fridman et al. 2020). Consecutive studies of the *P. luminescens* DJC genome identified two genes encoding for Tme-like effectors named Tme1A and Tme1B (**Chapter 4, Fig. 4.1A**). Initial studies of the *P. luminescens* effectors indicated that Tle4A exhibited antibacterial activity, whereas the Tme_{Pl}, Tle2 and Tle4 effectors did not (**Chapter 2, Fig. S3;**

Chapter 3, Fig. 3.6). This led to the question of whether other effectors related to the T6SSs are employed as a weapon against bacterial cells in *P. luminescens*.

Following the aim to identify antibacterial effectors, Tme1A and Tme1B were shown to deploy antibacterial activity upon cytoplasmic expression, whereas Tme1B exhibits stronger toxicity compared to Tme1A (**Chapter 4, Fig. 4.3A**). As Tme of *V. parahaemolyticus* led to loss of membrane potential similar to VasX of *V. cholerae,* a pore-forming colicin-like, time-lapse microscopy showed, that also Tme1A of *P. luminescens* leads to cell rounding by disruption of the cell membrane through pore formation (Fridman et al. 2020; Miyata et al. 2011; Miyata et al. 2013). Ssp6, a T6SS pore-forming effector found in *Serratia marcescens* was found to oligomerize to a pore and thus, impairing the integrity of the outer membrane (Mariano et al. 2019). Thus, self-interaction of Tme1A was tested in *in silico* analysis and confirmed via BACTH assays, supporting the hypothesis of the assembly of Tme1 to a multimeric pore in a targeted membrane (**Chapter 4, Fig. 4.1E and 4.1F**). Further, protein structure predictions of multimeric Tme1A and Tme1B indicated the formation of an inner lumen similar to the formation of a pore (**Chapter 4, Fig. 4.1E)**. However, further biochemical studies need to be performed to confirm the mode of action and pore assembly. In conclusion, Tme1A and Tme1B, two antibacterial effectors of *P. luminescens* were identified and their putative mode of action was elucidated. Further, through oligomerization in the target cell wall, these effectors are hypothesized to form a pore.

Previously it was shown, that the toxicity of the class of Tme effectors can be neutralized through the cognate immunity protein Tmi, commonly found encoded downstream of Tme (Fridman et al. 2020). Aiming to understand the effectors Tme1A and Tme1B, the cognate immunity proteins were analysed and found to neutralize cognate and non-cognate Tme1A and Tme1B, unlike the Tme-Tmi pairs of *V. parahaemolyticus*, where no cross-neutralization was observed family (**Chapter 4, Fig. 4.1A, 3C and 3D**) (Fridman et al. 2020). Consequent bioinformatic analyses of Tmi proteins found in diverse Gram-negative bacteria identified a conserved motif in the C-terminal loop of the Tmi proteins. Suggested through prediction of the protein-interaction structures, the Tmi1 proteins most likely inhibit the formation of a pore by

Tme1 through the interaction of C-terminal loop with the α-3 and α-4 helices of Tme1. Indeed, absence of the C-terminal loop in Tmi1A abolished the neutralization of Tme1A and therefore, supports this hypothesis (**Chapter 4, Fig. 4.4)**. Also in *P. aeruginosa*, a similar interaction pattern of the effector pairs Tle4-Tli4 and Tse3-Tli3 was observed to neutralize the toxic effectors (Lu et al. 2014a; Lu et al. 2014b). Concluding, the C-terminal loop of T6SS immunity proteins is essential to provide neutralization of T6SS effectors in *P. aeruginosa* as well as in *P. luminescens.*

Both effectors contain the conserved Tme motif, but lack additional domains such as a MIX or PAAR, which have been previously identified in the Tme effector family (Fridman et al. 2020). In a DNase effector found in *V. parahaemolyticus* the MIX domain is crucial for binding to the T6SS and secretion of the effector into a target cell (Fridman et al. 2022). Thus, here it was tested whether Tme1A can interact with HcP3, found encoded in the genomic neighbourhood (**Chapter 4, Fig. 4.2**). However, while no such interaction was observed, Tme1A and Tme1B interacted with various HcP's found encoded in the genome of *P. luminescens* DJC, thus indicating that the Tme effectors are transported by the T6SS along the HcP tube. In *P. aeruginosa*, Tse1-4 interact with HcP1 but not with HcP2 or HcP3, indicating specific HcP-effector interactions (Howard et al. 2021). The inner lumen of the HcP tube, with a diameter of approximately 40 Å, restricts the size of the toxin, yet the molecular weights of Tme1A and Tme1B (26-32 kDa) support the hypothesis that they are transported through the Hcp tube (Mougous et al. 2006).

In summary, Tme1A and Tme1B represent novel antibacterial effectors in *P. luminescens* that disrupt bacterial membranes through pore formation, highlighting their potential role in interbacterial competition (**Fig. 7.1)**. Their neutralization by cognate Tmi immunity proteins, mediated via a conserved C-terminal loop, underscores a finely tuned effector-immunity interplay. Given their antibacterial properties, these effectors hold promise for biotechnological applications, such as the development of novel antimicrobial agents or therapeutic strategies against resistant bacterial pathogens.

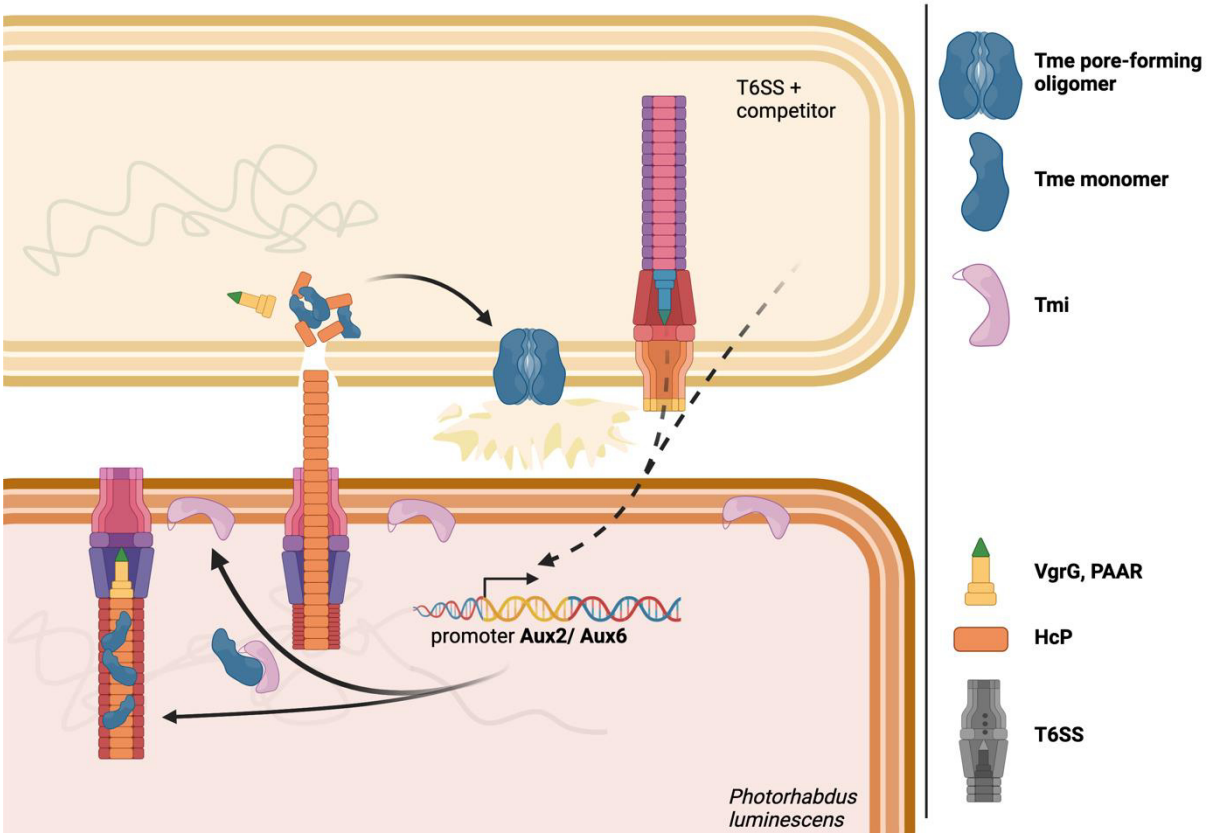

Fig 7.1. Model of the effector-immunity pair Tme1-Tmi1 in *P. luminescens*. The effector Tme1 is secreted into a target cell via the Type VI Secretion System. Thereby, activity of the respective promoter region leads to a co-production of the Tme1-Tmi1 pair, whereas the immunity protein binds to the effector via the C-terminal loop. Tme1 is then loaded into the HcP tube, ready for delivery into a target cell. The immunity proteins putatively remain in the cell to protect itself against intoxication. Once inside the target cell, Tme1 starts to form a pore in the bacterial membrane, leading to cell death of the target cell. A following counterattack by the target cell could in turn lead to reactivation of the T6SS and production of the Tme1 protein.

Initial studies showed that the T6SS effectors Tme1A and Tme1B are toxic to bacterial cells. However, no role in the lifestyle of *P. luminescens* could be assigned. Therefore, the goal was to identify their function in bacterial fitness. Through luminescence-based reporter assays performed in *P. luminescens* Δ*lux* strains, the basal activity of the *tme1A* promoter was detected in both 1° and 2° cells, although the promoter activity was significantly reduced in the 2° cells. In contrast, no activity of the *tme1B* promoter was observed, indicating that the two effectors have different roles in the life cycle of *P. luminescens* (**Chapter 4, Fig. 4.5A**). Moreover, the peak in promoter activity was observed during the exponential growth phase, which agrees with the killing capacity observed in interbacterial competition assays. Thus, it

could be demonstrated that the killing capacity of *P. luminescens* 1° cells is decreased lacking *tme1A*, whereas an increase of the killing capacity was observed in the 2° cells lacking *tme1A* (**Chapter 4, Fig. 4.5**). However, only a change of the killing capacity was observed against *Klebsiella pneumoniae* but not against *E. coli,* a T6SS-negative strain. A similar pattern was observed for *P. aeruginosa*, where T6SS-dependent killing was observed as a "T6SS duelling", thus resulting in T6SS activity when competing against other bacteria with a T6SS (Basler et al. 2013). Furthermore, different killing behaviours were observed in the *P. luminescens* 1° and 2° cell forms, suggesting that the T6SS is regulated differently depending on the phenotype. In summary, this thesis reveals that Tme1A and Tme1B have distinct roles in *P. luminescens*, with Tme1A contributing to interbacterial competition and differential killing capacity in 1° and 2° cells. Further, the results show that the immunity proteins Tmi1 can neutralize the Tme1 effectors through a motif in the C-terminal loop, most likely providing self-protection to the *P. luminescens* cells. The data further suggest that the Tme1 proteins could bind to the HcP tube of the T6SS, however it could not be determined through which T6SS the effectors are delivered.

Taken together, the T6SS-2 and T6SS-3 of *P. luminescens* DJC are involved in interbacterial competition, putatively secreting the antibacterial effectors Tme1A, Tme1B and Tle4A. The broad diversity of T6SS gene loci along with multiple T6SS effectors suggest a central role of these systems in the *P. luminescens*'s fitness to compete and survive in its ecological niche. Although none of the T6SSs was found to play a role in insect pathogenicity, the novel structure of the T6SS-3 with multiple lipases suggests a role of this secretion system towards the insect larvae. Further, the data suggest a master regulator that co-regulates different fitness factors like the T6SSs, PVCs, motility but also the secondary metabolism which has not been described before in other bacteria. However, the complexity of this system and its mechanisms require further analysis to rule out the specific roles of the different T6SSs in the lifecycle of *P. luminescens*. Yet, these findings provide valuable insights into the complex molecular mechanisms that govern bacterial competition and survival, which could have significant

implications for biotechnological applications, including the development of novel antimicrobial agents or strategies for controlling bacterial infections in agriculture or clinical settings.

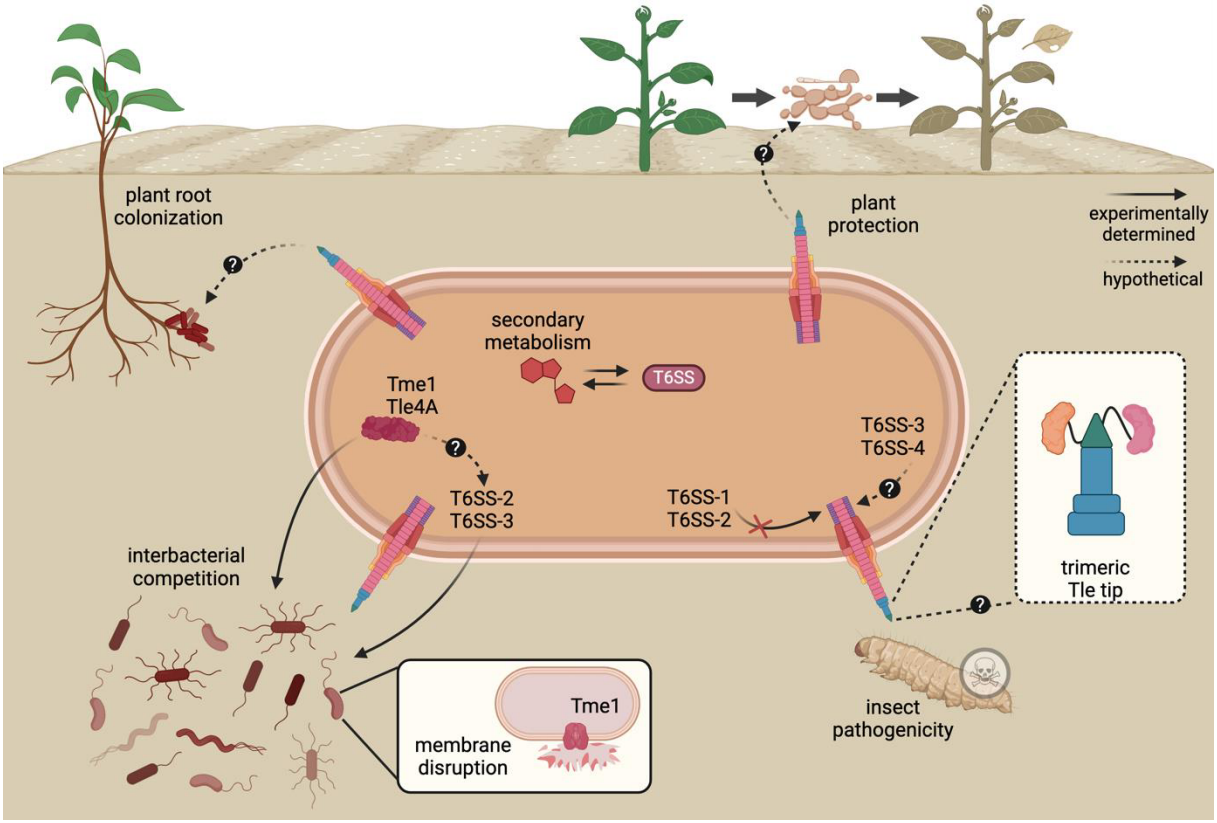

Fig. 7.2: Role of the different T6SSs in the life cycle of *P. luminescens*. The T6SS-2 and T6SS-3 are involved in interbacterial competition, yet it is still unclear which effectors are delivered via those two systems. Tme1A, Tme1B and Tle4A were shown to be antibacterial, whereas Tme1 disrupts the membrane of Gram-negative bacteria. Yet, no involvement of the T6SSs were observed for plant root colonization or plant protection. The T6SS-1 and T6SS-2 were shown to not play a role in insect pathogenicity. Thus, it is hypothesized that the trimeric tip of the T6SS-3 carrying a lipase effector cocktail is involved in killing of insect larvae. Moreover, the T6SSs in *P. luminescens* correlates with the secondary metabolism, leading to increased production of anthraquinone.

7.4 Role of bioluminescence for the *P. luminescens* biology

Our data show, that the T6SS gene clusters in *P. luminescens* play a vital role in the bacterium's fitness, facilitating interbacterial competition and enabling environmental adaptation. These systems enable *P. luminescens* to effectively compete with other microorganisms and thrive in

diverse conditions, thereby contributing to its overall survival and bacterial fitness. In addition to these mechanisms, *P. luminescens* exhibits bioluminescence. While bioluminescence is a phenomena which has gained a lot of interest by researchers, it is nowadays mainly used to perform luminescence-based assays, which offer a sensitive approach to study gene expression in various bacteria through the introduction of the *luxCDABE* gene operon (Winson et al. 1998; Gregor et al. 2018). However, due to the bioluminescence of *P. luminescens,* only fluorescence-based reporter assays could be performed so far (Münch et al. 2008). Yet, the application of fluorescence-based reporter assays in bacteria producing secondary metabolites is limited due to a high background signal derived from auto-fluorescent secondary metabolites, resulting in false positive or false negative signals (Winson et al. 1998). Indeed, also in *P. luminescens* 1° and 2° cells high auto-fluorescence was observed, with strong variation in signal strength dependent on the cultivation media (**Chapter 5, Fig. 5.4**).

The objective of this study was to ascertain the circumstances under which the various T6SSs and effectors were involved. To this end, several techniques were employed, including whole-cell proteomics, interbacterial competition assays with deletion mutants and fluorescence microscopy. Thus, to facilitate a more streamlined investigation, reporter assays based on luminescence should be established in *P. luminescens*. For this purpose, the *luxCDABE* operon was deleted in *P. luminescens* and following reintroduced via a reporter plasmid to enable the use of luminescence-based reporter assays (**Chapter 5, Fig. 5.5**). Thus, to establish the functionality of this new reporter strain and assay, different previously fluorescens-based reporter promoters were re-studied in this analysis to confirm the new reporter platform (Brameyer et al. 2014, 2015; Heinrich et al. 2016). The new reporter system was able to confirm the promoter activity of previously analysed genes; for example, the promoter of *ftsQ*, crucial for cell division during bacterial growth, was observed to exhibit similar activity levels in both the 1° and 2° cells, as expected (**Chapter 5, Fig. 5.5**). In conclusion, the successful implementation of luminescence-based reporter assays in lux-deficient strains of *P. luminescens* has provided a powerful tool for studying gene expression and cellular processes. This advancement not only overcomes the limitations associated with fluorescence-based

assays but also enhances our ability to investigate the intricate biological functions and regulatory mechanisms in this bioluminescent bacterium.

Building upon the successful establishment of luminescence-based reporter assays in *P. luminescens*, it is essential to further explore the role of bioluminescence itself in this organism. While bioluminescence is well-documented, its critical importance for the bacterium's interaction with its environment, putatively influencing its symbiotic relationship with nematodes and its pathogenicity towards insect larvae is not fully elucidated (Winson et al. 1998; Welham und Stekel 2009). Although bioluminescence is an energy intense process in bacterial cells and can consume up to 20% of the cell's energy, no change in bacterial growth were observed upon absence of bioluminescence (Ziegler und Baldwin 1981). Thus, it can be concluded that the lack of bioluminescence has no influence on bacterial growth under standard laboratory conditions, which in term allows the use of luminescence-based reporter assay in the *lux*-deficient strains. Additional stress tests performed of the *P. luminescens* 1° and 2° *lux*-deficient strains revealed no impact of temperature, salt or sugar stress (**Chapter 5, Fig. 5.2A**). However, under oxidative stress induced with 3% H_2O_2, the 2° *lux*-deficient strain showed a reduction in bacterial cell growth and was impaired in colony formation, thereby highlighting the biological role of bioluminescence in oxidative stress adaptation in the 2° cell form. Indeed, the enzymatic reaction of LuxAB, that catalyses the oxidation of reduced flavin, occurs under the consumption of O_2 (Welham und Stekel 2009). Thus, the production of bioluminescence can protect the cells against oxidative stress of reactive oxygen species, likewise in the haemolymph of insect larvae, where highly oxidative conditions are present (Welham und Stekel 2009; Rees et al. 1998). Nevertheless, cell death of *P. luminescens* 2°Δ*lux* cells occurred only at high hydroperoxide concentrations, similarly to *Vibrio harveyi luxA* and *luxB* strains, thus indicating that bioluminescence aids in adapting to oxidative stress but is not essential for survival (Szpilewska et al. 2003). Further analysis revealed that lack of bioluminescence does not influence proteolytic activity but significantly influences haemolytic activity, increasing in the 2° cell form but decreasing in the 1° cell form (**Chapter 5, Fig. 5.2B and 5.2C**). Putatively, the reduced energy consumption in the 2° cells is redirected to other

processes like haemolysis. Moreover, an increase of 2° cells found in the surroundings of plant roots was observed, implying benefits from the absence of bioluminescence (**Chapter 5, Fig. 5.3C**). Dark mutants like the Δ*lux* strains could have an evolutionary advantage as it was concluded in previous studies, stating that the lack of bioluminescence reduces the energy costs of bacteria and thereby the dark mutants can outcompete luminescent strains (Kenyan und Hastings 1961; Stabb 2005). In contrary, other studies concluded that dark mutants are rather rare and thus, don't bring an evolutionary advantage in opposite to the luminescent strains (O'Grady und Wimpee 2008). However, in *P. luminescens* strain DJC both conclusions were observed as the absence of bioluminescence affects the *P. luminescens* fitness differently depending on the cell form. While the 1° strain rather showed impaired interactions with eukaryotic hosts, such as reduced insect pathogenicity and decreased reproduction of infective juveniles, the 2° cell form benefits indicated by increased colonization of plant roots (**Chapter 5, Fig. 5.3**). Thus, it is most likely that the bioluminescence enhances the interactions of 1° cells with their eukaryotic hosts, although it is not essential. Putatively, the lack of bioluminescence reduces the capability of the 1° cell form to withstand the oxidative stress in the insect larvae (Waterfield et al. 2009). Furthermore, the availability of reactive oxygen species could be crucial for the insect larvae defence mechanisms (Waterfield et al. 2009). Thus, the lack of luciferase activity along with the increased concentration of reactive hydrogen species could aid the insect larvae to protect itself against the invading *P. luminescens* cells.

In conclusion, these data highlight the complex role of bioluminescence in *P. luminescens*, demonstrating its importance in oxidative stress adaptation and interaction with eukaryotic hosts in the primary cell form, while the secondary cell form benefits from the absence of bioluminescence, observed by increased plant root colonization and energy redirection to other processes such as haemolysis (**Fig. 7.3**). These insights provide new information on the differential impact of bioluminescence on the fitness of primary and secondary cell forms.

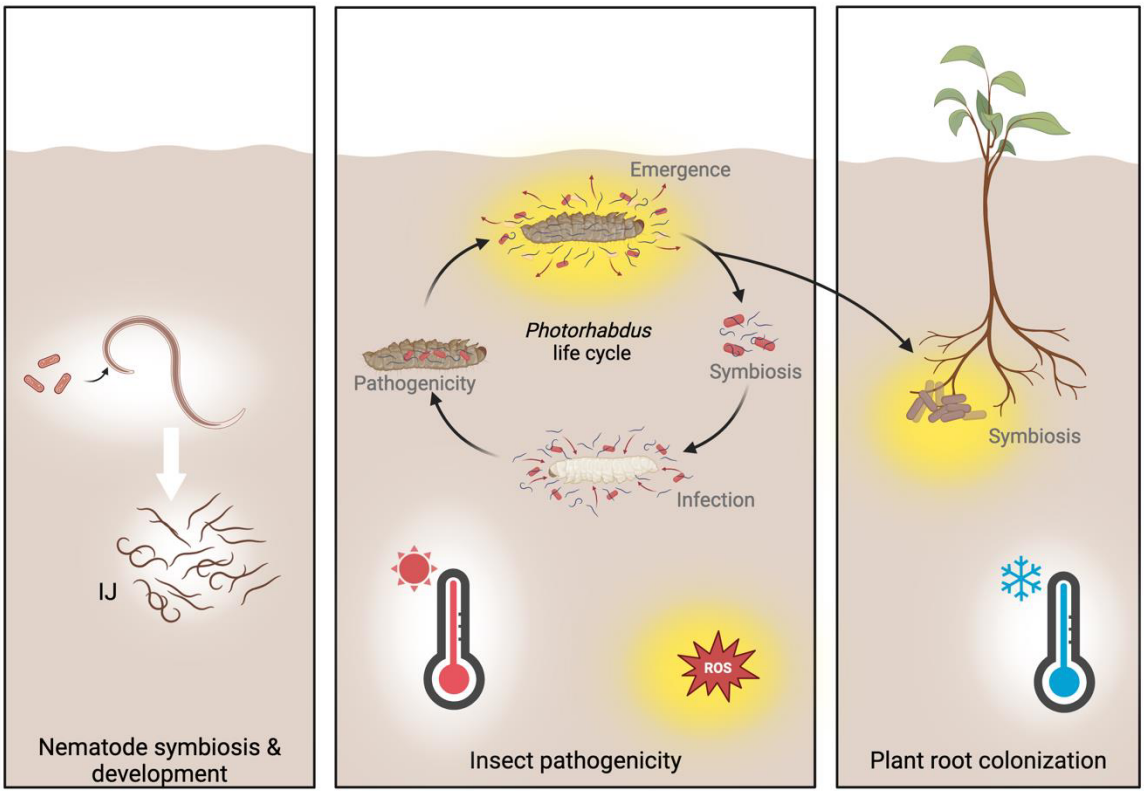

Fig. 7.3: The physiological role of bioluminescence in *P. luminescens*. The bioluminescence is not important for *Photorhabdus*-nematode symbiosis and nematodes development as well as to overcome the temperature stress. In contrary, bioluminescence is important to increase the *P. luminescens* 2° cells capacity to tolerate high concentrations of H_2O_2. Further, the bioluminescence seems to be important for insect pathogenicity although the lack of bioluminescence enhances the capability to colonize plant roots.

7.5 T6SS gene clusters in *Pseudomonas asiatica*: Ecological and applied perspectives

The T6SS in *Photorhabdus luminescens* plays a critical role in microbial interactions and competitive dynamics. Following detailed characterization of the T6SS, especially the T6SS-3 cluster with its range of diverse effectors, this study extends the analysis to *Pseudomonas asiatica*, a newly identified subspecies capable of degrading carboxymethyllysine (CML) and carboxyethyllysine (CEL). *P. asiatica* and *P. luminescens* occupy similar ecological niches, including the rhizosphere and the haemocoel of insect larvae, providing a relevant comparative

framework for understanding T6SS functions in overlapping environments (Mehler et al. 2022); **Chapter 6**).

The study of *Pseudomonas asiatica* is motivated by extensive research on *Pseudomonas* species, where T6SS functions have been observed to support various ecological and competitive roles (Bernal et al. 2017; Berni et al. 2019). For example, *Pseudomonas aeruginosa* employs T6SS to deploy toxins like VgrG2b, inducing membrane disruption in target cells, thereby enhancing its competitive edge and virulence (Sana et al. 2015). Similarly, *P. putida* utilizes T6SS mechanisms to enhance its ecological fitness, including in plant-associated environments, where it contributes to plant protection against pathogens (Bernal et al. 2017). Thus, *Pseudomonas asiatica* presents a unique model for studying potentially novel T6SS adaptations and interactions within microbial communities.

Genomic analysis of *Pseudomonas asiatica* has identified three distinct T6SS gene clusters, each encoding a complete T6SS (**Fig. 7.4**). This diversity in T6SS clusters suggests a complex capacity for interbacterial interactions and raises questions about the roles of specific effectors within these systems. T6SS-mediated secretion of antibacterial or antifungal effectors can be instrumental in enabling bacteria to compete with other microorganisms in shared environments, particularly in the rhizosphere. Investigating T6SS activity in *P. asiatica* thus provides an opportunity to examine whether it employs similar strategies to other *Pseudomonas* species and *Photorhabdus* or has evolved distinct mechanisms of microbial competition and survival. Preliminary findings in *P. asiatica* identified T6SS-associated effector-immunity pairs, including the known Tle effector from T6SS-3.

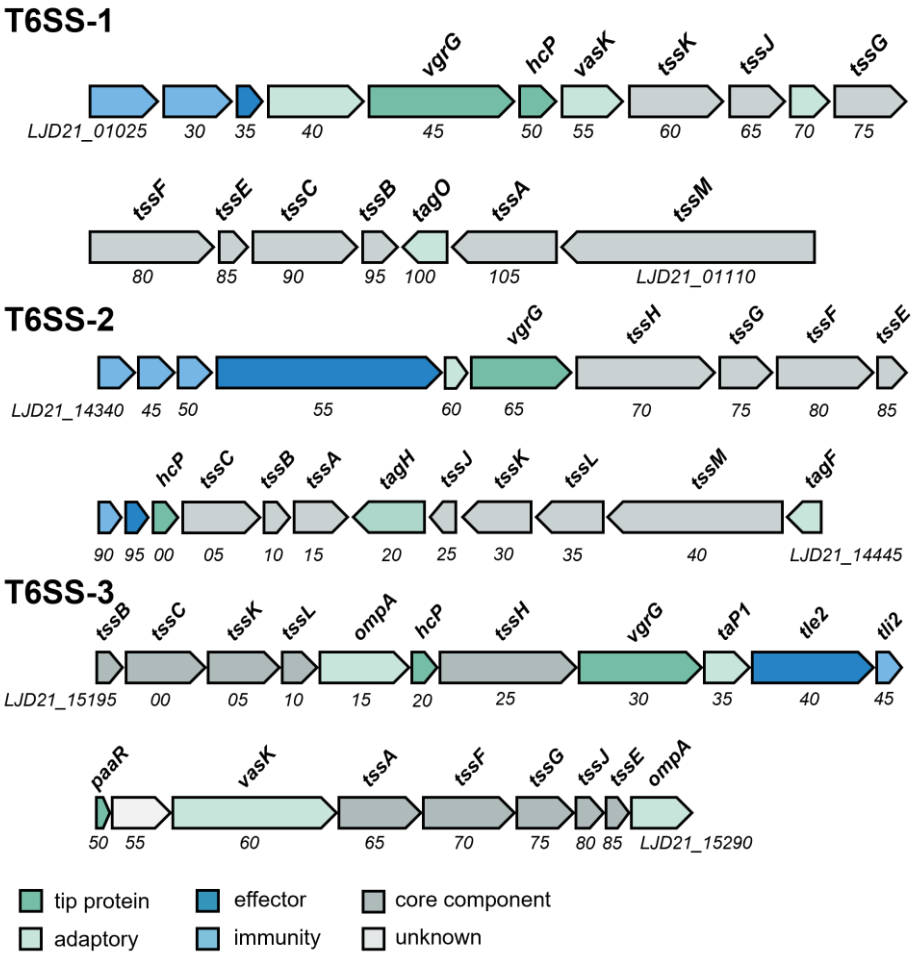

Fig. 7.4: Overview of the genomic organisation of the T6SS-1, T6SS-2 and T6SS-3 of *Pseudomonas asiatica* subsp. *bavariensis* JM1. T6SS effectors are shown in dark blue and corresponding immunity proteins are shown in light blue, tip proteins are shown in dark green, adaptor proteins are shown in light green and core components are shown in grey.

In summary, examining the T6SS of *Pseudomonas asiatica* enhances understanding of bacterial competition and adaptation strategies and aligns with the broader knowledge of T6SS roles across *Pseudomonas* species. Further investigation into the specific functions of T6SS in *P. asiatica* will be essential for understanding its potential applications in biotechnology, thereby advancing the central theme of this thesis on the significance of T6SS in microbial interactions and ecological adaptation.

7.6 The biotechnological potential of the T6SSs

Unlike conventional methods, biotechnology provides targeted, environmentally friendly approaches to minimize the effects of conventional approaches (Rathore und Singh 2022). One such approach is the use of microorganisms in environmental remediation, where their genetic manipulation can enable the degradation of pollutants (Tripathi et al. 2015). However, microbial competition in bioremediation can reduce efficiency, highlighting the importance of understanding mechanisms that control microbial interactions (Hays et al. 2015).

In this context, T6SSs offer a powerful tool for improving microbial competitiveness. By secreting antimicrobial effectors, T6SSs help bacteria outcompete rivals, making them useful for biotechnological applications. Similar to the Type I Secretion System (T1SS), which has been used for heterologous protein secretion and vaccine development, T6SSs can also be engineered to deliver therapeutic proteins or enzymes that target environmental toxins or promote plant growth, enhancing sustainability in agriculture (Burdette et al. 2018).

By employing these systems, the field of biotechnology can facilitate the development of novel approaches to address environmental challenges and improve human health. In light of this, microorganisms belonging to the *Photorhabdus* genus represent valuable models to study such competitive mechanisms.

7.7 Outlook

This work establishes initial insights into the T6SS functions in the insect pathogen *Photorhabdus luminescens* DJC, shedding light on their potential roles in bacterial competition and host interactions. While T6SS-2 and T6SS-3 demonstrate involvement in interbacterial competition, key questions remain regarding the roles of T6SS-1 and T6SS-4, particularly in the contexts of insect pathogenicity and root colonization. Future research should further investigate these systems' functionality through targeted fluorescence-tagging of TssC subunits, enabling visualization of T6SS activity *in situ* within various hosts. Host colonization assays, coupled with real-time fluorescence tracking, could provide insights into whether

specific T6SS clusters are involved in plant protection against pathogens or insect infection, both critical for defining T6SS roles in symbiotic and pathogenic phases.

Given that T6SSs are now recognized not only for their role in microbial competition but also as potential molecular delivery tools, there is an opportunity to explore their applications in biotechnology. The capacity of T6SSs to target and inject specific effectors into diverse cell types offers a promising route for developing cell-specific therapeutic delivery systems, potentially targeting pathogens or cancer cells in human health contexts. For example, effector protein engineering could allow the reprogramming of these systems to selectively inject therapeutic agents into target cells, an approach that could be transformative for precision medicine. Additionally, exploring the regulatory mechanisms of T6SS-3 activation under environmental stresses in *P. luminescens* opens doors to optimizing these systems for robust therapeutic applications that adapt dynamically to varying cellular conditions.

From a molecular perspective, further biochemical studies to elucidate the precise mechanisms of effector-VgrG binding and delivery would provide a foundation for these biotechnological applications. Protein interaction studies, such as bacterial two-hybrid assays, pull-down or high-throughput protein binding screens, could delineate T6SSs' delivery pathways. Understanding effector interaction motifs, such as the conserved loop and helix interactions seen in immunity proteins of *P. luminescens*, could lead to synthetic engineering of tailored effector delivery systems. Broadening the focus to include comparative genomic studies across *Photorhabdus* species could help identify conserved motifs that may inform more efficient effector design for cross-species applications.

On a larger ecological scale, T6SS-mediated interactions with environmental microbiota in the rhizosphere or insect gut microbiomes could be studied through metagenomic and microbiome profiling. Analyzing the influence of T6SSs on microbial community dynamics will enrich the understanding of these systems' ecological relevance, potentially allowing *P. luminescens* to be harnessed for agricultural biocontrol applications. Additionally, exploring the host immune responses to *P. luminescens* T6SSs in insect models may reveal novel immune-modulatory strategies that further expand the scope of T6SSs as tools for biotechnology.

Finally, the bioluminescent characteristics of *P. luminescens* might play a functional role in these systems, particularly under oxidative stress. Future studies, including transcriptome analysis of *lux* operon mutants under stress, may uncover new pathways of T6SS regulation and open avenues for utilizing bioluminescence as a reporter system within therapeutic delivery platforms. This integrative approach could ultimately extend the utility of T6SSs far beyond bacterial competition, positioning them as valuable assets in precision agriculture, therapeutic delivery, and ecological studies.

7.8 References of discussion

Asolkar, Trupti; Ramesh, Raman (2020): The involvement of the Type Six Secretion System (T6SS) in the virulence of *Ralstonia solanacearum* on brinjal. In: *3 Biotech* 10 (7), S. 324. DOI: 10.1007/s13205-020-02311-4.

Barret, Matthieu; Egan, Frank; Fargier, Emilie; Morrissey, John P.; O'Gara, Fergal (2011): Genomic analysis of the type VI secretion systems in *Pseudomonas* spp.: novel clusters and putative effectors uncovered. In: *Microbiology (Reading, England)* 157 (Pt 6), S. 1726–1739. DOI: 10.1099/mic.0.048645-0.

Basler, Marek; Ho, Brian T.; Mekalanos, John J. (2013): Tit-for-tat: type VI secretion system counterattack during bacterial cell-cell interactions. In: *Cell* 152 (4), S. 884–894. DOI: 10.1016/j.cell.2013.01.042.

Bernal, Patricia; Allsopp, Luke P.; Filloux, Alain; Llamas, María A. (2017): The *Pseudomonas putida* T6SS is a plant warden against phytopathogens. In: *The ISME journal* 11 (4), S. 972–987. DOI: 10.1038/ismej.2016.169.

Bernal, Patricia; Furniss, R. Christopher D.; Fecht, Selina; Leung, Rhoda C. Y.; Spiga, Livia; Mavridou, Despoina A. I.; Filloux, Alain (2021): A novel stabilization mechanism for the type VI secretion system sheath. In: *Proceedings of the National Academy of Sciences of the United States of America* 118 (7). DOI: 10.1073/pnas.2008500118.

Berni, Benjamin; Soscia, Chantal; Djermoun, Sarah; Ize, Bérengère; Bleves, Sophie (2019): A Type VI Secretion System Trans-Kingdom Effector Is Required for the Delivery of a Novel Antibacterial Toxin in *Pseudomonas aeruginosa*. In: *Frontiers in microbiology* 10, S. 1218. DOI: 10.3389/fmicb.2019.01218.

Böck, Désirée; Medeiros, João M.; Tsao, Han-Fei; Penz, Thomas; Weiss, Gregor L.; Aistleitner, Karin et al. (2017): In situ architecture, function, and evolution of a contractile injection system. In: *Science (New York, N.Y.)* 357 (6352), S. 713–717. DOI: 10.1126/science.aan7904.

Bondage, Devanand D.; Lin, Jer-Sheng; Ma, Lay-Sun; Kuo, Chih-Horng; Lai, Erh-Min (2016): VgrG C terminus confers the type VI effector transport specificity and is required for binding with PAAR and adaptor-effector complex. In: *Proceedings of the National Academy of Sciences of the United States of America* 113 (27), E3931-40. DOI: 10.1073/pnas.1600428113.

Boyer, Frédéric; Fichant, Gwennaële; Berthod, Jérémie; Vandenbrouck, Yves; Attree, Ina (2009): Dissecting the bacterial type VI secretion system by a genome wide in silico analysis: what can be learned from available microbial genomic resources? In: *BMC genomics* 10, S. 104. DOI: 10.1186/1471-2164-10-104.

Brameyer, Sophie; Kresovic, Darko; Bode, Helge B.; Heermann, Ralf (2014): LuxR solos in *Photorhabdus* species. In: *Frontiers in cellular and infection microbiology* 4, S. 166. DOI: 10.3389/fcimb.2014.00166.

Brameyer, Sophie; Kresovic, Darko; Bode, Helge B.; Heermann, Ralf (2015): Dialkylresorcinols as bacterial signaling molecules. In: *Proceedings of the National Academy of Sciences of the United States of America* 112 (2), S. 572–577. DOI: 10.1073/pnas.1417685112.

Burdette, Lisa Ann; Leach, Samuel Alexander; Wong, Han Teng; Tullman-Ercek, Danielle (2018): Developing Gram-negative bacteria for the secretion of heterologous proteins. In: *Microbial cell factories* 17 (1), S. 196. DOI: 10.1186/s12934-018-1041-5.

Cohen, Hadar; Baram, Noam; Fridman, Chaya Mushka; Edry-Botzer, Liat; Salomon, Dor; Gerlic, Motti (2022): Post-phagocytosis activation of NLRP3 inflammasome by two novel T6SS effectors. In: *eLife* 11. DOI: 10.7554/eLife.82766.

Crawford, Jason M.; Kontnik, Renee; Clardy, Jon (2010): Regulating alternative lifestyles in entomopathogenic bacteria. In: *Current biology : CB* 20 (1), S. 69–74. DOI: 10.1016/j.cub.2009.10.059.

Durand, Eric; van Nguyen, Son; Zoued, Abdelrahim; Logger, Laureen; Péhau-Arnaudet, Gérard; Aschtgen, Marie-Stéphanie et al. (2015): Biogenesis and structure of a type VI secretion membrane core complex. In: *Nature* 523 (7562), S. 555–560. DOI: 10.1038/nature14667.

Eckstein, Simone; Dominelli, Nazzareno; Brachmann, Andreas; Heermann, Ralf (2019): Phenotypic Heterogeneity of the Insect Pathogen *Photorhabdus luminescens*: Insights into the Fate of Secondary Cells. In: *Applied and environmental microbiology* 85 (22). DOI: 10.1128/AEM.01910-19.

Ffrench-Constant, Richard H.; Dowling, Andrea; Waterfield, Nicholas R. (2007): Insecticidal toxins from *Photorhabdus* bacteria and their potential use in agriculture. In: *Toxicon* 49 (4), S. 436–451. DOI: 10.1016/j.toxicon.2006.11.019.

Filloux, Alain; Hachani, Abderrahman; Bleves, Sophie (2008): The bacterial type VI secretion machine: yet another player for protein transport across membranes. In: *Microbiology (Reading, England)* 154 (Pt 6), S. 1570–1583. DOI: 10.1099/mic.0.2008/016840-0.

Flaugnatti, Nicolas; Le, Thi Thu Hang; Canaan, Stéphane; Aschtgen, Marie-Stéphanie; van Nguyen, Son; Blangy, Stéphanie et al. (2016): A phospholipase A1 antibacterial Type VI secretion effector interacts directly with the C-terminal domain of the VgrG spike protein for delivery. In: *Molecular microbiology* 99 (6), S. 1099–1118. DOI: 10.1111/mmi.13292.

Flaugnatti, Nicolas; Rapisarda, Chiara; Rey, Martial; Beauvois, Solène G.; Nguyen, Viet Anh; Canaan, Stéphane et al. (2020): Structural basis for loading and inhibition of a bacterial T6SS phospholipase effector by the VgrG spike. In: *The EMBO journal* 39 (11), e104129. DOI: 10.15252/embj.2019104129.

Fridman, Chaya M.; Keppel, Kinga; Gerlic, Motti; Bosis, Eran; Salomon, Dor (2020): A comparative genomics methodology reveals a widespread family of membrane-disrupting T6SS effectors. In: *Nature communications* 11 (1), S. 1085. DOI: 10.1038/s41467-020-14951-4.

Fridman, Chaya Mushka; Jana, Biswanath; Ben-Yaakov, Rotem; Bosis, Eran; Salomon, Dor (2022): A DNase Type VI Secretion System Effector Requires Its MIX Domain for Secretion. In: *Microbiology spectrum* 10 (5), e0246522. DOI: 10.1128/spectrum.02465-22.

Ghosh, Chandradhish; sarkar, Paramita; Issa, Rahaf; Haldar, Jayanta. (2019): Alternatives to Conventional Antibiotics in the Era of Antimicrobial Resistance. In: *Trends in microbiology* 27 (4). S. 323. DOI: 10/1016/j.tim.2018.12.010

Gregor, Carola; Gwosch, Klaus C.; Sahl, Steffen J.; Hell, Stefan W. (2018): Strongly enhanced bacterial bioluminescence with the ilux operon for single-cell imaging. In: *Proceedings of the National Academy of Sciences of the United States of America* 115 (5), S. 962–967. DOI: 10.1073/pnas.1715946115.

Hays, Stephanie G.; Patrick, William G.; Ziesack, Marika; Oxman, Neri; Silver, Pamela A. (2015): Better together: engineering and application of microbial symbioses. In: *Current opinion in biotechnology* 36, S. 40–49. DOI: 10.1016/j.copbio.2015.08.008.

Heinrich, Antje K.; Glaeser, Angela; Tobias, Nicholas J.; Heermann, Ralf; Bode, Helge B. (2016): Heterogeneous regulation of bacterial natural product biosynthesis via a novel transcription factor. In: *Heliyon* 2 (11), e00197. DOI: 10.1016/j.heliyon.2016.e00197.

Hood, Rachel D.; Singh, Pragya; Hsu, FoSheng; Güvener, Tüzün; Carl, Mike A.; Trinidad, Rex R. S. et al. (2010): A type VI secretion system of *Pseudomonas aeruginosa* targets a toxin to bacteria. In: *Cell host & microbe* 7 (1), S. 25–37. DOI: 10.1016/j.chom.2009.12.007.

Howard, Sophie A.; Furniss, R. Christopher D.; Bonini, Dora; Amin, Himani; Paracuellos, Patricia; Zlotkin, David et al. (2021): The Breadth and Molecular Basis of Hcp-Driven Type VI Secretion System Effector Delivery. In: *mBio* 12 (3), e0026221. DOI: 10.1128/mBio.00262-21.

Huang, Hao; Shao, Xiaolong; Xie, Yingpeng; Wang, Tingting; Zhang, Yingchao; Wang, Xin; Deng, Xin (2019): An integrated genomic regulatory network of virulence-related transcriptional factors in *Pseudomonas aeruginosa*. In: *Nature communications* 10 (1), S. 2931. DOI: 10.1038/s41467-019-10778-w.

Jiang, Feng; Wang, Xia; Wang, Bei; Chen, Lihong; Zhao, Zhendong; Waterfield, Nicholas R. et al. (2016): The *Pseudomonas aeruginosa* Type VI Secretion PGAP1-like Effector Induces Host Autophagy by Activating Endoplasmic Reticulum Stress. In: *Cell reports* 16 (6), S. 1502–1509. DOI: 10.1016/j.celrep.2016.07.012.

Jiang, Feng; Waterfield, Nicholas R.; Yang, Jian; Yang, Guowei; Jin, Qi (2014): A *Pseudomonas aeruginosa* type VI secretion phospholipase D effector targets both prokaryotic and eukaryotic cells. In: *Cell host & microbe* 15 (5), S. 600–610. DOI: 10.1016/j.chom.2014.04.010.

Joyce, Susan A.; Lango, Lea; Clarke, David J. (2011): The Regulation of Secondary Metabolism and Mutualism in the Insect Pathogenic Bacterium *Photorhabdus luminescens*. In: *Advances in applied microbiology* (76), S. 1–25. DOI: 10.1016/B978-0-12-387048-3.00001-5.

Jurėnas, Dukas; Payelleville, Amaury; Roghanian, Mohammad; Turnbull, Kathryn J.; Givaudan, Alain; Brillard, Julien et al. (2021): *Photorhabdus* antibacterial Rhs polymorphic toxin inhibits translation through ADP-ribosylation of 23S ribosomal RNA. In: *Nucleic acids research* 49 (14), S. 8384–8395. DOI: 10.1093/nar/gkab608.

Jurick II., Wayne M. (2022): Biotechnology approaches to reduce antimicrobial resistant postharvest pathogens, mycotoxin contamination, and resulting product losses. In: *Current opinion in biotechnology* 78, S. 102791. DOI: 10.1016/j.copbio.2022.102791.

Kapitein, Nicole; Bönemann, Gabriele; Pietrosiuk, Aleksandra; Seyffer, Fabian; Hausser, Ingrid; Locker, Jacomine Krijnse; Mogk, Axel (2013): ClpV recycles VipA/VipB tubules and prevents non-productive tubule formation to ensure efficient type VI protein secretion. In: *Molecular microbiology* 87 (5), S. 1013–1028. DOI: 10.1111/mmi.12147.

Kenyan, A.; Hastings, J. W. (1961): The isolation and characterization of dark mutants of luminescent bacteria. 121. Aufl.: Biol. Bull (S. 375). DOI: 10.1016/0304-4165(87)90076-6

Lamichhane, Jay Ram; Osdaghi, Ebrahim; Behlau, Franklin; Köhl, Jürgen; Jones, Jeffrey B.; Aubertot, Jean-noel. (2018) Thirteen decades of antimicrobial copper compounds applied in agriculture. A review. *Agron. Sustain. Dev.* **38**, 28. DOI: 10.1007/s13593-018-0503-9

Le, Nguyen-Hung; Pinedo, Victor; Lopez, Juvenal; Cava, Felipe; Feldman, Mario F. (2021): Killing of Gram-negative and Gram-positive bacteria by a bifunctional cell wall-targeting T6SS effector. In: *Proceedings of the National Academy of Sciences of the United States of America* 118 (40), e2106555118. DOI: 10.1073/pnas.2106555118.

Li, J.; Chen, G.; Wu, H.; Webster, J. M. (1995): Identification of two pigments and a hydroxystilbene antibiotic from *Photorhabdus luminescens*. In: *Applied and environmental microbiology* 61 (12), S. 4329–4333. DOI: 10.1128/aem.61.12.4329-4333.1995.

Li, Yanqi; Chen, Lin; Zhang, Pansong; Bhagirath, Anjali Y.; Duan, Kangmin (2020): ClpV3 of the H3-Type VI Secretion System (H3-T6SS) Affects Multiple Virulence Factors in *Pseudomonas aeruginosa*. In: *Frontiers in microbiology* 11, S. 1096. DOI: 10.3389/fmicb.2020.01096.

Lien, Yun-Wei; Lai, Erh-Min (2017): Type VI Secretion Effectors: Methodologies and Biology. In: *Frontiers in cellular and infection microbiology* 7, S. 254. DOI: 10.3389/fcimb.2017.00254.

Liu, X.; Matsumura, P. (1994): The FlhD/FlhC complex, a transcriptional activator of the *Escherichia coli* flagellar class II operons. In: *Journal of bacteriology* 176 (23), S. 7345–7351. DOI: 10.1128/jb.176.23.7345-7351.1994.

Lu, Defen; Shang, Guijun; Zhang, Heqiao; Yu, Qian; Cong, Xiaoyan; Yuan, Jupeng et al. (2014a): Structural insights into the T6SS effector protein Tse3 and the Tse3-Tsi3 complex from *Pseudomonas aeruginosa* reveal a calcium-dependent membrane-binding mechanism. In: *Molecular microbiology* 92 (5), S. 1092–1112. DOI: 10.1111/mmi.12616.

Lu, Defen; Zheng, Youshi; Liao, Naishun; Wei, Ling; Xu, Bo; Liu, Xiaolong; Liu, Jingfeng (2014b): The structural basis of the Tle4-Tli4 complex reveals the self-protection mechanism of H2-T6SS in *Pseudomonas aeruginosa*. In: *Acta crystallographica. Section D, Biological crystallography* 70 (Pt 12), S. 3233–3243. DOI: 10.1107/S1399004714023967.

Lucke, Miriam; Correa, Mario Gabriel; Levy, Asaf (2020): The Role of Secretion Systems, Effectors, and Secondary Metabolites of Beneficial Rhizobacteria in Interactions With Plants and Microbes. In: *Frontiers in plant science* 11, S. 589416. DOI: 10.3389/fpls.2020.589416.

Ma, Lay-Sun; Hachani, Abderrahman; Lin, Jer-Sheng; Filloux, Alain; Lai, Erh-Min (2014): *Agrobacterium tumefaciens* deploys a superfamily of type VI secretion DNase effectors as weapons for interbacterial competition in planta. In: *Cell host & microbe* 16 (1), S. 94–104. DOI: 10.1016/j.chom.2014.06.002.

Mariano, Giuseppina; Trunk, Katharina; Williams, David J.; Monlezun, Laura; Strahl, Henrik; Pitt, Samantha J.; Coulthurst, Sarah J. (2019): A family of Type VI secretion system effector proteins that form ion-selective pores. In: *Nature communications* 10 (1), S. 5484. DOI: 10.1038/s41467-019-13439-0.

Mehler, Judith; Behringer, Kim Ina; Rollins, Robert Ethan; Pisarz, Friederike; Klingl, Andreas; Henle, Thomas et al. (2022): Identification of *Pseudomonas asiatica* subsp. *bavariensis* str. JM1 as the first Nε -carboxy(m)ethyllysine-degrading soil bacterium. In: *Environmental microbiology* 24 (7), S. 3229–3241. DOI: 10.1111/1462-2920.16079.

Miyata, Sarah T.; Kitaoka, Maya; Brooks, Teresa M.; McAuley, Steven B.; Pukatzki, Stefan (2011): *Vibrio cholerae* requires the type VI secretion system virulence factor VasX to kill *Dictyostelium discoideum*. In: *Infection and immunity* 79 (7), S. 2941–2949. DOI: 10.1128/iai.01266-10.

Miyata, Sarah T.; Unterweger, Daniel; Rudko, Sydney P.; Pukatzki, Stefan (2013): Dual expression profile of type VI secretion system immunity genes protects pandemic *Vibrio cholerae*. In: *PLoS pathogens* 9 (12), e1003752. DOI: 10.1371/journal.ppat.1003752.

Mougous, Joseph D.; Cuff, Marianne E.; Raunser, Stefan; Shen, Aimee; Zhou, Min; Gifford, Casey A. et al. (2006): A virulence locus of *Pseudomonas aeruginosa* encodes a protein secretion apparatus. In: *Science (New York, N.Y.)* 312 (5779), S. 1526–1530. DOI: 10.1126/science.1128393.

Münch, Anna; Stingl, Lavinia; Jung, Kirsten; Heermann, Ralf (2008): *Photorhabdus luminescens* genes induced upon insect infection. In: *BMC genomics* 9 (1), S. 229. DOI: 10.1186/1471-2164-9-229.

O'Grady, Elizabeth A.; Wimpee, Charles F. (2008): Mutations in the lux operon of natural dark mutants in the genus *Vibrio*. In: *Applied and environmental microbiology* 74 (1), S. 61–66. DOI: 10.1128/AEM.01199-07.

Pisarz, Friederike; Glatter, Timo; Süss, Dhana-Theresa M.; Heermann, Ralf; Regaiolo, Alice (2024): The Type VI secretion systems of the insect pathogen *Photorhabdus luminescens* are involved in interbacterial competition, motility and secondary metabolism. In: *The Microbe* 3, S. 100067. DOI: 10.1016/j.microb.2024.100067.

Rathore, Anurag S.; Singh, Anurag (2022): Biomass to fuels and chemicals: A review of enabling processes and technologies. In: *J of Chemical Tech & Biotech* 97 (3), S. 597–607. DOI: 10.1002/jctb.6960.

Ray, Ann; Schwartz, Nika; Souza Santos, Marcela de; Zhang, Junmei; Orth, Kim; Salomon, Dor (2017): Type VI secretion system MIX-effectors carry both antibacterial and anti-eukaryotic activities. In: *EMBO reports* 18 (11), S. 1978–1990. DOI: 10.15252/embr.201744226.

Rees, J. F.; Wergifosse, B. de; Noiset, O.; Dubuisson, M.; Janssens, B.; Thompson, E. M. (1998): The origins of marine bioluminescence: turning oxygen defence mechanisms into deep-sea communication tools. In: *The Journal of experimental biology* 201 (Pt 8), S. 1211–1221. DOI: 10.1242/jeb.201.8.1211.

Repizo, Guillermo D.; Gagné, Stéphanie; Foucault-Grunenwald, Marie-Laure; Borges, Vitor; Charpentier, Xavier; Limansky, Adriana S. et al. (2015): Differential Role of the T6SS in *Acinetobacter baumannii* Virulence. In: *PloS one* 10 (9), e0138265. DOI: 10.1371/journal.pone.0138265.

Russell, Alistair B.; LeRoux, Michele; Hathazi, Krisztina; Agnello, Danielle M.; Ishikawa, Takahiko; Wiggins, Paul A. et al. (2013): Diverse type VI secretion phospholipases are functionally plastic antibacterial effectors. In: *Nature* 496 (7446), S. 508–512. DOI: 10.1038/nature12074.

Salomon, Dor; Gonzalez, Herman; Updegraff, Barrett L.; Orth, Kim (2013): *Vibrio parahaemolyticus* type VI secretion system 1 is activated in marine conditions to target bacteria, and is differentially regulated from system 2. In: *PloS one* 8 (4), e61086. DOI: 10.1371/journal.pone.0061086.

Sana, Thibault G.; Baumann, Christoph; Merdes, Andreas; Soscia, Chantal; Rattei, Thomas; Hachani, Abderrahman et al. (2015): Internalization of *Pseudomonas aeruginosa* Strain PAO1 into Epithelial Cells Is Promoted by Interaction of a T6SS Effector with the Microtubule Network. In: *mBio* 6 (3), e00712. DOI: 10.1128/mBio.00712-15.

Shalom, Gil; Shaw, Jonathan G.; Thomas, Mark S. (2007): In vivo expression technology identifies a type VI secretion system locus in *Burkholderia pseudomallei* that is induced upon invasion of macrophages. In: *Microbiology (Reading, England)* 153 (Pt 8), S. 2689–2699. DOI: 10.1099/mic.0.2007/006585-0.

Stabb, Eric V. (2005): Shedding Light on the Bioluminescence “Paradox”. In: *ASM News* (71), S. 2223–2229.

Sun, Yu; Wang, Lidong; Zhang, Ming; Jie, Jing; Guan, Qingtian; Fu, Jiaqi et al. (2024): *Acinetobacter nosocomialis* utilizes a unique type VI secretion system to promote its survival in niches with prey bacteria. In: *mBio* 15 (7), e0146824. DOI: 10.1128/mbio.01468-24.

Szpilewska, Hanna; Czyz, Agata; Wegrzyn, Grzegorz (2003): Experimental evidence for the physiological role of bacterial luciferase in the protection of cells against oxidative stress. In: *Current microbiology* 47 (5), S. 379–382. DOI: 10.1007/s00284-002-4024-y.

Thomas, Jacob; Watve, Samit S.; Ratcliff, William C.; Hammer, Brian K. (2017): Horizontal Gene Transfer of Functional Type VI Killing Genes by Natural Transformation. In: *mBio* 8 (4). DOI: 10.1128/mbio.00654-17.

Tripathi, Vishal; Fraceto, Leonardo F.; Abhilash, P. C. (2015): Sustainable clean-up technologies for soils contaminated with multiple pollutants: Plant-microbe-pollutant and climate nexus. In: *Ecological Engineering* 82, S. 330–335. DOI: 10.1016/j.ecoleng.2015.05.027.

Trunk, Katharina; Peltier, Julien; Liu, Yi-Chia; Dill, Brian D.; Walker, Louise; Gow, Neil A. R. et al. (2018): The type VI secretion system deploys antifungal effectors against microbial competitors. In: *Nature microbiology* 3 (8), S. 920–931. DOI: 10.1038/s41564-018-0191-x.

Unterweger, Daniel; Kitaoka, Maya; Miyata, Sarah T.; Bachmann, Verena; Brooks, Teresa M.; Moloney, Jessica et al. (2012): Constitutive type VI secretion system expression gives *Vibrio cholerae* intra- and interspecific competitive advantages. In: *PloS one* 7 (10), e48320. DOI: 10.1371/journal.pone.0048320.

Vacheron, Jordan; Péchy-Tarr, Maria; Brochet, Silvia; Heiman, Clara Margot; Stojiljkovic, Marina; Maurhofer, Monika; Keel, Christoph (2019): T6SS contributes to gut microbiome invasion and killing of an herbivorous pest insect by plant-beneficial *Pseudomonas protegens*. In: *The ISME journal* 13 (5), S. 1318–1329. DOI: 10.1038/s41396-019-0353-8.

Villadsen, John. (2007): Innovative technology to meet the demands of the white biotechnology revolution of chemical production. In: *Chemical Engineering Science* 62 (24), S. 6957. DOI: 10/1016/j.ces.2007.08.017

Wang, Xin; Wang, Qiyao; Xiao, Jingfan; Liu, Qin; Wu, Haizhen; Xu, Lili; Zhang, Yuanxing (2009): *Edwardsiella tarda* T6SS component evpP is regulated by *esrB* and iron, and plays essential roles in the invasion of fish. In: *Fish & shellfish immunology* 27 (3), S. 469–477. DOI: 10.1016/j.fsi.2009.06.013.

Waterfield, Nick R.; Ciche, Todd; Clarke, David (2009): *Photorhabdus* and a host of hosts. In: *Annual review of microbiology* 63, S. 557–574. DOI: 10.1146/annurev.micro.091208.073507.

Welham, Patricia A.; Stekel, Dov J. (2009): Mathematical model of the Lux luminescence system in the terrestrial bacterium *Photorhabdus luminescens*. In: *Molecular bioSystems* 5 (1), S. 68–76. DOI: 10.1039/b812094c.

Wettstadt, Sarah (2020): Should I kill or should I go: T6SS regulation networks in *Vibrio*. In: *Environmental microbiology* 22 (1), S. 1–4. DOI: 10.1111/1462-2920.14830.

Winson, M. K.; Swift, S.; Hill, P. J.; Sims, C. M.; Griesmayr, G.; Bycroft, B. W. et al. (1998): Engineering the luxCDABE genes from *Photorhabdus luminescens* to provide a bioluminescent reporter for constitutive and promoter probe plasmids and mini-Tn5 constructs. In: *FEMS microbiology letters* 163 (2), S. 193–202. DOI: 10.1111/j.1574-6968.1998.tb13045.x.

Yang, G.; Dowling, A. J.; Gerike, U.; ffrench-Constant, R. H.; Waterfield, N. R. (2006): *Photorhabdus* virulence cassettes confer injectable insecticidal activity against the wax moth. In: *Journal of bacteriology* 188 (6), S. 2254–2261. DOI: 10.1128/JB.188.6.2254–2261.2006.

Zhang, Anran; Han, Yu; Huang, Yuanming; Hu, Xiao; Liu, Ping; Liu, Xiaoshu et al. (2021): VgrG is separately transcribed from HcP in T6SS orphan clusters and is under the regulation of IHF and HapR. In: *Biochemical and biophysical research communications* 559, S. 15–20. DOI: 10.1016/j.bbrc.2021.04.092.

Zhang, Liqing; Xu, Jingsheng; Xu, Jin; Zhang, Hao; He, Liyuan; Feng, Jie (2014): TssB is essential for virulence and required for type VI secretion system in *Ralstonia solanacearum*. In: *Microbial pathogenesis* 74, S. 1–7. DOI: 10.1016/j.micpath.2014.06.006.

Ziegler, Miriam M.; Baldwin, Thomas O. (1981): Biochemistry of Bacterial Bioluminescence. In: Current Topics in Bioenergetics: Elsevier, S. 65–113. DOI: 10.1007/s13205-020-02311-4